The Role Of Epithelial Cells in COPD



Rassin Lababidi

St. Edmund Hall

Thesis submitted for the degree of Doctor of Philosophy in Medical Sciences

The most exciting phrase to hear in science, the one that heralds new discoveries, is not 'Eureka!' but 'That's funny…' - Isaac Asimov

Table of Contents

Abstract 9
Declaration 11
Acknowledgements 12
Abbreviations 14
Introduction 17
General Overview of COPD **17**
1.1 Epidemiology and Prevalence **19**
1.1.1 Geographical Burden 19
1.1.2 Gender Burden 21
1.1.3 Exacerbation Burden 21
1.1.4 Prevalence of Inflammatory Phenotypes 22
1.1.5 Co-morbidities 23
1.2 Pathology **24**
1.2.1 Emphysema 24
1.2.2 Chronic bronchitis 25
1.2.3 Pulmonary hypertension 26
1.3 Therapies and Treatments in COPD **28**
1.3.1 Classes of Bronchodilators 29
1.3.2 Steroids and Triple Therapies 29
1.3.3 Biologics in COPD 30
1.3.4 Antibiotic and Macrolide therapies ..... **Error! Bookmark not defined.**
1.4 Introduction to the Airway Microbiome in COPD **31**
1.4.1 Bacterial Colonization and Infections 31
1.4.2 Viral Infections in Exacerbations 34
1.4.3 Secondary infections and co-infections in COPD 36
1.5 Immunology of COPD and response to Infections **37**
1.5.1 Innate Immunity 38
1.5.2 The adaptive immune response 44
1.6 Lung Epithelial Cells in Health **47**
1.6.1 The Lung Epithelium 47
1.6.2 Epithelial defence against bacteria 49
1.6.3 Anti-viral Response in Lung Epithelial Cells 51

1.7 Lung Epithelial Cell Dysfunction in COPD 52
1.7.1 The Epithelium in COPD 52
1.7.2 Potential Therapeutics for the Epithelium in COPD 56
1.8 Tight Junctions in Epithelial Cells in Health and COPD 58
1.8.1 Junction proteins in the epithelium 58
1.8.2 Types of Tight Junction Molecules 58
1.8.3 Tight Junction dysfunction in asthma 61
1.8.4 COPD and Smoking 61
1.8.5 Effects of pathogens on adhesion molecules in bronchial epithelium 65
1.9 Aims, Objectives, & Hypothesis 66
Chapter 2: Materials & Methods 70
Materials 70
Methods 72
2.1 Ethics 72
2.2 Patient cohort and cell acquisition 72
2.3 Processing and Culturing of human bronchial epithelial cells on a monolayer 73
2.4 Culturing of human bronchial epithelial cells at Air-Liquid Interface 74
2.5 Measuring Transepithelial Resistance 75
2.6 Human bronchial epithelial cells stimulation with LPS and Poly I:C 75
2.7 Meso Scale Discovery Platform for Multiplex Measurements 76
2.8 Microscopy Staining 77
2.9 Mean Fluorescence Intensity and colocalization measurement 78
2.10 IFNλ 1/3, IFN-β1, and GM-CSF ELISAs 78
2.11 Colony forming Units Quantification and Stock Preparation of NTHi 79
2.12 NTHi Infection of HBECs 80
2.13 RV16 Propagation 82
2.14 RV16 Quantification 82
2.15 RV16 Infection 83
2.16 Harvesting of HBECs 83
2.17 RNA Isolation 84
2.18 Reverse Transcription and cDNA synthesis 85
2.19 Mastermix preparation for qPCR cycle run 86
2.20 Relative gene expression fold change calculation 87
2.21 FACS staining and analysis 88
2.22 Flow cytometry and analysis 89

2.23 RNA-seq Experimental Design 90
2.22 Library preparation and sequencing by GENEWIZ 90
2.24 RNA-seq analysis 91
2.25 Statistics 95
Chapter 3: Anti-Viral Response and Inflammation in Epithelial Cells in Response to Viral and Bacterial Infection 97
Introduction **97**
Results **101**
3.1.1 LPS stimulation effects on GM-CSF and TNF-α in HBECs at basal culture 101
3.1.2 Effect of LPS stimulation of HBECs on the pro-inflammatory cytokines GM-CSF and TNF-α at ALI 102
3.1.3 Pro-inflammatory cytokine response to NTHi infection at an early timepoint in basal culture HBECs 103
3.1.4 Effect of NTHi infection on inflammatory cytokines in basal cultured HBECs 104
3.1.5 Expression of pro-inflammatory cytokines in differentiated HBECs upon NTHi infection 105
3.1.6 Poly I:C stimulation of basal cultures affects pro-inflammatory cytokines in HBECs 107
3.1.7 Change in pro-inflammatory cytokine levels in response to Poly I:C in differentiated HBECs 108
3.1.8 HBEC infection with RV at an early time point does not change levels of GM-CSF and TNF-α 109
3.1.9 TNF-α and GM-CSF concentrations in HBECs after infection with RV in basal cultures 110
3.1.10 Response of pro-inflammatory cytokines in differentiated HBECs in response to RV infection 111
3.1.11 Changes in alarmins in HBECs after stimulation with LPS 112
3.1.12 Effect on Alarmins in HBECs in response to LPS stimulation at ALI 113
3.1.13 Effect on alarmin release from monolayer HBECs early post-infection with NTHi 115
3.1.14 Alarmin concentrations after NTHi infection in HBEC basal cultures 116
3.1.15 Changes in alarmins after NTHi stimulation in ALI cultures of HBECs 117
3.1.16 Alarmin levels post poly I:C stimulation of healthy and COPD HBECs 118
3.1.17 Alarmins expression after stimulation of HBECs with poly I:C at ALI 119
3.1.18 RV infection of HBECs does not change alarmin levels early on post-infection 121
3.1.19 Alarmin expression in basal cultures after RV infection 121
3.1.20 Alarmins in HBECs cultured at ALI after RV infection 123

3.1.21 Type I and Type III IFN response in HBECs in response to LPS stimulation 124
3.1.22 Type I and Type III IFN production in HBECs in response to LPS at ALI 125
3.1.23 IFN responses in HBECs after early infection with NTHi are unaffected 126
3.1.24 NTHi infection effect on Type I and Type III IFNs in HBECs in basal cultures 127
3.1.25 Production of IFNα2a, IFNβ1, and IFNλ1 after NTHi infection in differentiated HBECs 128
3.1.26 Type I and type III IFN concentrations in HBECs in response to poly I:C cultured on a monolayer 130
3.1.27 Effect of poly I:C stimulation on innate IFNs in differentiated HBECs 131
3.1.28 Early Expression of Type I and Type III IFNs in HBECs in response to RV infection 132
3.1.29 Type I and Type III IFN expression in HBECs in response to RV infection in basal cultures 133
3.1.30 Changes in IFNs in differentiated HBECs post-infection with RV 135
3.1.31 Gene expression of IFNRs after NTHi or RV infection in HBECs 137
3.1.31 Expression of the ISG OAS1 after infection of HBECs with NTHi or RV16 138
Discussion 140
3.2.1 The role of infection on pro-inflammatory cytokines in HBECs 141
3.2.2 Alarmin responses in COPD HBECs post-infection and stimulation 143
3.2.3 Innate anti-viral responses in HBECs post-infection 145
3.2.4 IFN signalling in HBECs in infections 147
3.2.5 Limitations and further investigations 148
Chapter 4: Barrier Integrity and Tight Junctions in Epithelial Cells in Response to Bacterial or Viral Infection 150
Introduction: 150
Results 153
4.1.1 Visualization of TJ proteins in unstimulated HBECs using confocal imaging 153
4.1.2 Expression of Tight Junction Molecules under basal conditions in HBECs 157
4.3 Colocalization of TJ proteins under basal conditions in HBECs 157
4.1.4 Transepithelial resistance in HBECs in response to LPS and under basal conditions 158
4.1.5 Effect of LPS on TJ protein localization in HBECs 159
4.1.6 Tight Junction Expression in Response to LPS Stimulation in HBECs 162
4.1.7 TJ molecule colocalization in HBECs after LPS stimulation 163
4.1.8 Changes in transepithelial resistance in response to NTHi infection 164

4.1.9 Localization of TJs CLDN-3, CLDN-4, and JAM-A in response to NTHi infection 164
4.1.10 Effect of NTHi infection on Tight Junction Expression in HBECs 167
..... 168
4.1.11 Colocalization changes in HBECs after NTHi HBECs 168
4.1.12 Transepithelial resistance in HBECs after poly I:C stimulation 169
4.1.13 Change and Localization of TJ proteins in HBECs after stimulation with Poly I:C 170
4.1.14 Poly I:C Stimulation of HBECs effect on Tight Junction Expression 173
4.1.15 Effect of Poly I:C stimulation on TJ protein colocalization 174
4.1.16 Changes in transepithelial resistance post-infection with RV 174
4.1.17 Spatial changes in Tight Molecules in response to infection of HBECs with RV16 175
4.1.18 Changes in Tight Junction Levels after RV16 Infection of HBECs 178
..... 179
4.1.19 Effect of RV16 infection of HBECs on Colocalization of CLDN-3, -4, and JAM-A 179
4.1.20 Gene expression of CLDN-3, CLDN-4, and JAM-A in HBECs after NTHi and RV16 infections 180
4.1.21 Tight Junction Molecules Occludin and ZO-1 gene expression after NTHi and RV16 infection 182
Discussion 185
4.2.1 TJ molecule expression differences in HBECs 185
4.2.2 Role of JAM-A expression in transmigration of leukocytes 187
4.2.3 TER and Spatial effects of TJ molecules in HBECs 188
4.2.4 Transcriptional Regulation of TJ Molecules 192
4.2.5 Limitations and Further Investigations 193
Chapter 5: RNA-seq Study of HBECs in COPD During Bacterial or Viral Infection 195
Introduction 195
Results 198
5.1.1 Dispersion Estimates of sequenced samples 198
5.1.2 Principle Component Analysis of the sequenced samples within different groups and culture conditions 199
5.1.3 Distance Matrix between samples within different HBEC groups and conditions 200
5.1.4 log 2-Fold changes and significance comparisons between HBEC groups and stimulations 203
5.1.5 DGE between unstimulated healthy HBECs and smoker or COPD HBECs in basal cultures 204

5.1.6 DEGs in differentiated HBEC cultures under basal conditions in COPD, smokers, and healthy HBECs 206
5.1.7 DEGs of healthy HBECs stimulated with NTHi in basal cultures 208
5.1.8 Effect of NTHi infection on smoker HBECs in basal cultures 209
5.1.9 NTHi Infected COPD HBECs DEGs in basal culture 211
5.1.10 Differentiated healthy HBECs are unaffected by NTHi infection 213
5.1.11 DEGs of smoker HBECs infected with NTHi in differentiated cultures 214
5.1.12 DEGs in NTHi infected COPD HBECs in ALI cultures 216
5.1.13 Response of healthy HBECs when infected with RV in basal cultures 217
5.1.14 No effect of RV infection on DEGs in smoker HBECs at basal cultures 218
5.1.15 COPD HBECs responses during RV infection in basal cultures 218
5.1.16 RV infection in differentiated healthy HBECs have no effect 219
5.1.17 DEGs in differentiated smoker HBECs post-infection with RV 220
5.1.18 Supervised analysis for DEGs involved in IFN signaling or innate anti-viral immunity 222
5.1.19 Gene counts and changes in PRRs in healthy, smoker, and COPD HBECs 227
5.1.20 DGE of Interleukins, Interleukin Receptors, and Cytokines in HBECs 230
5.1.21 DGE of TJ molecules in healthy, smoker, and COPD HBECs 235
Discussion 238
5.2.1 Variation between sequenced HBEC samples 238
5.2.2 DGE in COPD or smokers compared to healthy HBECs when unstimulated 238
5.2.3 Effect of NTHi on smoker HBECs in comparison to NTHi infected healthy HBECs 239
5.2.4 Changes in COPD HBECs post-infection with NTHi 246
5.2.5 RV16 Infection did not induce any DEGs in HBECs 250
5.2.6 Limitations and further investigations 251
Chapter 6: Concluding Discussion 253
6.1 Summary 253
6.2 Future Investigations 258
Chapter 7: The Covid-19 Pandemic Effect On the Thesis and Research 262
Appendix 264
References 279

Abstract

Chronic Obstructive Pulmonary Disease (COPD) is a complex disease of the airways that results in the decline of lung function with patients having emphysema or chronic bronchitis pathologies and is responsible for 7% of global deaths per year. Smoking is the largest risk factor for causing COPD and COPD patients can experience exacerbations which is defined as worsening of the symptoms which often leads to hospitalizations. The strongest risk factors for exacerbations are bacterial or viral infections. *Non-typeable haemophilus Influenzae* (NTHi) and Rhinovirus (RV) in particular are associated with up to half of COPD exacerbations. The epithelium is the first line of defense against pathogens and responsible for keeping the microbiome in check. COPD patients have been shown to have a dysfunctional epithelium.

In this thesis, I investigate the role of bronchial epithelial cells in healthy, smokers, and COPD patients to assess any difference in host immune responses and barrier integrity. They are examined under the context of an infection by the common pathogens that are found, NTHi and RV. In particular, I study type I and type III Interferon (IFN) production as well as the production of alarmins and pro-inflammatory cytokines. In addition, I assess the expression and spatial changes of Tight Junction (TJ) proteins Claudin (CLDN)-3, CLDN-4, and Junctional Adhesion Molecule A (JAM-A) in HBECs post-infection as well as barrier integrity. Finally, HBECs from basal and differentiated HBECs are infected and sequenced to capture gene expression of HBECs and assess for any differences.

COPD human bronchial epithelial cells (HBECs) immune and anti-viral responses are dysregulated as well as TJ protein expression compared to healthy HBECs post-infection with either NTHi or RV16. NTHi infected COPD HBECs had significantly higher concentrations of IFNλ1 and an significant increase in TNFα but did not upregulate TJ molecules during infection unlike in healthy HBECs. Smoker and COPD HBECs however had significantly higher levels of all TJ proteins measured at basal levels compared to health HBECs. My RNA-seq data demonstrated that COPD HBECs express significantly higher amounts of inflammatory genes post-infection with NTHi compared to healthy HBECs and smoker HBECs upregulate anti-viral genes post-infection with NTHi in basal cultures. Together, the data shows that COPD

HBECs behave differently than heathy HBECs and are dysfunctional as well as smoker HBECs post-infection in certain contexts.

Declaration

This thesis is submitted to the University of Oxford in fulfillment of the requirement for a degree of Doctor of Philosophy in Medical Sciences. The thesis contains no materials that were submitted to another university or institution for another degree or diploma. All work on this thesis is representative of my own original work unless indicated otherwise.

Rassin Lababidi

September 2021

Acknowledgements

The journey to a thesis is a long and mountainous road and I would not be here if not for the friends and family who helped and supported me along the way. I would first and foremost like to thank my supervisors Mona Bafadhel and Jennifer Cane for giving me this project and guiding me during my time in the lab.

I want to thank my lab colleagues and my friends and colleagues James and Ryan for supporting me throughout my time in the lab and for giving me their friendship outside of the lab. Oxford is an incredible place for meeting some of the smartest and kindest people you can find from around the world and so I would be amiss if I didn't thank the new and dear friends I made along the way. I want to especially thank Lilli, John, Martin, Mehdi, Gina, Conan, and Hannah for supporting me throughout my DPhil and for all the good times, hearty laughs and late nights, and precious memories that I have been given to keep. The next round is on me.

It goes without saying how much the friendship and support of my old close friends means to me but I know I wouldn't hear the end of it if I didn't mention it. I want to thank my best friends Karam, Karim, and Saba for their eternal support and friendship throughout thousands of miles away. Deep roots are indeed not reached by the frost. It is safe to say I wouldn't be here without them and I am amazed how we have all grown together over the years.

A very special thanks to my partner and love Rowie for her never ending support, kindness, patience, and love throughout all the incredible times we have had and when the road to my thesis was arduous. I am incredibly lucky to have you honin bertje. I also want to thank my dog Auri for her unconditional and undying love that she has given me over her six years. This journey would not be the same without her.

Finally, I want to profoundly thank my family, especially my parents, for their unconditional love and support throughout my life and when I decided to move thousands of miles away into uncertain yet bountiful waters. Mama, baba, and my siblings Anas, Yazan, and Ghaliah, I love you all very much and I wouldn’t be here without you. So it goes.

Abbreviations

A1AT- Alpha-1-Antitrypsin

AJ – Adheren Junction

ALI – Air-Liquid Interface

AMP – anti-microbial peptides

APC – Antigen Presenting Cell

cAMP – Cyclic Adenosine Monophosphate

AZM - Azithromycin

CLDN – Claudin

COPD – Chronic Obstructive Pulmonary Disease

CSE – Cigarette Smoke Extract

CS – Cigarette Smoke

DC – Dendritic Cell

DEG – Differentially Expressed Gene

DGE – Differential Gene Expression

EGF – Epithelial Growth Factor

EMT – Epithelial to Mesenchymal Transition

ERK – Extracellular Signal-Regulated Kinase

GM-CSF – Granulocyte Macrophage Colony Stimulating Factor

HBD – Human β-defensin

HBECs – Human Bronchial Epithelial Cells

ICS – Inhaled Corticosteroids

IEC – Intestinal Epithelial Cells

IFN – Interferon

IFNAR – Interferon Alpha/Beta Receptor

IFNLR1 – Interferon Lambda Receptor 1

Ig - Immunoglobulin

IL – Interleukin

ILC2 – Innate Lymphoid Cell 2

IRF – Interferon Regulatory Factor

ISG – Interferon Stimulated Gene

JAM – Junctional Adhesion Molecule

LPS – Lipopolysaccharide

MMP – Matrix Metalloproteinase

mDC – Myeloid Dendritic Cell

NE – Neutrophil Elastase

NET – Neutrophil Extracellular Trap

NK – Natural Killer

NKT Cell – Natural Killer T-cell

NO – Nitric Oxide

NOS – Nitric Oxide Synthase

Nrf2 - Nuclear Factor Erythroid 2-related Factor 2

NTHi – Non-typeable Haemophilus Influenzae

OCS – Oral Corticosteroids

PARP - Poly ADP-Ribose Polymerases

PCA – Principle Component Analysis

PCR – Polymerase Chain Reaction

pDC – Plasmacytoid Dendritic Cell

PR3 – Proteinase 3

PRR – Pattern Recognition Receptor

PTX3 – Pentraxin 3

PH – Pulmonary Hypertension

RIG-I – Retinoic Acid Inducible Gene I

ROS – Reactive Oxygen Species

RSV – Respiratory Syncytial Virus

RV – Rhinovirus

STAT – Signal Transducer and Activator of Transcription

SOCS – Suppressor of Cytokine Signaling

TER – Transepithelial Resistance

TGF-β – Transforming Growth Factor-β

TJ – Tight Junction

TLR - Toll-like Receptor

TNFα - Tumor Necrosis Factor α

TNFAIP - TNFα Inducible Protein

TRIM – Tripartite Motif

TSLP – Thymic Stromal Lymphopoietin

VEGF – Vascular Endothelial Growth Factor

VDR – Vitamin D Receptor

ZO – Zona Occludin

Introduction

General Overview of COPD

Chronic obstructive pulmonary disease (COPD) is a multi-factorial disease of the small airways, that leads to a decline in lung function as the disease progresses and is a leading cause of morbidity and mortality worldwide. According to the World Health Organization, it is already the 3rd biggest cause of death[1]. The progression of COPD is a mixture of emphysema and chronic bronchitis depending on the phenotypic characteristics of the patient[2]. Emphysema is characterized as the destruction of the alveolar air space; whilst chronic bronchitis is a clinical description of chronic inflammation and sputum production. Patients with COPD report symptoms such as wheezing, shortness of breath, tightness in the chest, and chronic coughing[2]. Exacerbations can also occur in patients with COPD and are defined as an acute worsening of the symptoms that require additional therapy and potential hospitilization to manage the symptoms and negative impact on patients' health.

COPD is mainly thought to be caused by chronic smoking including second hand smoke. In recent years however, long term exposure to various noxious particles, pesticides, pollutants, and toxins have been also shown to be risk factors in the disease[3,4]. In a clinical context, spirometry is used to measure any airflow obstruction of the lung using a bronchodilator and measuring the ratio of the airflow before to after the bronchodilator was taken, denoted as the FEV_1/FVC ratio[5]. People with some or all the symptoms as well as long term exposure to the risk factors and a FEV_1/FVC ratio of less than 0.7 post-bronchodilator are diagnosed with COPD. The severity of COPD is stratified into four categories of mild, moderate, severe, and very severe depending on the FEV_1% predicted and severity of the symptoms[5].

Mechanisms of the pathogenesis of COPD are not well understood however it is clear that chronic inflammation with multiple immune cells plays a prominent role in the pathogenesis. In addition, viral and bacterial infections are linked to the occurrence of exacerbations along with potential exposure to pollutants[6]. Recently, examination of inflammatory cells in the sputum and blood of patients with COPD has led to the understanding that inflammation in COPD can be grouped into two broad types: eosinophilic COPD and infection related - non-eosinophilic COPD[7,8]. Eosinophilic COPD can be defined as blood eosinophils being >2% of the circulating leukocyte count and/or >3% sputum non-squamous cells. Eosinophilic COPD accounts for approximately 30% of patients depending on the population being studied with the rest composed of non-eosinophilic COPD[8,9]. This stratification of inflammatory subtypes is largely based on the asthma literature where both subtypes are also found albeit with the eosinophilic phenotype in higher proportions in contrast to COPD[10]. Both subtypes may impact the epithelial barrier in the lung differently which may imply that treatments need to be targeted differently. The non-eosinophilic subtype will broadly induce a Type 17 response and neutrophilic phenotype while the eosinophilic subtype induces a Type 2 response which could lead to increase mucus production and hypersecretion.

Treatments for COPD have remained mostly stagnant over the past few decades. The three main categories of inhaled treatment have been anti-muscarinics, beta-agonists, and corticosteroids and are increasingly given together in a single inhaler. There have been some developments in targeted treatment approaches including potential use of monoclonal antibodies. The identification of the eosinophilic and non-eosinophilic inflammatory sub-types of COPD has led to novel studies to target treatment of eosinophilic COPD patients with oral corticosteroids during an exacerbation[11,12]. Macrolide antibiotics have also increasingly been used recently in non-bactericidal

doses as they have been shown to be anti-inflammatory and decreases exacerbation particularly if patients have certain symptoms[13,14].

1.1 Epidemiology and Prevalence

Although it is known that the global burden of COPD is high with a greater impact on older people, the range of the global burden is wide. Unfortunately, estimating this burden on a global level proves difficult due to factors such as diagnostic criteria and the availability of COPD data from some countries is low. Until recently for example, the disease burden of COPD in China and developing countries has been largely unstudied but suspected to be high due to factors such as extremely high pollution levels and occupational fumes and toxins as well as more established causal factors such as smoking. In the UK, the prevalence of COPD is 1.2 million with 30,000 deaths although it is estimated that up to two thirds of COPD cases are undiagnosed making the UK the third in terms of COPD deaths in Europe[15]. According to the World Health Organization the estimated number of people with COPD worldwide is around 380 million. The number is likely to be greatly underestimated due to COPD being underdiagnosed and unstudied.

1.1.1 Geographical Burden

In South America and the Caribbean, based on a relatively small number of studies and surveys, it was found that the proportion of people that have COPD has been found to be 11.6% with a range of 9.1-14.4% depending on the country[16]. In-hospital deaths have been found to have a wide range depending on the country with 6.7% in Brazil and 29.5% in Mexico for example[16]. North America was found to have a higher prevalence of COPD with a mean prevalence of 14.5% across the United States[17]. In

Europe, the estimated mean prevalence of COPD is 12.4% with the highest proportion of COPD incidence in West and Central Europe with 14.2% and 14.1% respectively[18]. Interestingly, it was found that countries with higher per capita gross national incomes generally had a higher prevalence of COPD[19]. This is likely at least partially due to wealthier countries having a higher proportion of an aging population which is where the incidence of COPD patients is highest.

It is estimated that of all global deaths, approximately 7% are attributed to COPD with approximately 4% of the world's daily affected life years (DALYs) although that is likely an underestimate as it does not account for deaths that COPD contributes to[20]. It should also be reiterated that it is likely that COPD is largely undiagnosed especially in low income countries.

China accounts for around 20% of the world's population and is among the top countries with the highest proportion of an aging population. Until recently, studies on the prevalence and mortality of COPD patients in China were initially limited in scope and had a wide range from 1.2-8.9% due to lack of access to diagnostic material with a treatment rate of 7.9%[21]. It was first estimated that the cases of COPD in China were around 42.5 million and in 2010, 934,000 people with died from COPD[22,23]. DALYs were also higher than average compared to other countries with approximately DALYs of 1576/100,000.

Recently, Wang et. al performed a nationwide study termed the China Pulmonary Health Study to more accurately quantify the disease burden and prevalence of COPD[24]. This study excluded participants that had no or unreliable spirometry to fit in with the diagnostic criteria for COPD and it was found that around 8.6% of participants had COPD[24]. This indicates that the prevalence of COPD in China is approximately

100 million people which is significantly higher than the previous estimate of 42.5 million people. Smoking and exposure to PM2.5 particulates were among the highest risk factors associated with COPD[24].

1.1.2 Gender Burden

The prevalence of COPD is higher in men then women worldwide. In a meta-analysis, around 9.2% of men and 6.1% of women were found to have COPD[25]. The proportion of men and women both increase in the age groups aged over 65 with men still having a higher proportion than women[25]. Severe and very severe forms of COPD also accounted for a higher proportion of the cases although that is likely because more severe cases of COPD are more likely to be diagnosed. In terms of survival, there were no significant differences in survival and mortality between men and women[26]. Women however, exhibited more severe dyspnea and airflow limitation with a higher likelihood to have an exacerbation than men[27].

1.1.3 Exacerbation Burden

Exacerbations play a role in the mortality of COPD. A study by Golpe et. al attempted to stratify COPD patients based on the first Spanish COPD guidelines into asthma-COPD overlap, non-exacerbators, frequent exacerbators with emphysema, and frequent exacerbators with chronic bronchitis[28]. The Asthma-COPD overlap phenotype is currently characterized as persistent airflow obstruction for adults over 40 that share features with both asthma such as partially reversible airflow, and COPD such as persistent airflow limitations and co-morbidities[29]. Frequent exacerbators were classified as patients with more or equal to two exacerbations per year and patients were followed for almost 8 years and survival rates were compared. It was found that the frequent exacerbators with emphysema group had the lowest survival rates by

more than 38% followed by the frequent exacerbators with chronic bronchitis group, the non-exacerbators group, and finally the Asthma-COPD overlap group with the highest survival rates at 12%[28]. This shows that frequent exacerbators have significantly greater mortality rates than non-exacerbators.

1.1.4 Prevalence of Inflammatory Phenotypes

Between 30-40% of COPD patients have been found to be eosinophilic with more than 3% eosinophils in sputum and around 25% have more than 2% eosinophils in the blood[30,31]. Eosinophilic COPD patients have been found to have significantly greater numbers of exacerbations than non-eosinophilic patients with a greater proportion of men than women being eosinophilic according to the Copenhagen General Study[32]. In addition, a study by Couillard et. al found that eosinophilic COPD patients had a significantly increased risk of 12-month hospital admission and an increased risk of readmission with no differences in length of hospital stay[33]. Blood eosinophils have also been shown to be a good predictor of exacerbations with eosinophilic cell counts shown to be a better predictor than eosinophil percentages[30,32]. A study of more than 10,100 COPD patients by Yun et. al has shown that increased counts of eosinophils have been shown to be at a higher risk for exacerbations than fluctuating eosinophil numbers[34]. However, despite the higher incidence of exacerbations, a study by Shin et. al found that COPD patients with persistently high blood eosinophils (>300 cells/µl) had better survival rates than patients with persistently low blood eosinophils (<300 cells/µl)[35]. Interestingly, ex-smokers with eosinophilic COPD seem to have a higher risk of exacerbating than current smokers with eosinophilic COPD[30]. This may be at least partially due to smoking inducing Type 17 and Type 1 responses[36]. Both of those responses have been shown to repress the Type 2 response that eosinophilia is

associated with. The immunological counterweight induced by smoking may thus delay the incidence of exacerbations in COPD[36].

1.1.5 Co-morbidities

COPD is often a disease that does not present individually with various comorbidities found in COPD patients. It has been estimated that over 97% of COPD patients present with one or more comorbidities with 53.5% of patients presenting with four or more comorbidities. Ischemic heart disease, pulmonary hypertension, chronic kidney disease, lung cancer, diabetes, anxiety, and depression are among the most common comorbidities found in COPD patients. Comorbidities have been found to decrease the quality of life and increase the frequency of exacerbations and mortality in COPD. Heart failure, diabetes, and heart diseases in general have been shown to have the strongest association with the increased mortality in COPD patients[28].

It is difficult to discern whether some comorbidities are caused by the symptoms and pathology of COPD or whether the disease shares similar etiological factors as COPD. For example, smoking can increase the risk of heart failure in general however inflammation in COPD can accelerate atherosclerosis thus increasing the risk. A study by Kunisaki et. al of 16,485 COPD patients has shown that there was approximately a 2.5-fold increased risk in heart failure 30 days post-exacerbation and a 2-fold increased risk at 90 days even in patients without a known history of cardiovascular diseases[37]. On the other hand, the disability and reduced autonomy and mobility that is caused by COPD can lead to patients have a feeling of increased anxiety, depression, and dyspnea.

Lung cancer is found in approximately 2.8% of COPD patients in pulmonary clinics[38]. Around 50% of patients diagnosed with lung cancer however have been found to have

COPD however with an association between increasing stages of lung cancer and the severity of COPD. Lung cancer and COPD have a shared etiological factor from smoking and the inflammation that smoking causes which could mean that smoking can cause lung cancer and COPD independently. While COPD is more associated with the destruction of the lung epithelium there are several ways where COPD and proliferative diseases like cancer can intersect. The inability to scavenge ROS for example, can lead to DNA damage in COPD which leads to mutations that lead to greater proliferation and anti-apoptotic features[39].

1.2 Pathology

The pathology of a heterogenous disease such as COPD is complex and can be variable or more severe depending on the stage and phenotype of the disease. As aforementioned, COPD is characterised by emphysema and chronic bronchitis and the pathology of COPD is summarized in **Figure 1.1**.

1.2.1 Emphysema

Emphysema is broadly defined as a lung condition characterized by permanent and abnormal enlargement of the respiratory airspaces, accompanied by destruction of their walls without obvious fibrosis[40]. To define the different types of emphysema, the lung acinus first needs to be defined. The lung acinus is the distal portion of the terminal airway bronchioles and is responsible for gas exchange which also comprises the alveolar sacs and ducts[41]. Lung acini are too small to be viewed on conventional CT scans however, new micro-CT has helped visualize the pulmonary acini[41].

There are four main types of emphysema: Centriacinar emphysema, panacinar emphysema, paraseptal emphysema, and paracicatricial emphysema. Centriacinar is the most common type of emphysema and is most associated with cigarette smoking.

Centriacinar mainly affect the bronchioles by leaving the alveoli relatively intact while the bronchioles are damaged. Conversely paraseptal emphysema is when the distal bronchioles are unaffected with destruction occurring in the alveolar sacs and ducts. Panacinar is the destruction of the alveoli and usually occurs from the deficiency of the preotease inhibitor alpha-1-antitrypsin (A1AT). It is found in approximately 2% of COPD patients and leads to the occurrence of emphysema and COPD much earlier in life than most other COPD patients[42]. Finally, paracicatricial emphysema is characterized as airspace enlargement.

There have been several studies in both humans and mice attempting to establish the etiological factors of emphysema. While the mechanisms for the pathogenesis of emphysema have not been definitively established, studies have consistently indicated that the pathology of emphysema is due to dysregulated production of proteases that destroy the lung tissue and microenvironment. Belouaaj et. al showed that mice deficient in serine protease releasing granules in neutrophils are unable to release the proteases proteinase 3 (PR3), Cathepsin G, and neutrophil elastase (NE) leading to the mice being protected from emphysema upon cigarette smoke exposure[43]. Mice with prolonged exposure also had greater infiltration of Tc17, Th17, and Treg cells in the lungs leading to increased neutrophil recruitment and production of TGF-β[44]. The role of TGF-β is of particular interest as TGF-β has been shown to be able to induce fibrosis and the production of serine proteases[45].

1.2.2 Chronic bronchitis

Chronic bronchitis is mainly categorized as chronic inflammation and airflow obstruction with cough and sputum production for three months a year for two consecutive years[46]. Inflammation induces the recruitment of leukocytes such as macrophages as well as granulocytes into the lungs. The immune system at mucosal

surfaces are under constant surveillance for any pathogens and toxins that may enter with epithelial cells and resident dendritic cells (DCs) and macrophages keeping microorganisms at bay and under tight control[47]. During infection innate immune cells such as granulocytes and macrophages signal the adaptive immune response, mainly lymphocytes such as T-cells and B-cells, to be recruited into the lungs to mount a more specific immune response. Severe COPD leads to a chronically higher number of T-cell and B-cell infiltrating the lungs[48]. It has been found that there is an increase in CD8+ Tc1 T-cell infiltration in the lung in patients with COPD which are usually recruited during viral or intracellular bacterial infections[49]. Importantly, epithelial layer thickening and mucus hypersecretion is induced during chronic bronchitis which is due to goblet cells activation, metaplasia, and hyperplasia[50,51]. Ciliary cells are a subtype of epithelial cells that play a role in removing noxious particles and mucus trapped pathogens out of the lungs through their beat like movement. They been found to be less efficient and able to beat less frequently in COPD despite COPD patients having more primary cilia, which leads to mucus buildup in the lungs[52,53]. Chronic bronchitis has also been associated with a lower quality of life as well as an increase in exacerbations[54].

1.2.3 Pulmonary hypertension

Both emphysema and chronic bronchitis can contribute to changes in the pulmonary vasculature which can subsequently lead to pulmonary hypertension. Pulmonary Hypertension (PH), described as an increase in pressure in the pulmonary artery, is commonly found in COPD patients[55]. Severe PH is rarely found in COPD however it has been shown that prevalence of PH increases with the severity of the disease[55]. Endothelial cells play a major role in regulating the vasculature. In the pulmonary arteries of COPD patients, vascular endothelial growth factors (VEGF) and their

respective receptors have been shown to be upregulated[56]. VEGF proteins are usually responsible of inducing the angiogenesis of endothelial cells[57]. Vascular lesions as well as thickening of the blood vessel walls and narrowing of the blood vessels are features that are also observed in COPD patients, probably due to the inflammatory environment in and around the lungs[58]. The inflammatory environment can contribute to the acceleration of cardiovascular diseases such as pulmonary embolism[59]. All these changes make oxygen less available in the lungs and can subsequently lead to a hypoxic lung environment which is found in some COPD patients[60]. Hypoxia can lead to increased degranulation of neutrophils and inflammation in the lungs and angiogenesis, creating a positive feedback loop that leads to increasingly aberrant vascular and lung remodelling[61]. The angiogenic and pro-inflammatory changes that occur in the lung can lead to damage and destruction of the epithelial barrier and its structure. Long term hypoxia may also impair the function of the epithelium in the lungs skew its function to counteract the multitude of changes and unable to maintain homeostasis.

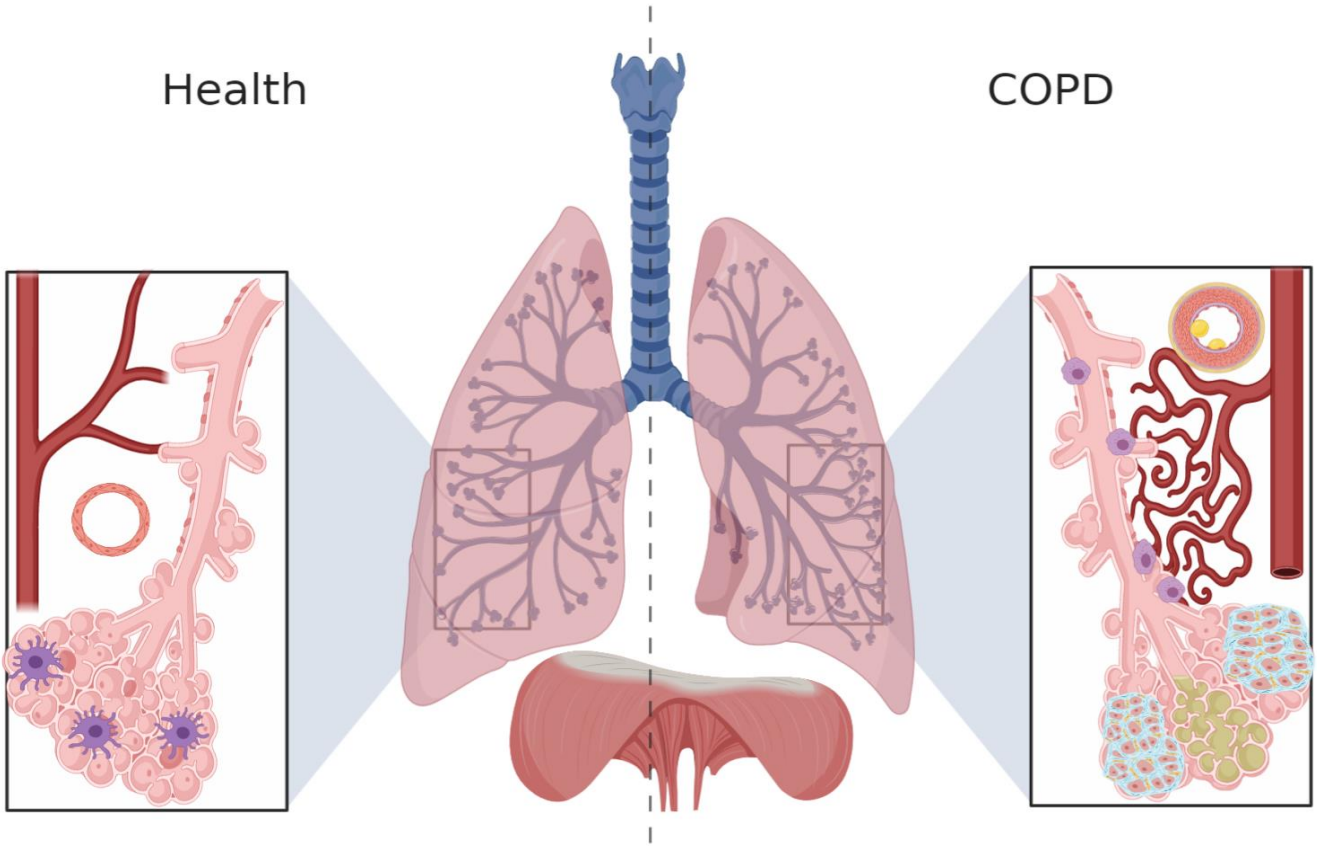


Figure 1.1: Pathology of COPD in the lungs. *Lungs in healthy people are free of obstruction with gases flowing freely and have surveillance immune cells for irritants or pathogens such as alveolar macrophages or dendritic cells. Lungs in COPD patients on the other hand are obstructed with mucus and infiltrating leukocytes such as macrophages or neutrophils and have increased airway destruction in the alveoli termed as emphysema. Blood vessels around COPD lungs are dysregulated and hypoxic with increased smooth muscle cells leading to hypertension as well as increased plaque formation potentially leading to pulmonary embolisms.*

1.3 Therapies and Treatments in COPD

There is a wide array of treatments for COPD with varying degrees of efficacy. The medication prescribed to the patient is dependent on the severity or stage of the disease. Immunological phenotypic characteristics of patients has also been proposed as a way to define disease severity and for treatment implementation such as eosinophil counts[62].

1.3.1 Classes of Bronchodilators

Most COPD patients are given bronchodilators which relax the airway smooth muscles to relieve symptom and have been shown to improve quality of life[62]. Bronchodilators can either be short or long acting, SA and LA respectively. The first type of bronchodilators are beta$_2$ acting agonists. They act by stimulating the beta$_2$ adrenergic receptors which induces the production of cyclic AMP (cAMP), antagonizing bronchoconstriction[63]. Another type of bronchodilator are the anti-muscarinic drugs, which block bronchoconstriction by inhibiting the binding of the neurotransmitter acetylcholine to the M3 muscarinic receptor on the airway smooth muscle[64]. Anti-muscarinics can either be short or long acting (SAMAs and LAMAs). Long-acting bronchodilators are given either alone or in combination in a single inhaler, with studies showing combination dual-bronchodilation are superior at alleviating the symptoms of COPD than when given individually[65].

1.3.2 Steroids and Triple Therapies

Inhaled corticosteroids (ICS) or oral corticosteroids (OCS) are given to patients with severe symptoms and exacerbations in combination with LABAs or LAMAs. Corticosteroids migrate through the cell membrane then bind and activate glucocorticoid receptors in the cell. Their effects are pleiotropic and have generally shown to be immunosuppressive and anti-inflammatory[66]. As a result, patients on ICS are more susceptible to infections such as candidiasis and pneumonia as well as causing skin bruising and a hoarse voice[67]. The Triple therapy combination treatment of ICS/LABA/LAMA however has been shown to be superior to both ICA/LABA and LABA/LAMA and improves lung function more and reduces exacerbations[68,69]. Unlike asthma, ICS has been shown to be ineffective in a majority of COPD patients with

reductions of exacerbations observed between only a quarter and third of patients and with no major effects on decline of FEV1 which brings its current conventional usage into question[70,71]. Recent studies have shown that ICS is effective only in the eosinophilic subpopulation of COPD patients and decreases the number of eosinophils in the lung[72,73].

1.3.3 Biologics in COPD

In the last decade or so, biologics have been emerging as a form of therapy in both COPD and asthma with more studies and clinical trials being done on asthma until recently. However, there is no clinically approved COPD biologic as of yet. IL-5 is an important activator of eosinophils and B-cells and can recruit eosinophils into the tissues along with eotaxin. IL-5 can be produced by various immune cell types particularly Type 2 cells such as Th2, Tc2, and ILC2 lymphocytes and eosinophils themselves. Thus, there have been efforts to inhibit the action of IL-5 in asthma and COPD either through sequestering it or inhibiting its respective receptor, IL-5R.

Mepolizumab is a clinically approved anti-IL-5 antibody in asthma. Clinical trials in eosinophilic COPD have reported that there is a decrease in exacerbations on treated groups versus placebo in COPD patients with higher eosinophils in the blood[12]. In contrast, the anti-IL-5R antibody benralizumab showed no significant reduction in exacerbations in moderate to severe COPD in Phase IIb and Phase III clinical trials[74,75].

Thymic Stromal Lymphopoietin (TSLP) is a cytokine and one of the main alarmins that orchestrates adaptive type 2 responses and inflammation. Studies have shown that TSLP is elevated in the BAL and epithelial cells of COPD and asthma patients compared to healthy controls particularly during viral infections[76,77]. The monoclonal

antibody against TSLP Tezepelumab, has been shown to significantly decrease exacerbations in uncontrolled asthma in a phase II clinical trial independent of blood eosinophil counts[78]. Since anti-TSLP has been shown to have a significant effect on asthmatics and TSLP has been shown to play a role in COPD, anti-TSLP clinical trials in COPD may lead to promising results.

TNF-α is an important pro-inflammatory cytokine. While anti-TNF-α monoclonal antibodies have been very effective in treating other chronic inflammatory diseases such as rheumatoid arthritis, they seemed to be ineffective in COPD clinical trials even having potential adverse effects on some patients[79].

1.4 Introduction to the Airway Microbiome in COPD

The microbiome in various organs has been shown to be vital in regulating the physiology and pathophysiology. The different bacterial and viral species that constitute the microbiome can be quantified and identified with various methods including qPCR, bacterial culture, plaque assays, and increasingly 16S RNA-seq analysis that can also stratify strains of the same species. While it was initially thought that the lung was sterile, it has been increasingly shown in the past decade or so that not only does it have a rich microbiome, but the constituting microbiota can influence diseases such as COPD[80].

1.4.1 Bacterial Colonization and Infections

Paradoxically, despite having chronic inflammation and leukocyte infiltration in the lungs, patients seem to be chronically infected with either pathogenic or opportunistic bacteria. Up to half of COPD patients have been shown to be colonized with potentially pathogenic bacteria with studies finding different ranges of incidence from 25-50% depending on the bacteria and method of detection[81,82]. In this instance, colonization

refers to a bacterial species that is either present in higher quantities in disease state or undetectable during healthy conditions. The main pathogens that are found in COPD patients are *Non-typeable Haemophilus Influenzae* (NTHi), *Streptococcus pneumoniae, Moraxella catarrhalis,* and *Pseudomonas aeruginosa* with around 40% of bacterial infection associated with exacerbations[82]. Frequent exacerbators have been found to have a higher incidence of lower airway bacterial colonization compared with infrequent exacerbators which further strengthens the association of bacterial colonization and exacerbations[83]. Bacterial colonization in the airways was also strongly associated to inflammation and smoking in COPD particularly with NTHi with elevated levels of sputum CXCL8 and IL-1β along with serum CRP[84,85].

The microbiome in the lungs of COPD patients are also altered between stable state and exacerbations. A longtitudinal study on 87 COPD patients where 476 sputum samples underwent 16S rRNA sequencing showed that exacerbating patients have increased levels of Proteobacteria from *Moraxella* and *Haemophilus* species. There was also a decrease in Firmicutes bacterial species that *Streptococcus* species belong to compared to bacteria at stable disease state[86]. These changes during exacerbations are diminished post treatment and during recovery with a reversion back to the microbiome in stable disease states[86]. The same study by Wang et.al then attempted to stratify between different COPD phenotypes during exacerbations. The biggest difference was found between the eosinophilic COPD exacerbations group and the bacterial COPD exacerbations group which are usually associated with a neutrophilic phenotype. Bacterial exacerbations had significantly less bacterial diversity than eosinophilic exacerbations and particular decrease in Firmicutes and increase in Proteobacteria corresponding to a decrease in *Streptococcus* species and increase in *Haemophilus* species respectively[86]. A study by Singh et. al of 168 COPD

patients showed that COPD patients with high sputum eosinophils of more than 3% sputum eosinophils had significantly less potentially pathogenic microorganisms compared to non-eosinophilic patients at less than 3% eosinophils in the sputum[87]. Patients with potentially pathogenic microorganisms also had a significant decrease in blood eosinophils post-exacerbation[87].

A longtitudinal study by Mahew et.al on 101 COPD patients with 584 sputum samples having 16S rRNA sequenced concurred the previous findings that proteobacteria abundance increased while Firmicutes abundance decreased with a significant increase in *Moraxella* species abundance in the sputum during exacerbations[88].The study also assessed whether the lung microbiome was altered with increasing severity of COPD. Increasing severity of COPD corresponded with a significant decrease in the abundance of Firmicutes and Bacteroidetes and a significant increase in Proteobacteria[88]. On a genus level, there was a significant increase in *Haemophilus* species and significant decrease in *Veillonella* species with increasing severity of COPD[88].

P. aeruginosa is another opportunistic pathogen that is found during exacerbations. A study found that approximately 13% of patients were found to have *P. aeruginosa* during exacerbations and two-thirds of detected *P. aeruginosa* were antibiotic resistant with *P. aeruginosa* having more frequent hospitalized exacerbations[89]. Patients can be given either corticosteroids or broad-spectrum antibiotics during exacerbations. Antibiotics can select for antibiotic resistant bacteria which can explain while there were more *P. aeruginosa* that were antibiotic resistant. Corticosteroids are used to treat COPD but are also broad acting immunosuppressive drugs that can facilitate the bacterial colonization. For example, a study found that systemic corticosteroid use was found to be a risk factor for *P. aeruginosa* colonization[90].

1.4.2 Viral Infections in Exacerbations

Viral infections have also been found to be associated with the occurrence of acute exacerbations in COPD. The viruses that are most strongly associated with acute exacerbations are human Rhinovirus (RV), Influenza, and Respiratory Syncytial Virus (RSV)[91]. RV can cause the common cold and are usually mild infections but are particularly problematic as there are over 99 serotypes in humans alone making vaccine development and detection difficult. Thus, in general, qPCR is used rather than serology to detect these viruses in the lungs. In one study on exacerbating COPD patients, respiratory viruses were detected in 39.2% of exacerbating patients[92]. RV was detected in over half of virus associated exacerbations with a smaller minority being caused by RSV, Influenza, or Coronaviruses[92]. In a study by Dimopoulos et.al, 53.5% of patients presenting with exacerbations had detectable virus in the lung with a third having more than one virus through microarray-based viral testing with 200 patients analyzed[93]. In the same study, RSV and Influenza were the most commonly found viruses followed by RV[93]. In 13.1% of patient where viruses were detected, bacterial colonizations were detected simultaneously specifically with the species *Pseudomonas aeruginosa* and NTHi [93]. COPD patients had significantly higher amounts of RV during exacerbations than stable state and were associated to them having increased frequencies of exacerbations thereafter[94]. Similar findings were shown by Kherad et. al where there were viruses detectable in 51% of nasopharyngeal swabs in 86 exacerbating COPD patients with 14 respiratory viruses measured by qPCR[91]. Viral amounts were also diminished following recovery from exacerbations treatment at only 11% of patients having a respiratory virus detectable[91]. The varying proportion of viral detection between the different studies can be due to various factors. Studies have used different cohorts and viral detection may be different

depending on if the sample is taken from sputum, BAL, or nasal swabs. In additional different reagent, kits, and primers for qPCR detection will create differences in detection. Despite that, it is clear that there is a strong association between respiratory viral infection and exacerbations in COPD.

While studies establish a strong association between respiratory viral infections and COPD exacerbations, it does not imply a causal relationship. Mallia et. al established an experimental human model of RV infection in COPD patients by using unobstructed controls as a comparison and infecting COPD patients with RV16 and measuring symptom scores on several days post-infection[95]. RV infected COPD patients had greater leukocyte infiltration and inflammation as well as viral load indicating successful infection[96]. More importantly, RV infection induced significantly more severe symptoms, inflammation, viral load, and airflow obstruction after infection in patients with COPD compared to healthy controls suggesting that RV infection was able to induce exacerbations in COPD patients[96]. This strongly indicates that viral infections can induce exacerbations in COPD. However, more functional and molecular studies are needed to see what facilitates viral replication and whether RV is more successful in replication in the epithelium in COPD.

The incidence of viral associated exacerbations could also be made worse by ICS treatment. Singanayagam et. al found that treatment of bronchial epithelial cells with ICS supressed innate and acquired anti-viral immunity in response to RV infection and significantly delayed RV clearance in the cells[97]. Type I IFNs as well as Interferon stimulated genes (ISGs) were significantly downregulated in COPD primary epithelial cells when treated with corticosteroids during RV infections which indicate that corticosteroids affect early anti-viral signalling as these effects were mitigated with IFN treatment. ICS treatments also enhanced mucus production and exogenous treatment

with Type I IFNs reversed all the negative effects[97]. ICS use was also significantly associated with an increase in secondary bacterial infections post exacerbation, which will be discussed in more detail in the following section[97].

1.4.3 Secondary infections and co-infections in COPD

Both viral and bacterial infections have been strongly associated with being a risk factor for exacerbations. However, this does not indicate that the relationship between bacterial and viral infections in COPD are independent in inducing exacerbations. COPD patients have been found to be chronically colonized with potentially pathogenic bacteria even during stable state and thus there must be factors that sway the response from stable state to the induction of exacerbations and increasing bacterial infections. There have been several studies that demonstrate that respiratory viral infections can facilitate a subsequent bacterial infection. Studies have previously shown that people infected with RV or Influenza A virus were significantly more likely to be subsequently infected with *S. pneumoniae* with an increased chance for bacterial biofilm formation[98,99]. Mice infected with IAV were found to have a higher bacterial load and invasion of *S. pneumoniae* 6-weeks post infection leading to significantly greater morbidity[98].

COPD patients admitted to a hospital had a significantly higher probability to be readmitted within 60 days if both bacterial and viral infection were detected in a patient than either a bacterial or viral infection individually[100]. Exacerbations where both RV and NTHi were detected also had a significantly higher bacterial load and serum IL-6[101].

Mallia et. al demonstrated that when COPD patients were infected with RV, bacterial load increased after viral infection in the sputum in comparison to smokers and healthy

controls when measured by colony counting on agar. This occurred even though COPD patients had the same bacterial load before infection which reverted back to basal levels after 3 weeks[102]. Incidentally, 3 weeks is also when viral load was cleared in the sputum. Subjects that were positive with potentially pathogenic microorganisms beforehand also had a greater increase of inflammatory cells and neutrophil infiltration after RV inoculation compared to COPD patients that were negative for potential pathogenic microorganisms[102]. Almost all COPD subjects however seemed to have worsening symptoms and airway obstruction indicating that all COPD subjects exacerbated regardless. There was also a significant induction of the antimicrobial peptides (AMPs) pentraxin 3 (PTX3) and α-defensin in COPD patients compared to smokers and healthy controls following RV inoculation[102]. However, human β-defensin-2 (HBD-2) was not induced in COPD patients while it was significantly higher in healthy controls following RV infection.

In a study by Molyneaux et. al where 14 COPD patients and 17 healthy control subjects had lung microbiome analysis after RV inoculation, 16S rRNA increased in sputum of COPD subjects compared to healthy controls on day 15 with no differences at baseline[103]. Proteobacteria were significantly increased and firmicutes decreased in COPD patients in response to RV infection on day 15[103]. In contrast, healthy controls had no significant microbiome changes through the course of infection.

1.5 Immunology of COPD and response to Infections

The immune response in COPD is one of the main effectors in the pathogenesis of the disease. Both the innate and adaptive immune response have been shown to play a role in either the chronic inflammatory or the emphysema aspect of the disease and their functional changes are summarized in **Figure 1.2**. Lymphocytes, neutrophils,

eosinophils, macrophages, mast cells, and DCs are all found to accumulate in the lungs in COPD patients. Granulocytes such as neutrophils and eosinophils are especially implicated in the disease and are even used to phenotypically stratify COPD patients based on eosinophil or neutrophil numbers in the lungs.

1.5.1 Innate Immunity

Inhaled irritants such as tobacco smoke are able to inhibit pattern recognition receptors (PRRs) such as toll-like receptors (TLRs) on innate immune cells leading to pro-inflammatory cytokine expression[104]. Cigarette smoke extract (CSE) has been shown to inhibit the expression of pro-inflammatory cytokines such as TNF-α, IL-6, and IL-1β through TLR4 in alveolar macrophages upon stimulation with either LPS or NTHi[104,105]. In fact, both TLR2 and TLR4 have been found to be downregulated on alveolar macrophages in smokers and COPD patients. Interestingly, while the classical pro-inflammatory cytokines and the master pro-inflammatory transcription factor NFκB are inhibited upon CSE exposure, CXCL8 is upregulated in alveolar macrophages upon CSE and LPS stimulation which leads to attracting more neutrophils into the lungs[104,105]. These data was recapitulated in COPD finding that CXCL8 is significantly upregulated in BAL compared to non-smokers and ex-smokers[106].

Macrophages

Macrophages are innate immune cells that are either derived from the yolk sac during embryogenesis or can be differentiated from blood circulating monocytes. Macrophages from COPD patients have been shown to be defective in phagocytosis which as an important mechanism for clearance of pathogens or cellular debris. Macrophages from COPD patients have been found to be able to phagocytose less

NTHi and *S.pneumoniae* compare to macrophages derived from healthy controls[107]. Hodge et. al showed that alveolar macrophages from BAL of COPD patients have a reduced ability to phagocytose UV induced apoptotic epithelial cells compared to healthy controls but not with polystyrene beads indicating that the defect is in a phagocytic receptor or substrate[108]. The study use an epithelial cell line however and not primary epithelial cells which may act differently. Usually macrophages and DCs are responsible for clearing out dead cells through phagocytosis. However, in COPD macrophage phagocytic ability is impaired and neutrophils have increased lung infiltration due to increased CXCL8 in the lung microenvironment.

Neutrophils

Neutrophils are granulocytes and are the first responders into the tissue during an infection. Neutrophils have a relatively shorter lifespan compared to macrophages and thus die shortly after reaching infected tissue. An increase in necrotic neutrophils and their granules in COPD may lead to increased inflammation creating a chronic inflammatory cycle. In addition, neutrophils in COPD patients migrate quicker towards chemotactic stimuli like CXCL8 however their accuracy towards the stimuli is impaired indicating that the site of inflammation is stochastic and undirected like a bull in a China shop[109].

The CXCL8 receptor CXCR2 is unchanged between COPD neutrophils and the neutrophils of healthy controls but are upregulated during COPD exacerbations[109,110]. Neutrophil Elastase (NE) is a protease that is released by neutrophils that is able to degrade most components of the extracellular matrix when released and can even damage host cells like epithelial cells and induce mucus hypersecretion[111]. NE has been shown to be increased in the BAL, sputum, and neutrophils themselves in COPD compared to healthy controls and increasing levels have been proposed to be

associated with exacerbation risk[112]. Recently, a study has shown that NE can become more potent by being released in neutrophil exosomes[113]. NE present in exosomes can avoid coming into contact with NE inhibitors such as α1-antitrypsin (α1-AT) and can directly bind and degrade the extracellular matrix[113]. These neutrophil derived exosomes have been found to be significantly higher in COPD patients than healthy controls[113].

Neutrophils can secrete their DNA, termed as Neutrophil extracellular traps (NETs), with granules and pro-inflammatory proteins such as NE associated with it to induce inflammation and trap potential pathogens. NET formation can be induced following the activation of CXCR2 by CXCL8 and can lead to cell death in the epithelium. Patients with COPD have a higher proportion of NET releasing neutrophils compared to neutrophils from healthy controls and is associated with disease severity. NETs have been found in a significantly larger amount of cases in the sputum of COPD patients than smokers or healthy controls with exacerbating COPD patients having greater amounts of NETs than stable COPD patients[114]. In addition, increasing frequency of NETs were found in the sputa of patients with higher severity of COPD[114]. Another study supported the aforementioned findings and also found that patients with higher NET formation had a diminished ability to phagocytose bacteria such as *P.aeruginosa* and *E. coli*[115].

Eosinophils

While neutrophils have been shown to play a prominent role in the pathogenesis of COPD, around a third of COPD patients are phenotypically eosinophilic and thus recently the role of the eosinophil in COPD pathogenesis has been brought into question. Eosinophils are another type of granulocyte that are far more sparsely found than neutrophils but are still associated with the host response against extracellular

infections and tissue repair. Eosinophils can also produce pro-inflammatory cytokines and degranulate albeit with a different granular protein content. Neutrophils are one of the first responders in the innate immune response and associated with Type 1 and Type 17 immune responses however, eosinophils are associated with Type 2 inflammation and cytokine secretion specifically IL-4, IL-5, and IL-13. Eosinophils are directed towards mucosal organs through the chemokine eotaxin-1, -2, and -3 as well as IL-5 which also plays a role in eosinophil survival and activation. In contrast to neutrophils in COPD, the role of eosinophils in COPD have not been studied as extensively except with its relation as a biomarker of exacerbation frequency and its association with the increased responsiveness to corticosteroids in eosinophilic patients[11].

NK Cells

NK cells are lymphoid cells that survey whether or not cells are infected with intracellular pathogens such as viruses by detecting irregular expression of MHC class I through their interactions with activating or inhibitory receptors on NK cells. If NK cells detect an infected cell, they can directly kill the cell through perforin or granzymes and can produce Type 1 cytokines such as IFN-γ. COPD patients had significantly greater quantities of NK cells in their peripheral blood than healthy non-smokers[116]. Circulating NK cells in COPD patients also produced significant less IFN-γ and had a higher expression of the inhibitory receptor CD158 than healthy non-smokers indicating that despite having greater quantities of NK cells, their function is impaired in COPD[116]. NK cells were also found to be in greater quantities in the airways of ex-smoking COPD patients compared to non-smokers and ex-smokers without COPD. A study showed that NK cells in the airways had significantly decreased receptor CD94 but greater amounts of granzymes and perforin proteins with increasing cytotoxic potential which

is contrary to the aforementioned study where there was greater amounts of the inhibitory receptor CD158[117].

Dendritic Cells

DCs are professional antigen presenting cells (APCs) that bridge the gap between the innate and adaptive immune system. The two main type of DCs are either myeloid DCs (mDCs) which are responsible for mediating classical immune responses and antigen presentation or plasmacytoid DCs (pDCs) which are antiviral and known to produce a large amount of Type I IFNs when activated. Both proportions of circulating mDCs and pDCs are significantly decreased in COPD patients compared with smokers and non-smokers[118]. However, in terms of absolute numbers, only pDCs are significantly decreased in COPD[118]. pDCs seemed to also have a greater activated phenotype in COPD with higher expression of activating co-stimulatory molecules such as CD40 and CD86 and a decrease in inhibitory molecules such as PD-L1[119,120]. In contrast to circulating DCs, the lungs seem to have an increased infiltration of DCs in COPD compared to smokers or healthy controls with numbers increasing with increasing severity of COPD[121]. The DC chemoattractant CCL20 also had significantly greater expression in the sputum and the airways in COPD compared to smokers without COPD and healthy controls[121]. This may indicate that blood DCs are reduced in COPD because they are being directed to the lungs in greater amounts to perform their effector functions.

Leukocyte Cell Type	Functional Change in COPD
Macrophages	Downregulation of TLR2 and TLR4
	Increased expression of CXCL8
	Decreased phagocytosis of NTHi and *S. pneumouniae*
	Decreased phagocytosis of apoptotic epithelial cells
	Increased macrophage infiltration in the lungs
Neutrophils	Increased infiltration in the lungs due to CXCL8
	Undirected migration despite increased infiltration
	Increase in CXCR2 during exacerbations
	Increase in NE by neutrophils including in sputum and BAL
	Increase in neutrophil exosome formation
	Increase in NET production with the increase proportional to severity of disease and during exacerbations
	Phagocytosis impaired in proportion to NET production increases
Eosinophils	Increased infiltration of eosinophils in the lungs
NK Cells	Greater amounts of NK cells in the blood and the airways
	Decreased IFN-γ production in the blood
	Higher expression of CD158 inhibitory receptor in the blood
	Greater production of perforins and granzymes in the airways
Dendritic Cells	Proportion of mDCs and pDCs significantly decreased in the blood
	Increase in co-stimulatory molecules CD40 and CD86
	Decrease in inhibitory molecule PD-L1
	Increased infiltration in the airways
T-cells	Increase of CD8+ Tc1 cells in blood and airways
	Decrease in proportion of Tc2 cells
	Increase of CCL3, the CD8+ chemoattraction, in the airways
	CD4+ Th17 cells increased in blood and lungs
	Upregulation of IL17A and IL-17F in the lungs
	Decrease in Tregs and FOXP3 expression
B-cells	Increased B-cell lung infiltration and associated with disease severity
	Upregulation of CXCL13 in the airways
	BAFF upregulated in the airways
	Increase in IgA production in the lungs
	IgA receptor downregulated in the epithelium

Table 1.1: Changes in the function of leukocytes in COPD

1.5.2 The adaptive immune response

The innate immune response is crucial in starting inflammatory processes even if it is aberrant and misdirected as seen in COPD. However, to help sustain chronic inflammation the role of the adaptive immune response is indispensable. Lymphocytes can not only infiltrate the lungs and mount an immune response themselves, but they can also direct the recruitment of more innate immune cells and sustain inflammation and mucus hypersecretion.

T-cells

T-cells are the main orchestrators of the adaptive immune response that develop in the thymus. They can be divided into two main types: CD4+ T-helper cells or CD8+ cytotoxic T-cells. In COPD, there are significantly higher numbers of infiltrating and circulating CD8+ Tc1 cells that mainly produce IFN-γ and IL-12p40[49]. The proportion of Tc2 cells are however decreased in stable COPD patients however this proportion could change if COPD patients were stratified into eosinophilic and non-eosinophilic endotypes[49]. Lungs of COPD patients also have the CD8+ chemokine CCL3 upregulated. Unlike macrophages, CD8+ T-cells upregulates TLRs and production of pro-inflammatory cytokines when exposed to cigarette smoke and in COPD patients[122].

The number of CD4+ Th17 cells are higher in the blood and lung tissues of COPD patients[44]. IL-17A and IL-17F are also upregulated in the lung biopsies of COPD patients which indicates that there is a Th17 or Tc17 response in the lungs which could contribute to the neutrophilic inflammation seen in the majority of COPD patients[123]. The number of the anti-inflammatory CD4+ T-cell subtype Tregs are markedly lower in COPD patients compared to healthy controls as well as the expression of the Treg

master transcription factor FOXP3[124]. The decrease in Treg could exacerbate inflammation in COPD and previous studies have shown that there is plasticity in CD4+ T-cell subtypes were Tregs can change into the Th17 subtype which is found to be upregulated in COPD.

NKT and iNKT cells are lymphocytes that can produce IFN-γ and IL-17. Both cell types have been found to be upregulated in the blood of COPD patients and exposure to cigarette smoke upregulates the production of IFN-γ and IL-17[125]

B-cells

B-cells are bone marrow derived lymphocytes that are part of the humoral antibody response against extracellular pathogens. They usually reside in the secondary lymphoid organs such as the lymph nodes and spleen and develop antigen dependent immune responses through T-cell and cytokine signalling. B-cells develop into either antibody secreting plasma cells or memory B-cells in the germinal centre. Similar to other leukocytes, higher infiltration of B-cells is found in COPD patients and is associated with disease severity[126]. CXCL13 is one of the main B-cell chemoattractant and is responsible for B-cell recruitment into the tissues as well as the formation of lymphoid follicles. In the lungs of COPD patients, CXCL13 is upregulated compared to healthy controls which could explain B-cell infiltration[127]. In addition to this, more lymphoid follicles are formed in the lungs of COPD patients[127]. BAFF is a protein that is responsible for the survival, maturation, and differentiation of B-cells. BAFF was found to be found in significantly higher amounts in the lungs of severe and very severe COPD patients which may help sustain inflammation in COPD[128].

B-cells' main function is to produce targeted Ig antibodies against microorganisms in different organs. IgA dimers are the most abundant and important antibody isotype

found in mucosal organs as they can translocate through mucosal barriers such as the epithelium to reach their microbial targets. Severe and very severe COPD patients have significantly higher levels of IgA in the lungs than healthy controls[128]. Airway epithelial cells from COPD patients were particularly potent in inducing IgA production in B-cells compared epithelial cells from healthy controls[128]. Despite the increased production of IgA in COPD the antibodies are still required to translocate across the epithelium to the lumen to target potentially pathogenic microorganisms. However, it has been found that in COPD the polymeric immunoglobulin receptor that is responsible for the translocation of IgA is downregulated which may lead to the accumulation of IgA in the lungs and their inability to reach their intended antigens[129]. In addition, what antigens the secreted IgAs target in the lung has not been well documented. There is evidence that COPD shares components with autoimmune diseases as autoimmune diseases also have chronic inflammation and the involvement of the adaptive immune response as seen in rheumatoid arthritis for example. Higher amounts of anti-tissue and anti-nuclear autoantibodies have also been detected in COPD patients compared to healthy controls[130]. All the changes that were elucidated for each type of leukocyte has been listed in **Table 1.1**.

The central site that is present during the chronic inflammatory cascade and is the first line of defense against noxious substances and pathogens is the epithelium which will be subsequently discussed in more detail along with its interplay with the immune system and role in COPD.

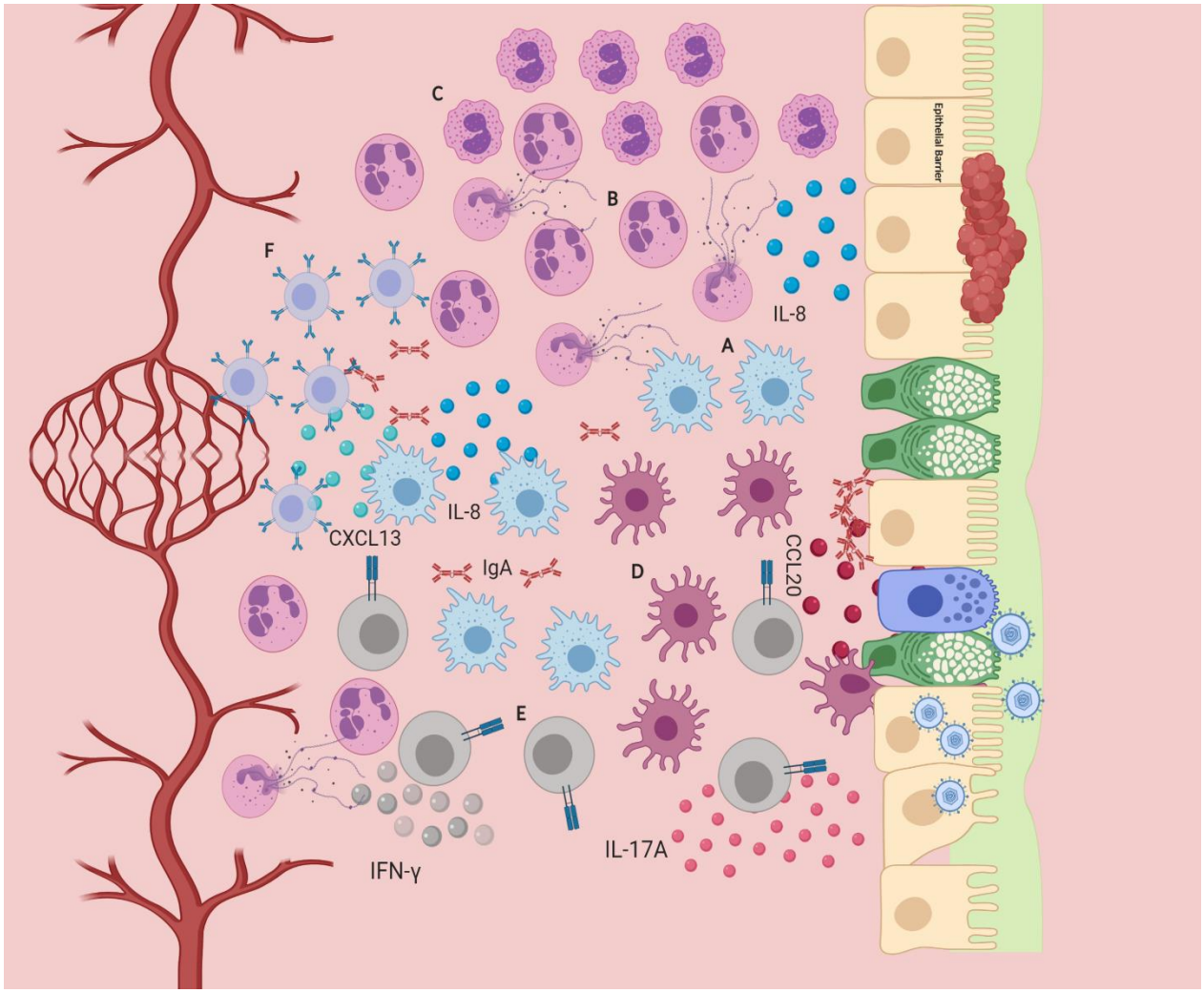


Figure 1.2: Immunological dysfunction and leukocyte infiltration in the lungs in COPD. ***(A)*** *Alveolar macrophages in COPD have a decreased ability for bacterial phagocytosis but produce higher levels of CXCL8 as well as lung epithelial cells.* ***(B)*** *Neutrophils or possibly* ***(C)*** *Eosinophils are then recruited to the lungs and degranulated which induces further inflammation and breakdown of the lung microenvironment.* ***(D)*** *Dendritic cells also infiltrate the lungs due to increase production of CCL20 from epithelial cells. Mucus production is increased possible due to the increased production of alarmins and TSLP.* ***(E)*** *T-cells and* ***(F)*** *B-cells are increased in COPD producing increased amounts of Type 1 and Type 17 cytokines as well as IgA antibodies that cannot translocate into the lumen to keep bacteria at bay.*

1.6 Lung Epithelial Cells in Health

1.6.1 The Lung Epithelium

Mucosal organs such as the lungs are exposed to the external environment, which ranges from pollutants and allergens to microorganisms such as bacteria or viruses

that may harm the body. However, the lung has developed several features and adaptations that separates and protects it from the external environment. In the lung, the epithelium is the first point of contact of exposure from the external environment. Epithelial cells consist of both a structural and chemical barrier in the lungs[131]. Structurally, they form tight junctions in between cells to block pathogens and irritants from invading the lungs. Junctional proteins include claudins, integrins, and zona-occludins[132,133]. Ciliated cells with cilia protrusions beat to remove any noxious substances or trapped pathogens out of the lungs. Basal cells are epithelial progenitor subtypes that are responsible for replenishing and maintaining the epithelial barrier.

Chemically, epithelial cells express mucin proteins such as MUC5AC and anti-microbial peptides (AMPs) to trap and remove microorganisms or keep them in steady numbers that do not cause pathogenesis under homeostatic conditions[131]. In addition, in recent years, the prominence of lung epithelial cells' bidirectional regulation of the immune system has been emerging. For example, pathogens that attempt to invade the lungs are sensed by epithelial cells which subsequently release pro-inflammatory cytokines and chemokines and once leukocytes are recruited into the lungs, they can induce the epithelium to secrete more AMPs and repair the damaged epithelial barrier. Following from that, the epithelium can ward off any potential pathogens which decreases any pro-inflammatory signalling and curtails the recruitment of leukocytes into the lungs.

Mucins are a class of glycoproteins that are mainly produced by epithelial cells. They are usually heavily glycosylated and are divided into two types of mucins: those that are tethered or secreted. Membrane-tethered mucins include MUC1 and MUC4[134]. The major secreted mucins are MUC5AC and MUC5B[134]. While MUC5B is constitutively expressed, MUC5AC is produced under inflammatory conditions. Both

tethered and secreted mucins can be protective against pathogens and irritants, however, secreted mucins are particularly important for mucocilliary clearance[135]. Mucins can also indirectly regulate the immune system by keeping potential pathogens and pro-inflammatory substance at bay. Notably, *muc5b* gene deficient mice have lung pathologies such as chronic inflammations as well as chronic bacterial infections[136]. This is most likely due to pathogens having increased contact with the pattern PRRs on epithelial cells, which heightens inflammation and signalling to other leukocytes such as neutrophils. FOXA3 is a prominent transcription factor in the epithelium that is responsible for the increase of goblet cell metaplasia and mucus production while also inhibiting the anti-viral IFN response[51].

In terms of the structure of the airways and epithelial cell subtypes in the lungs, the upper airways differ from the lower airways and finally the alveoli. In the upper airways, the epithelium is dominated by ciliated cells in order to remove and prevent from entry and potential pathogens or noxious particles. In the lower airways however, there is an increase in club cells as well as the increasing prevalence of goblet cells[137]. Club cells are responsible for the secretion of proteins such as AMPs, cytokines, and chemokines in order to help the epithelium maintain homeostasis. Basal cells are also in the epithelium and are progenitors for the different epithelial subtypes and can be used to replenish them post-infection. Finally, the alveoli have a different epithelial composition than the rest of the airways and mainly contain alveolar type I and alveolar type II cells[138].

1.6.2 Epithelial defence against bacteria

The lung epithelium's ability to induce the production of pro-inflammatory cytokines is blunted despite its ability to express several PRRs. While epithelial cells express the

prominent bacterial PRRs TLR4 and TLR2, they have lower expression of the co-receptors CD14 and CD36 respectively which would normally help induce pro-inflammatory signalling through the NFκB or TRIF pathways. PRRs such as TLR4 are also spatially concentrated intracellularly or on the basolateral side of the epithelium which is inaccessible to the outside environment further shielding it from an inflammatory environment[139]. Instead, the epithelium mainly relies on keeping bacteria under steady levels through the release of AMPs and mucosal immune surveillance by other leukocytes.

AMPs are divided into defensins and cathelicidins that are a host-response to potentially harmful microorganisms. Their effects are pleiotropic, and they are regulated by several mechanisms depending on the context and environment[140]. β-defensins are cationic peptides that can neutralize and disrupt the negatively charged surfaces of bacteria, promoting clearance, phagocytosis, and protecting from invasion[140]. Moreover, β-defensins can activate APCs by upregulating CD80 and CD86 or induce the production of proinflammatory cytokines such as IL-6[141,142]. LL-37, the only member of the cathelicidin family, can enhance the phagocytosis of bacteria by upregulation of integrins and FcRs as well as having immunomodulatory properties such as decreasing the production of proinflammatory cytokines while increasing the production of anti-inflammatory cytokines[143,144]. Therefore, it seems that the default state of the lung epithelium is tolerogenic. Only once a certain threshold is passed in terms of levels of bacterial stimulation and epithelial invasion does the lung epithelium mount a stronger immune response and signal the recruitment and activation of the rest of the immune system.

Epithelial cells can also regulate the immune system by the production of cytokines, chemokines, and triggering a differential adaptive immune response depending on the

inflammatory response. For example, epithelial cells can produce CXCL8 and CCL20, which are important cytokines for the recruitment of neutrophils and dendritic cells respectively[121,145]. Necrotic epithelial cells can release alarmins such as IL-25, IL-33, and TSLP to induce production of type 2 cytokines by eosinophils or type 2 innate lymphoid cells (ILC2s) and Th2/Tc2 cells[146].

Conversely, leukocytes can regulate epithelial cells in response to pathogens or pollutants such as cigarette smoke. Th17 cells producing IL-17 can induce the production of CXCL8 in epithelial cells[147]. Type 2 cytokines such as IL-5 can activate and recruit eosinophils and aid in the production of IgA[148]. IL-13 induces the production of mucins such MUC5AC and goblet cell differentiation in epithelial cells to help bacterial and viral clearance[149]. IFN-γ can induce the production of nitric oxide (NO) which can be toxic for any intracellular respiratory pathogens that have infected the epithelial cells with IL-22 increasing the production of AMPs[150,151].

1.6.3 Anti-viral Response in Lung Epithelial Cells

Unlike bacterial sensors in the epithelium, viral sensors in the epithelium such as TLR3 are responsive to viral and poly I:C which is a viral analogue that functions as an agonist for TLR3. Other types of viral PRRs such as RIG-I and MDA-5 are also expressed intracellularly[152]. Epithelial cells infected with virus can produce an anti-viral response through Type I and Type III interferon production which mainly bind to the IFNAR1 and IL-29R respectively then subsequently signal through the JAK/STAT pathway. The transcription of Interferon Stimulated genes (ISGs) are then induced by the transcription factors STAT1 and STAT2. ISGs have a myriad of functions that can inhibit viral replication if the virus has no efficient mechanisms to evade them[152]. More

virulent viruses such as influenza can induce higher amounts of pro-inflammatory cytokines and chemokines and inducing leukocyte infiltration.

Viruses such as influenza can induce epithelial cell death through cell lysis or apoptosis through Type I IFN signalling. RV can be detected by TLR2 on the extracellular of the epithelium and then recognized by TLR3, 7, and 9 once the virus starts replicating and shedding intracellularly[153]. RV can induce the production of the cytokines G-CSF and GM-CSF in bronchial epithelial cell lines or lavage fluid which helps recruit neutrophils to the site of infection to combat the virus[154,155]. CXCL8, CCL5, and CXCL10 can be secreted by epithelial cells which can recruit and activate granulocytes[156].

Effectively, the epithelium acts as a first line of defence against viruses and signals and recruits innate immune cells which can subsequently activate a more targeted adaptive immune response through IgA and IgG production or Tc1 cell activation and recruitment.

1.7 Lung Epithelial Cell Dysfunction in COPD

1.7.1 The Epithelium in COPD

COPD can lead to various pathologies in the epithelium such as a chronic inflammatory environment and the thickening of a fibrotic lung epithelium. However, despite having a thicker epithelium partly due to hyper- and metaplastic mucosal epithelial cells, epithelial cells in COPD have a higher rate of apoptosis and senescence as well which may be due to chronic inflammation and excessive ROS formation[157,158,39]. Cigarette smoke induces the production of ROS, which are then scavenged by the induction of the antioxidant response through the nuclear factor erythroid 2-related factor 2 (Nrf2) transcription factor[39]. COPD patients have been

shown to have a decreased expression of Nrf2 with an inferior ability to scavenge ROS, leaving them to damage DNA and harm cells[39]. Heme oxygenase 1, which is a gene induced by Nrf2, is a scavenger of ROS that is found to be upregulated in healthy smokers but not in COPD patients. Moreover, mucus hypersecretion has been shown in patients with COPD, either as a consequence of an increased proportion of mucus secreting goblet cells or an increased expression of the *muc* genes[50]. The transcription factor FOXA3 responsible for the differentiation of goblet cells has also been epigenetically hypermethylated in COPD to increase its expression[159]. COPD patients also have a significantly decreased count of basal cell progenitors in the lungs compared to non-COPD controls which are responsible for differentiating and renewing any required epithelial cell type such as ciliated cells for epithelial barrier protection[160]. Indeed, it has been shown that both smokers and COPD patients have a decrease of ciliated cells in the airways[161]. In addition, there are decreased proportion of club cells in smokers and COPD patients and an increase in the mucus secreting goblet cells which may be mediated by EGF[162].

Immunologically like alveolar macrophages in COPD, epithelial cells have a higher expression of CXCL8 in COPD, which is responsible for the chemotaxis of neutrophils[163] TLR4 expression data has been contradictory with one study showing an increase in TLR4 and another study demonstrating a decrease in TLR4 expression in COPD patients[164,165]. The expression of the DC chemoattractant CCL20 is increased by epithelial cells as well as DC infiltration in the lungs of patients with COPD[121]. IL-33, a prominent alarmin that is released after cell death, has been found to be highly secreted in the epithelial cells of COPD compared to healthy controls[166]. IL-33 normally induces the secretion of type 2 cytokines and has been shown to increase the expression of IL-13 on epithelial cells which in turn induces further mucus

secretion[167]. A study in mice has found that IL-33 can be upregulated then released in response to cigarette smoke followed by viral infection and its respective receptor ST2 upregulated on NK cells and macrophages[168]. However, in order to mediate a COPD-like exacerbation in mice, both smoking and a viral infection were required. In addition, IL-33 seemed to induce a Th1 like response rather than the conventional Th2 response that is associated with IL-33 signalling[168]. TSLP, another important alarmin, is also induced upon viral stimulation in significantly greater quantities in the epithelial cells of COPD patients compared to healthy controls[169]. It has also been shown that IL-17A can trigger the production of TSLP in the epithelial cells of COPD patients through IKKα mediated signalling[170].

TNFα is one of the most prominent pro-inflammatory cytokines along with IL-6 and IL-1β through signalling of NFκB. In COPD, TNF-α is produced at significantly higher levels in sputum and BAL compared to healthy controls in multiple studies although it remains understudied in the epithelium in the context of an infection[171]. The colony stimulating factors such as G-CSF and GM-CSF also facilitate inflammation in the lungs. GM-CSF is an activator and recruiter of granulocytes including neutrophils and eosinophils as well as macrophages which may be of relevance in COPD where macrophages and granulocytes are recruited and are significantly higher. GM-CSF has been found to be significantly upregulated in the sputum of COPD patients compared with healthy non-smokers however it is not yet known whether epithelial cells can produce GM-CSF in the context of an infection in COPD[172].

COPD exacerbations are strongly linked to viral infections and thus it would be inductive to deduce that the anti-viral immunity in the lungs is deficient or dysfunctional which is what is observed in asthma for example. The innate anti-viral response in COPD has not been well characterized with some studies showing there is a decrease

in type I and type III IFNs as well as the PRR RIG-I and other studies showing an upregulation in type I and type III IFNs gene expression upon RV infection[173,174]. Baines et. al showed that RIG-I and MDA-5 gene expression are significantly upregulated in response to RV16 infection as well as IFN-β and IFN-λ1[173]. Interestingly, the study by Baines et. al showed that despite the greater increase in IFNs in COPD epithelial cells upon RV infection, viral load remained significantly greater than healthy bronchial epithelial cells[173]. In addition, COPD bronchial epithelial cells were significantly less responsive to treatment with IFN-β with significantly less upregulation of RIG-I and MDA-5 compared to healthy controls[173]. However, quantifying RIG-I and MDA-5 are not directly downstream to IFN signalling thus it would have been more relevant to measure differences in IFN receptors, STAT1/2, or ISGs in response to Type I IFN treatment or RV16 infection.

A small number of studies have investigated the role of AMPs in COPD but their role has yet to be fully elucidated[,175,176]. Human β-defensin-1 levels are elevated while human β-defensin-2 expression is reduced in patients with COPD[176,177]. A study has shown that the IL-22R, which is responsible for mediating IL-22 signalling and subsequent AMP production, is also cleaved due to neutrophil proteases and does not function to induce the secretion of AMPs in COPD[178].

It is clear that in health there is tight homeostatic regulation of epithelial host response to external stimuli such as smoke, pollutants, bacteria and viruses. In COPD patients however, there is a small number of studies that have specifically examined the epithelium and its response to infections. The data on whether there is a differential response in eosinophilic and infection-driven non-eosinophilic COPD has also been largely unexplored. Changes in the epithelium of COPD patients has hence been summarized in **Figure 1.3**.

1.7.2 Potential Therapeutics for the Epithelium in COPD

In recent years and with the increase in understanding of the pathogenesis of COPD, more targeted therapeutics such as monoclonal antibodies are being developed. However, despite those treatments, there has been a bigger focus on targeting the effector leukocytes such as eosinophils with no clinical trials to attempt to repair and maintain the epithelial barrier. The epithelium is the first line of defense of the lungs and the most upstream tissue responsible for protecting the structure and function of the lungs.

Treatments may target pathways that can induce repair of the epithelium, upregulate adhesion molecules, and reverse EMT may restore the protective function of the epithelium and may protect from potential infections and pro-inflammatory mediators. However, more studies are needed to further elucidate potential pathways in COPD. Such treatments may be combined with anti-inflammatory therapeutics such as macrolides or existing monoclonal in order to have a wider and more holistic effect in the treatment of COPD.

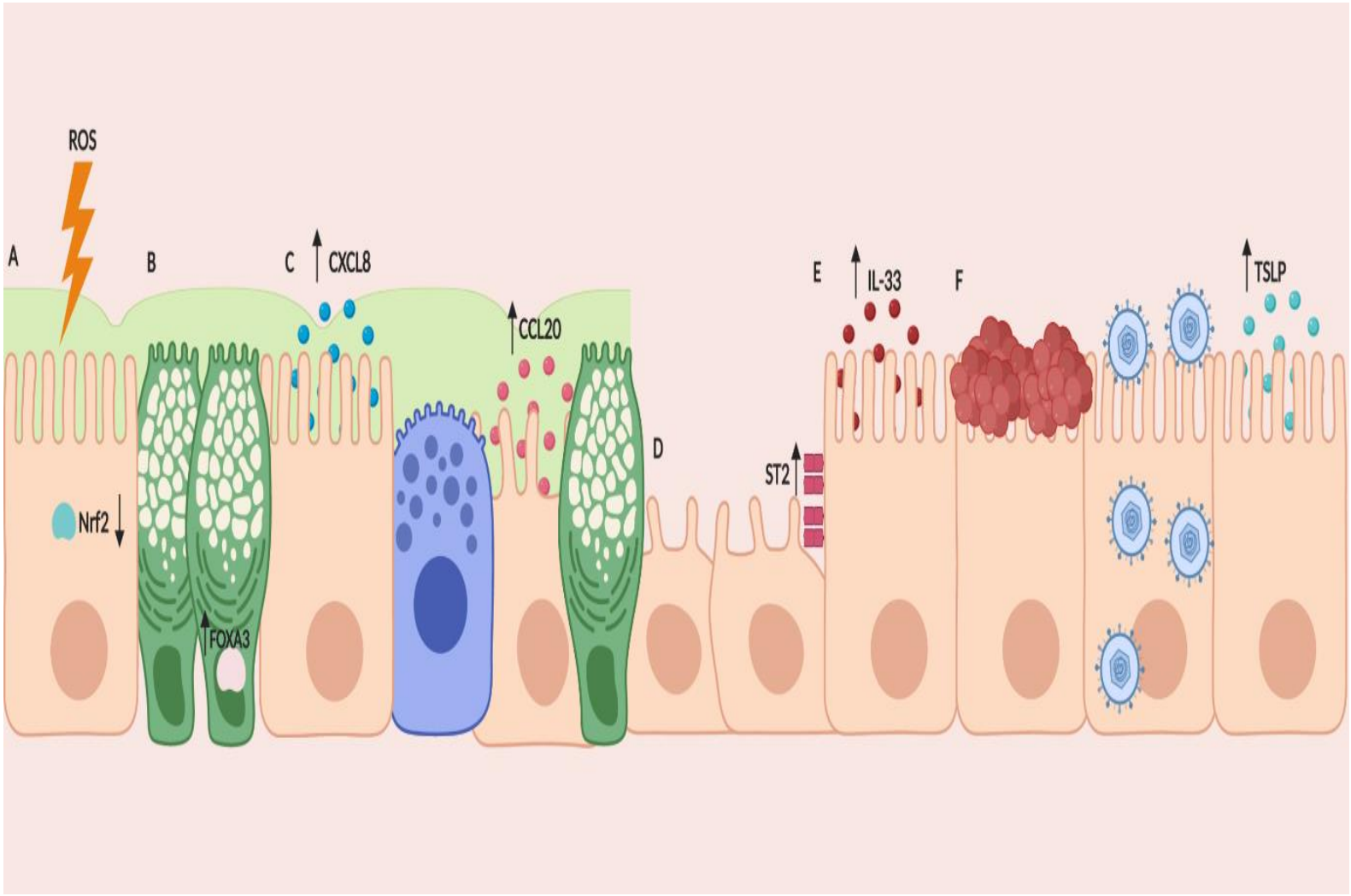


Figure 1.3: Changes in the epithelium in COPD from a healthy epithelium: *The lung epithelium is dysregulated in COPD **(A)** by being unable to scavenge ROS through the downregulation of the transcription factor Nrf2. **(B)** Upregulation in the transcription factor FOXA3 leads to goblet cell hyperplasia and increase of mucus production in the lungs. **(C)** Pro-inflammatory chemokines CXCL8 and CCL20 as well as monocyte chemokines are upregulated in COPD leading to increased neutrophil, macrophage, and DC recruitment. **(D)** Increase in epithelial cell apoptosis as well as an increase in **(E)** alarmins IL-33 and its receptor ST2. **(F)** Greater susceptibility to bacterial and viral infections such as from NTHi and RV with the literature on changes in AMP and IFN production and signalling still unclear with further elucidation required.*

1.8 Tight Junctions in Epithelial Cells in Health and COPD

The epithelial and endothelial barriers are important physical and chemical barriers to regulate the flow of nutrients and solutes as well as to protect the body from harmful toxins and pathogens. In the airways, the epithelium protects the body from harmful pathogens and noxious particles that are either resident or are inhaled. There are several types of adhesion molecules that controls the permeability of the epithelium and are tightly regulated in adapting to different contexts.

1.8.1 Junction proteins in the epithelium

The main junctional components in the epithelium are tight junctions (TJs) and adheren junctions (AJs)[179]. TJs are mainly composed of transmembrane proteins such as Claudins (CLDNs), Occludins (OCLNs) and junctional adhesion molecules (JAMs)[179]. Zona Occludins (ZO) are also part of the TJs that have been implicated some diseases recently such as cancers and IBD[180]. AJs are generally calcium dependent with E-cadherin playing a large role in maintaining epithelial integrity as well as the regulation of TJ formation[181].

1.8.2 Types of Tight Junction Molecules

There are over two dozen types of CLDNs in humans, composed of four transmembrane domains and two extracellular loops[182]. CLDNs regulate the extracellular fluid space between cells to regulate the flow of fluids such as water and ions like chloride through paracellular channels and regulating the permeability of the interstitial spaces[182]. CLDNs generally bind in a head to head manner either with the same CLDNs or in interactions with different TJ molecules such as ZO-1 or scaffolding proteins[183,184]. Phosphorylation of CLDNs at the C-terminal domain also plays a role in their organization and function[185]. However different phosphorylation events can

regulate CLDNs differently and are difficult to study thus, the mechanisms for CLDN regulation are not as well elucidated[185,186]. The most expressed CLDNs in alveolar cells are CLDN-3, -4, and 18[182]. However, being the most highly expressed does not mean that they are most import functionally, other modestly expressed TJs could have more prominent effects. CLDN-3 has been associated with increased permeability between alveolar junctions[187]. In contrast, CLDN-4 has been shown to have a functional role in fluid clearance in the alveolar spaces within the context of lung injuries[187,188]. CLDN-18 deficiency, a CLDN specific to the lungs, has also been shown to impair alveolar epithelial cell proliferation in mice[189,190].

CLDNs have not been as well studied in the upper airway compared to Occludins and ZO-1 but CLDNs-1, 3, 4, 7, 8, and 18 seem to be the most highly expressed CLDNs in the bronchioles[133]. The role TJ proteins in a healthy epithelium have been illustrated in **Figure 1.4**.

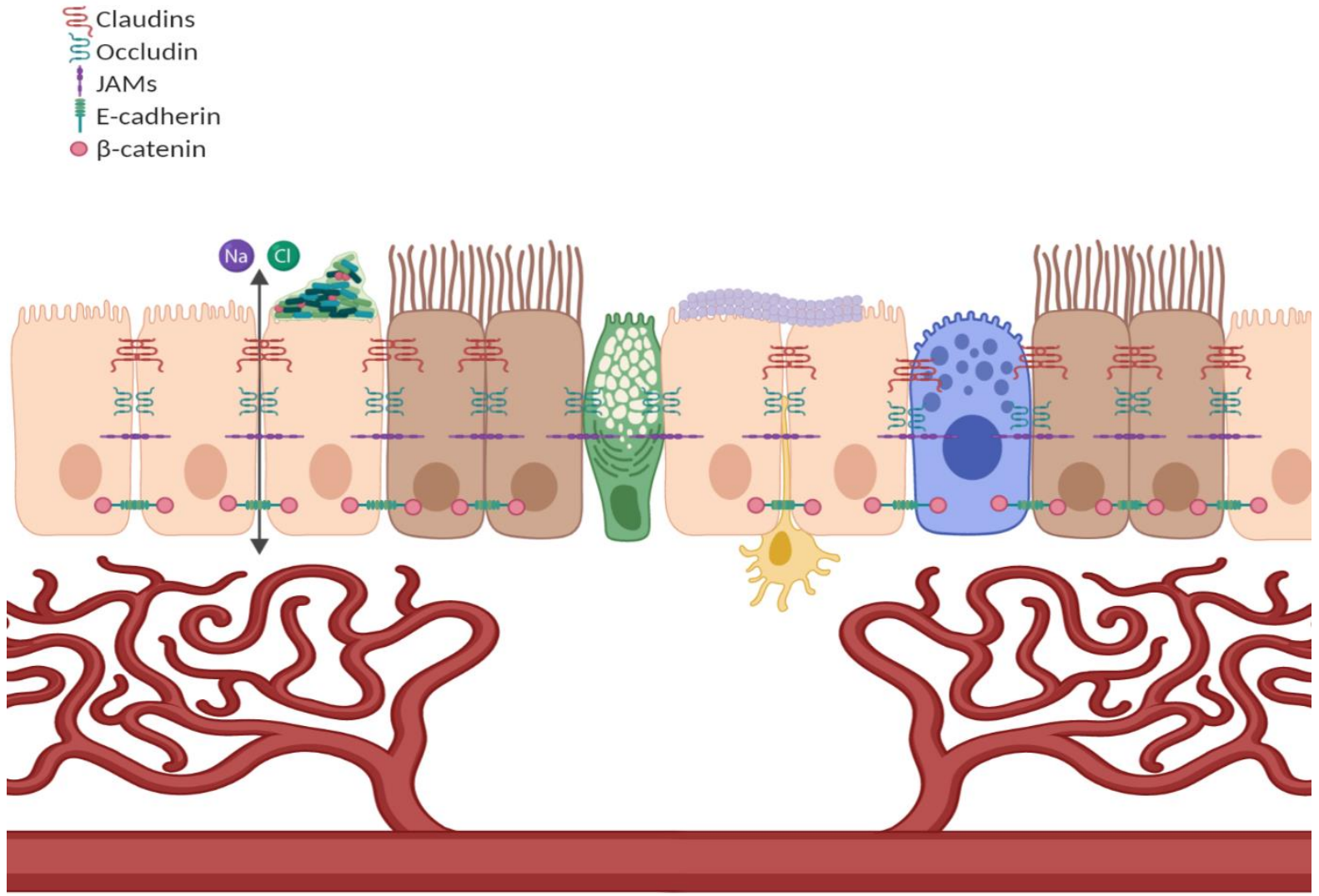


Figure 1.4: Epithelial junction in healthy lungs: *Barrier integrity in the lung is maintained by the tight regulation of TJ molecules such as Claudin, Occludin, and JAMs as well as the calcium dependent adheren junction molecule E-cadherin which also suppresses proliferation and regulates TJs. This also prevents pathogens from entering, and the microbiota is maintained at homeostatic numbers through anti-microbial peptides and immune surveillance. Paracellular permeability for ion and water exchange is regulated through Claudin forming channels.*

1.8.3 Tight Junction dysfunction in asthma

There are some studies on the effect of tight junctions and barrier integrity in asthma. For example, it has been found that asthmatic children have a significant increase in CLDN-1 and Occludin mRNA level compared to healthy epithelial cells[191]. However, when assessed at the protein levels, both CLDN-1 and Occludin are decreased in asthmatics indicating there are irregularities at the translational or assembly level in the asthmatic epithelium[191]. Asthmatics infected with RV-1B also had significantly decreased levels of CLDN-1, Occludin, and ZO-1 mRNA expression and while they were significantly decreased in healthy HBECs as well after 24 h, expression in asthmatics continued to decrease after 48 hours while healthy HBECs recovered[191]. Immunostaining showed that E-cadherin is decreased in the bronchioles of the lungs of asthmatics and CLDN-18 is also decreased at the mRNA level in asthmatic epithelial cells[192,193]. These changes may be due to epithelial growth factor (EGF) as it has been shown that EGF, a growth factor that regulates adhesion molecules, causes abnormal tyrosine phosphorylation events in the epithelium of asthmatics[194].

1.8.4 COPD and Smoking

Unlike asthma, there have not been as many studies on either the phenotype of junctional proteins in COPD or the mechanism that dysregulates that phenotype. In one study examining levels of CLDN-5, there seemed to be a decrease in CLDN-5 in COPD patients at either stable state or exacerbation compared to healthy controls[195]. However, CLDN-5 was measured in the plasma which is not very physiologically relevant in studying barrier integrity and is predominantly expressed in endothelial cells rather than the epithelium[195]. While there needs to be more studies on the epithelial junction in COPD, there are studies done on the epithelium under smoking conditions.

ZO-1 expression is decreased in the airways and HBECs of smokers and COPD patients compared to healthy controls at a protein and gene expression level[196]. CSE treated HBECs also had significantly decreased levels of ZO-1 and ZO-2 protein and relative mRNA expression levels compared to untreated controls as well as a lower transepithelial resistance (TER) in differentiated cultures[197]. The HBECs were able to be rescued by treating the cells with increasing doses of TGF-β indicating that it has a role in maintaining junctional integrity[197]. Interestingly, it has been shown that hypoxia leads to a decrease of ZO-1 which is found in the bronchioles of COPD patients[198]. ICAM-1 is an adhesion molecule that facilitates the migration of leukocytes into the tissue. It is also a receptor that Rhinovirus and NTHi bind to and upregulate during infection or colonization[199,200]. Increased levels of ICAM-1 was found in the bronchioles of COPD patients and smokers compared to healthy controls[201].

Cigarette smoke is also able to induce the production of ROS which can activate the epithelial growth factor receptor (EGFR) leading to the downregulation of adhesion molecules[202]. ROS can also induce the dissociation of adhesion molecules and importantly, the dissociation of E-cadherin leads to the release of β-catenin which activates the expression of matrix metalloproteases (MMPs) and extracellular matrix proteins such as fibronectin[203]. In addition, β-catenin is localized to the nucleus and acts as a co-factor to the transcription factors WNT, SLUG, and SNAIL which activates the process of epithelial to mesenchymal transition (EMT) which further disrupts epithelial integrity[204]. EMT has been found to be significantly increased in HBECs of COPD patients compared to healthy controls indicating that the epithelium is compromised in COPD[205]. EMT phenotypically changes the epithelium to become more motile which compromises epithelial barrier integrity and can facilitate the invasion of pathogens such as respiratory viruses and colonizing opportunistic

bacteria which are strongly associated to COPD exacerbations. In addition, EMT facilitates extracellular matrix protein production which may lead to lung fibrosis. This may be a cyclical process since for example increased NE production in COPD can dissociate adhesion of E-cadherin leading to more EMT[206].

Cytokines such as IL-17A and IFN-γ can also regulate junctional proteins such as E-cadherin however, their role in regulating junctional integrity in either COPD or in smokers has yet to be directly studied[207,208]. Studies inhibiting TNF-α in an inflammatory lung mouse model have shown that tight junction integrity is increased after inhibition of TNF-α suggesting that inflammation decreases barrier integrity, most likely to facilitate the movement of immune cells through to fight potential pathogens[209].

Interestingly, mice that are deficient in the Vitamin D Receptor (VDR) have a decrease in several TJ molecules including ZO-1, Occludin, CLDN-18, and CLDN-4[210]. This is also of interest as VDR deficient mice have previously been shown to have a COPD/emphysema phenotype with significantly more pro-inflammatory cytokines indicating the importance of tight junctions in COPD[210,211]. Changes in the epithelial barrier and TJs of COPD and smokers have been summarized in **Figure 1.5**.

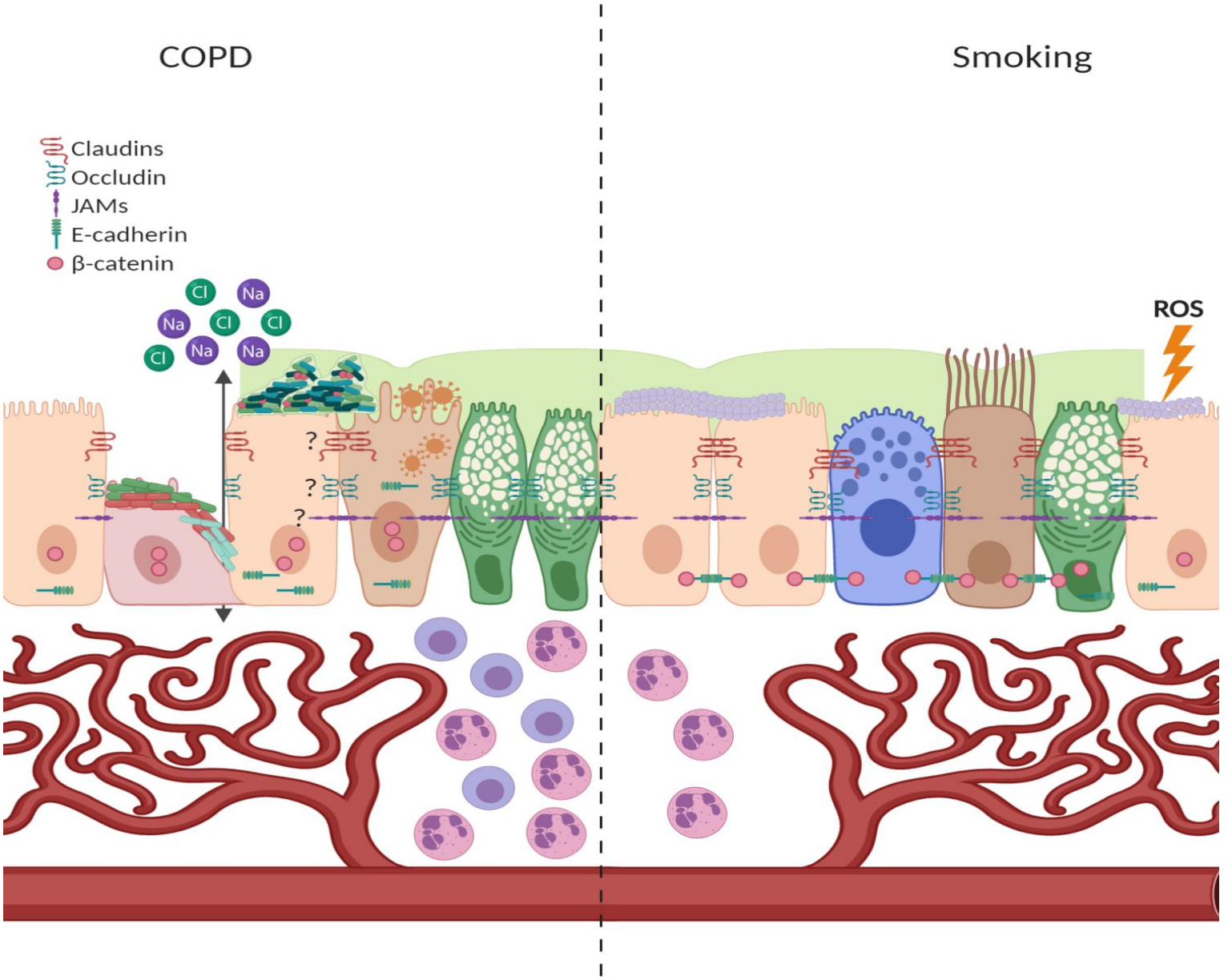


Figure 1.5: Epithelial barrier in the lungs of smokers and COPD patients. *COPD patients and smokers have an increase in EMT possible due to the dissociation of E-cadherin leading to the translocation of β-catenin into the nucleus beginning the process of EMT. E-cadherin can dissociate in smokers due to ROS production. Adhesion molecules such as ZO-1 and CLDNs are downregulated in both smokers and COPD patients. The increase in EMT and compromised epithelial barrier integrity can facilitate the invasion of pathogens into the lungs such as NTHi or respiratory viruses.*

1.8.5 Effects of pathogens on adhesion molecules in bronchial epithelium

There have been a few studies to assess the effect of RV and respiratory viral infections in general on tight junctions. HBECs infected with Influenza A virus and grown at ALI had a decrease in TER and while there was a decrease in the apical junction complex integrity, there were no significant decreases in any of the TJ molecules measured such as occludins, ZO-1, and CLDN-4[212]. In contrast, airway epithelial cells infected with Rhinovirus had decreased TER as well as decreases in the TJ molecules ZO-1, occluding, CLDN-1, and E-cadherin[213].

In mice infected with Respiratory Syncytial Virus, CLDN-1 and Occludin expression in the lungs are decreased after the first two days but recover to basal levels at day 4 onwards indicating a resolution in the infection[214].

While the effect of either bacterial or NTHi infections on the epithelial barrier in the lung have not been well studied, intestinal bacterial infections have been examined in greater detail. Mice infected with either NTHi or *Streptococcus pnemouniae* downregulate expression of CLDN-7 and CLDN-10 in the mouse lungs and have decreased TER[215]. This effect was recapitulated in human lung epithelial cells lines. Mice with TLR2 or TLR4 deficiency however do not exhibit these effects indicating that the downregulation of the TJ molecules are mediated by TLR2 and TLR4[215]. Interestingly, COPD patients and smokers have a downregulation of TLR4 compared to healthy controls in the lungs[165]. Infection of a highly virulent strain of *Haemophilus parasuis*, a closely related species to NTHi, on epithelial cells has shown that it can disrupt the key AJ protein E-cadherin[216]. E-cadherin then dissociates from β-catenin and activates the Wnt signalling pathway which is responsible for EMT[216]. This in turn facilitates the colonization of *H. parasuis* in the lungs.

1.9 Aims, Objectives, & Hypothesis

Objectives & Rationale

Viral and bacterial infections in COPD patients are strongly associated with chronic inflammation and the onset of exacerbation in COPD which indicates that there is a defect of the broader immune response in COPD. While there have been some studies with leukocyte responses to infections in COPD, the epithelial barrier's response to infections in COPD is far less studied. The epithelial immune response as well as changes in epithelial TJ proteins that are crucial to maintaining barrier integrity are particularly understudied and thus will be examined.

Hypothesis

I hypothesize that anti-viral and inflammatory responses following viral or bacterial infection will be either abrogated or dysfunctional in COPD HBECs with higher inflammation and alarmin production in response to infection. The epithelium TJs will be unresponsive during infection in COPD patients and have a weaker barrier and TJ expression under basal conditions and post-infection compared to healthy or smoker HBECs.

Aim 1: Elucidating differences between the epithelial immune and anti-viral response in response to NTHi and RV infections in healthy, smokers, and COPD epithelial cells

There have been studies to characterize some facets of the immune or anti-viral response in HBECs in COPD in response to RV infection or under stable state. However, the study findings have been mixed or mechanistically superficial ranging from no differences in IFN expression in response to RV between healthy and COPD HBECs to COPD patients having significantly higher expression of Type I and Type III

IFNs or TSLP when infected with RV or an analog. In addition, Type III IFNs are important responders to bacterial infections such as Shigella thus it would also be important to explore the expression of IFNs and their respective receptors under the context of an NTHi infection in COPD. There are also no studies as of yet to compare differences in the anti-viral response between the three pertinent groups of healthy, smokers, and COPD HBECs.

Objectives:

- Investigate the effects of infection with NTHi and RV in HBECs on alarmin and pro-inflammatory cytokine production or when stimulated with LPS or poly I:C
- Measure the concentrations of anti-viral proteins such as Type I and Type III IFNs when epithelial cells from all three groups are infected with NTHi or RV or stimulated with analogues
- Delineate the expression of Type I and Type III IFN receptors on HBECs between all three groups when infected with NTHi or RV as well as OAS1 expression

Aim 2: Investigate changes in tight junction proteins in the epithelium in COPD patients compared to smokers in healthy controls particularly under the context of NTHi or RV infection

Tight junction proteins are crucial to maintaining epithelial barrier integrity and prevent pathogen entry into the lungs. The expression and role of tight junctions has been largely unexplored in COPD particularly any changes in response to infection. Thus, this aim will explore any changes of TJ molecules in COPD patients compared to smoker or healthy HBECs in response to infection or stimulation.Objectives:

- Measure the TJ molecules CLDN-3, CLDN-4, and JAM-A in response to LPS or Poly I:C stimulation in HBECs from heathy, smokers, and COPD patients
- Measure the TJ molecules CLDN-3, CLDN-4, and JAM-A in response to NTHi or RV infection in HBECs
- Investigate spatial and colocalization changes in CLDN-3, CLDN-4, and JAM-A following stimulation with LPS or poly I:C as well as during infection with NTHi or RV in HBECs
- Quantify gene expression for tight junction genes CLDN-3, CLDN-4, JAM-A, Occludin, and ZO-1 after NTHi or RV infection in HBECs

Aim 3: Perform RNA-seq to analyze differential gene expression on HBECs from healthy, smokers, and COPD patients under NTHi and RV infection

RNA-seq experiments are particularly useful to analyze differentially expressed genes between different groups and conditions. Unlike asthma, the gene expression of the epithelium in COPD has not been subject to RNA-seq analysis compared to smokers and healthy controls under the context of infection. Thus, finding differentially expressed genes between healthy, smokers, and COPD patients would be crucial to elucidate any aberrant expression of prominent genes particularly under the context of infection of NTHi or RV.

Objectives:

- Explore any genes with the greatest expression differences in healthy, smokers, and COPD HBECs with or without NTHi and RV infection
- Investigate if differential gene expression (DGE) is different in HBECs when cultured at a monolayer or at ALI

- Assess for differential expression between healthy, smokers, and COPD HBECs in the anti-viral response during NTHi and RV infection with a particular focus on signalling and interferon stimulated genes
- Analyze for any differentially expressed TJ molecules between healthy, smokers, and COPD HBECs during RV and NTHi infection such as CLDNs and JAM molecules and under basal conditions

Chapter 2: Materials & Methods

Materials

Reagent	Manufacturer
Phosphate Buffer Saline	Sigma-Aldrich Life Science
PureCol	Advance Biomatrix Science
Lipopolysaccharide from *E.coli O111:B4*	Sigma-Aldrich Life Science
Poly I:C	Sigma-Aldrich Life Science
RV16	ATCC
Dulbecco's Modified Eagle's Medium (DMEM)	Sigma-Aldrich Life Science
L-Glutamine	Sigma-Aldrich Life Sciences
Non-Essential Amino Acids Solution (NEAA)	Gibco
Epithelial Growth Medium	PromoCell
Epithelial Growth Medium Supplements	PromoCell
Anti-Trypsin Inhibitor	Roche Life Sciences
Gentamicin-Sulfate Amphotericin (GA-1000)	Lonza
Penicillin-Steptomycin	Sigma-Aldrich Life Science
Dimethyl Sulfoxide (DMSO)	Sigma-Aldrich Life Science
Human JAM-A Antibody	R&D Systems
Human Claudin-4 Antibody	Abcam
Human Claudin-3 Antibody	R&D Systems
Trypsin-EDTA	Sigma Life Science
IFNλ1/3 ELISA Duoset	R&D Systems
IFNβ1 ELISA Duoset	R&D Systems
GM-CSF ELISA Duoset	R&D Systems
IFN-β ELISA Quantikine Kit	R&D Systems
Multiplex Analyte Plates	Meso Scale Discovery
Mammalian Protein Extraction Lysis Buffer	ThermoFisher Scientific
Human IFNAR1 Antibody	R&D Systems
Human IL-29R Antibody	R&D Systems
Human Pancytokeratin Antibody	Abcam
Human EpCAM Antibody	BD Biosciences
Bovine Serum Albumin	Sigma-Aldrich Life Sciences
Anti-fade Mounting Medium with DAPI	Vector Laboratories
Anti-Mouse IgG NL493	R&D
Anti-Goat IgG NL637	R&D
Anti-Rabbit IgG NL557	R&D

Tween-20	Sigma-Aldrich Life Science
Tritonx100	Acros Organics
4% Paraformaldehyde	Sigma-Aldrich Life Science
Phosphate Buffer Saline	Sigma-Aldrich Life Science
Brain Heart Infusion Media	Sigma-Aldrich Life Science
Hemin	Merck
NAD	MP Biomedicals
Reitnoic Acid 50 mg	Sigma-Aldrich Life Science
24-well Plate Transwells	Greiner
Live/Dead Zombie Aqua	Biolegend
EVOM2/3 Machine	World Precision Instruments (WPI)
QIAshredder	QIAGEN
RNeasy Plus Micro Kit	QIAGEN
RNAlater	In Vitrogen
RNase Zap	In Vitrogen
High Capacity cDNA Reverse Transcription Kit	ThermoFisher Scientific
Fast SYBR Green Master Mix	Applied Biosystems
Nunc Lab Tek II Chamber Slides	ThermoFisher
NEBNext Ultra II Directional RNA Library Prep Kit	New England Biosciences

Methods

2.1 Ethics

Ethical approval was obtained for the recruitment of a patient cohort under the guidelines of the Airway Epithelium Study (AES) to investigate immune pathways in epithelial cells in airway diseases and approved by the Oxford B Research Ethics Committee (REC No.18/SC/0068).

2.2 Patient cohort and cell acquisition

Patients with airways disease undergoing bronchoscopy or lung resection as part of their medical care, were invited to consent to donation of samples. All suitable patients were identified by the clinical team, who explained to them the nature of the research objectives and provide a participant information sheet at the first clinic attendance. Eligibility was confirmed by the clinical team, and the research team obtained consent. Brushes were obtained from the airways during the bronchoscopy for healthy and COPD donors.

Smoker donors' epithelial cells as well as some COPD and healthy HBECs were bought in and obtained from Lonza to supplement the sample number of clinically acquired HBECs. Demographics of samples utilized are outlined in **Table 2.1.**

	Healthy	**Smokers**	**COPD**
Number of Patients	4	7	7
Sex (M/F)	2/2	5/2	5/2
Average Age (SD)	52 (17.5)	56.7 (13.5)	68.7 (10.1)
Smoker Status (Non/Current/Ex)	4/0/0	0/7/0	0/3/4

Table 2.1: Demographics of HBEC donors utilized in the study.

2.3 Processing and Culturing of human bronchial epithelial cells on a monolayer

Epithelial cells brushings that were obtained from bronchoscopies were inserted into 3 ml of EGM supplemented media (Promocell) with the antibiotics 1% pencilin-streptomycin (Sigma-Aldrich Life Science) and 1:1000 GA-1000 (Lonza) per brush. Supplement EGM media contained 0.004 mg/ml of Bovine Pituitary Extract, 10 ng/ml of EGF, 5 µg/ml of insulin, 0.5 µg/ml of hydrocortisone, 0.5 µg/ml of epinephrine, 6.7 ng/ml of Triiodo-L-thyronine, 10 µg/ml of transferrin, and 0.1 ng/ml of retinoic acid. In a Level II Biological Safety Cabinet (BSII), the brushings were then inserted into a Pasteur pipette and supplemented EGM media was absorbed and blown out in order to detach cells from the brushes into the media. After the brushes have been cleared of cells, the cell filled media is transferred into a T12.5 flask coated with PureCol collagen (Advanced Biomatrix Science) for at least 30min at a 1:30 dilution. Media is changed the following day after being warmed to 37°C to remove any dead cells or debris with 3 ml of supplemented EGM media with the antibiotics.

Some donors were bought in commercially from Lonza and were thawed quickly at 37 degrees and then pipetted into a T75 flask with 7 ml of supplemented EGM media inside. HBECs were then cultured with the same method of cells obtained from bronchoscopies after growing in a T75 flask at passage 1.

All EGM culture media subsequently used was supplemented with EGM supplement pack (Promocell) and GA-1000 (Lonza) unless otherwise indicated. After the cells reach 70%-90% confluence, Trypsin-EDTA is used for 5-10 min to detach the cells then anti-trypsin inhibitor at 0.5 mg/ml (Roche Life Science) is added at a ratio of 1:1 to inhibit the effects of trypsin. HBECs are centrifuged at 200*g* for 5 min and then transferred to a T75 flask at a 1:4 dilution ratio in EGM culture media (Promocell) after

the supernatant is discarded. Cell culturing is done in a T75 flask thereafter until passage 6 when HBECs lose their morphology and have a decreased growth rate. For plating, cells were seeded at a density of 50,000 cells per well in a 24-well plate and media was changed every other day until confluence.

When HBECS were frozen, 500,000-1,000,000 cells were put into 90% supplemented EGM media and 10% DMSO with 1 ml pipette into a cryovial which was then inserted into a Mr. Frosty^{TM} Freezing Container (Thermofisher Scientific) and stored at -80 for 2 days. HBEC vials were then moved to a liquid nitrogen cryostore at -150 ^{o}C until the HBECs were thawed.

For thawing, HBECs were quickly thawed in a 37 degree water bath and then pipetted into a 1:30 collagen (Advanced Biomatrix Science) coated T75 flask with 7 ml of supplemented EGM media (Promocell).

2.4 Culturing of human bronchial epithelial cells at Air-Liquid Interface

HBECs were seeded into 0.4 µm pore size transwells (Greiner) at 50,000 cells per well with 500 µl at the basolateral side and 200 µl at the apical side of the transwells. Cells are incubated overnight or until confluency and then cultured using Air-liquid interface (ALI) media. Media used for culturing at ALI was made by 1:1 dilution of DMEM and EGM supplemented with 1 µl of EGM supplements per ml of ALI media without retinoic acid or triiodothyronine. Retinoic acid was then added fresh at 50 nM to the ALI media to be used for culturing HBECs at ALI to complete the ALI media.

Once cells became confluent by very little to no space between the cells, ALI media was removed on the apical side and washed with 300 µl of PBS then removed and kept air facing. The media on the basolateral side was also washed with 500 µl of PBS and replaced with 500 µl of ALI media. ALI media was then replaced every other day

on the basolateral side with no media on the apical side until the TER increased then plateaued around 28 days later.

2.5 Measuring Transepithelial Resistance

TER was measured at ALI or at a monolayer culture in transwells using an EVOM2 or EVOM3 machine (WPI) measuring resistance in Ohms. The STX2 electrode is cleaned with 70% ethanol then washed in PBS. The electrode is then put into the media with no cells to measure the blank resistance before measuring TERs. The STX2 electrode is then put vertically into the transwell with the shorter end into the apical side and the longer end into the basolateral side. The EVOM machine then displays the TERs and the electrode is subsequently cleaned with 70% ethanol and washed with PBS before moving onto the next well or sample. TERs were measured once a week for differentiated cultures until the TER has plateaued after which the HBECs at ALI are ready for experiments or can continue being cultured as described until an experiment was performed on them. TERs were also measured at a monolayer when the cells were confluence in order to determine barrier integrity and is discussed in more detail in **Chapter 4**.

2.6 Human bronchial epithelial cells stimulation with LPS and Poly I:C

HBECs were stimulated with either LPS or poly I:C for 24 hours diluted in EGM media and a media only control. LPS stimulation was done 20 ng/ml while Poly I:C stimulation was performed at 25 µg/ml. Similar concentrations of LPS have been used to stimulate epithelial cells with or without any responses in healthy epithelial cells depending on the context[139,217]. However, high concentration of LPS can cause cell death and thus a concentration of 20 ng/ml has been chosen as it can induce inflammation in other innate immune cells and COPD HBECs may have exaggerated responses. A poly I:C concentration of 25 µg/ml has been previously shown to induce an inflammatory

response in primary epithelial cells and thus the same dose was utilized in this study[218,219]. Supernatants were then harvested, and the cells were lysed with the supernatants also being harvested and stored at -80°C prior to testing then used for measurement of various analytes. All analytes measured were done in duplicates.

2.7 Meso Scale Discovery Platform for Multiplex Measurements

Quantification of cytokines and alarmins was done using undiluted samples on the Meso Scale Discovery (MSD) multiplex platform on U-Plex plates. All reagents were brought to room temperature where required. Biotinylated capture antibodies were coupled to a linker by mixing 200 µl of the biotinylated antibody to 300 µl of the assigned linker and mixed by vortexing then incubated at room temperature for 30 min. Stop solution was then added at 200 µl to the mixture and vortexed then incubated again at room temperature for 30 min. Linker coupled antibodies were then mixed by adding 600 µl of each into a 15 ml falcon tube then vortexing. The mixed solution was then brought up to 6 ml using stop solution resulting in a 1X concentration of coating solution. The coating solution was added to the MSD plates at 50 µl/well then sealed and incubated at room temperature for 1 hr while shaking. The plate was then washed 3 times with 150 µl/well of 1X MSD Wash Buffer.

Standard were prepared by adding 250 µl of MSD Diluent 43 to each standard resulting in a 5X solution then diluted into a 7-point standard through decreasing and subsequent 5-fold dilutions using MSD Diluent 43. 25 µl of standards, samples, and a blank was then put into each well with each well having 25 µl/well of MSD Diluent 41 beforehand then incubated at room temperature for 1 hour. The plate was then washed three times as previously described then detection antibody was diluted at 1:100 using MSD Diluent 45 and then added at 50 µl/well and incubated at room

temperature for 1 hours. The plates were then washed again three times and MSD GOLD read buffer was then added at 150 µl/well and then directly read by the MSD plate reader where analytes were also quantified. Each sample was run in duplicates and if the sample was below the limit of detection, the next lowest integer below the limit of detection was chosen until a concentration of 0.1 pg/ml. The lower and upper limits of detection for the various analytes measured are listed in the **Appendix**.

2.8 Microscopy Staining

Cells were seeded at 20,000 cells/well on an 8-chambered slide and fixed in 150 µl of 4% formaldehyde for 15 minutes. Cells were then washed with PBS three times and then blocked with 300 µl of 1% BSA (Sigma-Aldrich) in PBS for one hour. After blocking, cells were incubated with 150 µl of the primary antibodies against CLDN-3, CLDN-4, and JAM-A and diluted in 1% BSA overnight in 4 degrees or for two hours at room temperature to allow sufficient time for the primary antibody to bind. The chambers were then washed with 300 µl PBS three times and incubated with 150 µl of the respective secondary antibody attached to a fluorochrome in PBS with 1% BSA for an hour at room temperature. Cells were then washed three times in PBS and 300 nM of DAPI was added for 3 min in order to also visualize the nucleus of the cells. Three final washes of PBS were done and then the cells were visualized under either a Zeiss 780 inverted confocal microscope in order to examine the fluorescent TJ molecules with the same microscope settings utilized across experiments where no noise from the gain was detected in the healthy controls. Five images were taken for each condition at 100x and four images for 630x. For intracellular staining, cells were treated with 0.5% Triton-100X for 10 min after the cells were fixed with the same steps

were performed afterwards. All microscope images taken were analysed using FIJI image analysis software.

2.9 Mean Fluorescence Intensity and colocalization measurement

FIJI was used to measure mean fluorescence intensities of TJ proteins in each respective channels as a quantitative measure for images taken at 100x magnification. For 100x images, five images were taken for each donor and condition combination before MFI was quantified as previous studies on TJs have taken 4-6 images per condition[220]. Each image was uploaded onto FIJI in a czi format and channels were split for each respective protein measured and DAPI. Mean fluorescence intensity (MFI) was measured with FIJI and the data aggregated and subsequently analyzed. Colocalization analysis was done in FIJI using the EzColocalization plugin to assess colocalization between different TJ molecules for images at 630x. Images were taken at 630x in order to have a high enough resolution to distinguish protein localization. The metric utilized was the Pearson correlation coefficient in order to assess colocalization with an R score of 0-0.29 seen as very weakly colocalized, 0.3-0.49 weak colocalization, 0.5-0.69 is moderate colocalization, and a score of 0.7-1 is a strong colocalization. The higher the Pearson correlation coefficient, the more colocalized the proteins measured are with 0 being not colocalized at all and 1 being perfectly colocalized proteins.

2.10 IFNλ 1/3, IFN-β1, and GM-CSF ELISAs

ELISAs were performed according to the manufacturers instruction including for capture and detection antibody dilutions (R&D Systems). Capture antibodies were diluted in sterile PBS were pipetted into 96-well plates at 100 µl/well and incubated at room temperature overnight. After the capture antibody was discarded, the wells were washed with wash buffer composed of 0.05% Tween (Sigma-Aldrich Life Science) in

PBS (PBS-T) 3 times. Wells were blocked with 1% BSA (Sigma-Aldrich Life Science) for at least 1 hour at 300 µl/well then washed. Supernatants or lysates were then transferred into the wells at 100 µl/well as well as diluted standards then incubated for 2 h at room temperature. Supernatants were then discarded then the wells washed as described previously. Diluted detection antibodies were then put into each well at 100µl/well then incubated for 2 h at room temperature then washed as described previously. Diluted Strepavidin-HRP conjugate was then diluted at 1:40 in 1% BSA then put into each well at 100 µl/well for 20 min at room temperature away from direct light exposure then washed. Reagent substrate in the kit were then mixed at a 1:1 ratio and 100 µl were added to each well for 20 min at room temperature away from direct light. Stop Solution was finally added at 50 µl/well to inhibit reaction induced color changes. Plate was read using Spectrostar Nano plate reader (BMG Labtech) at a wavelength of 450 nm with 570 nm for background correction. All incubation steps were performed on a plate shaker at approximately 600 rpm.

2.11 Colony forming Units Quantification and Stock Preparation of NTHi

Sterile Brain Heart Infusion (BHI) was diluted in PBS at 1:10 to make up 15 ml of PBS supplemented with BHI and subsequently the supplemented PBS was put in 12 Eppendorf tubes at 900 µl each. Aliquots of 100 µl from NTHi stocks or samples were taken and put in the Eppendorf tubes to make 12 10-fold dilutions from a 10^{-1} dilution to a 10^{-12} dilution while vortexing each Eppendorf tube at each subsequent dilution. Chocolate agar plates were equilibrated to room temperature and divided into four quadrants for each plate. Each quadrant was labelled with a specific dilution and 20 µl of the corresponding NTHi dilutions were pipetted into their respective quadrants in triplicates. The chocolate agar plates were incubated at 35 degrees overnight and then

the colonies were counted with the quadrants with the clearest number of colonies counted.

The following equation was used to calculate the CFUs/ml:

CFUs/ml = (No. of colonies/3 x dilution factor)/0.05

2.12 NTHi Infection of HBECs

BHI was supplemented with 10 µg/ml of Hemin and 2 µg/ml of NAD to make supplemented BHI (sBHI) and between 10 ml of sBHI was placed in a 50 ml falcon tube. A scratching of frozen NTHi strain 398 was taken or 50µl and then inoculated into the sBHI. The sBHI inoculated with NTHi was then incubated at 35 degrees and shaken at 200 rpm until the NTHi reaches its exponential growth phase. The exponential growth phase was determined by putting 1 ml of the sBHI inoculated with NTHi into a cuvette and measuring the OD490 and OD600 while using sBHI alone as a blank. When the OD490 or OD600 are greater than 0.33 and 0.21 respectively then the bacteria were growing at an exponential rate as determined by the bacterial growth curve **(Figure 2.1)**.

NTHi was then diluted in EGM media without antibiotics at a MOI of 0.1-1000 to infect HBECs. Media was then removed from growing HBECs and replaced with the NTHi containing EGM media in duplicates at 350 µl in a 24-well plate. Infected HBECs were then incubated for 2 hours at 35 degrees to allow time to infect the HBECs. After 2 hours, the media was removed and washed three times with 400 µl of EGM media and then replaced with EGM media containing gentamicin at 200 µg/ml for another 1.5 hours. Subsequently, the media was removed and replaced with EGM media and incubated at 35 ^{o}C either at an early timepoint of 4 hours as epithelial changes have been demonstrated at an early timepoint or at 24 hours[165,221].

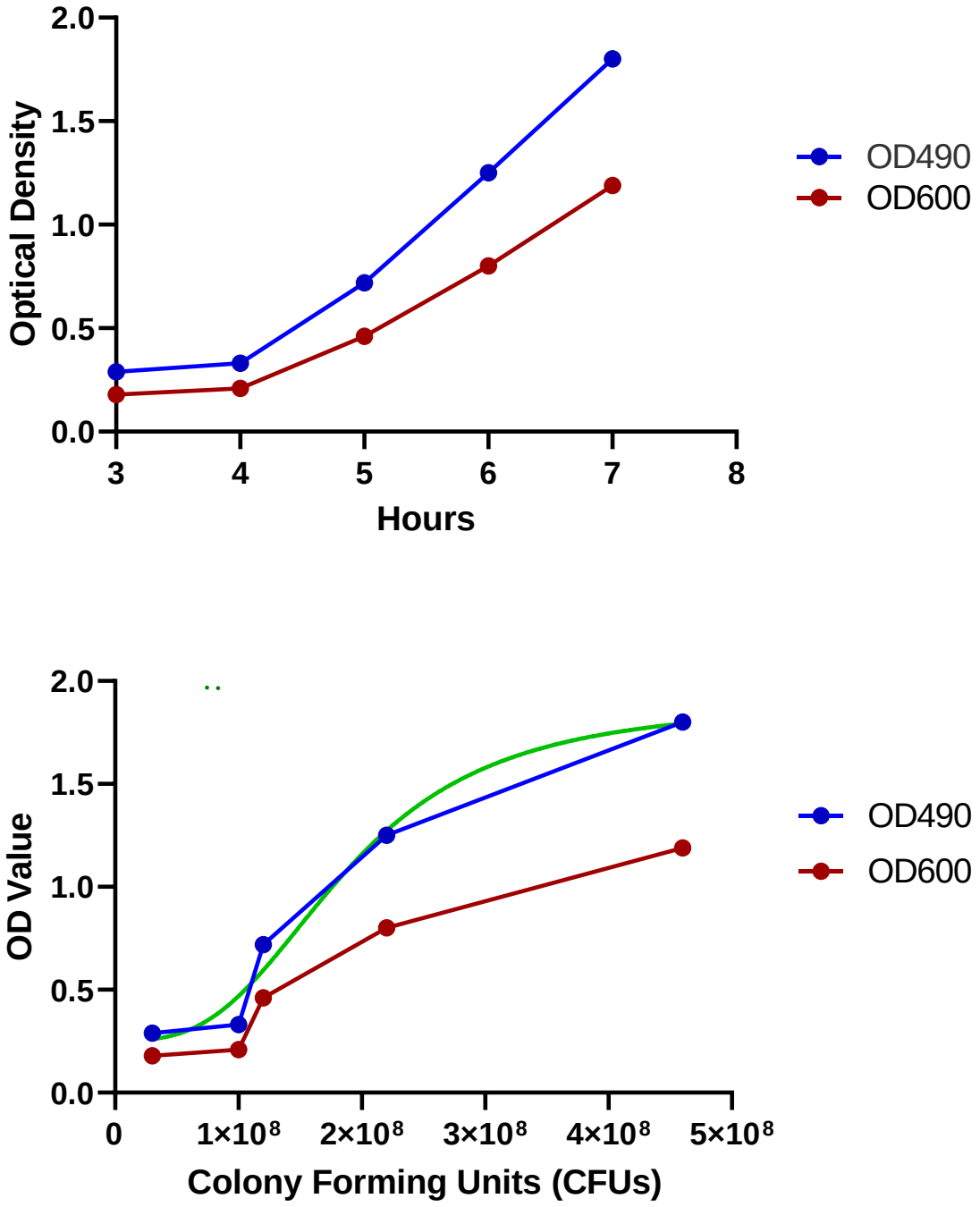


Figure 2.1: Quantified ODs and CFUs/ml over time to determine exponential growth. *ODs were measured over **(A)** Time in hours and **(B)** CFUs were quantified for each OD value determined per unit time.*

2.13 RV16 Propagation

HeLa cells were used to propagate RV16 due to their high doubling rate over many passages on a monolayer and a dampened innate anti-viral response in comparison to primary epithelial cells and being an established cell line. HeLa cells were cultured in DMEM medium supplemented with NEAA (Gibco), 10% FCS (Sigma-Aldrich Life science), 1% penicillin-streptomycin (Sigma-Aldrich Life science), and 1% L-glutamine (Sigma-Aldrich Life science) in a T150 flask until cells were 90% confluent. Media was then removed from the flask and washed with sterile PBS. RV16 diluted in 5 ml of supplemented DMEM media altered to 2% FCS and was then added to the HeLa cells and incubated for 1 hours at room temperature while swirling to mix every 15 min. Original supplemented DMEM was then added to RV16 containing flask until volume reached 20 ml and cells were incubated at 35 degrees. Cells were checked daily until 50% of HeLa cells have died in the flasks and subsequently supernatants were collected. Supernatants were frozen at -80 and thawed twice then centrifuged at 500*g* for 5 min to remove any debris. Virus containing supernatants were then aliquoted in O-ring capped tubes and stored at -80 degrees.

2.14 RV16 Quantification

HeLa cells were plated in 96-well plates at 10,000 cells/well that were coated with collagen diluted in 1:30 for half an hour beforehand and the cells were incubated overnight until they have reached confluence. A dilution curve was created for RV16 diluting it from 10^{-1} to 10^{-8} in supplemented DMEM media altered with 2% FCS with a media only as a negative control then 100 µl were added to each well with 6 replicates per dilution factor. The plate was then incubated at room temperature for an hour and swirled to mix every 15 min. Media was then removed and washed with PBS and then replaced with supplemented DMEM media. Cells were then incubated at 35 degrees

and wells were checked daily for viability starting at 72 hours until more than 50% of the cells at a particular dilution factor have died. The next lowest dilution where less than 50% of cells have died were also recorded and the $TCID_{50}$ was then calculated using both dilution factors with the pfu/ml being 0.69 of the $TCID_{50}$.

$TCID_{50}$ Calculations:

1. Proportionate Distance = (% Dead cells at dilution where more than 50% cells are dead)-50% / (% Dead cells at next dilution where less than 50% cells are dead) - (% Dead cells at dilution where more than 50% cells are dead)
2. 50% End Point: Log of dilution where more than 50% cells are dead eg. -7 or -4
3. Concentration of RV16 in well = 10- Proportionate distance + log of low dilution
4. $TCID_{50}$/ml = $TCID_{50}$/0.1
5. PFU/ml = 0.69 x $TCID_{50}$/ml

2.15 RV16 Infection

RV16 is diluted in EGM media at the desired MOI from a range of 0.01 to 1. Media is then removed from HBEC cells and replaced with RV16 containing media. HBECs are then incubated at 35 degrees for 1 hr. RV16 is then removed from the cells and washed with EGM 3 times then replaced with fresh EGM for 24 hours or until the end of the infection time point. HBECs were infected in duplicates for each donor.

2.16 Harvesting of HBECs

Supernatants were collected from stimulated and infected HBECs in order to harvest secreted proteins while the harvesting of intracellular proteins was done using 300 µl Mammalian Protein Extraction Lysis Buffer were added to the cells and then removed

and stored. For RNA, 300 µl of RNAlater were added to the cells in order to inhibit RNases and degradation of RNA and then stored until RNA was ready to be isolated. All supernatants, lysates, and RNA were stored at -20 or -80 degrees.

2.17 RNA Isolation

RNA was isolated using the QIAGEN RNeasy plus micro kit and protocol was closely followed as per the manufacturer's instructions. RLT lysis buffer plus was added to the cells at 350 µl to each well in a 24-well plate to lyse the cells. Samples were then removed and put into a microcentrifuge tube then vortexed. The sample was then put into a QIAshredder spin column (QIAGEN), placed in a 2 ml collection tube, then centrifuged at max speed to homogenize the sample. The homogenized lysate is then transferred into a gDNA Eliminator column which was placed in a 2 ml microcentrifuge tube and centrifuged for 30 seconds at more than 8000*g* to remove the DNA.

The flow through (The solution that went through the column) is then taken and 350 µl of 70% ethanol is added to it and mixed. The sample is then transferred to a RNeasy Minielute spin column placed in a 2 ml collection tube then centrifuged for 15s at more than 8000*g*. The flow through is then discarded and 700 µl of Buffer RW1 is added into the Minielute spin column to wash the spin column and centrifuged again for 15s at the same speed. The flow through is again discarded and 500 µl of RPE Buffer was added to the Minielute spin column and subsequently centrifuged at the same settings. The flow through was discarded and 500 µl of 80% ethanol was added to the spin column then centrifuged for 2 min at a speed of more than 8000*g*. The collection tube and flow through were then discarded and the spin column was put into a new 2ml collection tube. The cap of the spin columns was opened and then centrifuged at full speed for 5 min. The flow through and collection tube were discarded, and the spin

column was put into a new 1.5 ml collection tube and 14 µl of RNase free water was added to the centre of the spin column membrane. The spin column was then centrifuged at full speed for 1 min to elute the RNA and RNA was subsequently quantified and the purity assessed using a Nanodrop machine.

2.18 Reverse Transcription and cDNA synthesis

cDNA was then synthesized from the RNA that was isolated from the samples using the high capacity reverse transcription kit (Thermofisher Scientific) as per the manufacturer's instructions. 6 µl of each isolated RNA sample was diluted with the different reagents required as outlined in **Table 2.2**. The RNA sample was mixed with the reagents in a MicroAmp Optical PCR 96-well reaction plate (Applied Biosystems) with a total of 20 µl and then centrifuged for 10s at 300g to remove air bubbles and susbsequently inserted into a thermocycler to be heated at 37 ^{o}C for 2 hours then cooled to 4 degrees. Samples were then stored at -20 until qPCR experiments were performed.

Reagent	Volume (µl)
10X RT Buffer	2.0
25X dNTP mix (100 mM)	0.8
10X RT Random Primers	2.0
Multiscribe Reverse Transcriptase	1.0
RNase Inhibitor	1.0
Nuclease Free H_2O	7.2
RNA Sample	6.0
Total Volume	20

Table 2.2: Reagent mix for reverse transcription and cDNA synthesis from RNA samples.

2.19 Mastermix preparation for qPCR cycle run and primer design

Primers were designed using the Primer-BLAST tool on the NCBI website by inputting the accession number of the gene of interest. Primers for each gene were made with a length of approximately 150 base pairs to maximize amplification and PCR efficiency. The primers were validated by looking at the melting point after a PCR run or running a Northern blot gel and imaging it to ensure that the band size is similar to the predicted molecular weight. If there were multiple melting points or the melting point is vastly different than the predicted melting point for a gene after a PCR reaction, then the primer was redesigned and tested again to ensure the correct target was being amplified.

The mastermix for a qPCR reaction was prepared by first mixing 10 µl of the Fast SYBR Green Master Mix (Applied Biosystems) with 0.5 µl of a 10 µM stock of the forward and reverse primers of the gene of interest. 4 µl of DNA free water was then added to the mastermix with 5 µl of the cDNA of the respective samples to make up a total reaction volume of 20 µl in the well of a MicroAmp Optical PCR 96-well reaction plate (Applied Biosystems). The PCR place was then centrifuged at 300g for 10s to remove air bubble and deposit the reaction mix to the bottom of the well and subsequently inserted into a CFX96 Real Time System Bio-Rad qPCR machine with the amplification cycle design outlined in **Table 2.4**.

Gene	Forward	Reverse
cldn3	5′-CAACACCATTATCCGGGACT-3′	5′-CTTGGTGGCCGTGTACTTCT-3'
cldn4	5′-AGCCTTCCAGGTCCTCAACT-3′	5′-AGCAGCGAGTCGTACACCTT-3
ZO-1	5'-GCCCGTGCCCCGCTCGCTCTC-3'	3'-CCGCCCGCTCCTCACGCCACAG-5'
occludin	5'-AGGCCTGATGAATTCAAACCG-3'	3'-CTGGGTAAAAAGAGTAGGCTGGC-5'
jam-a	5′-GTGAAGTTGTCCTGTGCCTACTC-3′	5′-ACCAGTTGGCAAGAAGGTCACC-3′
IFNLR1	5'-CAGAATGTGACGCTGCTCTC-3'	5'-CGCGTCCCTTGAACTTGTTG-3'
IFNAR1	5'-CGCGAACATGTAACTGGTGG-3'	5'-CGACAGACTCATCGCTCCTG-3-
IFNAR2	5'-GCACTAAAGACGCTTCTTCCC-3'	5'-AGGTGATCAAAATTCTGAAGTGTC-3'
GAPDH	5'-AGCCACATCGCTCAGACAC-3'	5'GCCCAATACGACCAAATCC-3'

Table 2.3: Primers used for qPCR experiments. Primers were designed by myself and purchased from Merck.

Amplification Step	**Temperature (°C)**	**Time (Min:Sec)**
Initial Start	95	0:20
Denaturation	95	0:05
Annealing & Polymerization	60	0:30
Denaturation, Annealing, and Polymerization steps were done 44 times		
Cooling	40	0:30

Table 2.4: Amplification cycle settings for the qPCR experiments performed.

2.20 Relative gene expression fold change calculation

Cycle threshold (C_T) values of the genes of interest and reference gene were extracted from the machine for analysis. GAPDH was used as a reference gene as it has been used multiple times as a reference gene and does not significantly change across groups and conditions. A difference between one C_T value is the equivalent of an

amplification cycle which is a 2x difference ie. The higher the C_T value the lower amount of DNA of the gene of interest. For example, a 3 C_T value difference is 2^3 which is a 8-fold difference. Fold changes was calculated in comparison to unstimulated HBECs of the particular donor of a group as follows:

1. ΔC_T = C_T value of gene of interest - C_T value of GAPDH
2. $\Delta\Delta C_T$ = ΔC_T of infection condition of interest - ΔC_T of unstimulated condition
3. Fold change = $2^{-\Delta\Delta CT}$

2.21 FACS staining and analysis

Cells were washed twice with 2 ml of PBS in 1% BSA and 10 µM of EDTA after being detached and transferred into polypropylene tubes. PBS with 1% BSA and 10 M of EDTA was used in order to avoid clumping of HBECs in the tube as that was observed in previous attempts when only PBS was used. HBECs were centrifuged at 300g for 5 min and the supernatant was discarded. Fluorescent antibodies against EpCAM1, IFNAR1, and IFNLR1 were then diluted at their respective dilutions to stain the HBECs with titrations performed beforehand in order to deduce optimal concentrations **(Figure 2.2)**. Antibodies were then added to the HBECs at 20µl and were incubated in the dark at 4 degrees for 20 min. HBECs were then washed twice with the PBS mix solution and centrifuged at 300g for 5 min with the supernatants discarded. A viability dye was then added to the cells at 1:500 and then incubated for 15 min in the dark at room temperature. Cells were then washed twice with PBS solution mix and centrifuged at 300g for 5 min. HBECs were then fixed with 4% PFA for 15 min at room temperature and vortexed then washed and centrifuge twice again as previously described before proceeding to flow cytometry.

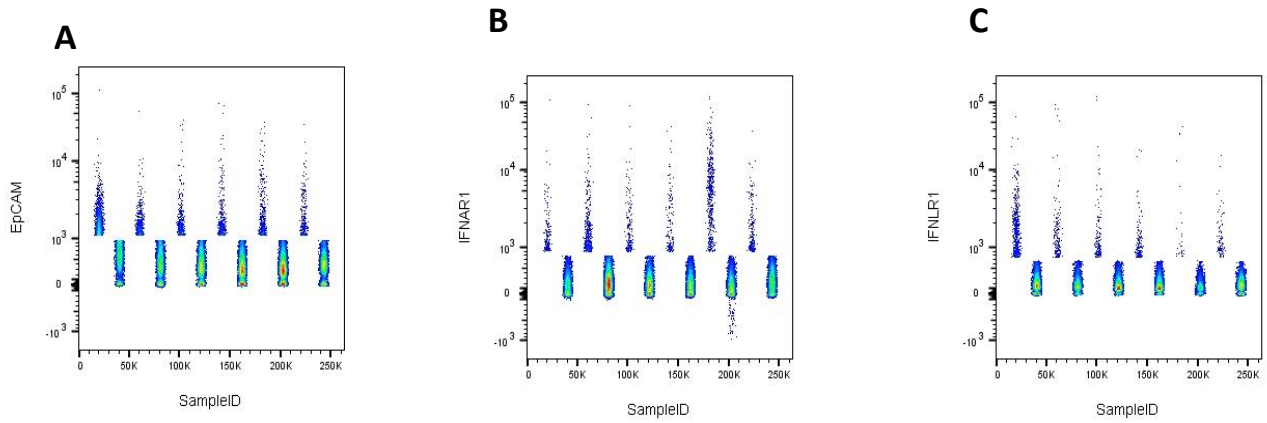


Figure 2.2: Titrations of antibodies for flow cytometry. *Antibody titrations done on **(A)** EpCAM, **(B)** IFNAR1, and **(C)** IFNLR1 from undiluted concentrations to 1:80. Points on the far right of each plot are unstained controls.*

2.22 Flow cytometry and analysis

Flow cytometry was performed on the samples using a modified LSRII machine with the antibody stained and unstained samples using the FACS DIVA software recording 10,000-20,000 events. Data was then analyzed using the FlowJo v10 software with the gating strategy is outlined (**Figure 2.3)**. Due to the Live/Dead dye used having high autofluorescence, gating on live cells was excluded as the gating would be unreliable and thus some dead cells may have been gated on.

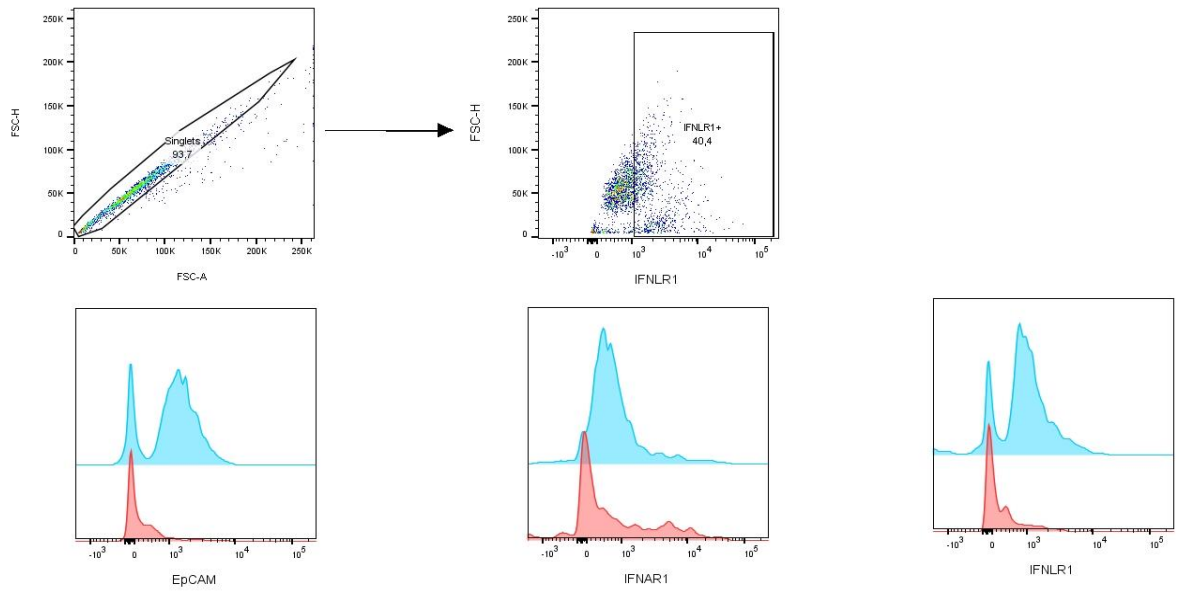


Figure 2.3: Gating strategy utilized for flow cytometry. *Singlets were gated on and then cells positive for the respective marker were gated on compared to the unstained control.*

2.23 RNA-seq Experimental Design

Bulk RNA-seq was performed on HBECs in order to identify differential gene expression between different groups and conditions. HBECs were from healthy, smoker, and COPD donors cultured at either a monolayer or ALI and were either unstimulated or stimulated with NTHi at a MOI of 10 or RV16 at a MOI of 0.01 for 24 hours. The total number of samples sent for library preparation and sequencing is 91. 30 million reads were chosen per sample in order to get an in depth read from each biological replicate and to offset any rRNA impurities within the sequenced samples and low sample sizes.

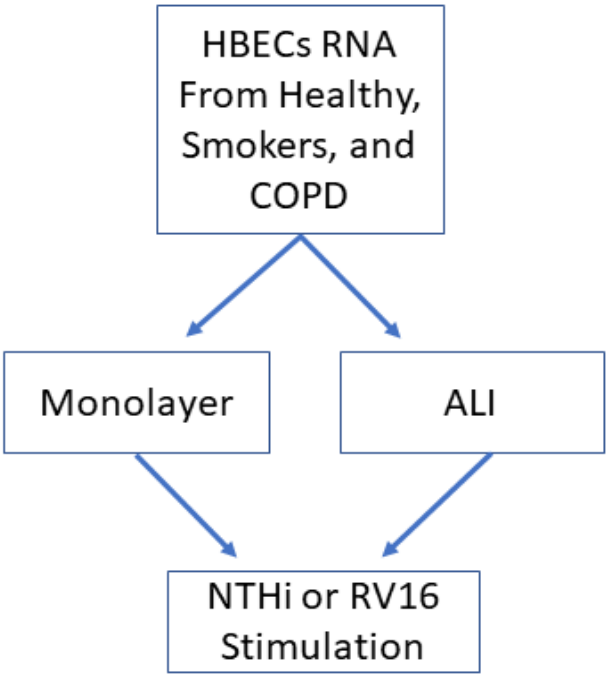


Figure 2.4: Diagram of different groups, conditions, and culturing methods for samples used for bulk RNA-seq.

2.22 Library preparation and sequencing by GENEWIZ

Samples were sent to GENEWIZ to perform QC, library preparation, and sequencing. RNA samples were quantified using Qubit 4.0 Fluorometer (Life Technologies) and RNA integrity was checked with RNA Kit on Agilent 5400 Fragment Analyzer (Agilent Technologies). An RNA quality number (RQN) above 7.0 from a scale of 1-10 was considered good enough for sequencing and the samples on average had a RQN of 8.5. RNA sequencing library preparation was prepared using NEBNext Ultra II

Directional RNA Library Prep Kit for Illumina following manufacturer's instructions (New England Biosciences). Briefly, mRNAs were first enriched with Oligo(dT) beads. Enriched mRNAs were fragmented. First strand and second strand cDNA were subsequently synthesized. The second strand of cDNA was marked by incorporating dUTP during the synthesis. cDNA fragments were adenylated at 3'ends, and indexed adapter was ligated to cDNA fragments. Limited cycle PCR was used for library amplification. The dUTP incorporated into the cDNA of the second strand enabled its specific degradation to maintain strand specificity. Sequencing libraries were validated using NGS Kit on the Agilent 5300 Fragment Analyzer (Agilent Technologies), and quantified by using Qubit 4.0 Fluorometer (Invitrogen). The sequencing libraries were multiplexed and loaded on the flowcell on the Illumina NovaSeq 6000 instrument according to manufacturer's instructions. The samples were sequenced using a 2x150 Pair-End (PE) configuration v1.5. Image analysis and base calling were conducted by the NovaSeq Control Software v1.7 on the NovaSeq instrument. Raw sequence data (.bcl files) generated from Illumina NovaSeq was converted into fastq files and de-multiplexed using Illumina bcl2fastq program version 2.20. One mismatch was allowed for index sequence identification.

2.24 RNA-seq analysis

Analysis and conversion of the raw data of sequence reads to hit counts was performed by bioinformaticians at GENEWIZ. After investigating the quality of the raw data, sequence reads were trimmed to remove possible adapter sequences and nucleotides with poor quality using Trimmomatic v.0.36. The trimmed reads were mapped to the Homo sapiens reference genome available on ENSEMBL using the STAR aligner v.2.5.2b. The STAR aligner is a splice aligner that detects splice junctions and incorporates them to help align the entire read sequences. BAM files

were generated as a result of this step. Unique gene hit counts were calculated by using feature Counts from the Subread package v.1.5.2. Only unique reads that fell within exon regions were counted. Base reads were looked at for GC content and distribution as well as read quality of the bases which had an average read quality of 35.8 **(Figure 2.5a,b)**.The hit counts were then sent back and then I uploaded them onto RStudio version 1.41106 along with the sample metadata and R language v4.1.0 was used to analyze the data. Packages that were utilized to analyze and visualize the bulk RNA-seq data are outlined in **Table 2.5**.

Normalization of read counts was done using the DESeq2 package which normalizes the hit counts and has its own method for taking variability between samples such as size factor and read counts into consideration. The DESeq dataset was then filtered to exclude genes that have hit counts with 0 reads. Differential gene expression between different groups and conditions were compared with log2Fold changes, p-values, and adjusted p-values calculated. However, in order to take into account outliers within genes and a smaller sample size the lfcShrink() function was used using the ashr method and outputs such as log2Fold changes were subsequently produced[222].

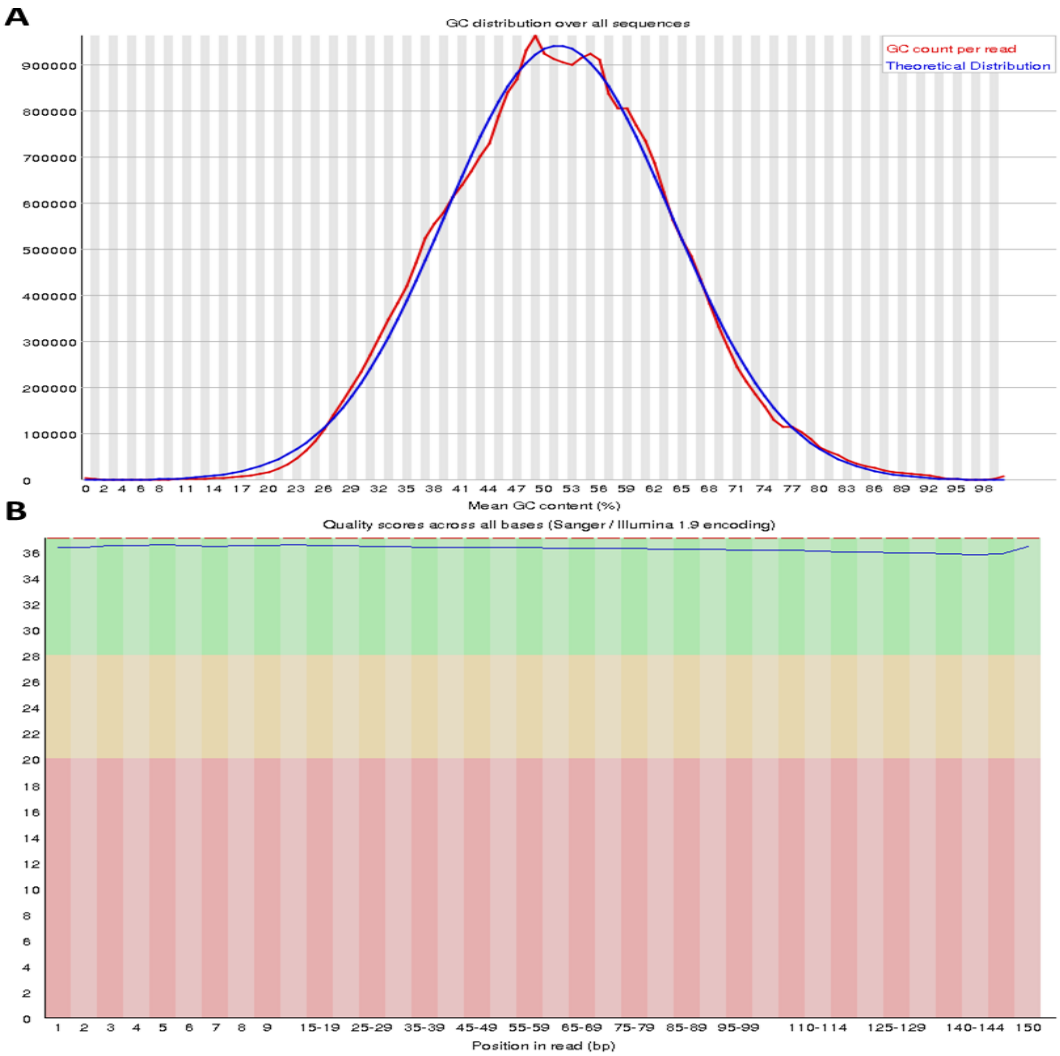


Figure 2.5: Base read GC content and quality scores. ***(A)*** *Mean GC content of the base reads compared to a theoretical distribution in a sample.* ***(B)*** *Quality score of the read bases with each position in the read with a score above 28 being high.*

Package	Description
ashr	Methods for adaptive Shrinkage, using Empirical Bayes
base	The R base package
BiocManager	Gives access to the Bioconductor package Reporsitory
BiocGenerics	Generic functions used in Bioconductor

BiocWorkflowTools	Tools to aid the development of Bioconductor Workflow Packages
biomartr	Retrieval or genome data and gene names from ensemble IDs
datasets	The R dataset package
DESeq2	Differential gene expression based on the negative binomial distribution for RNA-seq analysis
dplyr	Grammar package for data manipulation
EnhancedVolcano	Synthesizes publication ready volcano plots with enhanced coloring and labelling
GenomicInfoDb	Utilities for manipulating chroosoe names, including modifying them to follow a particular naming style
GenomicInfoDbData	Species and taxonomy ID look up table used by GenomicInfoDb
ggplot2	Create elegant data visualizations using the grammar of graphics
gpubr	ggplot2 based publication read plots in order to layout created plots
gridExtra	Grid graphic package with miscellaneous functions
magrittr	A forward pipe operator for R

MatrixGenerics	Statistic functions that operate on matrix-like objects
matrixStats	Functions that apply to rows and columns of matrices and vectors
pheatmap	Generates pretty heat maps from a matrix-like input
RColorBrewer	ColorBrewer Palettes used to color plots
readr	Read rectangular text data
readxl	Read Excel files
Stats	The R stats package
stringr	Simple and consistent wrapper for common string operations
superheat	A graphical tool for exploring complex datasets using heatmaps
tibble	Simplifies data frames
tidyr	Tidies messy data
tidyselect	Selects from a set of strings
tidyverse	Set of packages to tidy up messy data

Table 2.5: Set of R packages used for the analysis and visualization of RNA-seq data and their respective descriptions

2.25 Statistics

All statistical analysis was done on GraphPad Prism 9.2 with t-tests being done to compare significance between two conditions with the alpha p-value being 0.05. The results were checked if they were parametric by doing the D'Agostino & Pearson, Shapiro-Wilk, and Kolmogorov-Smirnoff normality tests. If the data were parametric, a

Welch correction test was performed to calculate significance. However, if the data was non-parametric, the Mann-Whitney test was performed. A paired t-test analysis was done for parametric or non-parametric data in an experiment if the same donor or groups were used such as the ratio paired t-test. One-way ANOVAs and two-way ANOVAs were also done in certain datasets with multiple groups.

Chapter 3: Anti-Viral Response and Inflammation in Epithelial Cells in Response to Viral and Bacterial Infection

Introduction

Chronic inflammation in the lungs is a hallmark of COPD pathogenesis. The lung epithelium is the first line of defense in the lungs and the first sensor of the external environment that can lead to signalling for an immune response. Thus, it can be the first to signal the innate immune system and trigger inflammation in the lungs. More specifically, the epithelium can release multiple alarmins and among the most important of the alarmins are IL-25, TSLP, and IL-33. All the aforementioned alarmins can be released by epithelial cells and have been shown to mainly induce leukocyte production of type 2 cytokines IL-4, IL-5, and IL-13 which subsequently leads to type 2 inflammation[223]. Within the context of COPD, it has been shown that IL-33, which is constitutively expressed inside the cells, is found higher amounts in the serum of COPD patients and inside the bronchial epithelial cells compared healthy controls[167]. COPD HBECs also had significantly greater TSLP production when stimulated with dsRNA compared to healthy controls[77]

TNF-α is an important pro-inflammatory cytokine that is induced through the transcription factor NFκB after pathogen sensing through PRRs. In COPD, TNF-α has been shown to be produced at significantly higher levels in sputum and BAL in comparison to healthy controls in multiple studies[171]. GM-CSF is an activator and recruiter of myeloid cells and prominent granulocytes such as neutrophils and eosinophils as well as macrophages. This is of particular relevance in COPD where either chronic neutrophilic or eosinophilic inflammation is observed in the lungs. GM-CSF has been found to be significantly upregulated in the sputum of COPD patients

compared with healthy non-smokers however it is not known whether epithelial cells are the source of the difference and in the context of a viral or bacterial infection[172].

The production of Type I and Type III IFNs are crucial cytokines as a first line of defense against viral infections in the lungs and can be produced in epithelial cells. IFN-λ in particular and its receptor IFNLR1 is mainly expressed by epithelial cells making it more specialized as a barrier cytokine rather than a pleiotropic one like Type I IFNs[224]. The induction of these cytokines is not only important for clearing viruses through the innate immune response but can also induce Type 1 responses such as increased presentation of MHC Class I, cytotoxic T-cell mediated killing, and the production of IFN-γ. In COPD, how the role of Type I and Type III IFNs and how they are changed is not yet clear. A study by Baines et. al has shown that IFN-λ and IFN-β1 expression was significantly higher in the HBECs of COPD patients in comparison to healthy controls in response to a RV infection[173]. Another study looking at the lung tissue of COPD patients showed that levels of IFN-β1 was significantly lower in the tissue of COPD patients than healthy controls however, it was not within a context of a viral infection but in patient lung biopsies[225]. A study by Veerati et. al did look at the anti-viral response in differentiated HBECs and found that unlike the findings in the study by Baines et. al, COPD HBECs had delayed Type I and Type III expression at 72-96 h post-infection compared to healthy controls. A significant increase in IFNs was also observed at 24-48 hours post-infection even at very low RV doses[226]. The aforementioned studies had different designs such as different timepoints, techniques, doses, or RV strains which may have contributed to different findings as well as the variation with in biological replicates. In addition, they did not investigate the role of the anti-viral response on smoker HBECs or IFN responses outside of viral infections.

IFNs, and particularly Type III IFNs, do not only respond to viral infection. The role of Type III IFNs has been shown to be more versatile and has been shown to be expressed in response to bacterial infections as well[227]. It has been shown for example that IFN-λ can be induced after infection with *P. aeruginosa* in mice. Interestingly, however, IFN-λ signalling through its receptor seems to inhibit bacterial clearance compared to mice deficient in IFN-λ signalling[228].

The aforementioned cytokines are all important and implicated in a myriad of inflammatory processes and the fact that COPD seems to have a diverse set of stochastic and chronic inflammatory attributes leaves a lot to explore. The literature on the expression and signalling of these cytokines in the epithelium in COPD is not yet clear particularly in the context of infection of the common bacterial or viral pathogens associated with exacerbations. For example, expression of the IFN receptors such as IFNAR2 and IFNLR1 are unexplored as well as IFNs and alarmins in response to NTHi infection.

In this chapter, I explore how these inflammatory and anti-viral cytokines manifest themselves in response to infection in the HBECs of healthy controls, smokers, and COPD patients. I take a multi-layered approach to exploring all types of cytokines discussed here when HBECs are infected with either RV16 or NTHi, two prominent pathogens linked to exacerbations in COPD. LPS and Poly I:C are also used as bacterial and viral analogues respectively. Protein levels of the cytokines are measured at 4 and 24 h after infection of HBECs with NTHi or RV16 cultured at a monolayer with different doses explored at 24 h. The cytokines are also measured after infection or stimulation of HBECs for 24 h when cultured at ALI to explore the effects in differentiated HBECs. Finally, gene expression of IFN receptors are explored in response to 24 h of NTHi or RV16 infection in HBECs in the three groups to get a

better idea of changes in IFN signalling as well as measurement of the ISG OAS1 post-infection.

Results

3.1.1 LPS stimulation effects on GM-CSF and TNF-α in HBECs at basal culture

The bacterial analogue LPS was used to stimulate HBECs at 20 ng/ml for 24 hours and the pro-inflammatory cytokines TNF-α and GM-CSF were subsequently measured by ELISA or the MSD multiplex platform.

TNF-α concentrations were unchanged in response to LPS stimulation in healthy and COPD HBECs. However, TNF-α concentrations were not measured in smoker HBECs after LPS stimulation due to a lack of plate availability **(Figure 3.1a)**.

GM-CSF levels were also unchanged in response to LPS stimulation in healthy, smoker, and COPD HBECs and no differences found between the three groups pre- and post-infection **(Figure 3.1b)**.

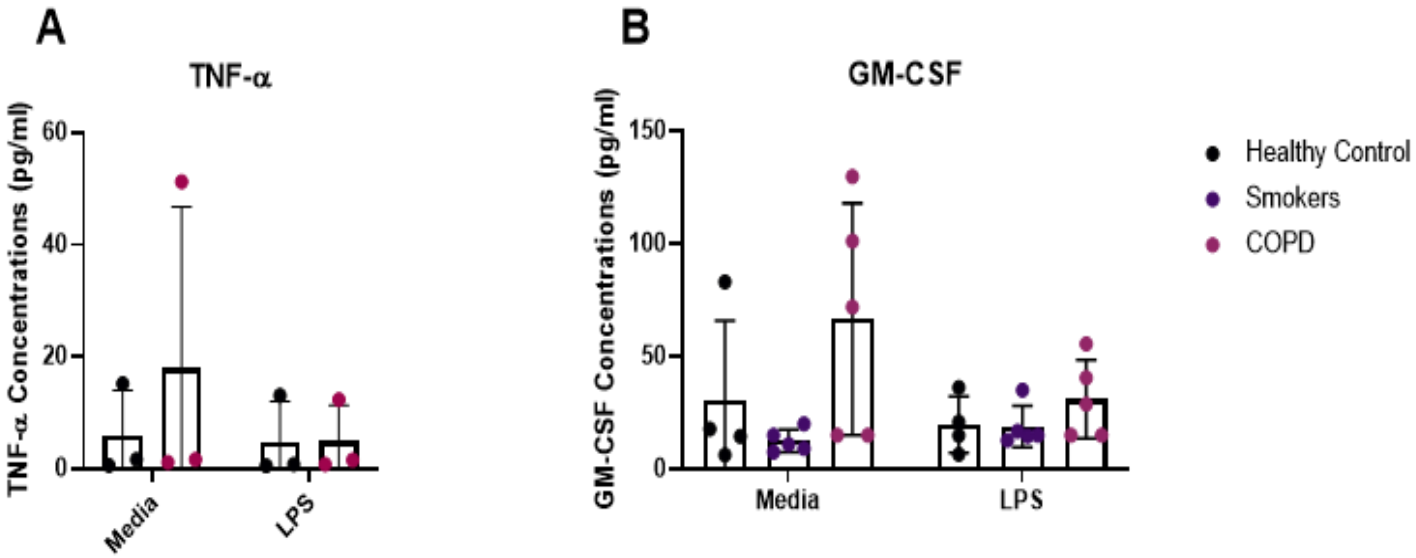


Figure 3.1: Pro-inflammatory Cytokine measures after LPS stimulation in HBECs after 24 H. *The cytokines **(A)** TNF-α and **(B)** GM-CSF were measured in supernatants by multiplex after 24 hours of 20 ng/ml of LPS stimulation. N numbers: Healthy=4, Smokers=5, COPD=7. Error bars are representatives of SEM. Welch test and ratio-paired t-tests performed.*

3.1.2 Effect of LPS stimulation of HBECs on the pro-inflammatory cytokines GM-CSF and TNF-α at ALI

HBECs from healthy, smokers, and COPD patients were cultured at ALI then stimulated with LPS at 20 ng/ml for 24 h. GM-CSF and TNF-α were then measured using the MSD multiplex platform from both the apical side, as well as the basolateral side of the cells on the transwells. This would theoretically mimic the side facing the lung lumen (Apical) as well as the lung tissue (Basolateral). However, most studies only measure the apical side however measuring both sides can also ascertain how physiologically relevant both sides are to the lung environment.

There were no significant differences in levels of GM-CSF on the apical side in response to LPS stimulation in any of the three groups despite and increasing trend observed in healthy HBECs in response to LPS (p=0.1554) **(Figure 3.2a,c)**. Similarly, there were no significant differences at the basolateral side either.

There were no significant differences in levels of TNF-α on the apical sides in response to LPS in all three groups. TNF-α levels were also not significant on the basolateral side although there did seem to be an apparent difference between stimulated healthy HBECs **(Figure 3.2b,d)**.

Overall, no differences were observed in either GM-CSF or TNF-α protein expression in response to LPS in all three groups.

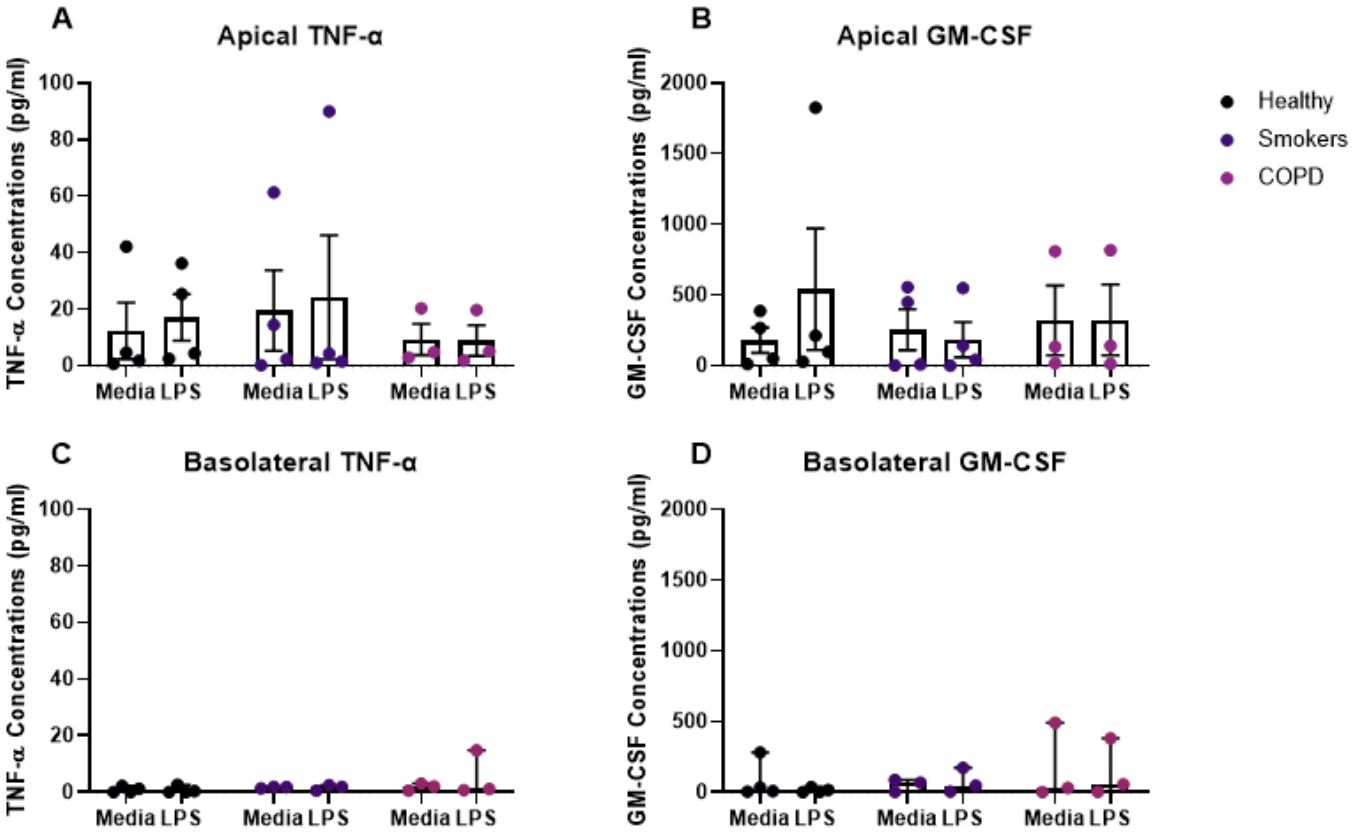


Figure 3.2: Inflammation in response to LPS Stimulation of HBECs at ALI. *HBECs were stimulated with 20 ng/ml of LPS for 24 hours and levels of* ***(A)*** *TNF-α and* ***(B)*** *GM-CSF were measured on the apical side as well as the* ***(C-D)*** *Basolateral side of the transwells. Error bars are representative of SEMs and one-way ANOVAs performed. N: Healthy=4, Smokers=3-4, COPD=3.*

3.1.3 Pro-inflammatory cytokine response to NTHi infection at an early timepoint in basal culture HBECs

In order to investigate whether there was an inflammatory response to NTHi at a relatively early time point, levels of GM-CSF and TNF-α were measured 4 hours post-infection with 10 MOI of NTHi.

There were no significant differences found in both TNF-α and GM-CSF levels within HBECs groups and between groups in response to NTHi infection after 4 hours indicating that the time point assess is too early for an inflammatory response **(Figure 3.3a,b)**.

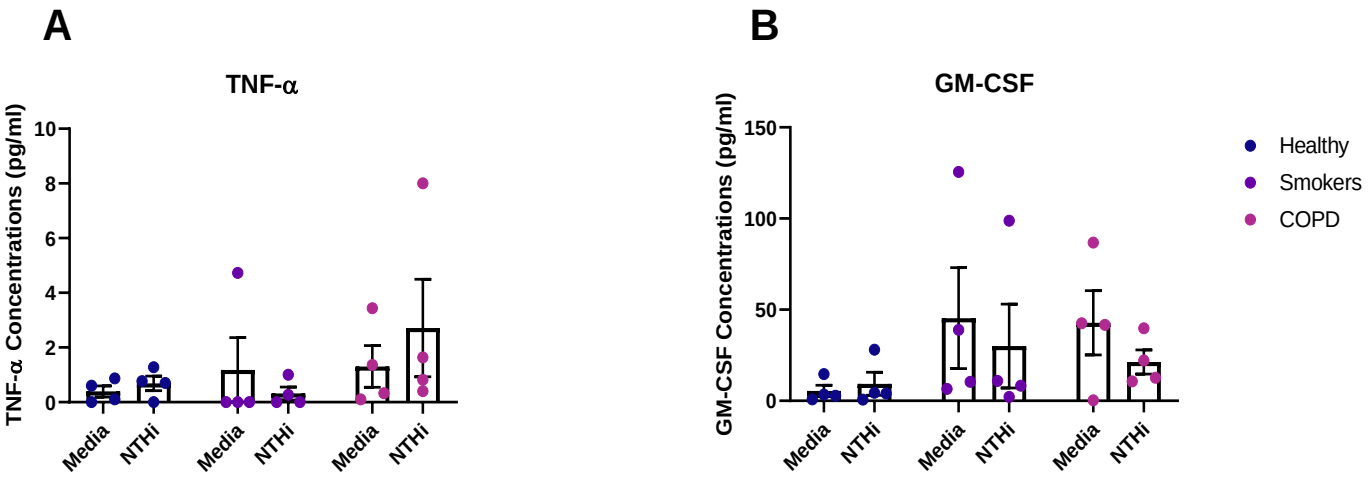


Figure 3.3: Pro-inflammatory Cytokine measures after early NTHi infection in HBECs. *The cytokines **(A)** TNF-α and **(B)** GM-CSF were measured in supernatants by multiplex after 4 hours of NTHi infection at a MOI of 10. Error bars are representatives of SEM. Welch tests and ratio paired t-tests performed. N: Healthy=4, Smokers=4, COPD=4.*

3.1.4 Effect of NTHi infection on inflammatory cytokines in basal cultured HBECs

The inflammatory cytokines GM-CSF and TNF-α were measured in all three groups after a dose-dependent infection of NTHi from an MOI of 0.1 to 1000 after 24 hours.

There was a significant concentration-dependent increase within the three groups after NTHi infection with the most marked increase in COPD HBECs and smallest increase found in smokers (Two-way ANOVA, p<0.0001) **(Figure 3.4a)**. However, despite the variation observed with the concentration-dependent increase between the three groups, the differences between the three groups were not significant at any MOI after NTHi infection (Two-way ANOVA, p= 0.0858) **(Figure3.4a)**.

There were no significant changes in GM-CSF concentrations between all three groups with increasing doses of NTHi and there was no changes or trends within groups with different MOIs of NTHi **(Figure 3.4b)**.

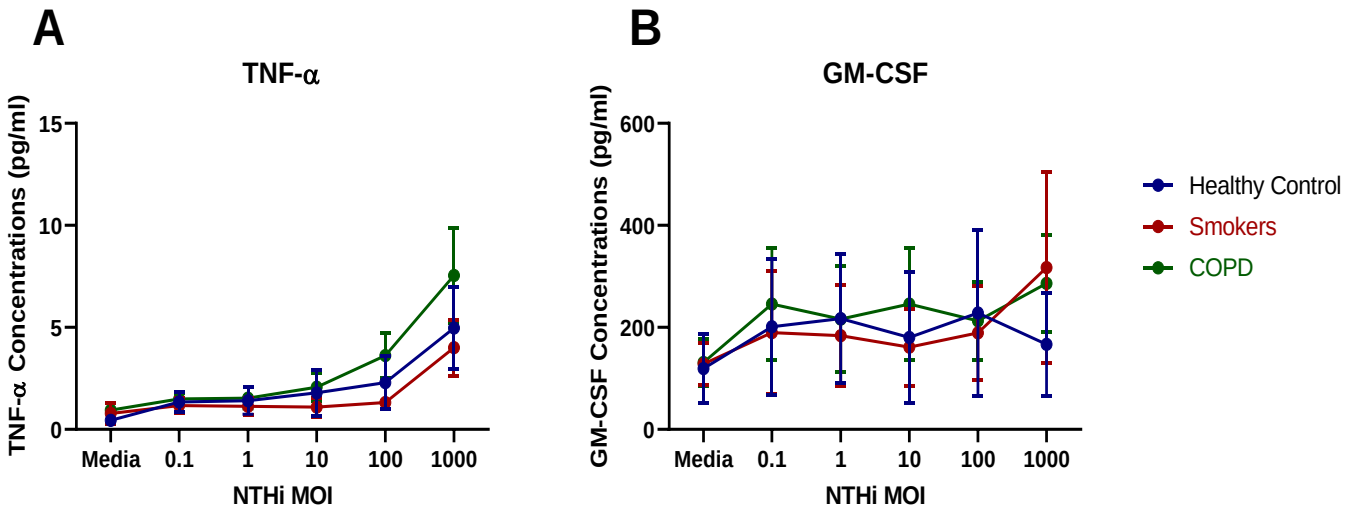


Figure 3.4: Pro-inflammatory Cytokine measures after NTHi infection in HBECs after 24 H. *The cytokines (A) TNF-α (Two-way ANOVA, p<0.0001) and (B) GM-CSF were measured in supernatants by multiplex after 24 hours of NTHi infection from a MOI of 0.1-1000. N numbers: Healthy=4, Smokers=5, COPD=7. Error bars are representatives of SEM. Two-way ANOVAs performed as well as multiple Manny-Whitney t-tests.*

3.1.5 Expression of pro-inflammatory cytokines in differentiated HBECs upon NTHi infection

NTHi was used at a MOI of 10 at 24 h in differentiated HBECs. TNF-α levels at the apical side were unchanged upon NTHi infection in all three groups. There seemed to be a response to NTHi at the basolateral side in COPD HBECs however changes to TNF-α expression were not significant (p=0.1634) **(Figure 3.5a.c)**.

There were no significant differences observed in GM-CSF protein expression on the apical side after NTHi infection in all three groups. Similarly, no significant differences were observed in levels of GM-CSF after NTHi infection despite infected COPD HBECs appearing to have higher levels than infected healthy HBECs (p=0.4158) **(Figure 3.5b,d)**.

There were no changes overall in pro-inflammatory cytokines TNF-α and GM-CSF expression. There were also no significant percentage changes in TNF-α or GM-CSF between stimulated HBECs from media only controls.

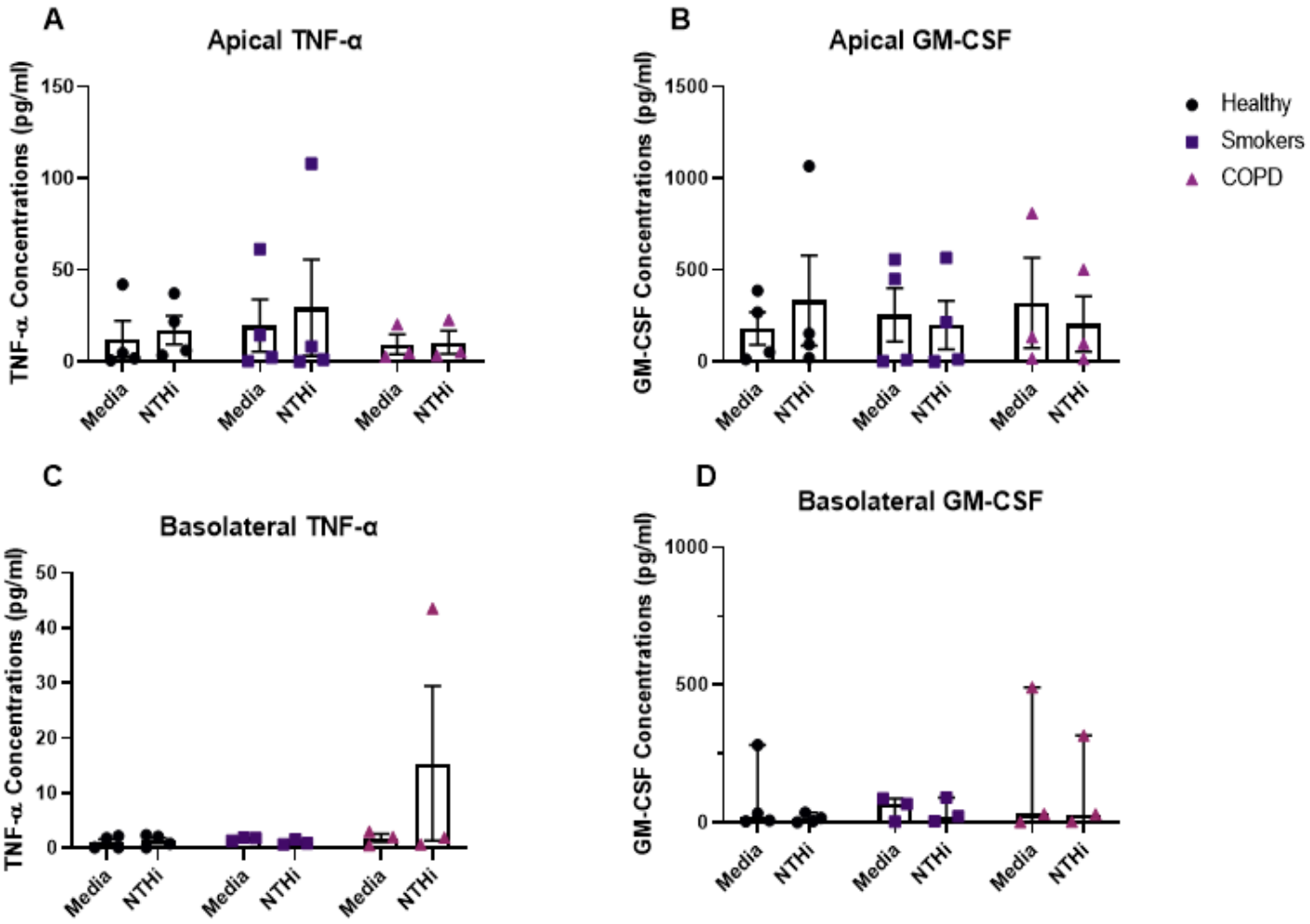


Figure 3.5: Response of Inflammatory cytokines to NTHi stimulation of HBECs at ALI. *HBECs were infect with 10 MOI of NTHi for 24 hours and levels of* ***(A)*** *TNF-α and* ***(B)*** *GM-CSF were measured on the apical side as well as the* ***(C-D)*** *Basolateral side of the transwells respectively. Error bars are representative of SEMs. Welch tests and ratio paired t-tests performed N: Healthy=4, Smokers=3-4, COPD=3.*

3.1.6 Poly I:C stimulation of basal cultures affects pro-inflammatory cytokines in HBECs

HBECs were stimulated with 25 µg/ml of poly I:C for 24 hours and TNF-α and GM-CSF were measured. No significant changes were observed in TNF-α concentrations COPD and healthy HBECs in response to poly I:C stimulation and no differences were seen between the two groups but there appeared to be an increase in COPD HBECs (p=0.114). **(Figure 3.6a)**

Levels of GM-CSF were also had no significant changed after poly I:C stimulation in healthy and COPD HBECs but there was an increasing trend particularly in COPD HBECs (p=0.10 and p=0.17 respectively). Smokers however had a significant increase in GM-CSF after poly I:C stimulation with approximately a 13-fold increase (p=0.0066) **(Figure 3.6b)**. No differences were observed between the three groups before or after stimulation and there were no significant percentage changes either in COPD and healthy HBECs from baseline after poly I:C stimulation.

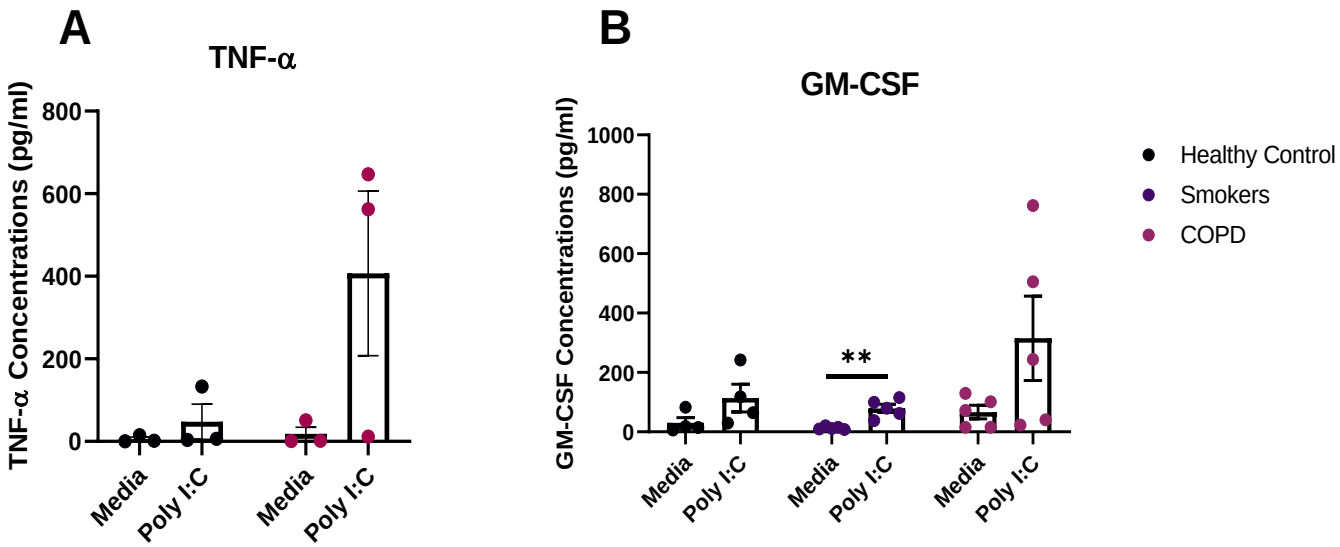


Figure 3.6: Inflammation in basal cultured HBECs after poly I:C stimulation. *Healthy, smokers, and COPD HBECs were stimulated with 25 µg/ml for 24 hours and **(A)** TNF-α and **(B)** GM-CSF were subsequently measured in supernatants. Error bars are representative of SEM. **: p<0.005. N: Healthy=3-4, Smokers=5, COPD=3-5. Mann Whitney and Wilcoxon tests performed.*

3.1.7 Change in pro-inflammatory cytokine levels in response to Poly I:C in differentiated HBECs

The viral analogue poly I:C was used to stimulated HBECs at ALI as well. HBECs in all three groups were stimulated at 25 µg/ml for 24 h. Levels of GM-CSF were unchanged in all three groups in response to poly I:C stimulation when measured apically **(Figure 3.7a)**. No significant differences were observed in GM-CSF expression at the basolateral level as well **(Figure 3.7c)**.

TNF-α expression at the apical side remained unchanged in all three groups after poly I:C stimulation although there was in increasing trend particularly in healthy and COPD HBECs (p=0.1294 and p=0.0648) **(Figure 3.7b)**. Similarly, TNF-α levels were not significantly changed at the basolateral side in all three groups however there was some increase in TNF-α in response to poly I:C in COPD HBECs **(Figure 3.7d)**.

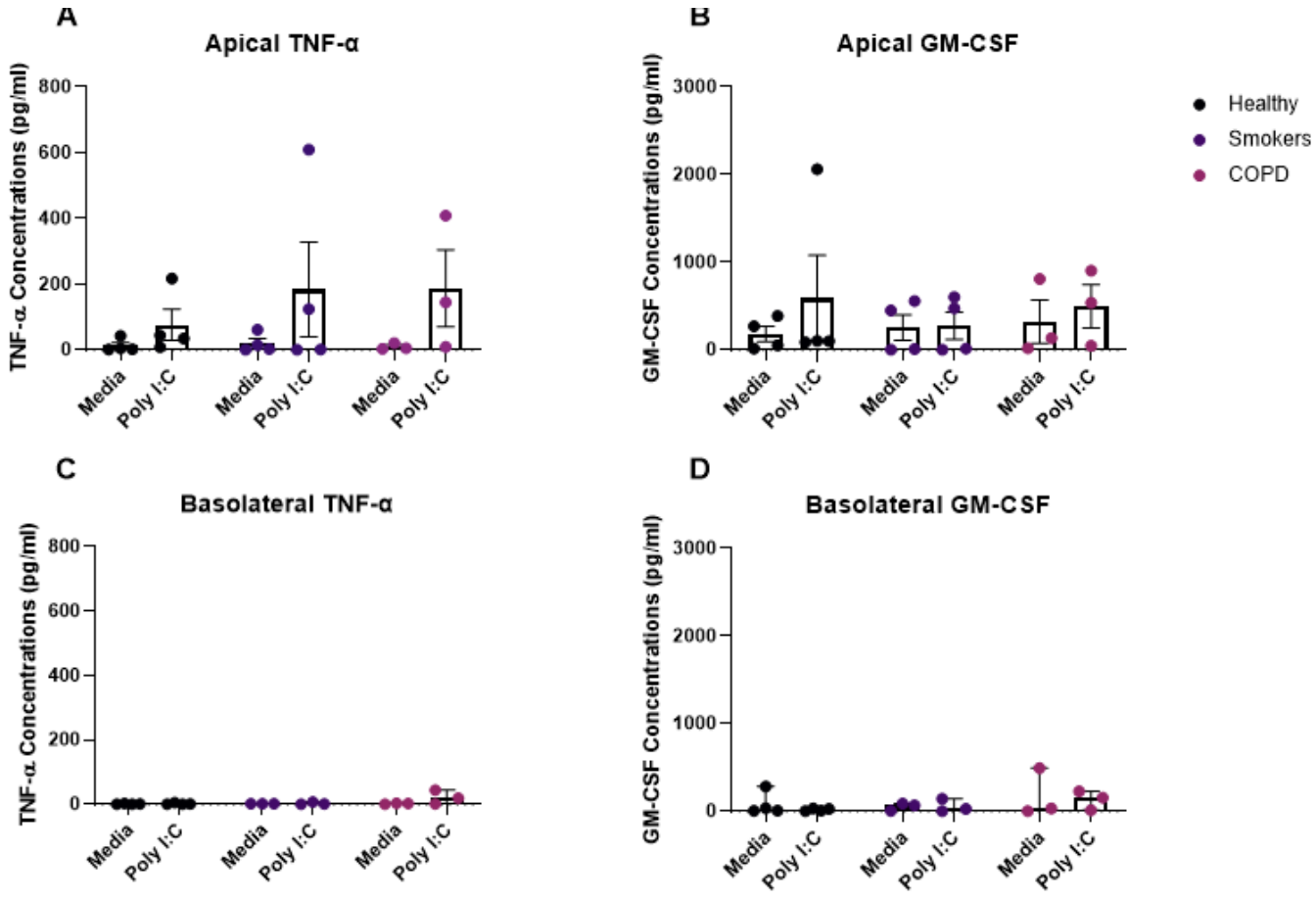


Figure 3.7: No differences in inflammation in differentiated HBECs after poly I:C stimulation. *Healthy, smokers, and COPD HBECs were stimulated with 25 µg/ml of Poly I:C for 24 hours and* ***(A)*** *TNF-α and* ***(B)*** *GM-CSF were subsequently measured on the apical side and on* ***(C,D)*** *the basolateral side of the transwells. Error bars are representative of SEM. Welch t-tests and ratio-paired t-tests performed. N: Healthy=4, Smokers=3-4, COPD=3.*

3.1.8 HBEC infection with RV at an early time point does not change levels of GM-CSF and TNF-α

HBECs were infected with RV16 at an MOI of 0.01 for 4 hours and the inflammatory cytokines TNF-α and GM-CSF were measured.

HBECs in all three groups did not respond to RV16 infection in terms of changes to GM-CSF and TNF-α. In addition, there were no differences observed between healthy, smokers, and COPD HBECs **(Figure 3.8a,b)**.

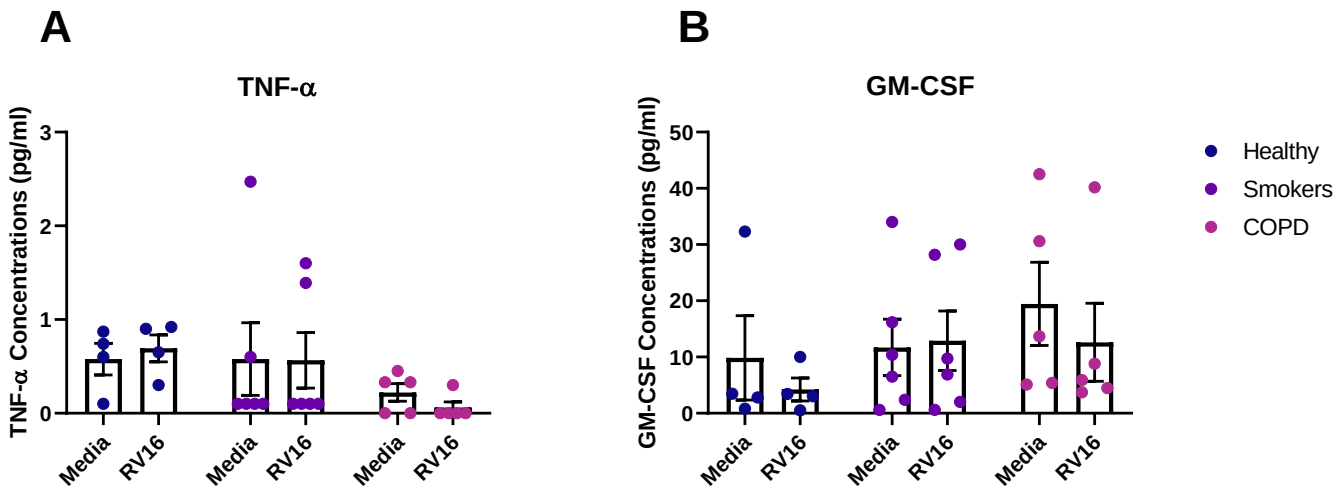


Figure 3.8: Inflammatory cytokines at an early timepoint after RV16 infection. *HBECs were infected with 0.01 MOI of RV16 for 4 hours and secreted* ***(A)*** *TNF-α and* ***(B)*** *GM-CSF were subsequently measured. Healthy=4, Smokers=6, COPD=5. Error bars are representative of SEMs and one-way ANOVAs performed. Welch tests performed ratio paired t-tests performed****.***

3.1.9 TNF-α and GM-CSF concentrations in HBECs after infection with RV in basal cultures

The effect on inflammatory cytokines TNF-α and GM-CSF after 24 h of RV infection were then assessed by measuring supernatants. HBECs were infected with an increasing MOI of RV16 from 0.01 to 1 MOI in basal cultures.

There were no significant differences observed between the different groups in both TNF-α and GM-CSF protein levels at any dose of RV16. In addition there were no significant effects on TNF-α or GM-CSF or trends observed within groups either (Two-way ANOVA. p=0.95 and p=0.96) **(Figure 3.9a,b)**.

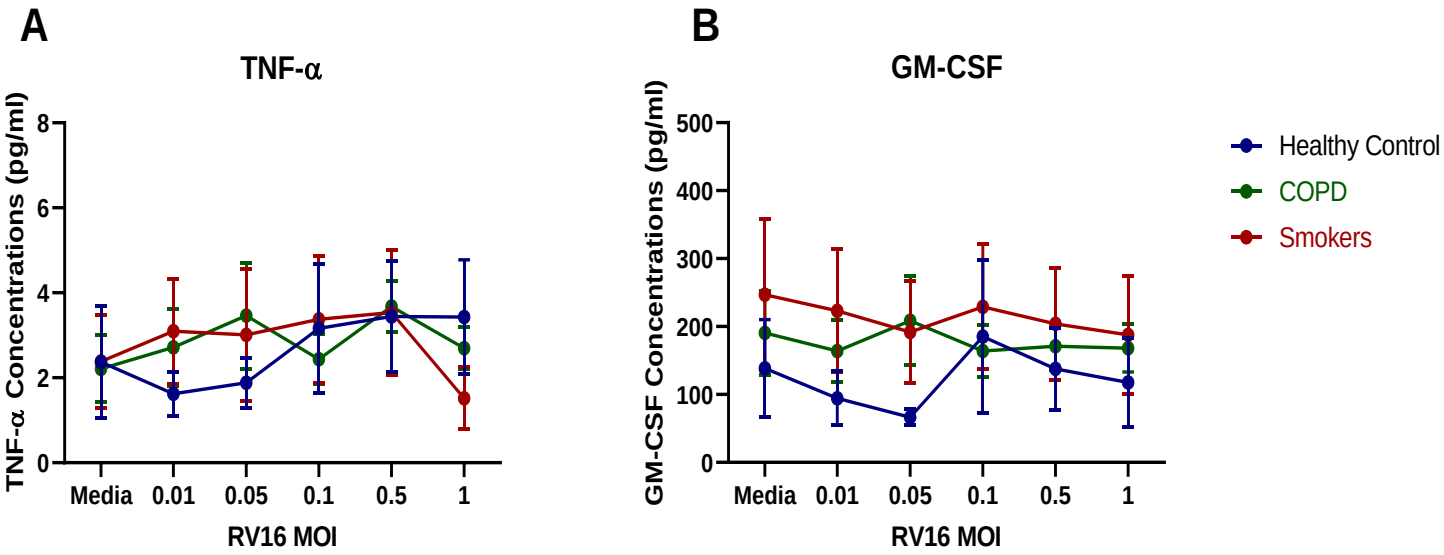


Figure 3.9: Concentration-dependent infection of RV16 does not affect inflammation in HBECs. *Three groups of HBECs were infected with RV16 at a dose of 0.01-1 MOI for 24 hours with the secreted cytokines* ***(A)*** *TNF-α and* ***(B)*** *GM-CSF measured. N: Healthy=4, Smokers=5, COPD=6. Error bars are representative of SEMs. Two-way ANOVAs and multiple unpaired t-tests were performed*

3.1.10 Response of pro-inflammatory cytokines in differentiated HBECs in response to RV infection

HBECs in healthy, smoker, and COPD patients were then infected with RV16 at a MOI of 0.01 for 24 h and GM-CSF and TNF-α were then measured. There were no changes in GM-CSF at the apical level in response to RV16 infection in all three groups **(Figure 3.10a)**. There were also no changes in basolateral changes of GM-CSF after RV16 infection **(Figure 3.10b)**.

Protein levels of TNF-α were unchanged in all three groups on the apical surface after RV16 infection as well **(Figure 3.10c)**. TNF-α levels at the basolateral side were unchanged as well however there was an increasing trend in COPD HBECs after RV16 infection **(Figure 3.10d)**.

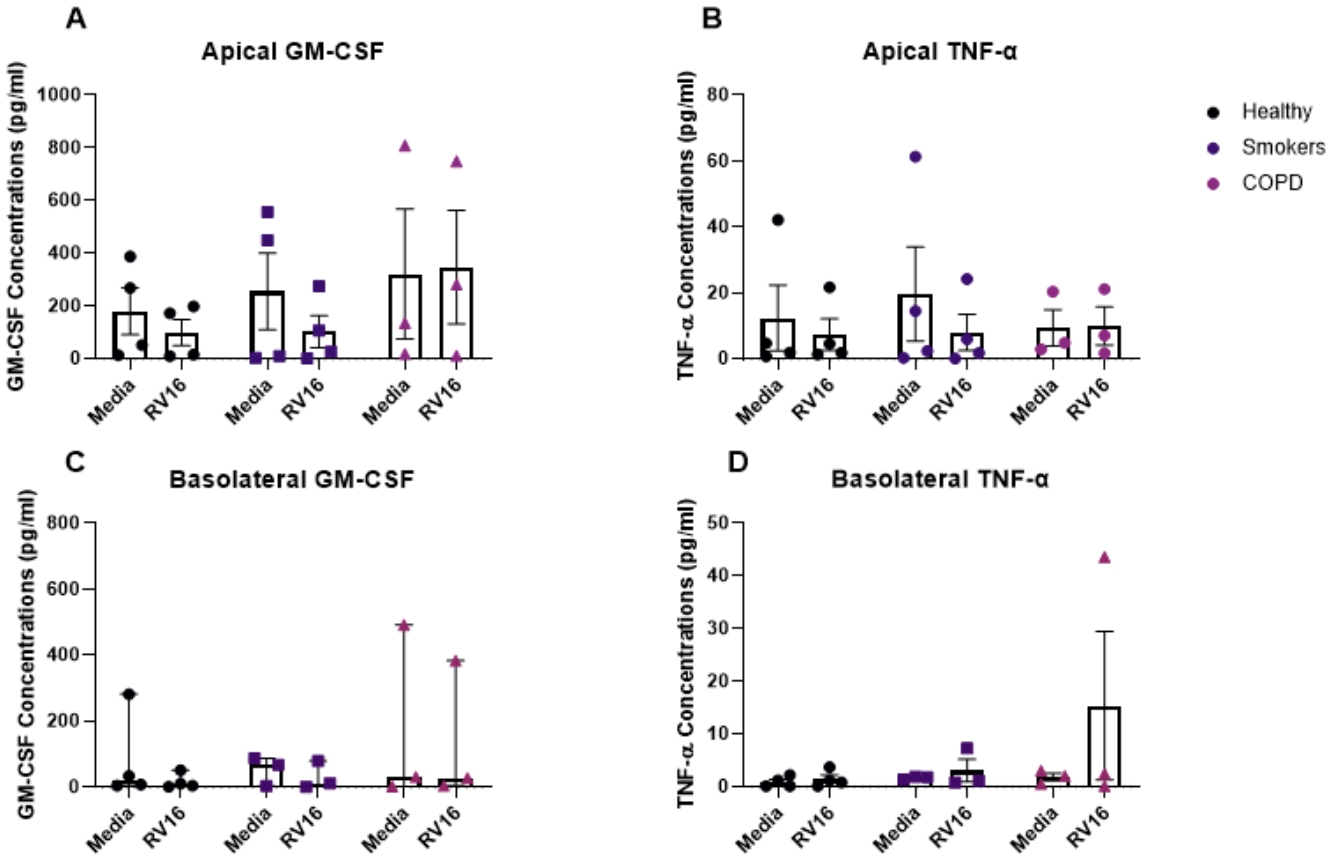


Figure 3.10: Inflammatory cytokines in differentiated HBECs in response to RV16 infection. *Healthy, smokers, and COPD HBECs were infected with 0.01 MOI of RV16 for 24 hours and* ***(A)*** *TNF-α and* ***(B)*** *GM-CSF were subsequently measured on the apical side and on* ***(C,D)*** *the basolateral side of the transwells respectively. N: Healthy=4, Smokers=3-4, COPD=3. Error bars are representative of SEM and one-way ANOVAs performed.*

3.1.11 Changes in alarmins in HBECs after stimulation with LPS

The effect of 20 ng/ml of LPS stimulation on alarmin concentrations after 24 hours was assessed through quantification of alarmins in healthy and COPD HBECs.

Concentrations of IL-25 were generally low however there was a significant 2-fold decrease in IL-25 after LPS stimulation in COPD HBECs (p=0.0382) **(Figure 3.11a)**.

No significant differences in TSLP were observed in response to LPS in healthy and COPD groups and no differences under basal conditions **(Figure 3.11b)**. IL-33 levels were undetectable or in very low quantities pre and post stimulation with LPS in healthy and COPD HBECs **(Figure 3.11c)**. Analytes were not measured in smoker HBECs due to a lack of plate availability to measure smoker samples.

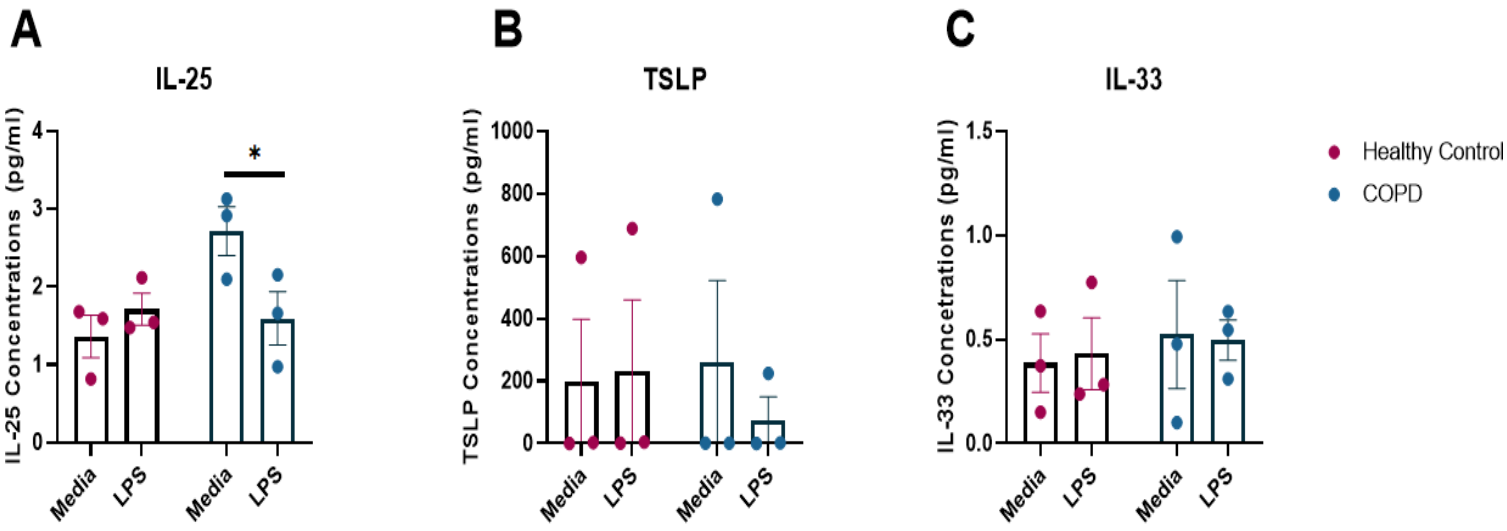


Figure 3.11: Change in Alarmins after LPS stimulation of HBECs in basal cultures. *HBECs in all three groups were stimulated with 20 ng/ml of LPS for 24 hours and levels of* ***(A)*** *IL-25 and* ***(B)*** *TSLP and* ***(C)*** *IL-33 concentrations were measured in supernatants. N: Healthy=3 and COPD=3. Error bars are representative of SEMs.* *******: p<0.05. Manny-Whitney and Wilcoxon correction tests performed.*

3.1.12 Effect on Alarmins in HBECs in response to LPS stimulation at ALI

The alarmins IL-25, TSLP, and IL-33 were also measured after 24 h of LPS stimulation at 20 ng/ml where HBECs were cultured at ALI. IL-25 levels were generally low in healthy, smokers and COPD HBECs at basal levels with means of 4.0, 1.7, and 0.8 pg/ml respectively on the apical side. There were no significant changes in IL-25 levels

after LPS stimulation either **(Figure 3.12a)**. IL-25 expression was also low on the basolateral side under basal conditions and while there were no significant changes in IL-25 expression there was a trend in decreasing IL-25 after LPS stimulation in smokers (p=0.14) **(Figure 3.12d)**.

TSLP levels secreted at the apical side were low in smokers and COPD HBECs (Means: 1.7 and 14.8 pg/ml) and however they were not significantly lower than levels found in healthy HBECs (Mean: 136.5 pg/ml) and there were no significant differences with LPS stimulation **(Figure 3.12b)**. Levels of TSLP were also low in smoker HBECs at the basolateral side however they were not significantly lower than healthy HBECs despite an observed increase (p=0.15) **(Figure 3.12e)**. No significant changes were observed after LPS stimulation at the basolateral side either in all three groups.

Protein levels of IL-33 were undetectable in almost all HBEC donors in all groups whether they were from healthy, smoker, or COPD patients and were not detectable after LPS stimulation both apically and on the basolateral side **(Figure 3.12c,f)**.

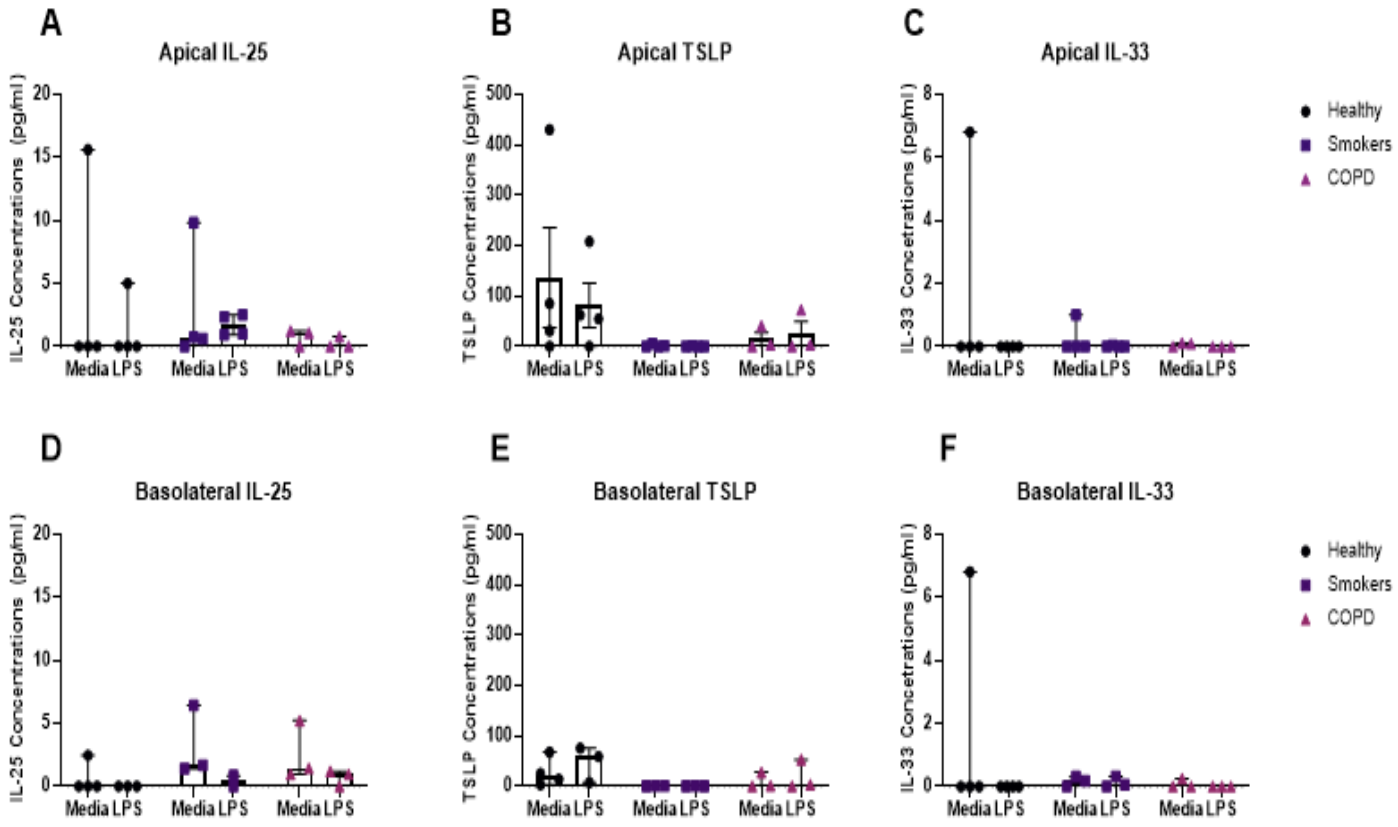


Figure 3.12: No change in Alarmins after LPS stimulation of HBECs in differentiated cultures. *HBECs in all three groups were stimulated with 20 ng/ml of LPS for 24 hours and levels of* ***(A)*** *IL-25 and* ***(B)*** *TSLP and* ***(C)*** *IL-33 were measured on the apical side as well as the* ***(D-F)*** *Basolateral side of the transwells. N: Healthy=4, Smokers=4, COPD=3. Error bars are representative of SEMs and one-way ANOVAs performed.*

3.1.13 Effect on alarmin release from monolayer HBECs early post-infection with NTHi

Alarmins were then assessed at an early time point of 4 hours in basal cultured HBECs post-infection with NTHi at an MOI of 10. There were no significant differences in IL-25 production either within groups or between groups of HBECs post-infection with levels of IL-25 being largely undetectable **(Figure 3.13a)**.

Similarly, no changes were observed in TSLP post-infection with NTHi between all HBECs groups and within groups post-infection **(Figure 3.13b)**. Levels of IL-33 were mostly undetectable in all groups pre and post-infection with NTHi **(Figure 3.13c)**.

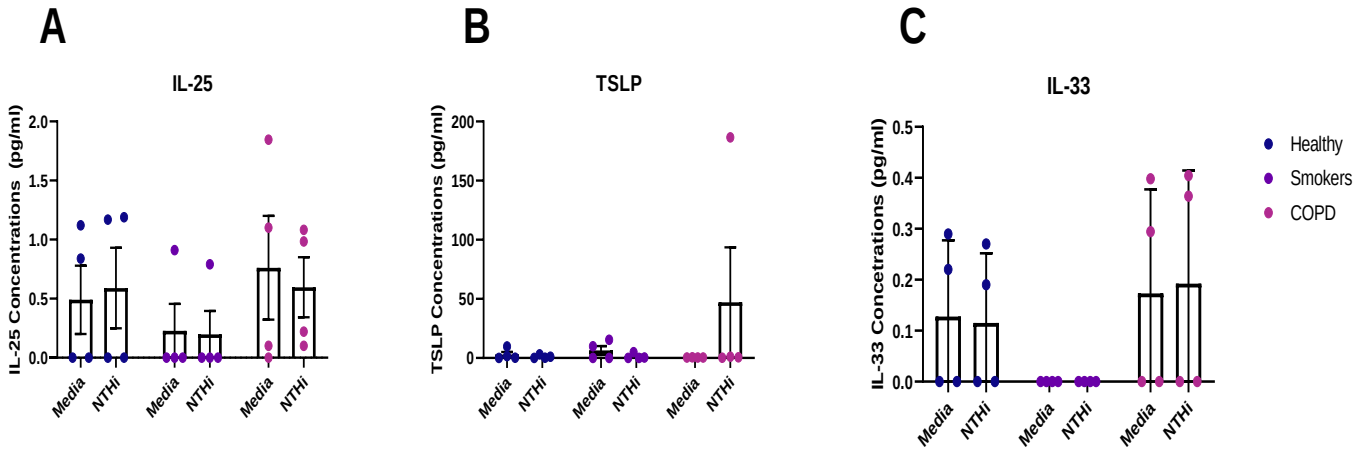


Figure 3.13: Alarmin Concentrations were unaffected after early Infection of NTHi in HBECs. *The cytokines* ***(A)*** *IL-25 and* ***(B)*** *TSLP and* ***(C)*** *IL-33 were measured in supernatants by multiplex after 4 hours of NTHi infection at an MOI of 10. N: Healthy=4, Smokers=4, COPD=4. Error bars are representatives of SEM. Welch tests and ratio paired t-tests performed.*

3.1.14 Alarmin concentrations after NTHi infection in HBEC basal cultures

The alarmins IL-25, TSLP, and IL-33 were also measured after a concentration-dependent infection with NTHi. IL-25 in healthy HBECs was largely undetectable with increasing MOIs of NTHi. There was an increase in IL-25 in COPD and smoker HBECs at higher doses of NTHi however there was no significant trend with increasing doses of NTHi (Two-way ANOVA, p=0.0523) **(Figure 3.14a)**. Within groups, there were no significant differences in IL-25 between COPD and healthy HBECs after NTHi infection despite observable differences. However, there were significant differences between smoker and healthy HBECs at MOIs of 0.1 and 10 (p=0.016 and p=0.0476) **(Figure 3.14a)**.

In terms of TSLP concentrations, a concentration-dependent increase was observed in all three groups of HBECs after NTHi infection (Two-way ANOVA, p=0.0056) **(Figure 3.14b)**. There were however no significant differences in TSLP between the three groups despite observable differences between them.

Lastly, levels of IL-33 were largely undetectable in all three groups despite NTHi infection and thus did not respond to NTHi infection **(Figure 3.14c)**.

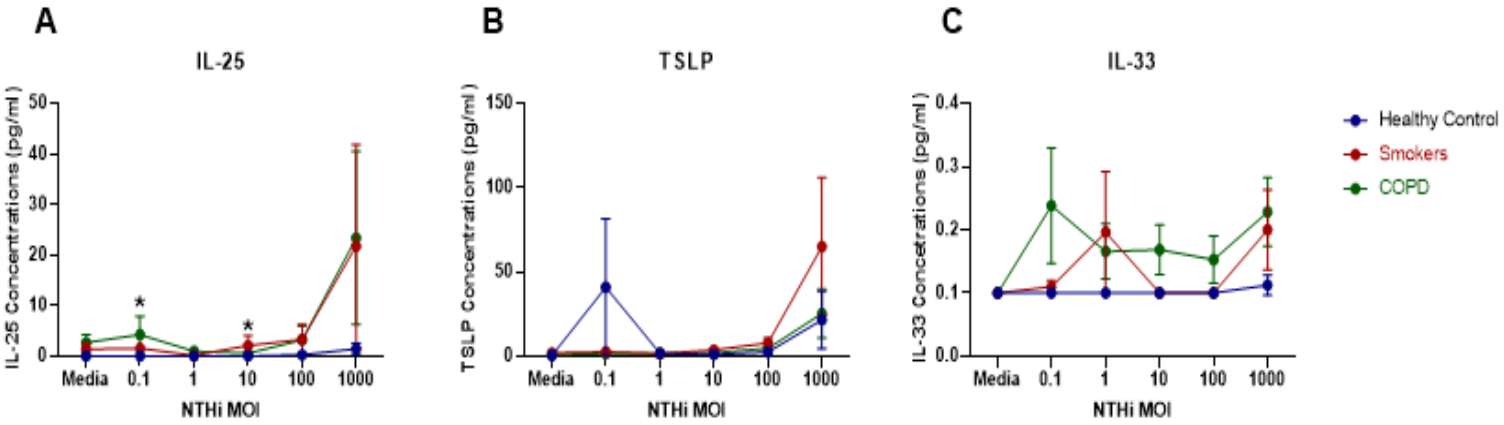


Figure 3.14: Alarmin Concentrations after concentration-dependent Infection of NTHi in HBECs after 24 H from 0.01-1 MOI. *The cytokines* ***(A)*** *IL-25 and* ***(B)*** *TSLP (Two-way ANOVA, p=0.0056) and* ***(C)*** *IL-33 were measured in supernatants by multiplex after 24 hours. N numbers: Healthy=4, Smokers=5, COPD=7. * indicates p<0.05. Error bars are representatives of SEM. Two-way ANOVAs and multiple unpaired t-tests performed.*

3.1.15 Changes in alarmins after NTHi stimulation in ALI cultures of HBECs

HBECs cultured at ALI were infected with NTHi at a MOI of 10 for 24 hours. Levels of IL-25 remained largely undetectable with no significant changes observed even after infection on the apical side **(Figure 3.15a)**. Similarly, no changes were found in IL-25 after infection on the basolateral side **(Figure 3.15d)**.

TSLP expression did not differ in all three groups after NTHi infection on the apical side of the cultures **(Figure 3.15b)**. Similarly, no significant differences in TSLP were

observed on the basolateral side after NTHi infection **(Figure 3.15e)**. IL-33 remained largely undetectable as well despite NTHi infection on both sides of the transwells **(Figure 3.15c,f)**.

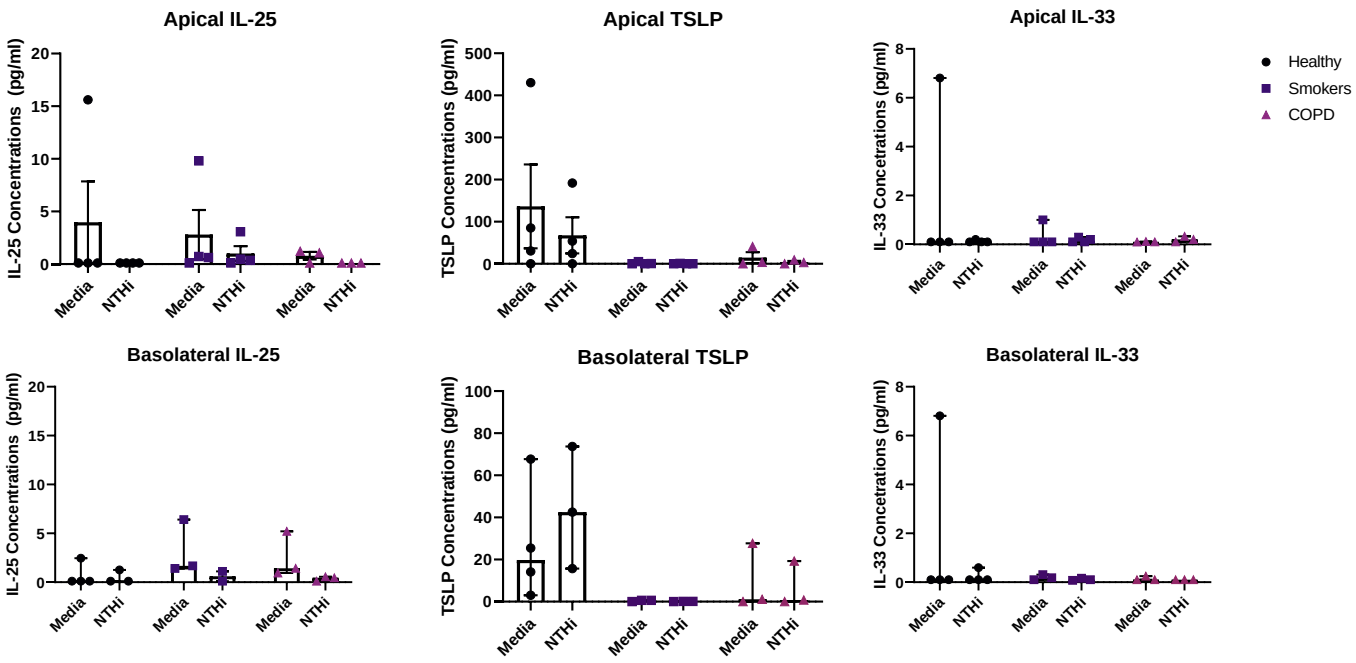


Figure 3.15: Alarmins post-infection with NTHi in HBECs in differentiated cultures. *HBECs in all three groups were stimulated with 10 MOI of NTHi for 24 hours and levels of* ***(A)*** *IL-25 and* ***(B)*** *TSLP and* ***(C)*** *IL-33 were measured on the apical side as well as the* ***(D-F)*** *Basolateral side of the transwells respectively. N: Healthy=4, Smokers=4, COPD=3. Error bars are representative of SEMs and one-way ANOVAs performed.*

3.1.16 Alarmin levels post poly I:C stimulation of healthy and COPD HBECs

Healthy and COPD HBECs were stimulated with 25 µg/ml of poly I:C for 24 hours and the alarmins IL-25, TSLP, and IL-33 were measured. There were no significant changes observed in IL-25 levels after poly I:C stimulation although there was an observable increase in COPD HBECs after stimulation despite the lack of significance (p=0.208) **(Figure 3.16a)**. Differences between healthy and COPD HBECs were not significant.

Similarly, there were no significant changes in TSLP after poly I:C stimulation in healthy and COPD HBECs however there was an observable increase in both groups (p=0.06 and p=0.09) **(Figure 3.16b)**. IL-33 was not detectable in all other stimulations or infections in HBECs however IL-33 was higher after poly I:C stimulation in healthy and COPD HBECs. There was an observed increase in IL-33 in healthy and COPD HBECs after poly I:C stimulation but the increase was no significant (p=0.061 and p=0.15) **(Figure 3.16c)**. Alarmins in smokers were not measured due to a lack of plate availability.

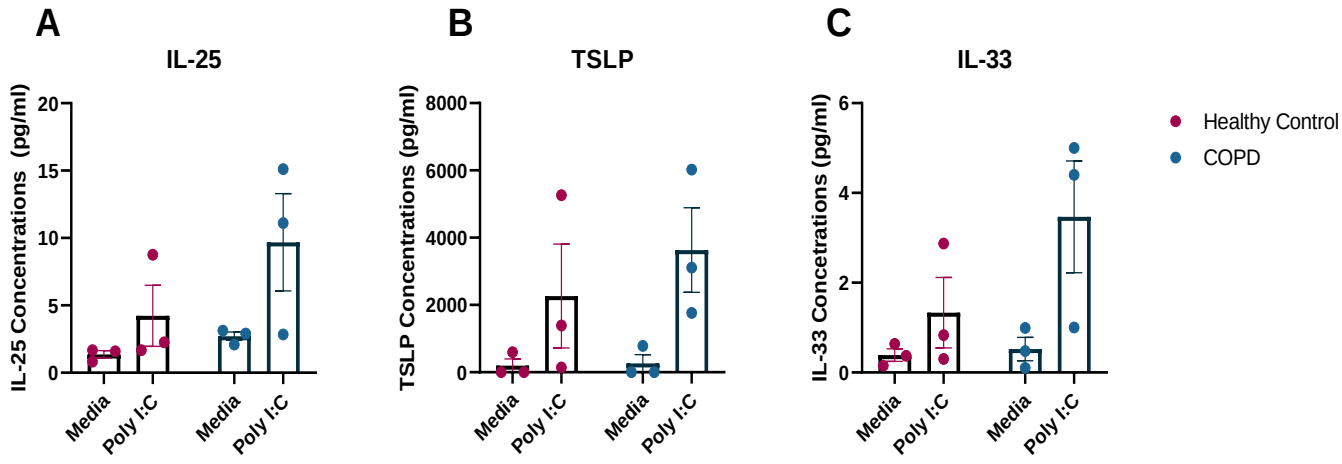


Figure 3.16: Effect on Alarmins in response to Poly I:C in basal HBECs. *HBECs were at a monolayer in all three groups were stimulated with 25 µg/ml of poly I:C for 24 hours and levels of* ***(A)*** *IL-25 and* ***(B)*** *TSLP and* ***(C)*** *IL-33 were measured in supernatants using a multiplex platform. N: Healthy=3 and COPD=3. Error bars are representative of SEMs. Mann-Whitney and Welch correction t-tests performed.*

3.1.17 Alarmins expression after stimulation of HBECs with poly I:C at ALI

The cells then underwent stimulation with 25 µg/ml of poly I:C for 24 h when cultured at ALI. There were no changes in IL-25 expression after poly I:C stimulation on the apical side **(Figure 3.17a)**. There was a decreasing trend after poly I:C stimulation in smoker and COPD HBECs on the basolateral side however the decrease was only significant in smoker HBECs with approximately a 7-fold decrease (p=0.018) **(Figure**

3.17d). The initial levels of IL-25 however were quite small going from 3.16 pg/ml to 0.43 pg/ml.

There were no significant changes in TSLP expression after poly I:C stimulation under basal conditions apically however there was a mean increase in COPD HBECs after stimulation although it was not significant (Means: 14.8 and 68.6 pg/ml, p=0.185) **(Figure 3.17b)**. A similar trend in TSLP was observed in COPD HBECs after poly I:C stimulation on the basolateral side as well (p=0.19) **(Figure 3.17e)**.

Finally, IL-33 remained largely undetectable in all three groups after poly I:C stimulation on the apical side as well as the basolateral **(Figure 3.17c,f)**.

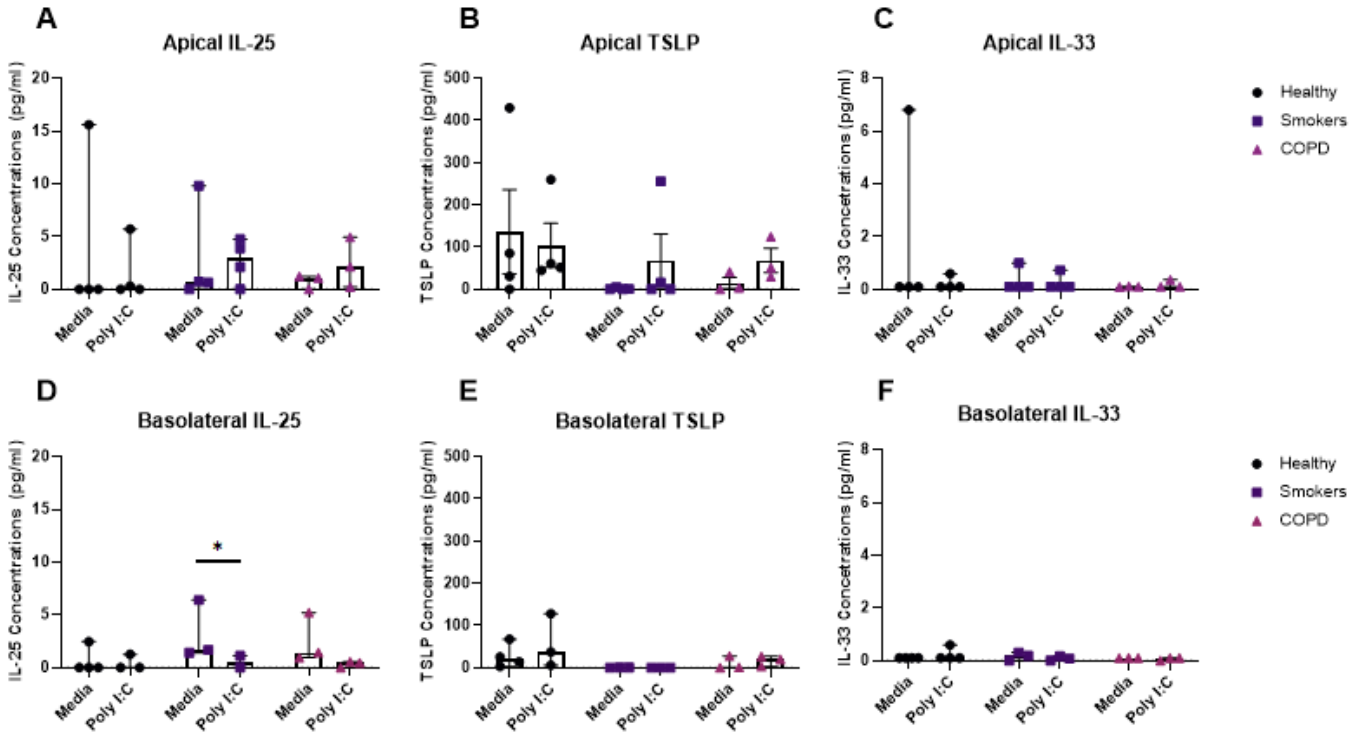


Figure 3.17: Effect on Alarmins in response to poly I:C in differentiated HBECs. *HBECs were at ALI in all three groups were stimulated with 20 ng/ml of LPS for 24 hours and levels of* ***(A)*** *IL-25 and* ***(B)*** *TSLP and* ***(C)*** *IL-33 were measured on the apical side as well as the* ***(D-F)*** *Basolateral side of the transwells respectively. N: Healthy=4, Smoker=3-4, COPD=3. Error bars are representative of SEMs. Mann-Whitney, Welch Correction, and ratio paired t-tests performed * : p<0.05.*

3.1.18 RV infection of HBECs does not change alarmin levels early on post-infection

Alarmins were measured 4 hours post-infection with 0.01 MOI of RV. IL-25 quantities were largely undetectable in all three groups and there were no differences found post-infection in HBECs or between three groups **(Figure 3.18a)**. However, there was a significant 54% decrease from baseline in infected COPD HBECs but IL-25 levels were either low or undetectable particularly post-infection (p=0.0233).

No changes were observed in TSLP either between the three groups or post-infection with RV16 infection and IL-33 was largely undetectable in almost all conditions and thus no comparisons were possible **(Figure 3.18b,c)**.

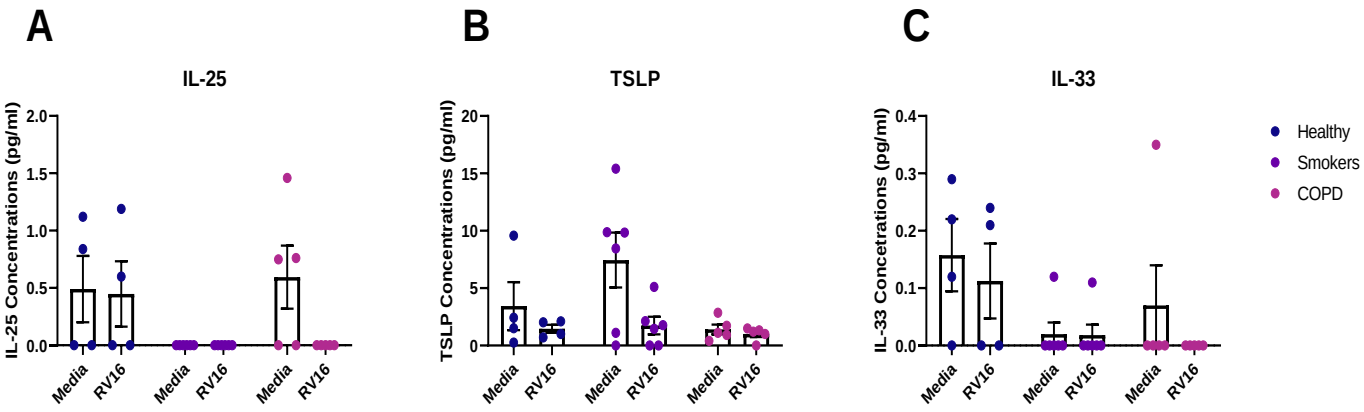


Figure 3.18: Effect on Alarmins in response to an early timepoint RV16 infection. *HBECs were at a monolayer culture in all three groups were stimulated with 0.01 MOI of RV16 for 24 hours and levels of **(A)** IL-25 and **(B)** TSLP and **(C)** IL-33 were measured in supernatants. N: Healthy=4, Smokers=6, COPD=5. Error bars are representative of SEMs Welch t-tests and ratio paired t-tests performed.*

3.1.19 Alarmin expression in basal cultures after RV infection

The aforementioned alarmins were then measured after a dose infection with RV16 from 0.01 to 1 MOI after 24 hours of infection. IL-25 expression were 3-fold greater in healthy HBECs than the levels found in COPD HBECs at MOIs of 0.1 and 0.5 (p=0.035

and p=0.012). Expression of IL-25 was also significantly higher in healthy HBECs than smoker HBECs at MOIs of 0.1, 0.5, and 1 (p=0.016, p=0.0047, and 0.022) **(Figure 3.19a)**. There were however no differences observed within groups and it should be noted that levels of IL-25 were generally low and occasionally undetectable particularly in smoker HBECs (Two-way ANOVA: p=0.53) **(Figure 3.19a)**.

There were no significant differences in the protein levels of TSLP between groups of HBECs in response to RV infection. In addition, there were no significant differences within groups after infection with RV regardless of the dose utilized to infect the HBECs (Two-way ANOVA: p=0.3624) **(Figure 3.19b)**.

Levels of IL-33 were mostly undetectable in all groups and conditions in HBECs even after RV infection **(Figure 3.19c)**.

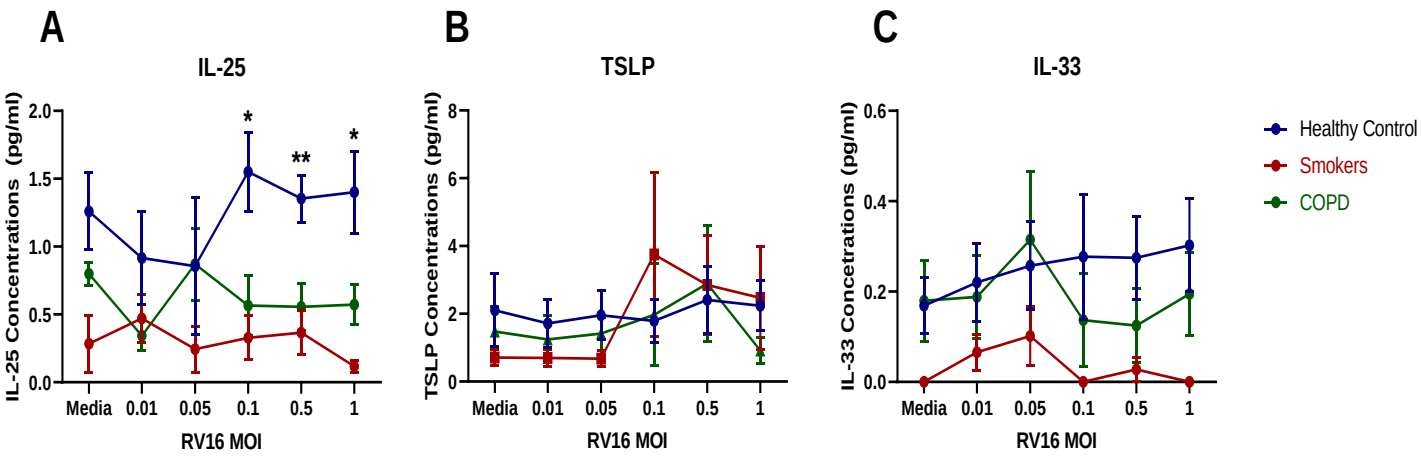


Figure 3.19: Effect on Alarmins in response to different doses of RV16 infection. *HBECs were at ALI in all three groups were stimulated with RV16 for 24 hours from MOIs of 0.01-1 and concentrations of **(A)** IL-25 and **(B)** TSLP and **(C)** IL-33 were measured. N; Healthy=4, Smokers=5, COPD=6. Error bars are representative of SEMs. * : p<0.05, **: p<0.005. Two-way ANOVAs and multiple unpaired t-tests performed.*

3.1.20 Alarmins in HBECs cultured at ALI after RV infection

HBECs cultured at ALI were then infection with 0.01 MOI RV16 for 24 hours and the secreted alarmins IL-25, TSLP, and IL-33 were subsequently measured. Protein expression of IL-25 was unchanged in response to RV16 infection in all three groups on both sides of the transwells **(Figure 3.20a,d)**.

There were no significant changes in secreted TSLP on the apical side after RV infection however there was a decreasing trend in healthy HBECs with the means going from 136.5 to 38.9 pg/ml **(Figure 3.20b)**. No significant changes driven by RV16 infection were observed in TSLP on the basolateral side either **(Figure 3.20e)**. IL-33 remained largely undetectable in all three groups with or without infection in all three groups and thus no changes were observed **(Figure 3.20c,f)**.

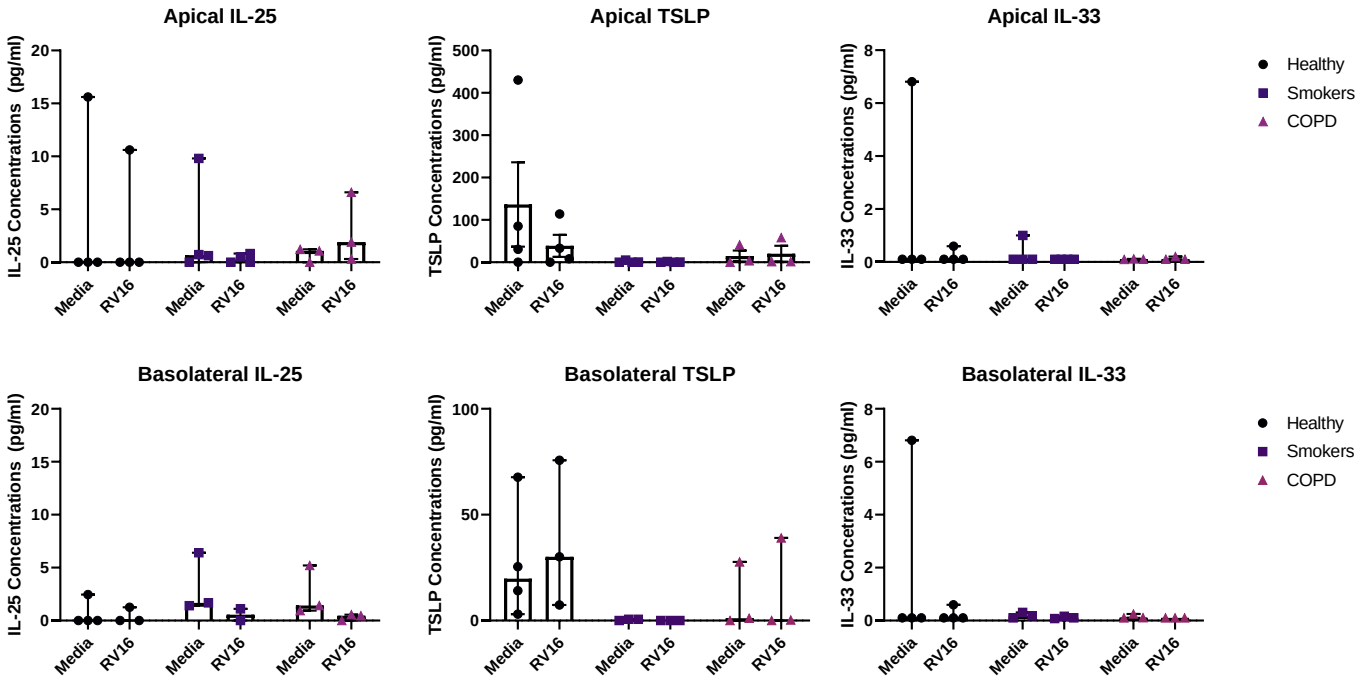


Figure 3.20: Alarmin expression in response to RV16 in differentiated HBECs. *HBECs were at ALI in all three groups were infected with 0.01 MOI of RV16 for 24 hours and levels of* ***(A)*** *IL-25 and* ***(B)*** *TSLP and* ***(C)*** *IL-33 were measured on the apical side as well as the* ***(D-F)*** *Basolateral side of the transwells. N: Healthy=4, Smoker=3-4, COPD=3. Error bars are representative of SEMs and one-way ANOVAs performed.*

3.1.21 Type I and Type III IFN response in HBECs in response to LPS stimulation

The innate anti-viral response was then assessed by measurement of IFNα2a, IFNβ1, and IFNλ1 after 20 ng/ml of LPS stimulation after 24 hours. IFNα2a concentrations were either very low or undetectable in healthy and COPD HBECs and thus no differences were observed **(Figure 3.21a)**.

IFNβ1 levels were also unchanged in response to LPS stimulation in all three groups however there was a sizeable difference between stimulated healthy and stimulated smoker HBECs despite having no significance (p=0.1035) **(Figure 3.21b)**.

In alignment with IFNβ1, there were no significant difference after LPS stimulation in IFNλ1 concentration in all three groups of HBECs and no differences between groups at basal levels or post stimulation **(Figure 3.21c).**

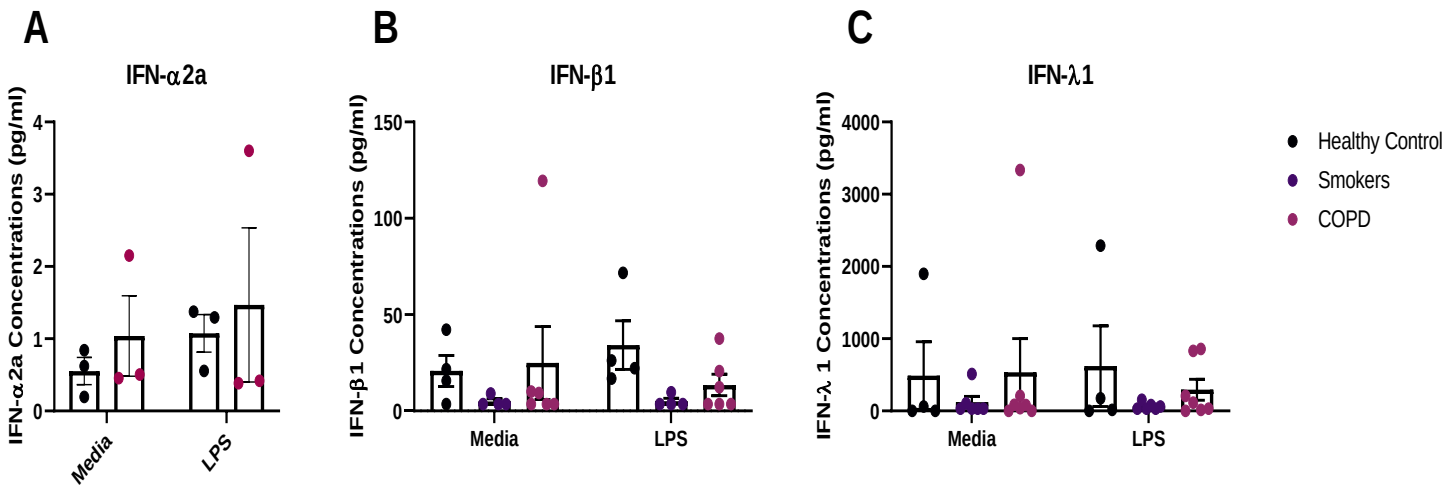


Figure 3.21: Innate anti-viral response in HBECs is unchanged after LPS stimulation. *HBECs in all three groups were stimulated with 20 ng/ml of LPS for 24 hours and levels of* ***(A)*** IFNα2a *and* ***(B)*** IFNβ1 *and* ***(C)*** IFNλ1 concentrations *were measured in supernatants. N: Healthy=3-4, Smokers=4-6, COPD=6-7. Error bars are representative of SEMs one-way ANOVAs performed. Manny-Whitney and Wilcoxon correction t-tests performed.*

3.1.22 Type I and Type III IFN production in HBECs in response to LPS at ALI

The type I and type III IFNs were then measured after 20 ng/ml of LPS stimulations for 24 hours in HBECs cultured at ALI. IFNα2 levels were undetectable in all three groups on both the apical and basolateral side of the transwells at basal levels and after LPS stimulation **(Figure 3.22a,d)**. There were no significant differences in levels of IFNβ1 on the apical side between different groups or after LPS stimulation although there was an observed increase in COPD HBECs from smokers at basal levels although it was not significant (Means: 44.2 and 2.7 pg/ml, p=0.0571) **(Figure 3.22b)**. On the basolateral level, there were no significant differences in IFNβ1 between all three groups at basal levels with no response after LPS stimulation although there was an increase in smoker HBECs after LPS stimulation (p=0.18) **(Figure 3.22e)**.

In terms of levels of IFNλ1 in response to LPS, there were no significant changes in IFNλ1 production either at basal levels in all through groups or after LPS stimulation on the apical side **(Figure 3.22c)**. On the basolateral side, IFNλ1 was largely undetectable in all three groups and was unchanged in response to LPS **(Figure 3.22f)**.

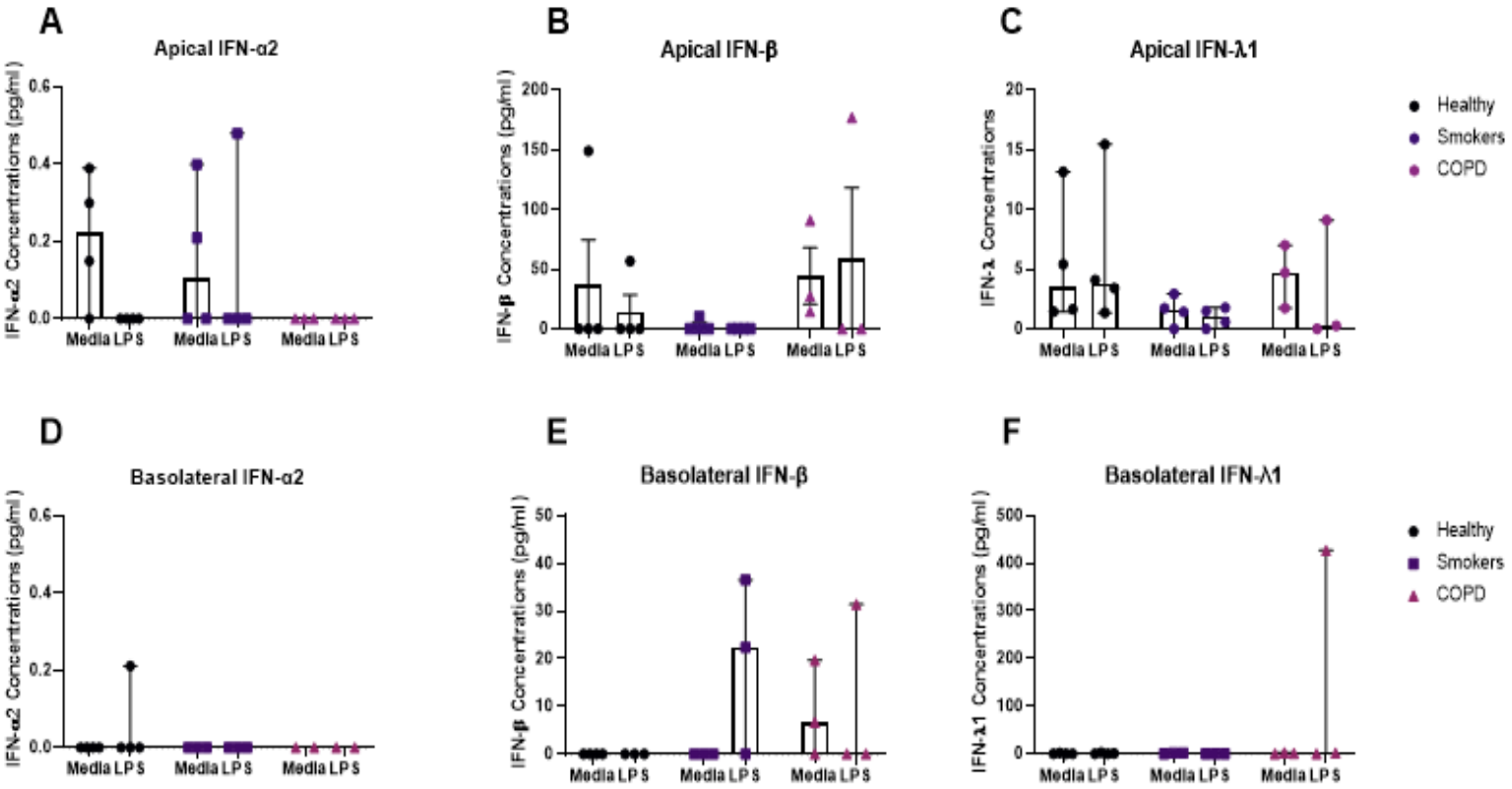


Figure 3.22: Innate anti-viral response in differentiated HBECs after LPS stimulation is unchanged. *HBECs in all three groups were stimulated with 20 ng/ml of LPS for 24 hours and levels of* ***(A)*** IFNα2a *and* ***(B)*** IFNβ1 *and* ***(C)*** IFNλ1*were measured on the apical side as well as the* ***(D-F)*** *Basolateral side of the transwells. N: Healthy=4, Smokers=3-4, COPD=3. Error bars are representative of SEMs. Welch t-tests and ratio paired t-tests performed.*

3.1.23 IFN responses in HBECs after early infection with NTHi are unaffected

Type I and type III IFNs were quantified at an early time point of 4 hours post-infection with NTHi at 10 MOI. IFNα2a was undetectable in all three groups pre and post-infection **(Figure 3.23a)**.

No changes were observed in IFNβ1 post-infection with NTHi in either healthy, smokers, or COPD HBECs with no differences observed within groups as well **(Figure 3.23b)**. Finally, similar to IFN β1, no differences were observed in quantities of IFNλ1 post-infection of HBECs with NTHi and no difference found between groups as well **(Figure 3.23c)**.

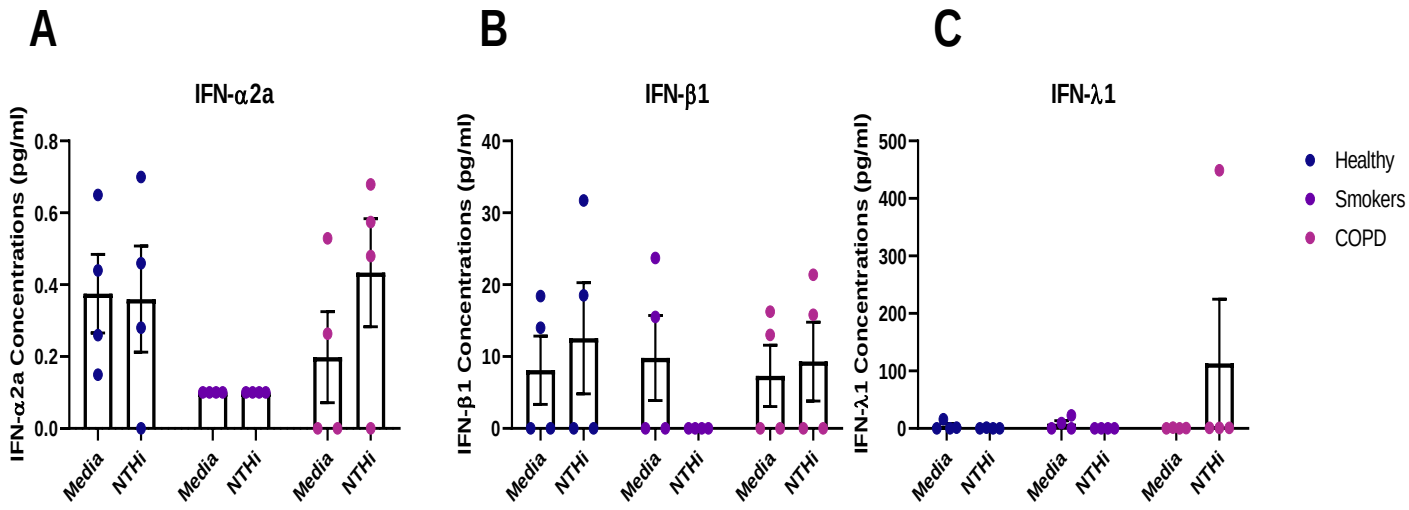


Figure 3.23: Effect of NTHi infection in an early time point on Type I and Type III IFN Concentrations in HBECs. *Concentrations of the cytokines **(A)** IFNα2 and **(B)** IFNβ1 and **(C)** IFNλ1 were measured in supernatants by multiplex after 24 hours of NTHi infection at an MOI of 10. N: Healthy=4, Smoker=4, COPD=4. Error bars are representatives of SEM. Manny-Whitney and Wilcoxon correct tests performed.*

3.1.24 NTHi infection effect on Type I and Type III IFNs in HBECs in basal cultures

The type I and type III IFNs were measured after a concentration-dependent NTHi infection in the three groups of HBECs after 24 hours. Levels of IFNα2a were largely undetectable in all three groups with no response to NTHi infection and thus there were no changes found within or between groups of HBECs **(Figure 3.24a)**.

IFNβ1 concentrations decreased after NTHi infection in all three groups however unlike healthy HBECs, IFNβ1 levels started to increase again in COPD and smoker HBECs after infecting with NTHi at MOIs greater than 10 (Two-way ANOVA, p=0.0367) **(Figure 3.24b)**. This indicates that inhibitory signalling after NTHi infection against IFNβ1 production is dysfunctional in smoker and COPD HBECs. However,

differences in IFNβ1 concentrations between the three groups were not significantly different in response to NTHi infection **(Figure 3.24b)**.

Concentrations of IFNλ1 were largely undetectable in healthy HBECs however there was a concentration-dependent increase in levels of IFNλ1 in smoker and COPD HBECs in response to NTHi infection (Two-way ANOVA, p=0.0381) **(Figure 3.24c)**. There was also a significant difference in IFNλ1 between healthy and COPD HBECs in response to NTHi at an MOI of 100 with COPD HBECs having over 20-fold more IFNλ1 concentrations (p=0.006) **(Figure 3.24c)**.

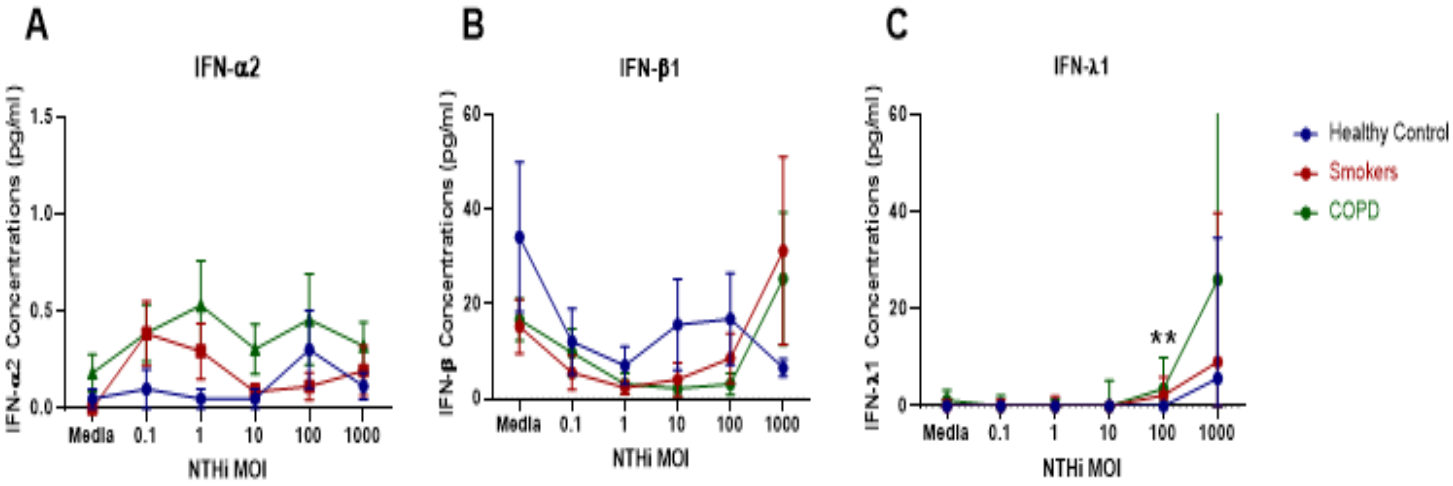


Figure 3.24: Effect of Concentration-dependent Infection of NTHi on Type I and Type III IFN Concentrations in HBECs. *The cytokines **(A)** IFNα2 and **(B)** IFNβ1 (Two-way ANOVA, p=0.0367) and **(C)** IFNλ1 (Two-way ANOVA, p=0.0381) were measured in supernatants by multiplex after infection with NTHi for 24 hours from MOIs of 0.1-1000. N numbers: Healthy=4, Smokers=5, COPD=7. ** indicates p<0.005. Error bars are representatives of SEM. Two-way ANOVAs and multiple unpaired t-tests performed.*

3.1.25 Production of IFNα2a, IFNβ1, and IFNλ1 after NTHi infection in differentiated HBECs

IFNα2 remained largely undetectable after infection with NTHi at a MOI of 10 for 24 hours on both sides of the transwells **(Figure 3.25a,d)**. There were no significant differences in IFNβ1 expression after NTHi infection on the apical side in smoker and healthy HBECs. However, there was a significant decrease of over 40-fold in IFNβ1

after infection in COPD HBECs going from 44.2 pg/ml to undetectable levels which is a similar response to what was observed in monolayer cultures (p=0.0085) **(Figure 3.25b)**. There were no significant differences in IFNβ1 on the basolateral side however despite an apparent decrease observed in COPD HBECs as well after NTHi infection (p=0.189) **(Figure 3.25e)**.

IFNλ1 levels were no significantly altered after NTHi infection on all three groups on the apical side although there was an increase observed in smoker HBECs from from 1.55 to 4.7 pg/ml (p=0.19) **(Figure 3.25c)**. There were no significant changes in IFNλ1 expression after NTHi infection on the basolateral side in healthy, smoker, and COPD HBECs **(Figure 3.25f)**.

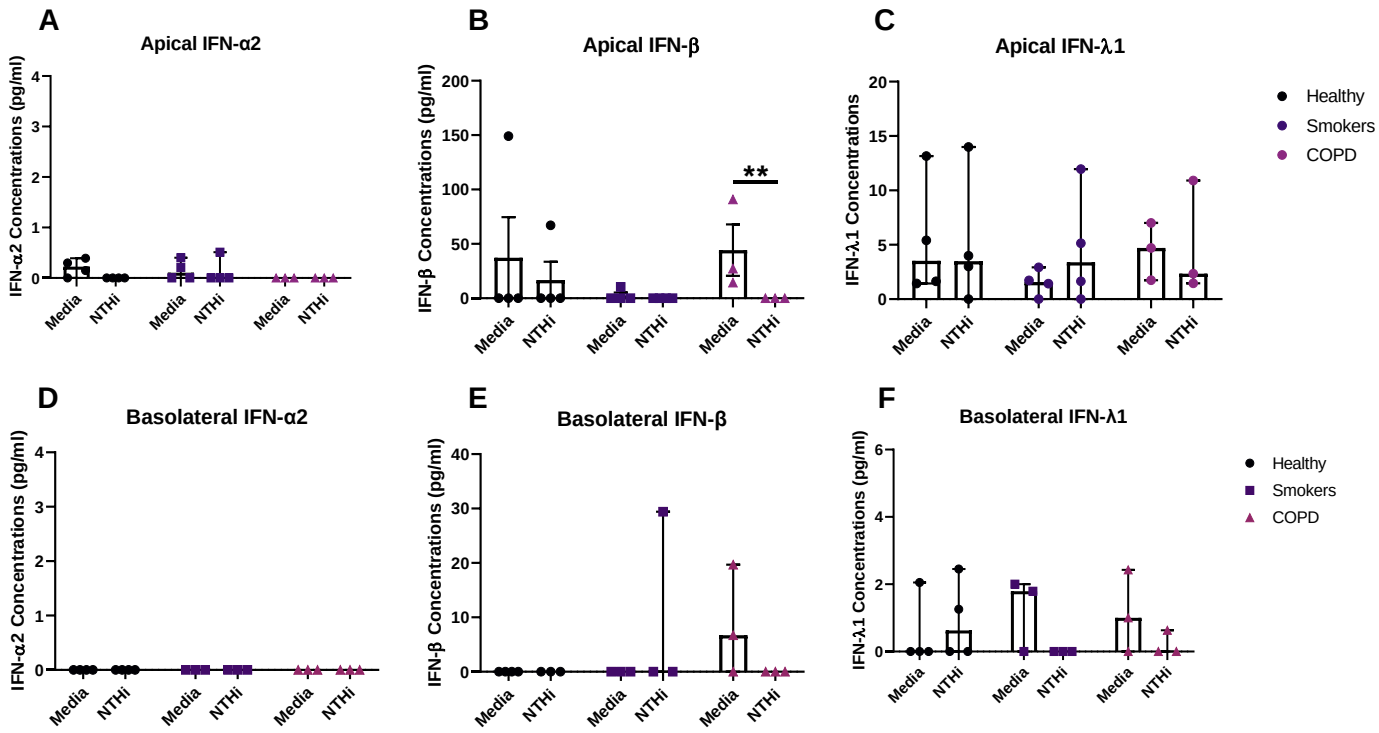


Figure 3.25: IFN levels in differentiated HBECs post-infection with NTHi. *HBECs in all three groups were infected with NTHi at a MOI of 10 for 24 hours and levels of* ***(A)*** IFNα2 *and* ***(B)*** IFNβ1 *and* ***(C)*** IFNλ1 *were measured on the apical side as well as the* ***(D-F)*** *Basolateral side of the transwells. N: Healthy=4, Smokers=3-4, COPD=3. Error bars are representative of SEMs. ** : p<0.005. Welch tests and ratio paired t-tests performed.*

3.1.26 Type I and type III IFN concentrations in HBECs in response to poly I:C cultured on a monolayer

The innate anti-viral response was assessed in HBECs after poly I:C stimulation by the measurement of IFNα2a, IFNβ1, and IFNλ1. Levels of IFNα2a has generally been low or undetectable however there was a large increase observed after poly I:C stimulation in COPD HBECs going from 0.50 to 16.8 pg/ml but the increase was not significant (p=0.079) **(Figure 3.26a)**.

Concentrations of IFNβ1 were significantly increased after poly I:C stimulation in healthy and COPD HBECs by around 1.5-logs (p=0.0442 and p=0.0026) **(Figure 3.26b)**. In addition levels of IFNβ1 in healthy and COPD HBECs were significantly greater than smoker HBECs after stimulation (p=0.029 and p=0.038) **(Figure 3.26b)**.

IFNλ1 levels were significantly increased in COPD HBECs after poly I:C stimulation but not in healthy or smoker HBECs (p=0.047). IFNλ1 was significantly greater in stimulated healthy and COPD HBECs compared to stimulated smokers as well (p=0.019 and p=0.035) **(Figure 3.26c)**.

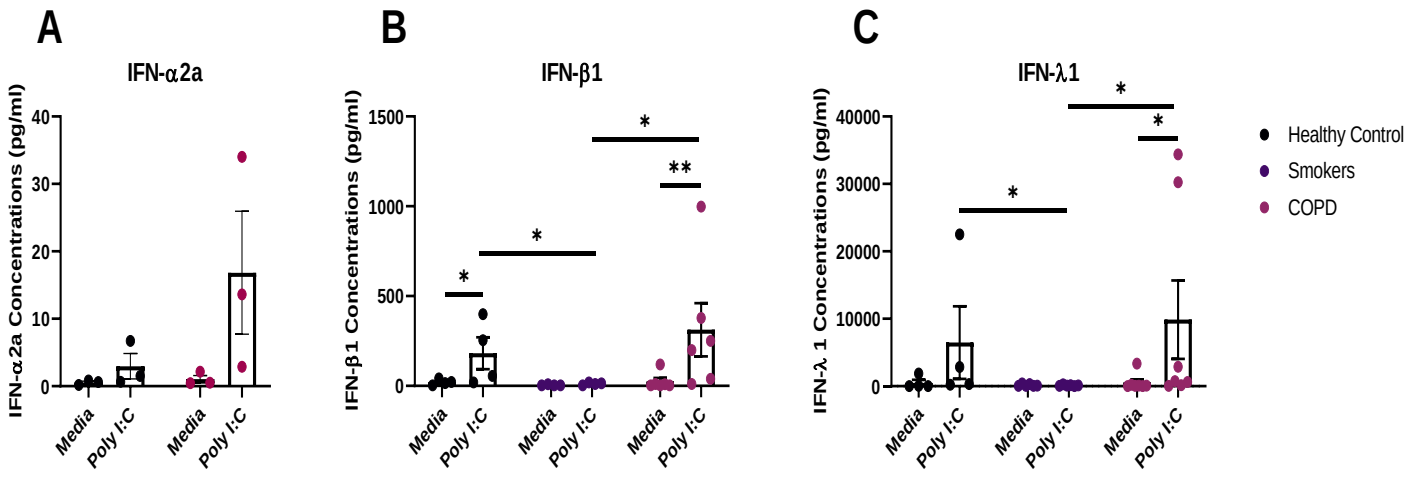


Figure 3.26: HBECs respond to poly I:C stimulation through innate anti-viral cytokine secretion. *Healthy, smokers, and COPD HBECs were stimulated with 25 µg/ml of poly I:C for 24 hours and the concentrations of **(A)** IFNα2a, **(B)** IFNβ1, and **(C)** IFNλ1 were measured. *: p<0.05, **: p<0.005. N: Healthy=3-4, Smokers=4-5, COPD=6-7, Error bars are representative as SEMs. Welch t-tests and Wilcoxon correction tests performed.*

3.1.27 Effect of poly I:C stimulation on innate IFNs in differentiated HBECs

IFNα2 production remained unchanged after stimulation of HBECs with poly I:C after 24 h in all three groups by being largely undetectable on both surfaces with no significant changes between or within groups **(Figure 3.27a,c)**. There were no significant changes in IFNβ1 after poly I:C stimulation in all three groups despite a sizeable increase observed in healthy HBECs (Means: 37.3 to 6532 pg/ml, p=0.342) **(Figure 3.27b)**. Similarly, no changes were observed in IFNβ1 production after poly I:C stimulation on the basolateral level **(Figure 3.27e)**.

There was an observable increase in IFNλ1 production on the apical side after poly I:C stimulation in healthy HBECs, from 5.41 to 1201 pg/ml, as well as smoker HBECs, from 1.55 to 7542 pg/ml, despite not being significant (p=0.129 and p=0.058) **(Figure 3.27c)**. No significant changes were observed in COPD HBECs after stimulation. There were no significant changes in IFNλ1 after stimulation on the basolateral side despite an increasing trend in COPD HBECs **(Figure 3.27f)**.

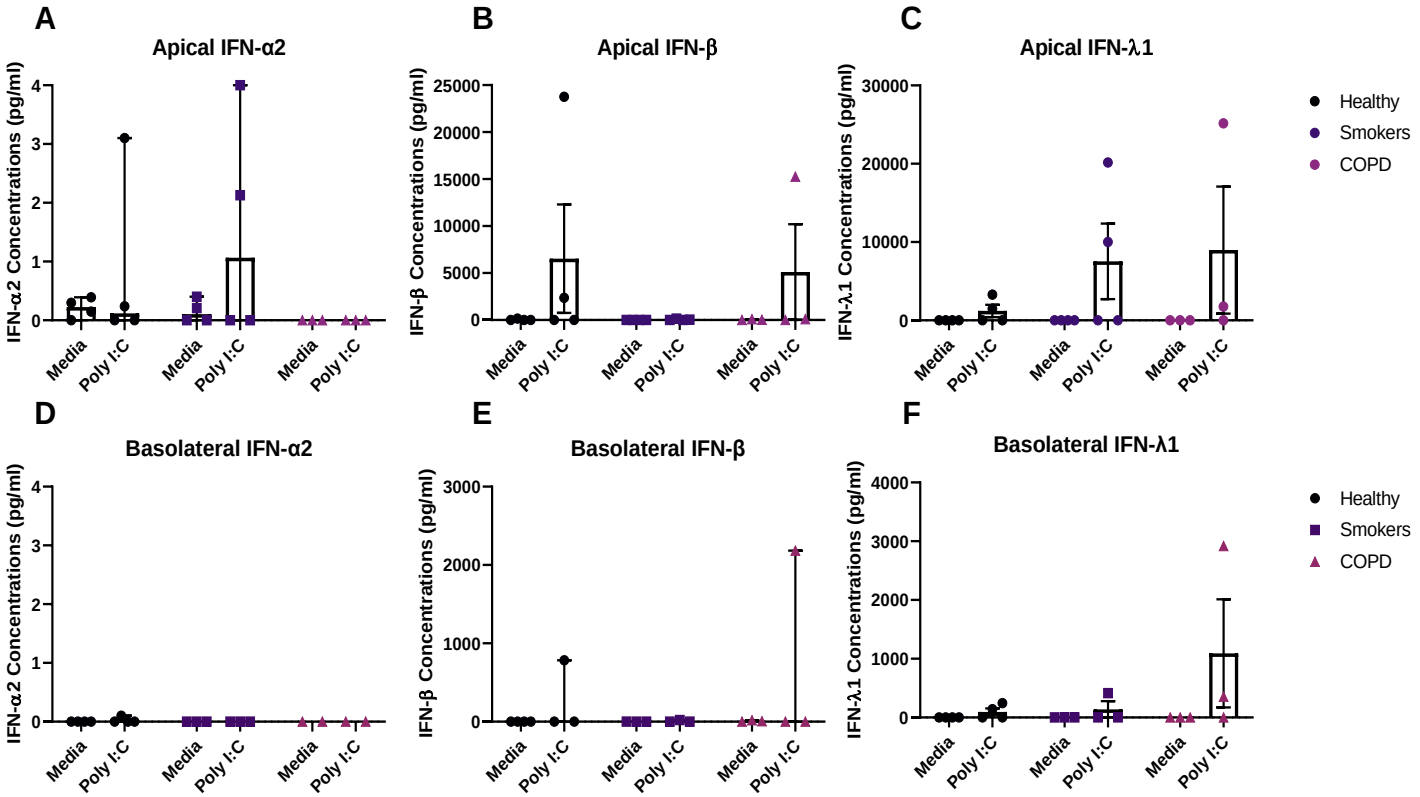


Figure 3.27: IFN levels in differentiated HBECs following poly I:C sitmulation. *HBECs in all three groups were stimulated with poly I:C for 24 hours and levels of* ***(A)*** IFNα2a *and* ***(B)*** IFNβ1 *and* ***(C)*** IFNλ1 *were measured on the apical side as well as the* ***(D-F)*** *Basolateral side of the transwells. N: Healthy=4, Smokers=3-4, COPD=3. Error bars are representative of SEMs. Welch tests and ratio-paired t-tests performed.*

3.1.28 Early Expression of Type I and Type III IFNs in HBECs in response to RV infection

Anti-viral cytokines were measured at an early time point of 4 hours after infection of HBECs with 0.01 MOI of RV16. IFNα2a concentrations were mostly undetectable and thus no differences were observed between any of the conditions in response to RV16 infection **(Figure 3.28a)**.

IFNβ1 levels were undetectable in smoker and COPD HBECs pre infection with RV16 with no significant changes in response to RV16. In additions there were no differences pre and post-infection in healthy HBECs and no significant differences between health HBECs and smoker or COPD HBECs **(Figure 3.28b)**.

Similar to what was observed in IFNβ1, no changes were observed in all three groups post-infection in IFNλ1 concentrations and no differences between healthy, smokers, and COPD HBECs **(Figure 3.28c)**.

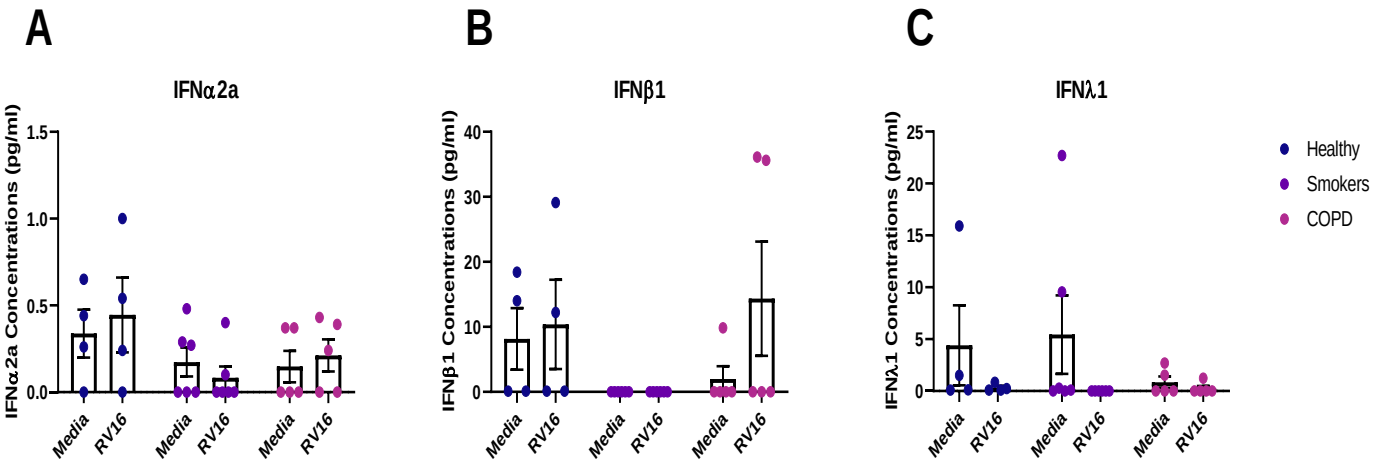


Figure 3.28: IFN levels in basal cultures HBECs post-infection with RV16 at an early timepoint. *HBECs in all three groups were infected with RV16 at a MOI of 0.01 for 4 hours and levels of* ***(A)*** IFNα2a *and* ***(B)*** IFNβ1 *and* ***(C)*** IFNλ1 *were measured. N: Healthy=4, Smokers=6, COPD=5. Error bars are representative of SEMs. Mann-Whitney and Wilcoxon correction tests performed.*

3.1.29 Type I and Type III IFN expression in HBECs in response to RV infection in basal cultures

The IFN response was then assessed through measurement of type I and type III IFNs after a dose infection of 0.01 to 1 MOI of HBECs with RV16 24 hours post-infection. IFN-α2a levels were largely undetectable in most groups and conditions and thus were not able to be quantified **(Figure 3.29a)**.

While there were no significant differences in levels of IFN-β1 within the three groups of HBECs after RV infection, there were significant differences between groups (Two-way ANOVA: p=0.5229 and p=0.0072). Healthy HBECs had significantly higher production of IFN-β1 than COPD HBECs at MOIs of 0.05, 0.1, and 1 with at least a 5-fold difference (p=0.009, p=0.004, and p=0.009) **(Figure 3.29b)**. In addition, healthy

HBECs had significantly higher levels of IFN-β1 than smoker HBECs at MOIs of 0.05 and 0.1 (p=0.0499 and p=0.03). While there were no trends in any of the three groups, IFN-β1 production was significantly decreased in COPD HBECs after RV16 infection in particular at the MOIs of 0.05 and 0.1 however levels of IFN-β1 remained more consistent in healthy HBECs (p=0.0453) **(Figure 3.29b)**.

In terms of IFNλ1 production, there were no significant changes observed within groups in response to RV16 infection despite a noticeable dependent increase in healthy HBECs (Two-way ANOVA: p=0.575) **(Figure 3.29c)**. There were also no significant differences between healthy and COPD HBECs in response to RV16 infection. However, IFNλ1 levels were significantly higher in healthy HBECs than smoker HBECs at MOI of 0.1 with approximately an 8-fold difference (p=0.037) **(Figure 29c)**.

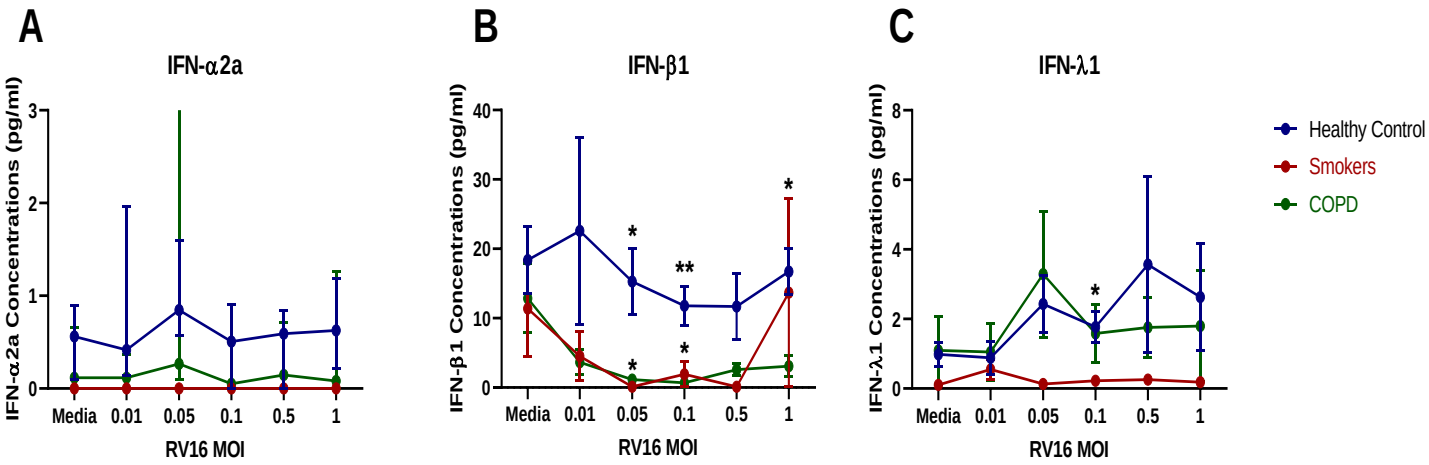


Figure 3.29: IFN levels in basal cultures HBECs post-infection with RV16. *HBECs in all three groups were infected with RV16 at a MOIs of 0.01-1 for 24 hours and levels of* ***(A)*** IFNα2a *and* ***(B)*** IFNβ1 *and* ***(C)*** IFNλ1 were quantified in supernatants*. N: Healthy=4, Smokers=5, COPD=6. Error bars are representative of SEMs. * : p<0.05. **: p<0.005. Two-way ANOVAs and multiple unpaired t-tests performed.*

3.1.30 Changes in IFNs in differentiated HBECs post-infection with RV

There were no changes in levels of IFNα2 after infection with 0.01 of RV16 after 24 h on both sides of the transwells **(Figure 3.30a,d)**. There were no significant differences in IFNβ1 production on the apical side after RV16 infection in all three groups **(Figure 3.30b)**. There were no significant changes in IFNβ1 after infection on the basolateral side either in all three groups of HBECs **(Figure 3.30e)**.

Levels of IFNλ1 were significantly increased over 20-fold after RV16 infection in smoker HBECs on the apical side going from 1.55 to 34.5 pg/ml (p=0.036). There was an increasing trend in COPD HBECs as well from 4.5 to 20.5 pg/ml, but it was not significant (p=0.34) **(Figure 3.30c)**. There were no significant changes on the basolateral levels of IFNλ1 in all three groups after RV16 infection **(Figure 3.30f)**.

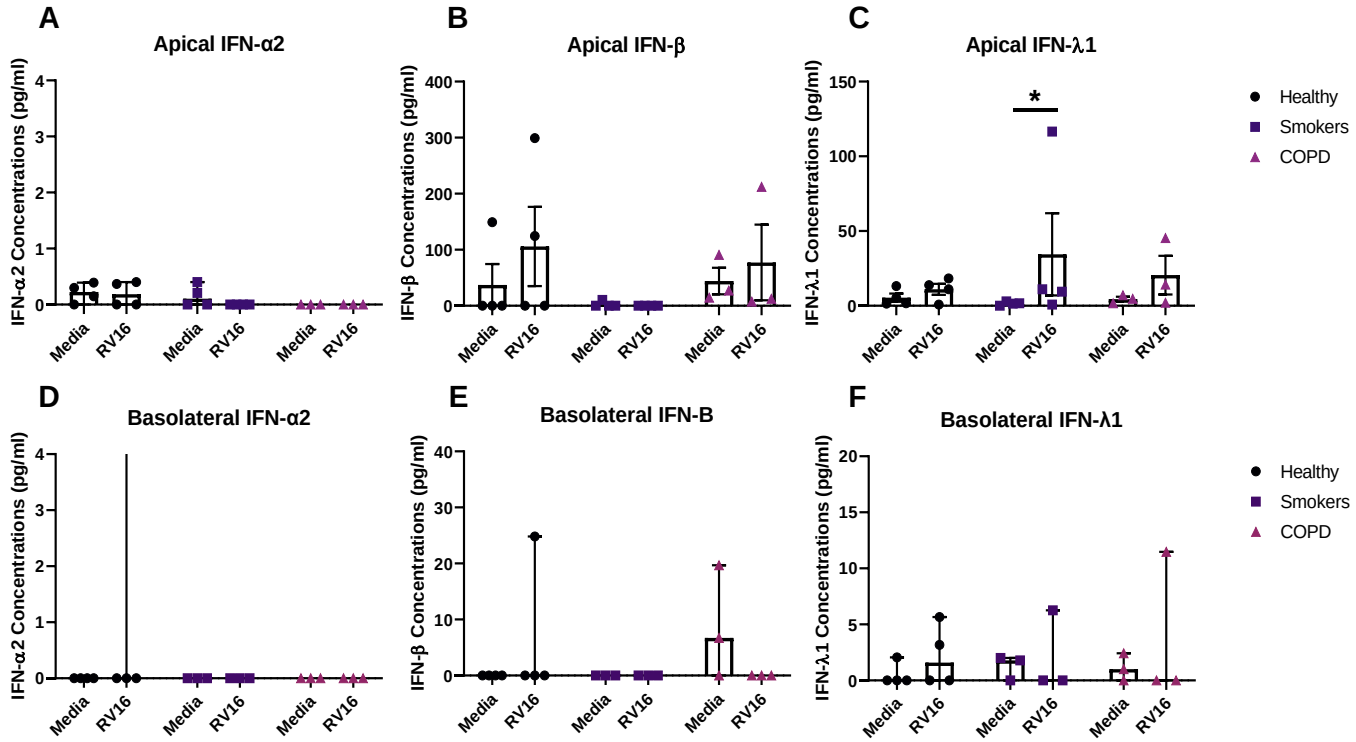


Figure 3.30: IFN levels in differentiated HBECs post-infection with RV16. *HBECs in all three groups were infected with RV16 at a MOI of 0.01 for 24 hours and levels of* ***(A)*** IFNα2a *and* ***(B)*** IFNβ1 *and* ***(C)*** IFNλ1 *were measured on the apical side as well as the* ***(D-F)*** *Basolateral side of the transwells respectively. N: Healthy=4, Smokers=3-4, COPD=4. Error bars are representative of SEMs. Welch t-tests and ratio paired t-tests performed. * : p<0.05.*

3.1.31 Gene expression of IFNRs after NTHi or RV infection in HBECs

In order to determine the expression of other signalling genes that are involved in the type I and type III IFN pathway, I measured gene expression of the IFNRs in HBECs cultured at a monolayer after NTHi or RV16 infection compared to unstimulated HBECs in all three groups by qPCR as described in **Section 2.19**. For type I IFN receptors, there were no significant changes in IFNAR1 expression after stimulation with either NTHi or RV16 in all three groups **(Figure 3.31a-c)**. There was, however, significant upregulation of IFNAR2 in healthy HBECs after RV16 stimulation with a 1.44-log fold increase in comparison to unstimulated HBECs (p=0.0022) **(Figure 3.32a)**. There were no significant changes in IFNAR2 expression in smoker and COPD HBECs after either NTHi or RV16 stimulation **(Figure 3.32b,c)**.

For the type III IFNR, expression of IFNLR1 was measured after infection in all three groups. However, there were no significant changes in IFNLR1 gene expression after NTHi or RV16 infection in all three groups of HBECs **(Figure 3.33a-c)**.

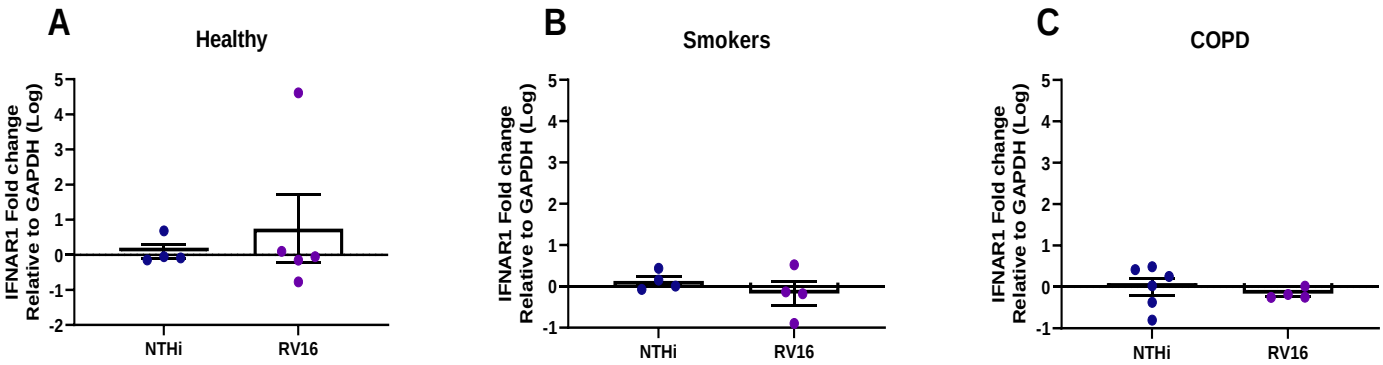


Figure 3.31: Gene expression of IFNAR1 after infection with NTHi or RV16. *HBECs were infected with 10 MOI of NTHi or 0.01 MOI of RV16 and changes were IFNAR1 were measured by RT-qPCR in* ***(A)*** *Healthy,* ***(B)*** *Smoker, and* ***(C)*** *COPD HBECs relative to unstimulated controls. N: Healthy=4-5, Smokers=4, COPD=4-6. Error bars are representative of SEMs. Ratio paired t-tests performed.*

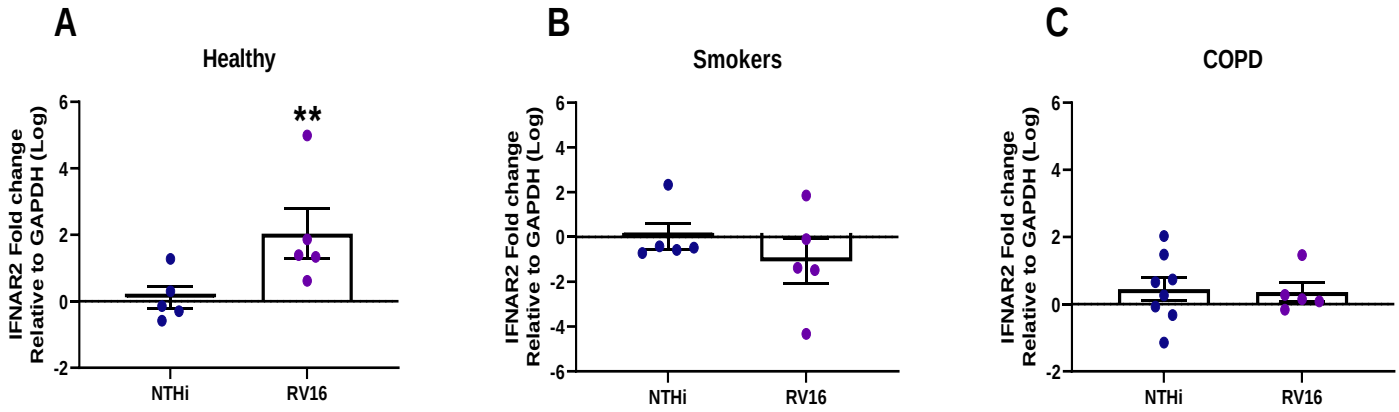


Figure 3.32: Infection with RV16 upregulates IFNAR2 gene expression in healthy HBECs. *HBECs were infected with 10 MOI of NTHi or 0.01 MOI of RV16 and changes were IFNAR2 were measured by RT-qPCR in* ***(A)*** *Healthy,* ***(B)*** *Smoker, and* ***(C)*** *COPD HBECs relative to unstimulated controls. N: Healthy=5, Smokers=5, COPD=5-8. Error bars are representative of SEMs. Ratio paired t-tests performed. ** : p<0.005.*

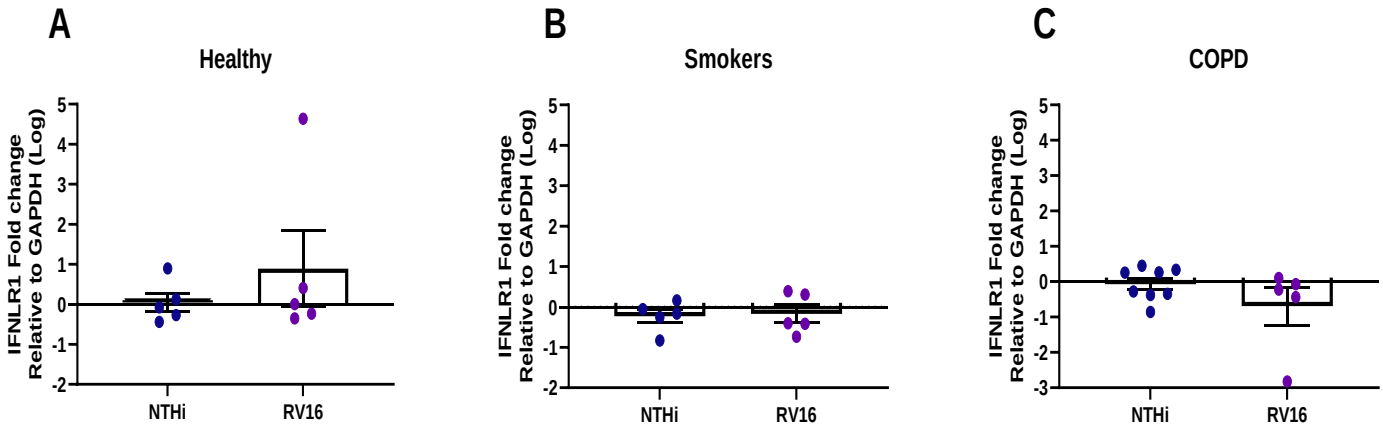


Figure 3.33: IFNLR1 mRNA levels in HBECs after infection with NTHi or RV16. *HBECs were infected with 10 MOI of NTHi or 0.01 MOI of RV16 and changes were IFNAR1 were measured by RT-qPCR in* ***(A)*** *Healthy,* ***(B)*** *Smoker, and* ***(C)*** *COPD HBECs relative to unstimulated controls. N: Healthy=5, Smokers=5, COPD=5-8. Error bars are representative of SEMs. Ratio paired t-tests performed.*

3.1.31 Expression of the ISG OAS1 after infection of HBECs with NTHi or RV16

The relative gene expression of the ISG OAS1 was then measured in all three groups by qPCR after infection with NTHi or RV16 as a proxy for the expression of ISGs and

IFN signalling in HBECs. There was an approximately 1-log fold increase in OAS1 expression in healthy HBECs after RV16 stimulation compared to unstimulated controls (p=0.0048) **(Figure 3.34a)**. There were, however, no significant changes in COPD and smoker HBECs after infection with either NTHi or RV16 **(Figure 3.34b,c)**.

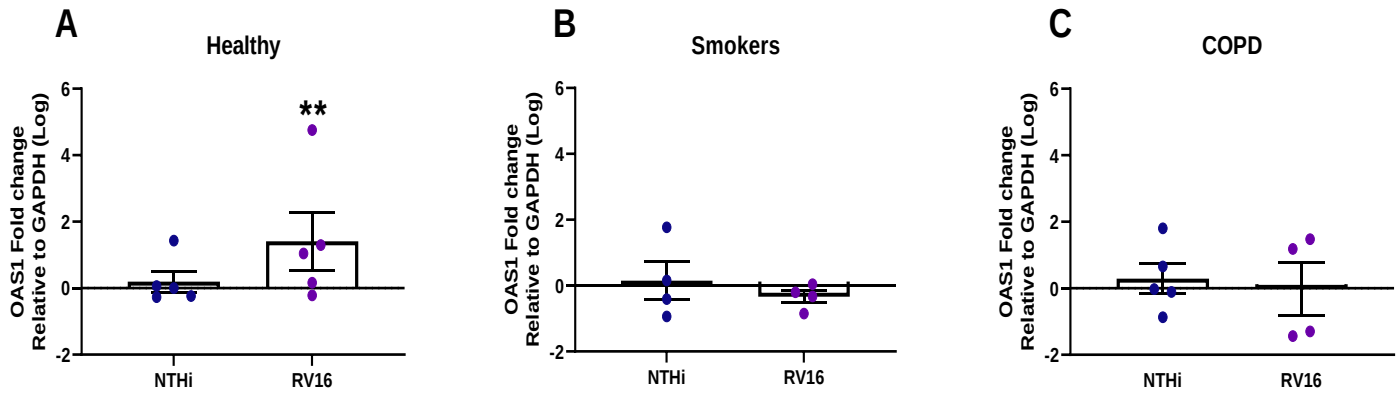


Figure 3.34: Infection with RV16 increases OAS1 gene expression in healthy HBECs. *HBECs were infected with 10 MOI of NTHi or 0.01 MOI of RV16 and changes were OAS1 were measured by RT-qPCR in **(A)** Healthy, **(B)** Smoker, and **(C)** COPD HBECs relative to unstimulated controls. N: Healthy=5, Smokers=4, COPD=4-5. Error bars are representative of SEMs. Ratio paired t-tests performed. ** : p<0.005.*

Discussion

The results demonstrate a few broad trends among the different conditions and analytes measured. Firstly, the measurement of the analytes at an early timepoint post-infection showed no significant differences between healthy, smokers, and COPD HBECs regardless of the analyte measured indicating that a 4-hour time point may be too early for a quantifiable response in all three groups. The 4-hour point was chosen in order to investigate earlier responses in HBECs and to examine whether there were any differences in the analytes between groups in the early time responses.

Secondly, concentrations of all the cytokines and alarmins measured were generally higher when the cells were successfully cultured and differentiated at ALI at least on the apical side. The basolateral side generally had lower concentrations which may indicate a physiological role or a limitation of the ALI model. Another potential reason may be that the media volume used on the basolateral side when culturing is more than double the volume utilized on the apical side (500µl and 200µl respectively) and thus the analytes are more diluted on the basolateral side. The 2.5x volume difference between the apical and basolateral side however is not sufficient enough to explain several of analyte differences between both compartments and there are a significantly higher difference on the apical side in IFNs for example.

Finally, what was observed, and what many studied have previously shown, is that there is substantial variation observed between biological replicates in human primary samples regardless of the group or condition tested. This is mainly due to, unlike cell lines or mice, there is a high amount of genetic diversity between humans which becomes particularly apparent when studying complex diseases like COPD.

For cell viability, it was indirectly observed post-infection through a trypan blue count or looking for cytopathic effects or changes in cell morphology under a brightfield microscopy. Cell death was observed more in smokers and COPD HBECs however more accurate methods for measuring cell death were not performed such as MTT assays and Annexin V staining.

3.2.1 The role of infection on pro-inflammatory cytokines in HBECs

COPD is a disease that is characterised by chronic inflammation. TNF-α concentrations were unchanged after LPS stimulation which indicates that either the dose was not sufficient to induce its production in epithelial cells or that the time points measured were too early or late to capture its induction. A study by Mubarak et. al however showed that LPS does not induce epithelial cells to produce pro-inflammatory cytokines such as CXCL8 at several timepoints but can be induced by poly I:C[229]. They also showed that LPS was able to induce pro-inflammatory cytokines in alveolar macrophages instead. This indicates that macrophages may be more easily primed to be inflammatory than epithelial cells potentially because epithelial cells are constantly exposed to the external environment and microbiome. On the other hand, the results here show a significant increase in amounts of TNF-α from HBECs after NTHi infection, in basal cultures at least, which is a more physiologically relevant model than LPS. While there were differences between the three groups with COPD patients having the highest TNF-α secretion, the differences were not significant. The relationship between NTHi and RV is not mutually exclusive and in fact there seemed to be a higher rate of co-infection with NTHi in COPD patients after a RV infection[102]. A study by Unger et. Al showed that TNF-α is significantly increased after NTHi infection in HBECs as demonstrated by this study as well however, when they infected

the cells with RV beforehand, levels of TNF-α were significantly decreased after NTHi infection[230]. This was further supported by demonstrating that RV inhibited the NFkB pro-inflammatory pathway which would have suppressed the ability for NTHi to induce it. Indeed, the data from my experiments showed infection of HBECs in all three groups did not induce any pro-inflammatory cytokine production after RV infection including TNF-α however whether the NFκB pathway was inhibited was unexamined. In addition, and interestingly, the by Unger et. al also showed that pre-infection with RV before NTHi decreased clearance of NTHi with higher CFUs of NTHi found when cells were pre-infected with RV[230].

Poly I:C has previously been shown to increase levels of TNF-α and indeed a similar trend was observed in the data shown here in both differentiated and basal cultures despite the increases not being significant[231]. Furthermore, COPD patients had higher means of TNF-α than healthy HBECs which indicates that COPD HBECs are more susceptible to inflammation than healthy HBECs.

In contrast to TNF-α, neither LPS nor NTHi induced production of GM-CSF in all three groups. GM-CSF is not the only stimulating cytokine for granulocyte or macrophage recruitment, activation, or survival however it was chosen instead of G-CSF or M-CSF as it is able to induce both granulocytes and macrophages unlike the other two cytokines. In addition, GM-CSF is upstream of other pro-inflammatory mediators and cytokines such as IL-6 or IL-8 by signalling through STAT5 and ERK. Interestingly however, other studies on healthy epithelial cells have also shown that LPS is not a potent inducer of GM-CSF[232,233]. The data from **Chapter 3** indicate that LPS is not a potent inducer of GM-CSF in primary healthy, smoker, and COPD HBECS as well and that COPD HBECs don't have exaggerated GM-CSF production.

Poly I:C upregulated GM-CSF in all three groups however it was only significant in smokers. COPD HBECs also had higher levels of GM-CSF after stimulation indicating, similar to TNF-α, that it is predisposed to exaggerated inflammatory responses or at least exaggerated cytokine production with potentially defective downstream signalling. Previous studies have in nasal epithelial cells have also shown an upregulation of GM-CSF in response to poly I:C stimulation[234]. Upon infection with RV16 however, there were no changes in GM-CSF production in all three groups in differentiated or basal cultures despite COPD HBECs having non-significant levels of GM-CSF at basal levels than healthy or smoker HBECs. A study by Sanders et. al demonstrated that upon infection of BEAS2B cells with RV, GM-CSF levels did not significantly increase either[235].

3.2.2 Alarmin responses in COPD HBECs post-infection and stimulation

The alarmins IL-25, TSLP, and IL-33 have been shown to be expressed by epithelial cells and have all been shown to induce the production of type 2 cytokines in different leukocytes which contribute to an inflammatory environment.

IL-25 is an alarmin that can induce the production of type 2 cytokines and can inhibit Th1 or Th17 response in diseases like IBD[236,237]. In asthmatic patients, IL-25 has been shown to be significantly higher than in healthy controls[238,239]. Asthmatic patients also had significantly higher IL-25 compared to healthy controls post-infection with RV[240]. CSE however was not able to induce the production of IL-25 indicating that CSE is not sufficient for IL-25 production[241]. IL-25 has been found to be unchanged when mice were stimulated with LPS which is similar to the findings in healthy HBECs in this study[242]. However, IL-25 is significantly downregulated in COPD HBECs after LPS stimulation and it is unclear why this is occurring. One reason could potentially be that

COPD HBECs are trying to skew responses away from type 2 cytokines which is why IL-25 is being downregulated.

TSLP has previously been shown to be induced in epithelial cells by dsRNA stimulation of HBECs. Furthermore, COPD patients had significantly higher concentrations of TSLP upon stimulation with dsRNA than healthy HBECs[169]. another study has also shown that poly I:C can concentration-dependently increase the production of TSLP in healthy nasal epithelial cells[243]. Despite not being significant, poly I:C induced an increased production of TSLP in healthy and COPD HBECs with COPD HBECs having a higher mean than healthy HBECs in my study which corroborate the aforementioned findings. However, no changes were observed in TSLP in all three groups upon RV16 infection indicating that RV16 can either evade or inhibit TSLP production.

Broadly speaking, IL-33 was generally undetectable in all groups regardless of the stimulation that HBECs were subjected to with the exception of some detectable IL-33 observed after poly I:C stimulation for 24 h. Byers et. al has shown that IL-33 is actually higher in COPD HBECs than non-COPD HBECs[167]. However, Byers et. al only measured lung lysates which only quantifies intracellular IL-33 while I measured secreted IL-33 which would be able to mediate its effector functions. While it is interesting that COPD HBECs had higher IL-33 intracellularly, IL-33 is already constitutively expressed in the cells and stored intracellularly until the right context, such as an infection and cigarette smoke exposure, wherein IL-33 is then released to exert its effector function[168]. To assess whether IL-33 is detectable by the assay, I used some lysates from HBECs that were measured and IL-33 was detectable in this case indicating that IL-33 is intracellular but not being secreted in HBECs (Data not shown). Interestingly, levels of IL-33 in the lungs of COPD patients were only higher

in GOLD IV patients compared to smokers but not healthy controls and in fact smoking seemed to downregulate its respective receptor ST2 in the aforementioned study[168].

3.2.3 Innate anti-viral responses in HBECs post-infection

Type I and type III IFNs are responsible for fighting against viral and some bacterial infections through the induction of ISG expression. IFN signalling can also inhibit cell proliferation, induce apoptosis, and disrupt barrier function in the process in order to kill infected cells. IFNAR1 is the low affinity receptor for type I receptors while IFNAR2 has been shown to be the high affinity receptor with IFNβ having the strongest affinity to the IFNARs.

Type III IFNs have been shown to play a prominent role in mucosal immunity which includes the lung barrier. The epithelial barrier is particularly important for type III IFN signalling since IFNLR1 is predominantly expressed on epithelial cells[244]. This includes responding to bacterial infection such as *Listeria monocytogenes* however IFNλ has also been shown to be induced by respiratory bacterial pathogens such as *P. aeruginosa*[245]. In the data shown here, IFNλ1 seemed to increase concentration-dependently with NTHi infection and is significantly higher in COPD HBECs. This could be due to either COPD HBECs being refractory to IFN signaling or that IFNλ1 is not playing a protective role in this particular context. For the latter, previous studies have shown that the release of type I and type III IFNs actually increased biofilm formation of *P. aeruginosa*[246]. The persistence of a bacteria either intracellularly or extracellularly may further perpetuate inflammation and barrier disruption

In contrast, NTHi decreased IFNβ1 production in HBECs up to an MOI of 100 in smoker and COPD HBECs and thus NTHi may be inhibiting IFN responses or IFNβ1 is not needed or detrimental to the immune response against NTHi. This was observed

in both basal and differentiated cultures. A study in mice has previously shown that infection of DCs by pathogenic bacteria does not trigger IFNβ1 production and IFNβ1 does not always have a protective effect against bacterial infections[247,248]. The trend in my data did not hold for high doses of NTHi in smoker and COPD HBECs were IFNβ1 production starts increasing again which may be detrimental and a failure to suppress IFNβ1 expression.

Poly I:C also upregulated IFNλ1 in COPD and healthy HBECs but was only significant in COPD HBECs in basal cultures. The higher upregulation of IFNλ1 in COPD HBECs may indicate that COPD HBECs are attempting to compensate for a blunter IFN response due to being more IFN signalling desensitization. There was no increase of IFNβ1 or IFNλ1 in smoker HBECs which is similar to gene expression data of smoke expose HBECs where IFN production was unresponsive to poly I:C stimulation[249]. RV16 increased concentrations of IFNλ1 in healthy HBECs and was significantly greater than smoker HBEC concentrations but there was no concentration-dependent increase in COPD or smoker HBECs. Interestingly, IFNλ1 was only significantly upregulated in smoker HBECs in differentiated cultures which is in contrast to basal cultures which indicates a limitation to models of cells cultured at a monolayer. A non-significant increase was observed however in COPD HBECs in differentiated cultures as well. RV16 was able to inhibit production of IFNβ1 in smokers and COPD HBECs compared to basal conditions which is indicated by the significant decrease in IFNβ1 post-infection. Healthy HBECs however was able to maintain persistent levels of IFNβ1 after RV16 infections which may indicate that RV16 is not as effective in inhibiting type I IFNs in healthy HBECs.

Different strains of RV can elicit variable amount of IFN responses. RV16 in particular produces the lowest amount of IFNβ out of all other strains tested[250]. Interestingly,

titers of RV may be different depending on the strain utilized. A study using RV39 to infect HBECs found significantly more RV39 in COPD HBECs than healthy HBECs despite higher quantities of type I IFNs[251]. Veerati et. al on the other hand used RV-A1, which belongs to the same group as RV16, and found that viral titres are similar across healthy, asthmatic, and COPD HBECs post-infection across several days[226]. In addition, RV16 has been used as an experimental model to induce exacerbation and assess symptoms in COPD patients[96]. Interestingly, levels of RV16 were significantly greater in COPD patients than healthy control subjects although the differences were seen at later timepoints[226].

3.2.4 IFN signalling in HBECs in infections

IFN signalling is tightly regulated during an infection as too much signalling can result in a large amount of cells death and other pathologies. Systemic lupus erythematosus for example is associated with excessive IFN production. Thus, cells have several mechanisms they can undergo in order to avoid excessive IFN signalling through IFN desensitization.

Endocytosis of IFNRs for example, is a mechanism to regulate IFN signalling after the induction of type I and type III IFNs. Another mechanism is when cells become desensitized to IFNs through JAK-STAT signalling is through activation and upregulation repressor proteins like SOCS1[252]. SOCS1 is a phosphatase that acts upon phosphorylated STAT proteins and inhibits JAK-STAT signalling and ISG production through dephosphorylation of STATs. USP18 in particular, can maintain IFN desensitization through prolonged periods by binding to IFNAR2[253]. Cells that were primed with IFNβ beforehand had a reduced ability to undergo IFN signalling through STAT1 through the upregulation of USP18[253].

Desensitization however, is required only to prevent an excessive IFN response and to return to homeostasis after an infection is cleared where IFN production and signalling is essential for protection of the lungs from viruses or bacteria.

IFN desensitization may at least partially explain expression levels of IFNs in the HBECs of COPD patients. Healthy HBECs were able to upregulate the high affinity IFN receptor IFNAR2 after infection with RV16 which may enhance IFN signalling which is further indicated by upregulation of the ISG OAS1 post-infection with RV16. On the other hand, COPD or smoker HBECs were not able to upregulate any of the IFNRs as well as the ISG OAS1 in response to infection indicating unresponsive IFN signalling or being more susceptible to desensitization mechanisms.

3.2.5 Limitations and further investigations

The data shown in this chapter are interesting and warrants further investigation to get a fuller picture of the innate immune response in the lung epithelium. However, there are several limitations in this chapter. Firstly, there is a high variation between the biological replicates within the different groups. This is unsurprising however it does mean that establishing a trend between different groups or conditions is challenging and thus a higher amount of donors in each group is needed to make the data more reliable. For example there are several experiments were there was an increasing trend in the production of TNF-α or TSLP in COPD HBECs after stimulation however significance was not demonstrated with our chosen alpha number of 0.05 but increasing the donor numbers may have established a significant result.

Another limitation is the dose of RV16 that was utilized in some of the experiments. A dose of 0.01 MOI was chosen in the early time point experiment as well as the experiments in differentiated cultures. A reason for this dose was to try to investigate

any early responses within different cultures and groups and changes that are sensitive to lower doses of RV16. In addition, a study by Veerati et. al was able to demonstrate significant changes in IFN responses in HBECs after infection with RV doses even lower than the ones utilized in this chapter such as an MOI of 0.001 and 0.01[226]. A RV dose experiment was done in basal cultures at a 24 hours timepoint however it would have been also been useful to have dose experiments at the earlier timepoint utilized and in differentiated culture at 24 hours. This can also be applicable to NTHi infection where a NTHi dose experiment at an early timepoint and differentiated cultures should be further investigated. In addition, a positive control to assess whether the HBECs were induced at the concentration used post-infection would have been useful such as measuring the pro-inflammatory cytokine IL-1β. Importantly however, a MOI of 0.01 for RV16 was sufficient to induce the upregulation of IFNAR2 and OAS1 mRNA in healthy HBECs suggesting that perhaps changes would be more discernible on a transcriptional level.

Further investigations into changes of IFN signalling in HBECs would also be interesting such as changes in levels of phosphorylation in STAT1 or IRF3 or the production of different ISGs as COPD HBECs may be refractory to IFN signalling through upregulation of repressors such as SOCS1. In addition, an investigation of later timepoints like 48 or 72 hours post-infection or stimulation may delineate differences in response times between the three groups and allow other mediators to affect the genes and proteins measured here.

Chapter 4: Barrier Integrity and Tight Junctions in Epithelial Cells in Response to Bacterial or Viral Infection

Introduction:

The epithelium is an indispensable barrier that protects the lung and body from external pathogens, toxins, and is tightly regulated to maintain homeostasis. Barrier failure can result in lung injury, flooding, and inflammation. Barrier integrity is maintained by a host of different factors but most importantly by the adhesion molecules and connective tissue that keeps the external environment at bay. TJs are a type of adhesion molecules that are expressed in the lungs and can form multiprotein complexes and cell-cell contact sites. TJs are segmented mainly into CLDNs, JAMs, and ZOs.

Exacerbations in COPD are strongly associated with viral and/or bacterial infections and thus it may be possible that the worsening of symptoms due to infection may be at least partly due to a dysfunctional epithelial barrier. Therefore, it would be interesting and of potential clinical benefit to measure and assess whether the expression of TJ proteins that are highly expressed in the lungs, would be different in COPD patients and upon infection. Smoking is also a one of the largest risk factors in causing COPD and thus assessing expression of TJ proteins in smoker may also be interesting as an intermediary step between a healthy epithelium and the epithelium of COPD patients. Protein expression and function can be highly regulated including tight junction molecules and it may be at a transcriptional, translational, or post-translational level.

Another factor that can influence barrier integrity is the spatial behavior of TJ molecules on epithelial cells and whether any spatial changes are observed after infection. Examining and visualizing TJ proteins in healthy, smokers, or COPD HBECs under a confocal microscope will help assess whether there are any spatial changes between the aforementioned groups and if there are changes in the TJ proteins after bacterial or viral infections. Analysis for any differences in TJ molecule colocalization in the three groups and whether or not there are any changes in TJ colocalization before and after infections.

CLDN-3 and CLDN-4 are among the highest expressed TJ molecules in the airways and have been shown to have roles in regulating paracellular movement of solutes and water for example. There is also some evidence in rat epithelial cells that CLDN-3 increase paracellular permeability while CLDN-4 expression increases transepithelial resistance[187]. JAM-A is another TJ protein that is expressed in the lungs and has been showed to aid in neutrophil migration to the lungs as well as inducing EMT and apoptosis which are both characteristics observed in the lungs of COPD patients[254,255].

I sought to investigate the role of the TJ molecules CLDN-3, CLDN-4, and JAM-A in healthy, smoker, and COPD HBECs under the different contexts of NTHi or RV16 infection as well as their respective analogs, LPS and Poly I:C. The TJ proteins were first examined under a confocal microscope to look for any spatial changes and differences between the three groups with or without stimulation as well as differences in colocalization effects. Expression and intensity were also measured through microscopic visualization to assess protein levels of the TJ molecules. In order to examine whether the differences in TJ expression was at a transcriptional or protein

level or both RT-qPCRs were performed after NTHi or RV16 infection measuring CLDN-3, CLDN-4, and JAM-A as well as other TJ molecules Occludin and ZO-1.

Results

4.1.1 Visualization of TJ proteins in unstimulated HBECs using confocal imaging

The TJ molecules CLDN-3, -4, and JAM-a were stained and visualized in monolayers of healthy, smoker, and COPD HBECs under a confocal microscope at 100x and 630x magnifications. An illustration is drawn to demonstrate the different types of spatial descriptions and localizations used in HBECs for the TJ molecules examined in this study in different conditions and groups **(Figure 4.1)**.

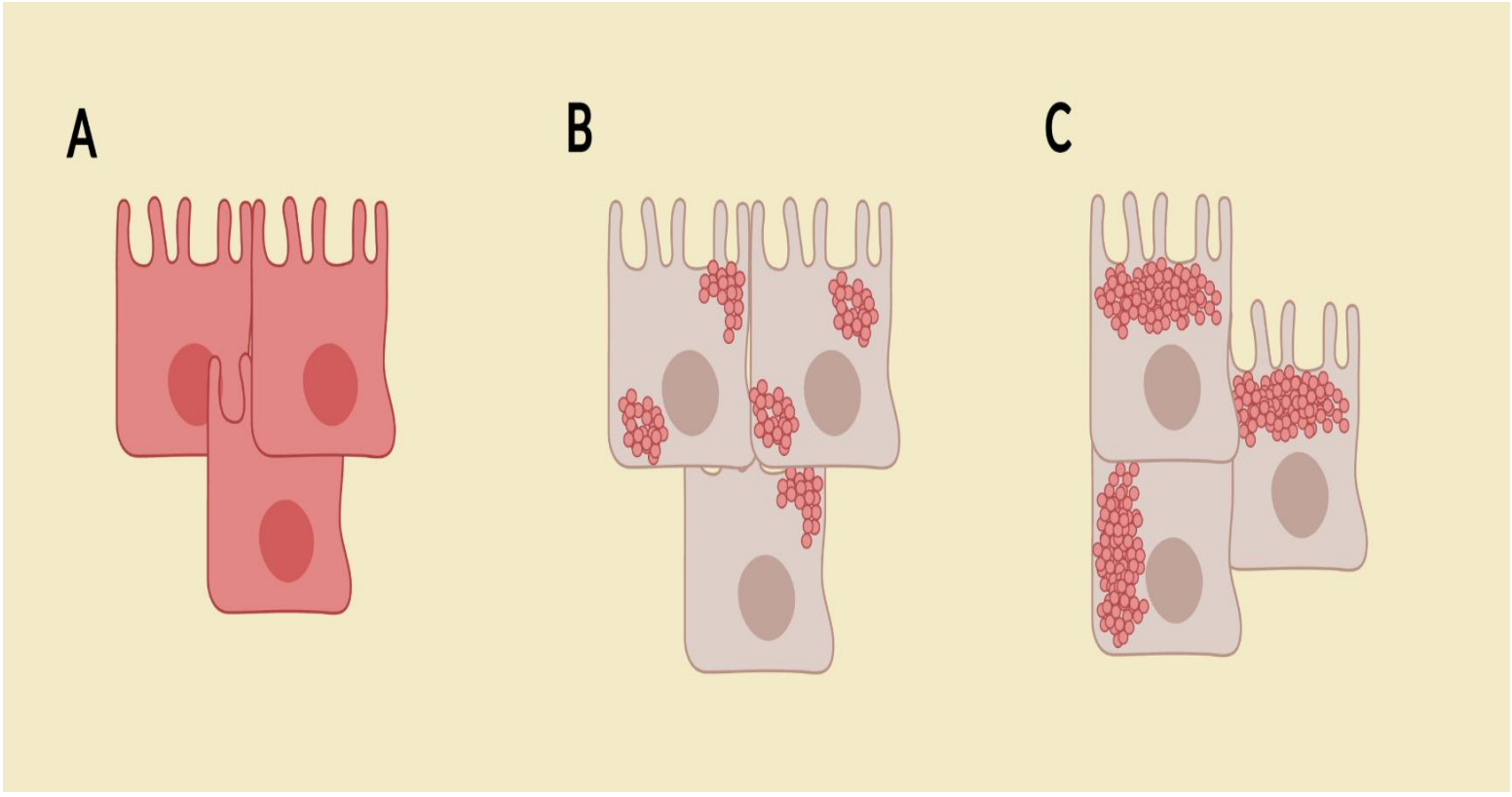


Figure 4.1: Types of Tight Junction spatial changes observed in HBECs. *The different types of tight junction spatial changes observed in HBECs where they can be **(A)** Diffused across the cell surface or **(B)** Clustered on the cells or **(C)** Be polarized at a particular side of the cell with a possibility of tight junction proteins being polarized and clustered.*

The HBECs were first only stained with DAPI and the secondary antibodies that were used in order to detect if there is significant background or non-specific fluorescence. There was very little background and unspecific fluorescence found when staining without the primary antibody establishing that there is the secondary antibody is not binding to the HBECs **(Figure 4.2)**.

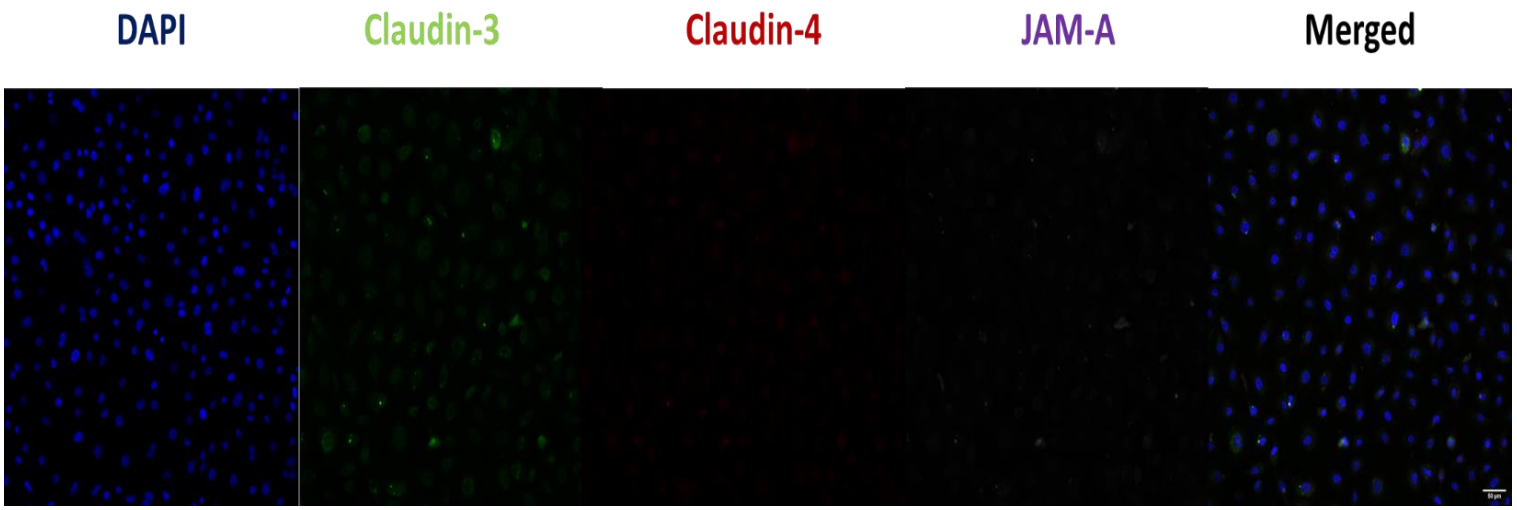


Figure 4.2: Background and unspecific fluorescence in HBECs. *HBEC background and non-specific fluorescence after staining with only secondary antibodies for CLDN-3, CLDN-4, and JAM-A with DAPI at 100x magnification*

Under unstimulated conditions, CLDN-3 is diffused across the cell surface in healthy HBECs while CLDN-3 seems to localize to be more clustered or polarized on the cell surface in smoker HBECs. CLDN-3 behaves similarly to smoker HBECs in COPD patients however the tendency for CLDN-3 to cluster and polarize on the cell surface seems to be slightly less.

CLDN-4 was also more diffused across the cell surface of healthy HBECs as seen in CLDN-3. CLDN-4, like CLDN-3, was polarized in COPD and smoker HBECs under basal conditions however clustering was not as strong as what was observed in CLDN-3 **(Figure 4.3a, b)**.

JAM-A in healthy HBECs was also diffused across the cell surface however there was also localization observed at the junctions of the cells. JAM-A also localized on the junctional ends of HBECs in smoker and COPD groups however similar to what was seen in CLDN-3, polarization and clustering of JAM-A was also observed on the cell surface of HBECs. Generally, under basal conditions the confocal images indicate that the TJ molecules measured are diffused across the cell surface in healthy HBECs. In smoker and COPD HBECs however, CLDN-3, CLDN-4, and JAM-A tend to exhibit a different behavior by clustering and polarizing on the cell surface **(Figure 4.3a, b)**.

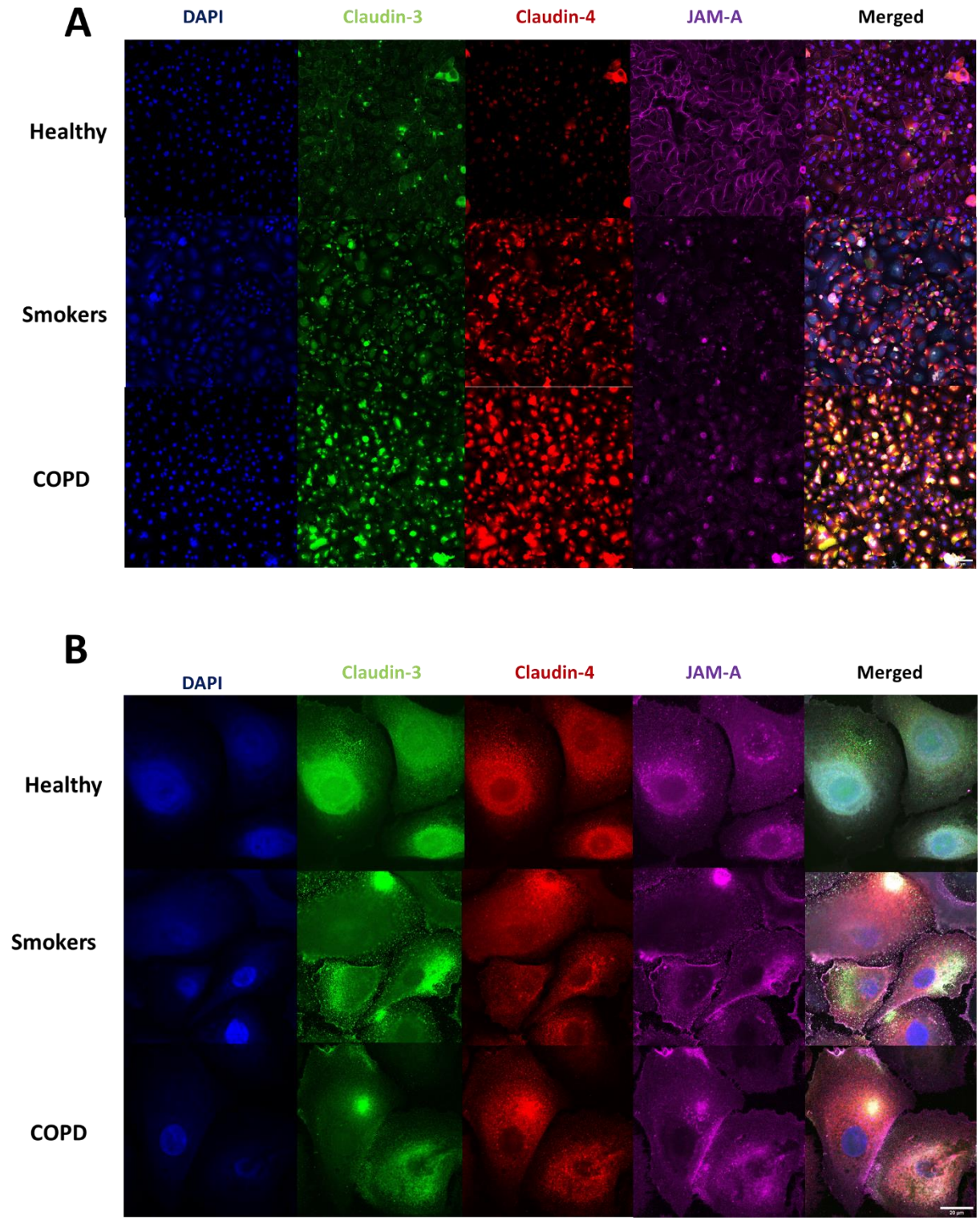


Figure 4.3: CLDN-3, CLDN-4, and JAM-A stained in unstimulated HBECs. *TJ molecules CLDN-3, CLDN-4, and JAM-A visualized in unstimulated healthy, smoker, and COPD HBECs under a confocal microscopy at (**A**) 100X, scale = 100 µm and (**B**) 630X magnifications, scale = 20 µm. TJ proteins in healthy HBECs were clustered and diffused while being polarized or clustered in smoker and COPD HBECs*

4.1.2 Expression of Tight Junction Molecules under basal conditions in HBECs

HBECs were cultured at a monolayer and then basal expression of TJ molecules were measured. Basal expression of the TJs CLDN-3, -4, and JAM-A in HBECs differed significantly in healthy controls compared to COPD and smoker HBECs. Smokers and COPD HBECs had significantly higher expression of CLDN-4 compared to healthy controls under basal conditions. Smokers and COPD HBECs had approximately 2.5-fold and 3-fold higher expression of CLDN-4 respectively (Medians: 5079 and 6474) compared to healthy controls (Median: 2073, $p<0.0001$). There were no significant differences in CLDN-4 expression however between smokers and COPD HBECs under basal conditions ($p = 0.052$). As with CLDN-4, expression of CLDN-3 in smokers and COPD patients (Medians: 4568 and 4621) were significantly higher than healthy controls (Median: 2553, $p=0.0001$ and $p<0.0001$) with approximately a 1.8-fold increase. There were also no significant differences in CLDN-3 expression between smokers and COPD patients ($p= 0.5846$). Finally, JAM-A also had significantly higher expression in smokers and COPD patients (Medians: 3498 and 2544) compared to healthy controls (Median: 1908) with 1.8-fold and 1.3-fold increases respectively ($p<0.0001$ and $p=0.0017$). No significant differences were found in JAM-A expression in COPD and smoker groups ($p=0.1057$). Overall, the data shows that COPD and smokers have significantly greater TJ expression compared to healthy HBECs in unstimulated conditions with no significant differences between smokers and COPD HBECs.

4.3 Colocalization of TJ proteins under basal conditions in HBECs

Next, a colocalization analysis was performed between CLDN-3, -4, and JAM-A for HBECs in all three groups under basal conditions. Colocalization strength was

determined using Pearson's correlation coefficient with a R score of 1 indicating complete colocalization. CLDN-3 and CLDN-4 strongly colocalized in healthy HBECs under basal conditions (R=0.78) while CLDN-3 and CLDN-4 moderately colocalized in smoker and COPD HBECs (R=0.52 and R=0.65 respectively). CLDN-3 and JAM-A were however weakly colocalized in healthy HBECs (R=0.47) while they were moderately colocalized in smoker (R=0.59) and COPD HBECs (R=0.57). CLDN-4 and JAM-A were weakly colocalized in healthy HBECs (R=0.41), smoker (R=0.13), and COPD HBECs (R=0.26) had very weak colocalization.

4.1.4 Transepithelial resistance in HBECs in response to LPS and under basal conditions

The TER was measured in healthy, smoker, and COPD HBECs under basal conditions and after stimulation with 20 ng/ml of LPS after 24 hours. The HBECs were cultured at a monolayer on a transwell and TER was subsequently measured. There were no significant differences in HBEC TER under basal conditions between all smoker and healthy HBECs and COPD and healthy HBECs (p=0.19 and p=0.14 respectively). There were also no changes in TER in response to LPS stimulation in healthy, smoker, and COPD HBECs (p=0.08, p=0.20, p=0.20 respectively) **(Figure 4.4)**.

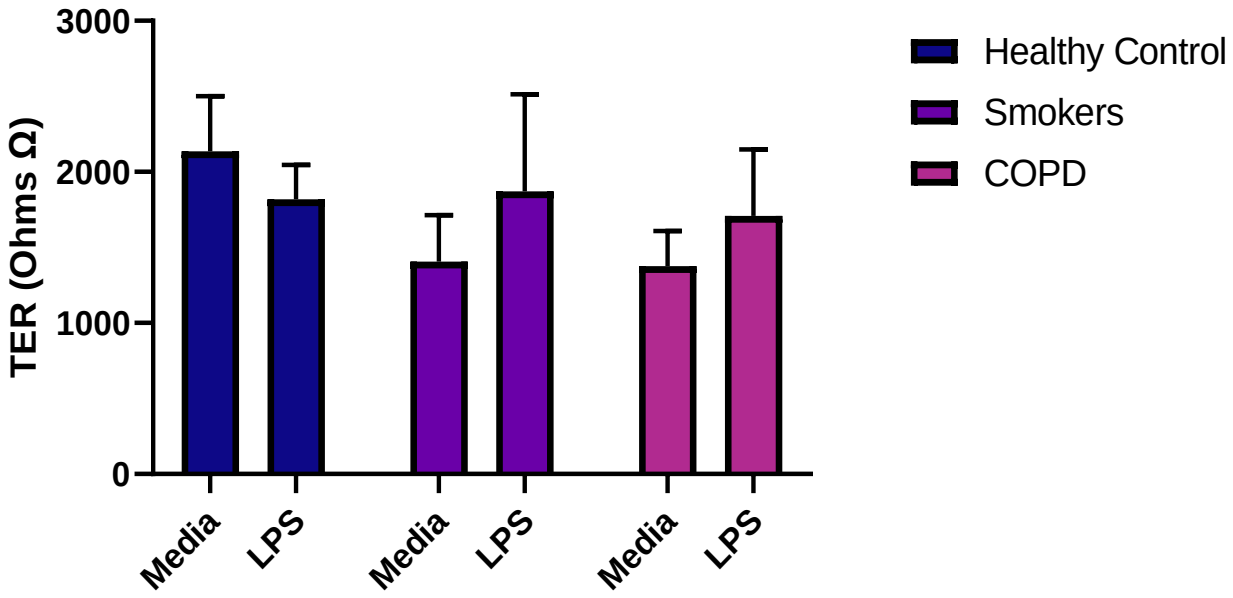


Figure 4.4: Transepithelial resistance in HBECs after LPS stimulation remains the same. *HBECs were stimulated with 20 ng/ml of LPS for 24 h and TERS were subsequently measured at basal levels and after stimulation. N: Healthy=4, Smokers=3, COPD=4. Error bars are representative of SEMs. Mann-Whitney and Wilcoxon correction tests performed.*

4.1.5 Effect of LPS on TJ protein localization in HBECs

HBECs from all three groups were also visualized under a confocal microscope 24 h after LPS stimulation at 20 ng/ml. Unlike in basal conditions, CLDN-3 responded to LPS by heavily clustering and polarizing on the cell surface of healthy HBECs. However, CLDN-3 was mostly dispersed on the cell surface of smoker HBECs after LPS stimulation which is in contrast to what was observed when the HBECs were unstimulated. In COPD HBECs, polarization was observed with some clustering however it was not observed to the same degree as in unstimulated COPD HBECs or healthy HBECs stimulated with LPS **(Figure 4.5a, b)**.

CLDN-4 was also polarized and clustered in healthy HBECs in response to LPS stimulation but not to the same degree as CLDN-3. Polarization of CLDN-4 was also observed in smoker HBECs after LPS stimulation but without clustering and to a lesser

extent than what was observed in unstimulated smoker HBECs. In HBECs of COPD patients, CLDN-4 was found to be polarized and without CLDN-4 clustering as well but less so than the polarization observed in healthy HBECs **(Figure 4.5a, b)**.

Following a similar trend to CLDN-3 and CLDN-4, JAM-A was heavily polarized and cluster after LPS stimulation in healthy HBECs with some JAM-A localized to the intercellular junctions. Smoker HBECs had JAM-A localized to the intercellular junctions to a greater degree in response to LPS than what was observed in healthy HBECs indicating higher junctional formation and less marked polarization and clustering of JAM-A. JAM-A localization in COPD HBECs followed a similar trend in that JAM-A was more localized to the intercellular junctions with less clustering and polarization of JAM-A observed compared to LPS stimulated healthy HBECs **(Figure 4.5a, b)**.

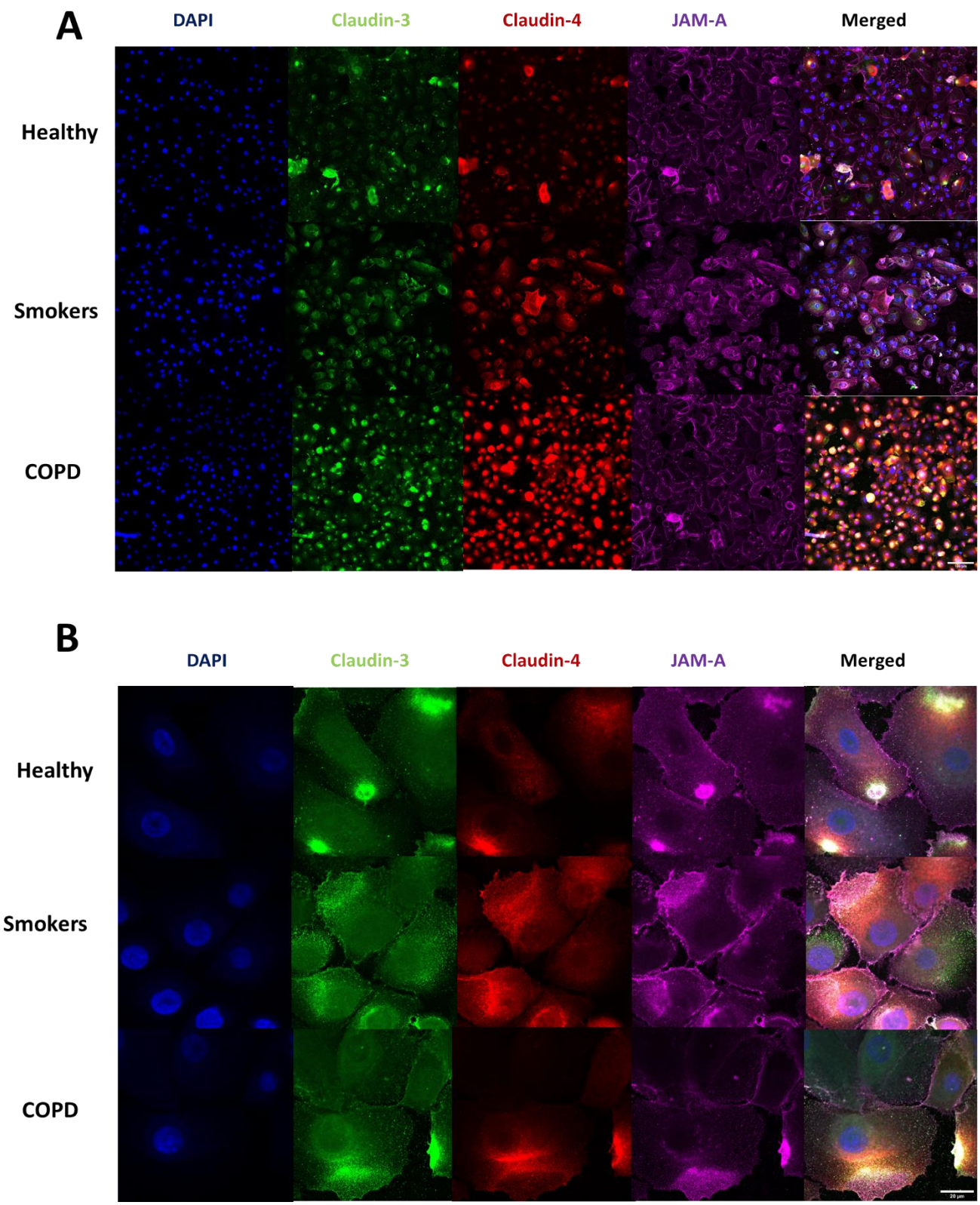


Figure 4.5: CLDN-3, CLDN-4, and JAM-A visualized in LPS stimulated HBECs. *TJ molecules CLDN-3, CLDN-4, and JAM-A visualized in healthy, smoker, and COPD HBECs after 24 h of LPS stimulation at 20 ng/ml under a confocal microscopy at (**A**) 100X, scale=100 µm and (**B**) 630X magnifications, scale=20 µm. TJ proteins in healthy*

HBECs became clustered or polarized with little change from basal conditions in smoker and COPD HBECs.

4.1.6 Tight Junction Expression in Response to LPS Stimulation in HBECs

HBECs were stimulated with 20 ng/ml of LPS for 24 hours in order to measure and visualize the tight junctions CLDN-3, CLDN-4, and JAM-A after stimulation with the bacterial analogue. There were no significant differences in CLDN-4 expression in response to LPS stimulation in healthy, smokers, and COPD HBECs (Medians: 4309, 3367, and 4322 respectively) (p=0.1738, p=0.4791, p=0.4111) **(Figure 4.6b)**. No differences in CLDN-3 expression were also observed in healthy, smoker, and COPD HBECs in response to LPS stimulation (Medians: 3490, 3744, 3872) (p=0.1611, p=0.0626, p=0.4073) **(Figure 4.6a)**. JAM-A expression was also unchanged in response to LPS stimulation in healthy, smoker, and COPD HBECs (Medians: 2643, 3032, 2690 (p=0.1520, p=0.8009, p=0.662). These results indicate that TJ molecules are unresponsive to LPS stimulation in any of the three groups **(Figure 4.6c)**.

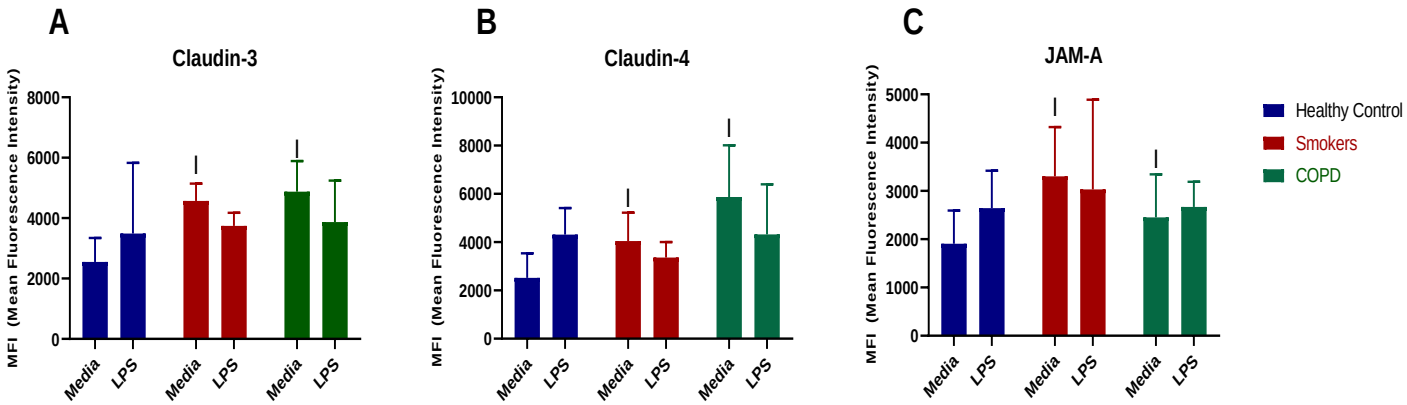


Figure 4.6: CLDN-3, CLDN-4, and JAM-A expression in LPS stimulated HBECs. *MFI of the TJ molecules **(A)** CLDN-3, **(B)** CLDN-4, and **(C)** JAM-A in healthy, smoker, and COPD HBECs after 24 h of LPS stimulation at 20 ng/ml compared to media treated HBECs. Error bars are representative of medians with 95% CI. Welch t-tests, and ratio paired t-tests performed. I: P<0.05 compared to unstimulated healthy controls (N: Healthy= 4, smokers=7, COPD=5).*

4.1.7 TJ molecule colocalization in HBECs after LPS stimulation

The Pearson correlation coefficient was used to measure TJ colocalization in 630x images with 0 being no colocalization at all and 1 being perfectly colocalized proteins. being no pCLDN-3 and CLDN-4 were moderately colocalized in all three groups after LPS stimulation with Pearson's correlation coefficients being 0.63 in healthy and smoker HBECs and R=0.69 in COPD HBECs **(Figure 4.7a)**. CLDN-3 and JAM- A were moderately colocalized in healthy HBECs (R=0.65) while being weakly colocalized in smoker HBECs (R=0.47) **(Figure 4.7b)**. CLDN-3 and JAM-A were also moderately colocalized in COPD HBECs (R=0.53) **(Figure 4.7b)**.

CLDN-4 and JAM-A were very weakly colocalized in all three groups after LPS stimulation with healthy HBECs having an R score of 0.29 and smoker and COPD HBECs having R scores of 0.18 and 0.29 respectively **(Figure 4.7c)**.

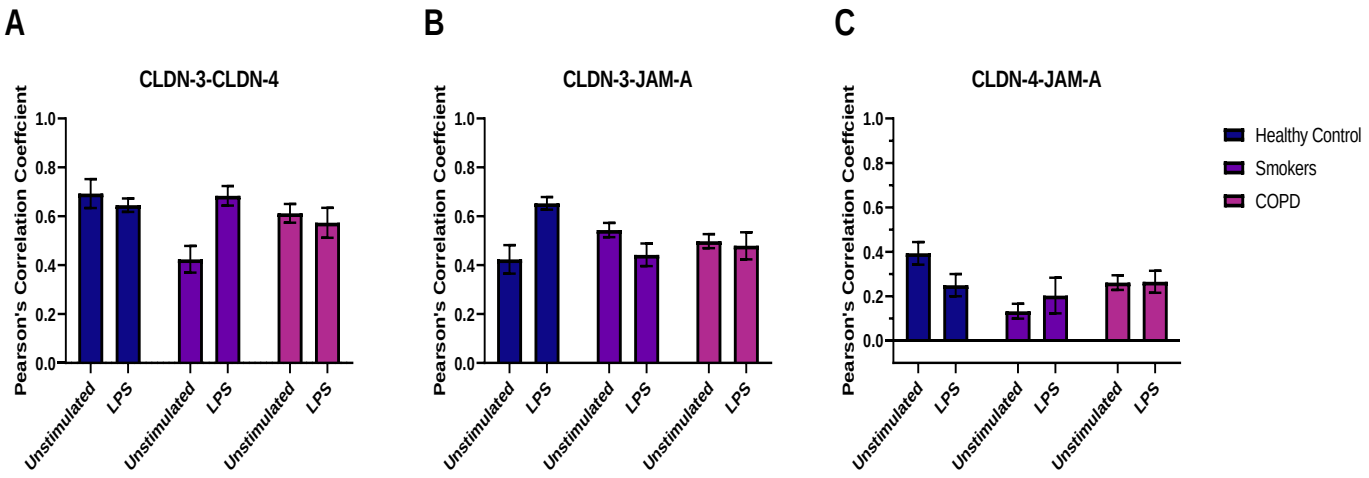


Figure 4.7: Colocalization analysis of TJ molecules after LPS stimulation: *Pearson correlation coefficient to assess colocalization between the TJ molecules **(A)** CLDN-3 and CLDN-4, **(B)** CLDN-3 and JAM-A, and **(C)** CLDN-4 and JAM-A in healthy, smoker, and COPD HBECs after 24 h of LPS stimulation at 20 ng/ml compared to media treated HBECs. Error bars are representative of means with SEM.*

4.1.8 Changes in transepithelial resistance in response to NTHi infection

HBECs were infected with 10 MOI of NTHi for 24 hours and TERs were subsequently measured for any changes. There were no significant changes in TERs in healthy, smokers, and COPD HBECs in response to NTHi infection (p=0.44, p=0.53, and p=0.11 respectively) **(Figure 4.8)**

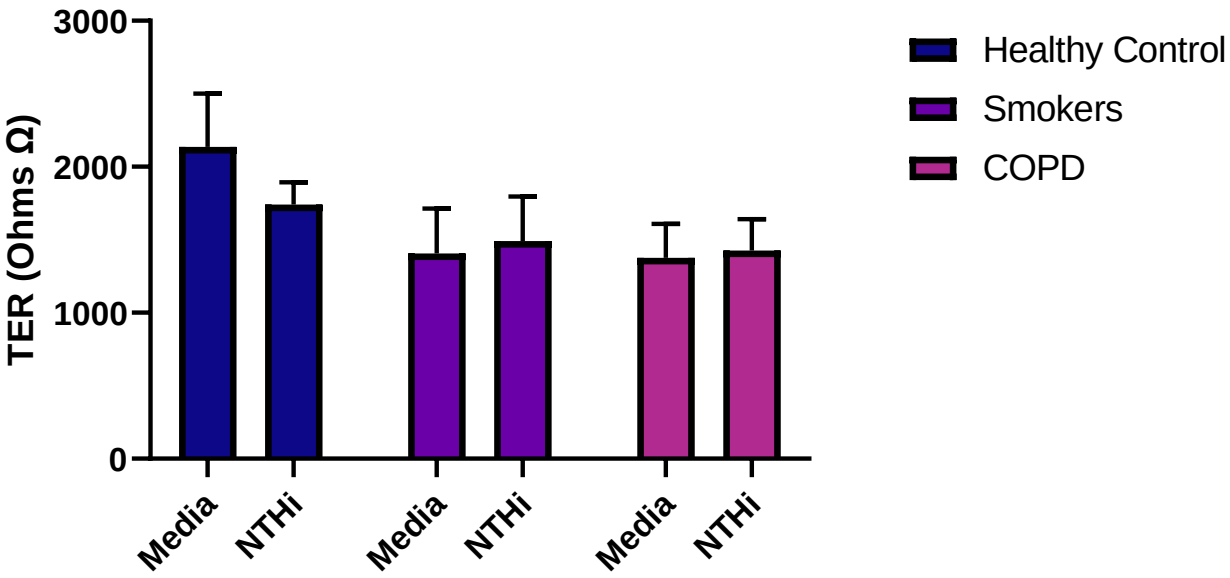


Figure 4.8: Transepithelial resistance in HBECs post-infection with NTHi remains unchanged. *HBECs were infected with 10 MOI of NTHi for 24 h and TERs were subsequently measured at basal levels and after stimulation. N: Healthy=4, Smokers=3, COPD=4. Error bars are representative of SEMs. Mann-Whitney and Wilcoxon correction tests performed.*

4.1.9 Localization of TJs CLDN-3, CLDN-4, and JAM-A in response to NTHi infection

In order to assess the localization of the TJs CLDN-3, -4, and JAM-A in HBECs in response to a physiologically pertinent infection, HBECs were infected with NTHi for 24 hours at an MOI of 10 then visualized. CLDN-3 had a significant amount of clustering and polarization in healthy HBEC when infected with NTHi which was similar to what was observed when stimulated with LPS. In sharp contrast to the behavior observed under LPS stimulation, smoker HBECs had significantly more clustering and

polarization observed in response to NTHi infection. Similarly, COPD HBECs also had clustering and polarization of CLDN-3 after NTHi infection to the same degree that was observed in healthy HBECs **(Figure 4.9a, b)**.

Polarization of CLDN-4 was also observed in healthy HBECs however CLDN-4 was not as heavily clustered as CLDN-3 in response to NTHi. Smokers HBECs exhibited a similar trend in CLDN-4 localization to healthy HBECs with polarization observed but little clustering of CLDN-4 on the cell surface. COPD HBECs however had little to no clustering or polarization of CLDN-4 on the cell surface in response to NTHi infection **(Figure 4.9a, b)**.

JAM-A was heavily polarized and clustered in healthy HBECs after NTHi infection with little to no JAM-A localization at the intercellular junctions. Localization of JAM-A in smoker HBECs was similar to healthy HBECs with significant clusters and polarization of JAM-A observed however there was also more JAM-A observed at the intercellular junctions of the HBECs. COPD HBECs exhibited a similar clustering and polarizing behaviors to smoker HBECs in response to NTHi infection with several clusters observed as well as localization of JAM-A at the intercellular junctions of the cells. Overall, the images indicate that CLDN-3 responds by clustering and polarizing on the cell surface in all three groups after NTHi infection but the same trend is not as marked in CLDN-4 with only some polarization observed in healthy and smoker HBECs. JAM-A also had significant clustering and polarization in all three groups however it was also found to be localized at the intercellular junction of the cell in COPD and smoker HBECs **(Figure 4.9a, b)**.

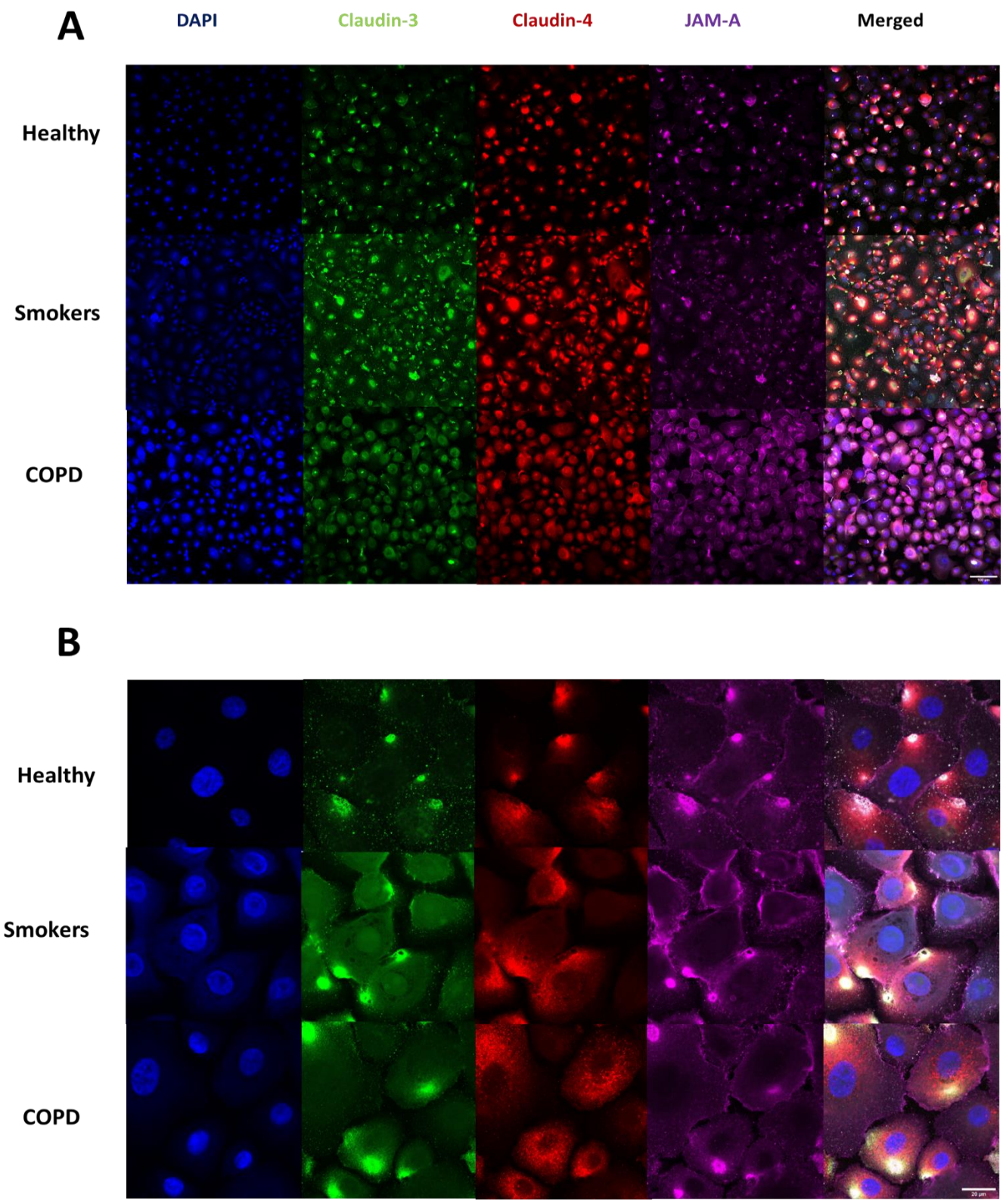


Figure 4.9: CLDN-3, CLDN-4, and JAM-A visualized in NTHi infected HBECs. *TJ molecules CLDN-3, CLDN-4, and JAM-A stained and visualized under a confocal microscope in healthy, smoker, and COPD HBECs after 24 h of NTHi infection of 10 MOI at (**A**) 100X, scale=100 µm and (**B**) 630X magnifications, scale=20 µm. All HBECs groups exhibit clustering and polarization. All groups has clustered and polarized TJ molecules in HBECs but not as strongly with CLDN-4 in COPD HBECs as well as JAM-A intercellular localization in all groups.*

4.1.10 Effect of NTHi infection on Tight Junction Expression in HBECs

In order to study TJ molecules and barrier integrity in a more physiologically relevant setting, NTHi was used to stimulate HBECs for 24 h at 10 MOI. This was done to examine if similar to LPS, no response would be observed in TJ molecule expression when NTHi, a bacteria that is commonly found in COPD, is used. In contrast to LPS stimulation, NTHi infection significantly upregulated CLDN-3, -4, and JAM-A by approximately 2-fold, 2.8-fold, and 2-fold respectively in healthy HBECs (Medians: 5446, 6890, 3860) ($p<0.0001$, $p <0.0001$, $p<0.0001$) **(Figure 4.10a, b, c)**. There were no significant changes in CLDN-3 and CLDN-4 (Medians: 3218 and 3716) in smoker HBECs in response to NTHi infection ($p=0.3586$ and $p=0.4509$) **(Figure 4.10a, b)**. However, JAM-A expression was significantly decreased by around 40% in response to NTHi in smoker HBECs (Median: 1940, $p=0.0472$) **(Figure 4.10c)**. COPD HBEC expression of the TJ molecules CLDN-3, -4, and JAM-A were unchanged when infected with NTHi (Medians: 5922, 7504, and 3562) ($p=0.1916$, $p=0.3626$, 0.2581) **(Figure 4.10a, b, c)**. Unlike LPS, healthy HBECs were significantly more responsive to NTHi infection by upregulating their TJ molecules while smokers and COPD HBECs seem to be largely unresponsive to NTHi.

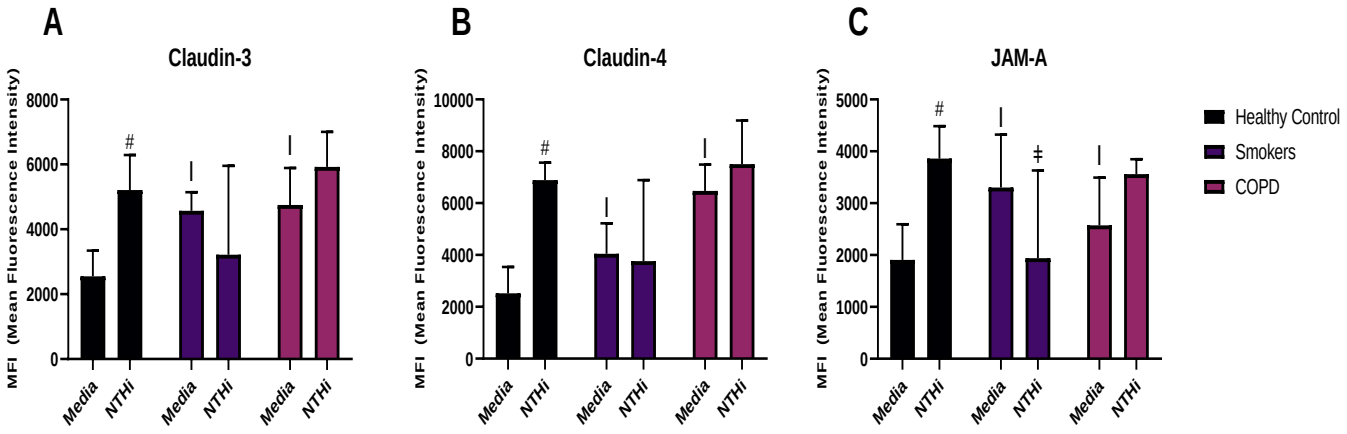


Figure 4.10: CLDN-3, CLDN-4, and JAM-A expression in response to NTHi infection in HBECs. *MFI of the TJ molecules **(A)** CLDN-3, **(B)** CLDN-4, and **(C)** JAM-A in healthy, smoker, and COPD HBECs in response to 24 h of NTHi infection at 10 MOI. Error bars are representative of medians with 95% CI. #/\: P<0.05 compared to unstimulated healthy controls. Welch t-tests, and ratio paired t-tests performed ǂ: P<0.05 compared to unstimulated smokers (N: Healthy= 3, smokers=3, COPD=6). Healthy HBECs upregulate TJ proteins measured post-infection but not in smoker or COPD HBECs.*

4.1.11 Colocalization changes in HBECs after NTHi HBECs

Following NTHi infection, CLDN-3 and CLDN-4 were still strongly colocalized in healthy HBECs (R=0.70) and smoker and COPD were still moderately colocalized as they were under basal conditions (R=0.51 and R=0.63 respectively) **(Figure 4.11a)**. CLDN-3 and JAM-A became moderately colocalized in healthy HBECs after NTHi stimulation (R=0.64) while CLDN-3 and JAM-A remained moderately colocalized in smoker and COPD HBECs (R=0.63 and R=0.56 respectively) **(Figure 4.11b)**. CLDN-4 and JAM-A remained weakly colocalized in healthy HBECs (R=0.40) and remained very weakly colocalized in smoker and COPD HBECs (R=0.27 and R=0.21) after infection with NTHi **(Figure 4.11c)**.

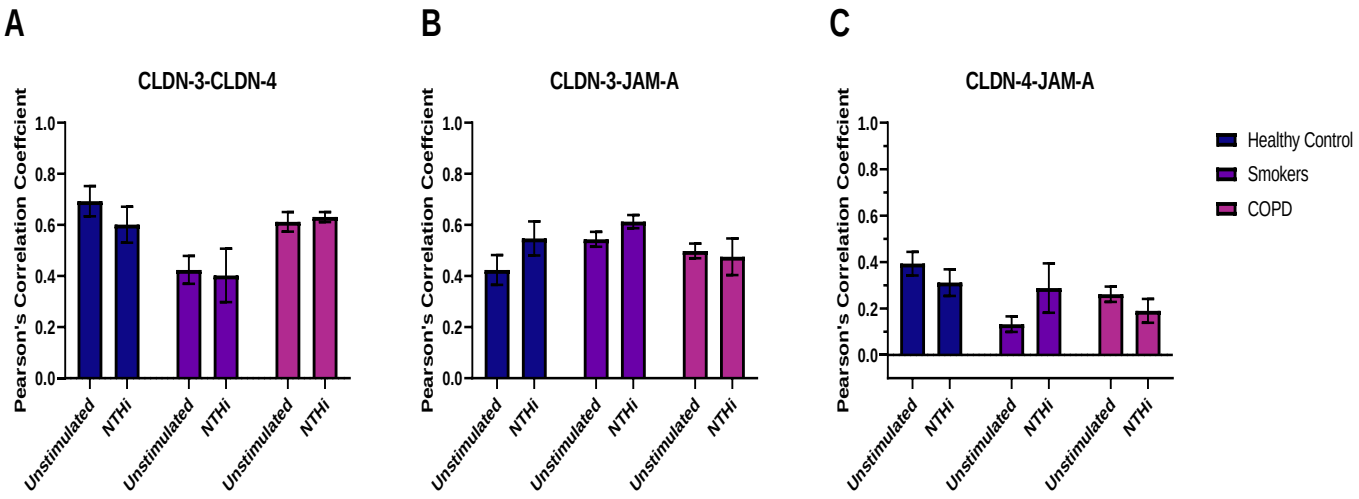


Figure 4.11: Colocalization analysis of TJ molecules after NTHi infection: *Pearson correlation coefficient to assess colocalization between the TJ molecules **(A)** CLDN-3 and CLDN-4, **(B)** CLDN-3 and JAM-A, and **(C)** CLDN-4 and JAM-A in healthy, smoker, and COPD HBECs after 24 h of NTHi infection at 10 MOI compared to media treated HBECs. Error bars are representative of means with SEM.*

4.1.12 Transepithelial resistance in HBECs after poly I:C stimulation

TERs were measured with the viral analogue poly I:C stimulating HBECs for 24 hours at a concentration of 25 µg/ml. There were no significant changes in the TERs of either healthy, smoker, or COPD HBECs in response to poly I:C stimulation (p=0.54, p=0.11, p=0.31 respectively) **(Figure 4.12)**.

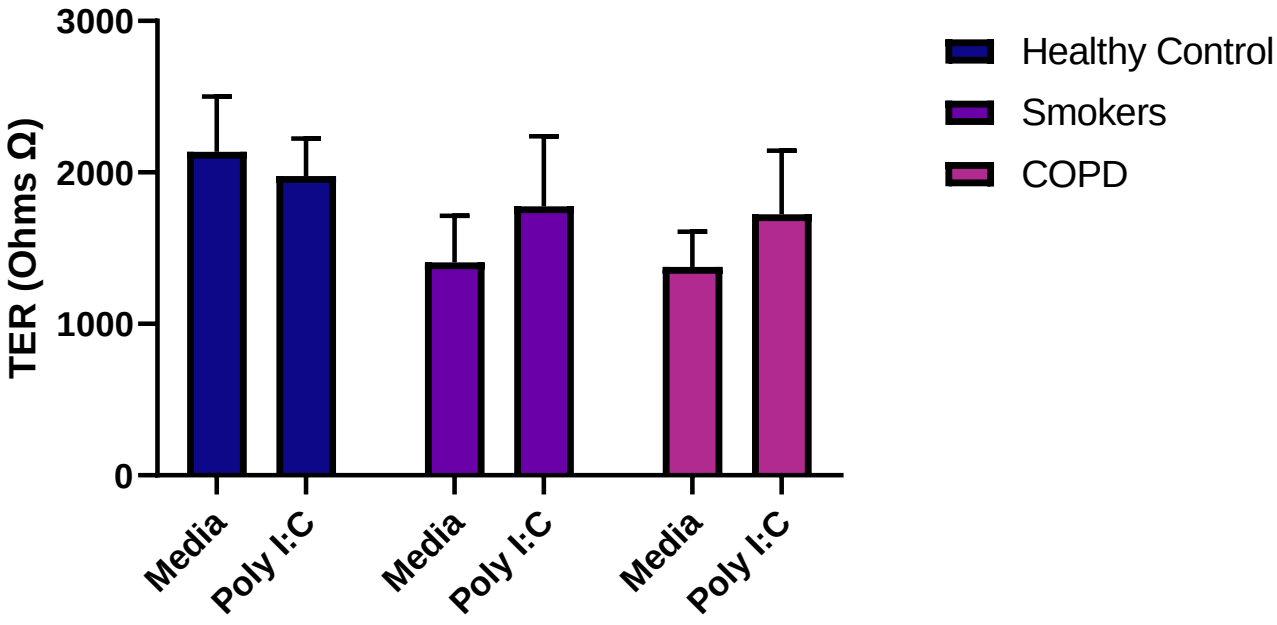


Figure 4.12: No significant differences in transepithelial resistance in HBECs after poly I:C stimulation. *HBECs were stimulated with 25 µg/ml of poly I:C for 24 h and TERs were subsequently measured at basal levels and after stimulation. N: Healthy=4, Smokers=3, COPD=4. Error bars are representative of SEMs. Mann-Whitney and Wilcoxon correction tests performed.*

4.1.13 Change and Localization of TJ proteins in HBECs after stimulation with Poly I:C

The effects of poly I:C on TJ proteins HBECs was then investigated by first looking at any spatial changes in CLDN-3, CLDN-4, and JAM-A after 24 h of poly I:C stimulation at a dose of 25 µg/ml. While CLDN-3 was diffused across the cell surface in unstimulated healthy HBECs, CLDN-3 became heavily polarized and clustered after stimulation with poly I:C. In contrast, CLDN-3 became widely diffused across the cell surface after poly I:C stimulation in both smoker and COPD HBECs with a slight amount of polarization observed in COPD HBECs **(Figure 4.13a, b)**.

Some polarization and clustering of CLDN-4 was observed in healthy HBECs in response to poly I:C but to a lesser degree than what was observed with CLDN-3.

However, CLDN-4 followed the same trend as CLDN-3 in COPD and smoker HBECs with CLDN-4 being diffused across the cell surface with little to no polarization in response to poly I:C stimulation **(Figure 4.13a, b)**.

JAM-A in healthy HBECs was also heavily polarized and clustered after poly I:C stimulation with little to no localization at the intercellular junctions observed. poly I:C stimulated smoker HBECs had JAM-A diffused across the cell however some intercellular junction localization as well a polarization was also observed and thus localization of JAM-A seemed to be disorganized and seemingly not following any spatial trend. In COPD HBECs, JAM-A was heavily localized at the junctions of the cells in response to poly I:C with little to no polarization of JAM-A observed **(Figure 4.13a, b)**.

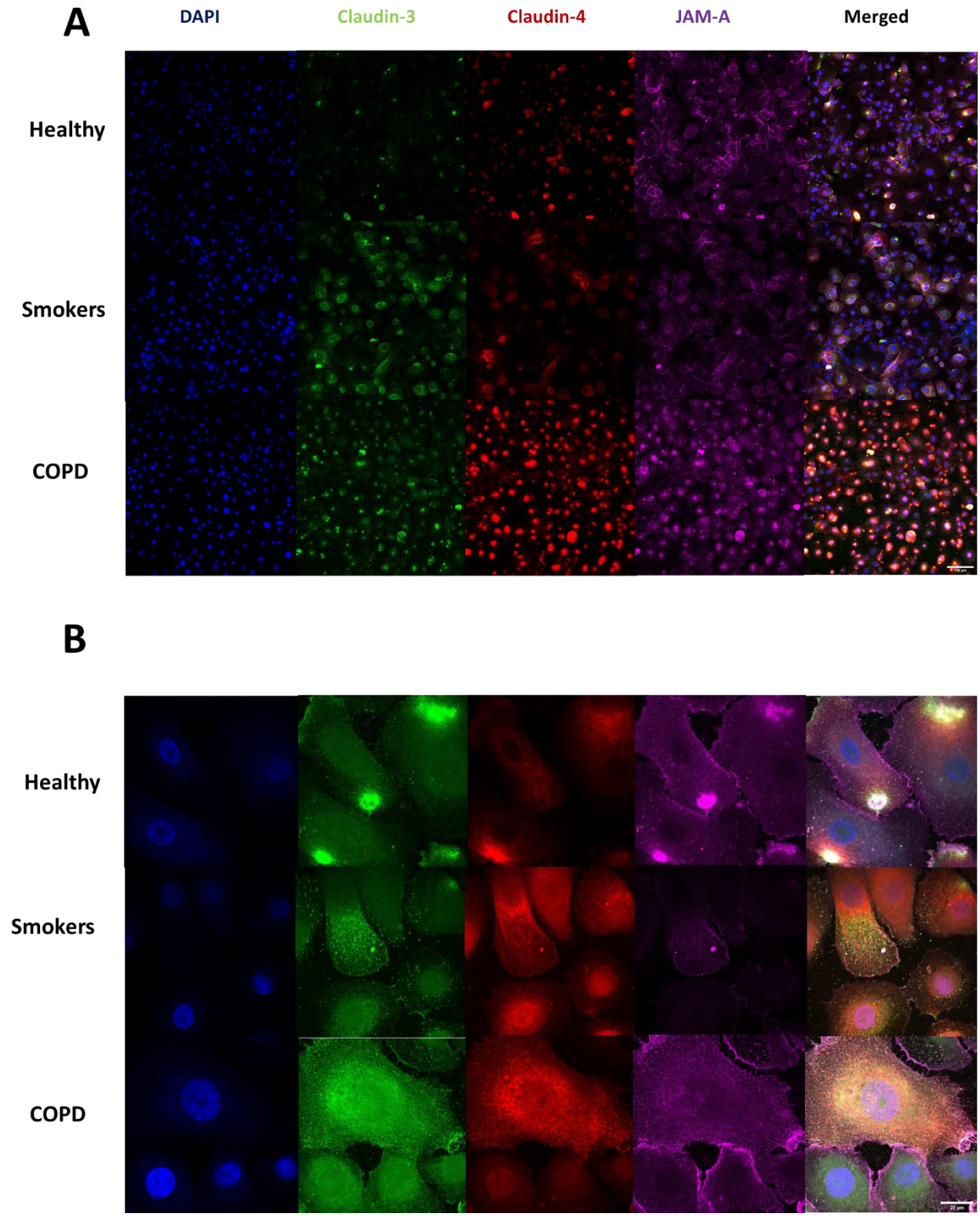


Figure 4.13: CLDN-3, CLDN-4, and JAM-A visualized in Poly I:C stimulated HBECs. *TJ molecules CLDN-3, CLDN-4, and JAM-A stained and visualized under a confocal microscope in healthy, smoker, and COPD HBECs after 24 h of Poly I:C stimulation at 25 µg/ml at (**A**) 100X, scale=100 µm and (**B**) 630X magnifications, scale=20 µm. While TJ proteins clustered in healthy HBECs they were largely diffused in smoker and COPD HBECs*

4.1.14 Poly I:C Stimulation of HBECs effect on Tight Junction Expression

In order to understand the effect of viral stimuli on HBEC barrier integrity in all three groups, expression of CLDN-3, CLDN-4, and JAM-A were measured after poly I:C stimulation. There were no significant changes in levels of either CLDN-3, -4, or JAM-A in response to Poly I:C stimulation in healthy HBECs (Medians: 2553, 4175, 2115) (p=0.8001, p=0.2047, p=0.7464) **(Figure 4.14a, b, c)**. Smoker HBECs had no significant changes in CLDN-3, -4, and JAM-A levels as well after poly I:C stimulation (Medians: 3812, 3611, 2849) (p=0.1378, p=0.8243, p=0.6066) **(Figure 4.14a, b, c)**. HBECs from COPD patients however had a significant decrease in CLDN-3 expression in response to poly I:C with approximately a third decrease in CLDN-3 levels (Median: 3330, p=0.0497) **(Figure 4.14a)**. CLDN-4 and JAM-A levels had no significant changes in COPD HBECs after poly I:C stimulation (Medians: 4810 and 2237) (p=0.4331 and p=0.0625) **(Figure 4.14b, c)**. Taken together, the results indicate that TJs levels were largely unchanged in response to poly I:C with the exception of a decrease in CLDN-3 observed in COPD HBECs.

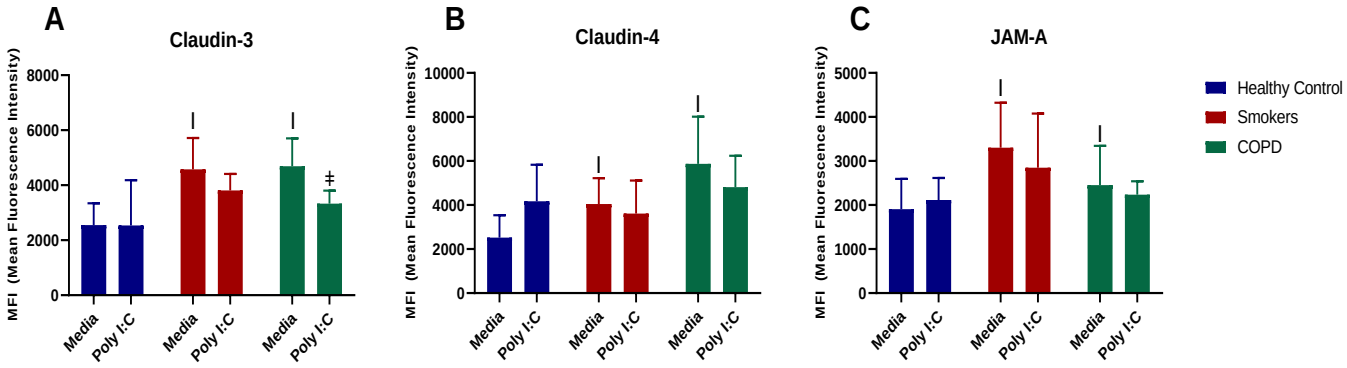


Figure 4.14: CLDN-3, CLDN-4, and JAM-A expression in Poly I:C stimulated HBECs. *MFI of the TJ molecules **(A)** CLDN-3, **(B)** CLDN-4, and **(C)** JAM-A in healthy, smoker, and COPD HBECs after 24 h of Poly I:C stimulation at 25 µg/ml compared to media treated HBECs. Error bars are representative of medians with 95% CI. Welch t-tests, and ratio paired t-tests performed* ǀ*: P<0.05 compared to unstimulated healthy controls.* ǂ*: P<0.05 compared to unstimulated COPD (N: Healthy= 4, smokers=7, COPD=5).*

4.1.15 Effect of Poly I:C stimulation on TJ protein colocalization

CLDN-3 and CLDN-4 became moderately colocalized in healthy HBECs after Poly I:C stimulation (R=0.69) while CLDN-3 and CLDN-4 became strongly colocalized in smoker HBECs (R=0.75) **(Figure 4.15a).** Colocalization of CLDN-3 and CLDN-4 remained unchanged in HBECs of COPD patients (R=0.67) **(Figure 4.15a)**.

CLDN-3 and JAM-A became moderately colocalized in healthy HBECs (R=0.67) in response to Poly I:C while they remained moderately colocalized in smoker (R=0.51) and COPD HBECs (R=0.54) **(Figure 4.15b)**. CLDN-4 and JAM-A were still weakly colocalized after Poly I:C stimulation (R=0.31). CLDN-4 and JAM-A colocalization increased however in smoker (R=0.31) and COPD (R=0.38) but were still weakly colocalized together **(Figure 4.15c)**.

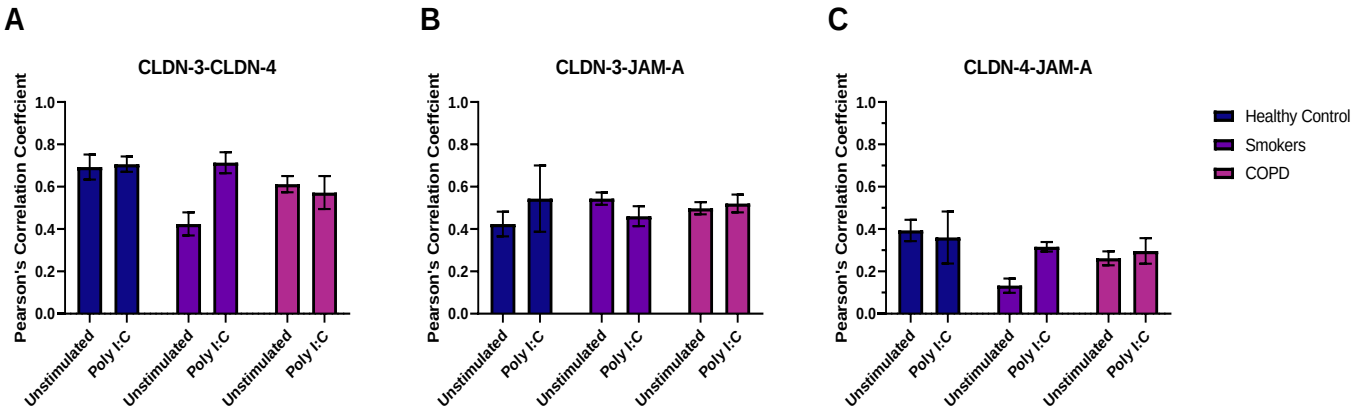


Figure 4.15: Colocalization analysis of TJ molecules after Poly I:C stimulation: *Pearson correlation coefficient to assess colocalization between the TJ molecules **(A)** CLDN-3 and CLDN-4, **(B)** CLDN-3 and JAM-A, and **(C)** CLDN-4 and JAM-A in healthy, smoker, and COPD HBECs after 24 h of Poly I:C stimulation at 25 µg/ml compared to media treated HBECs. Error bars are representative of means with SEM.*

4.1.16 Changes in transepithelial resistance post-infection with RV

Measurements of the TERs were taken post-infection with 0.1 MOI of RV16 for 24 hours in all three groups of HBECs. There were no significant changes in TERs in all

three groups of healthy, smokers, and COPD HBECs post-infection with RV16 however there was an increasing trend observed in healthy HBECs in response to RV16 infection (p=0.16, p=0.07, and p=0.22 respectively) **(Figure 4.16)**.

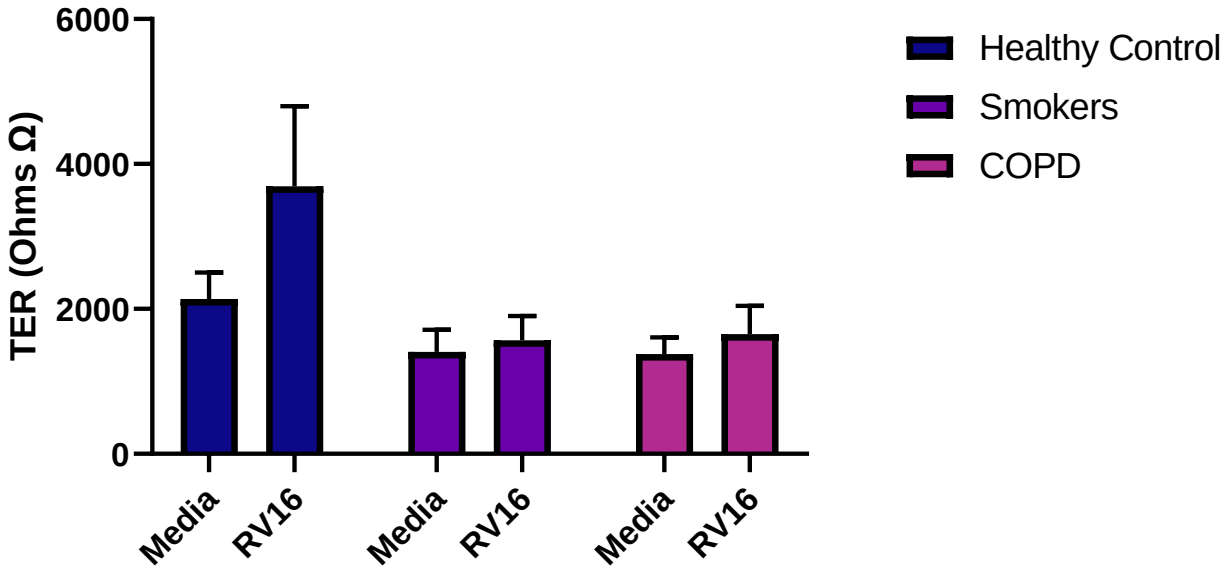


Figure 4.16: Effect of RV16 infection on Transepithelial resistance. *HBECs were infected with 0.1 MOI of RV16 for 24 hourrs and TERs were subsequently measured at basal levels and after stimulation. N: Healthy=4, Smokers=3, COPD=4. Error bars are representative of SEMs. Mann-Whitney and Wilcoxon correction tests performed.*

4.1.17 Spatial changes in Tight Molecules in response to infection of HBECs with RV16

HBECs were subsequently infected with RV16 for 24 h at 0.1 MOI in order to assess any changes in TJ molecules after infection of a live virus that is commonly associated with COPD exacerbations. Similar to what was seen after Poly I:C stimulation, CLDN-3 was heavily polarized and clustered in healthy HBECs after infection with RV16. Smoker and COPD HBECs infected with RV16 also match the trend of Poly I:C stimulation with CLDN-3 being diffused across the cell surface in smoker and COPD HBECs and some polarized of CLDN-3 observed in the HBECs of COPD patients **(Figure 4.17a, b)**.

CLDN-4 exhibited polarization in healthy HBECs after RV16 infection but no clustering. Smoker HBECs showed neither clustering or polarization of CLDN-4 after infection and was mostly dispersed on the HBECs. CLDN-4 was polarized on the HBECs of COPD patients in response to RV16 but did not cluster **(Figure 4.17a, b)**.

JAM-A, as observed with CLDN-3, was clustered and polarized on healthy HBECs after RV16 infection without junctional localization. In smoker HBECs, JAM-A mostly localized to the intercellular junctions though not as strongly as in COPD patients where intercellular junction localization as well as some polarization was observed though not to the same extent as in healthy HBECs **(Figure 4.17a, b)**.

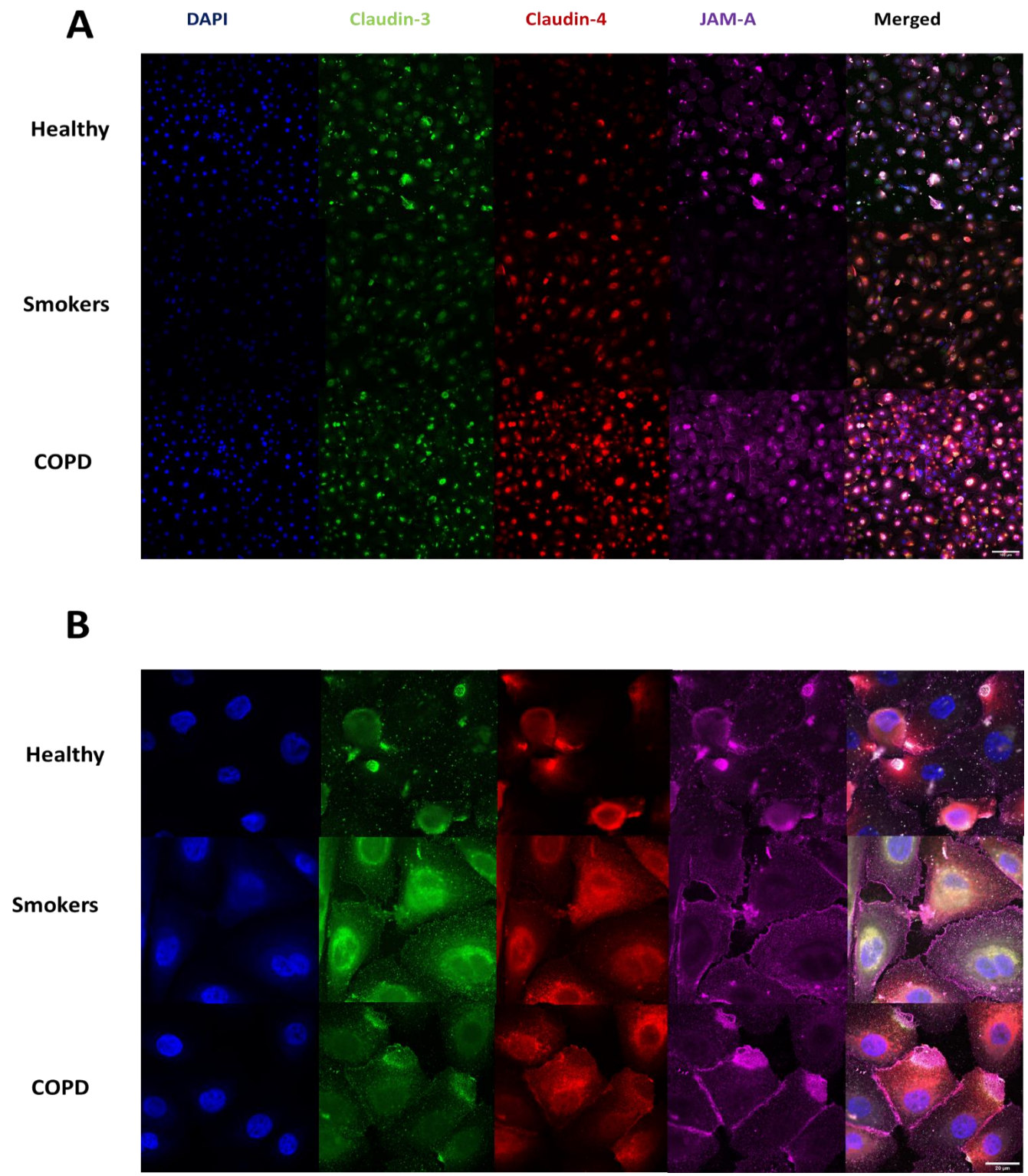


Figure 4.17: CLDN-3, CLDN-4, and JAM-A visualized in RV16 infected HBECs. *TJ molecules CLDN-3, CLDN-4, and JAM-A stained and visualized under a confocal microscope in healthy, smoker, and COPD HBECs after 24 h of RV16 infection at a dose of 0.1 MOI at (**A**) 100X, scale=100 µm and (**B**) 630X magnifications, scale=20 µm. Clustering and polarization was observed in healthy HBECs but was largely absent in smoker and COPD HBECs with mostly TJ protein diffusion across the cell surface or some polarization occurring.*

4.1.18 Changes in Tight Junction Levels after RV16 Infection of HBECs

Unlike with Poly I:C stimulation, the TJ molecules in healthy HBECs were significantly upregulated in healthy HBECs in response to RV16. CLDN-3, -4, and JAM-A increased by 2-fold, 2-fold, and 1.4-fold respectively in healthy HBECs after RV16 stimulation (Medians: 5207, 6274, and 2720) ($p<0.0001$, $p=0.0002$, $p=0.0114$) **(Figure 4.18a, b, c)**. In contrast, smokers had a significant decrease in levels of CLDN-3 and JAM-A when infected with RV16 with a decrease of approximately a third and 40% respectively (Medians: 2903 and 1967) ($p=0.0420$ and $p<0.0001$) **(Figure 4.18a, c)**. Levels of CLDN-4 remained unchanged however in smoker HBECs after RV16 infection (Median: 2787, $p=0.4600$) **(Figure 4.18b)**. HBECs of COPD patients did not respond to RV16 infection and thus levels of CLDN-3, -4, and JAM-A did not significantly change (Medians: 6166, 6096, and 3040) ($p=0.2150$, $p=4108$, $p=0.5728$) **(Figure 4.18a, b, c)**. Overall, the results show that healthy HBECs are significantly more responsive than COPD HBECs by upregulating expression of the measured TJ molecules in response to RV16 infection while TJ molecule expression in COPD HBECs remain unchanged. Smoker HBECs had a significant decrease in the levels of CLDN-3 and JAM-A as opposed to the trend in healthy HBECs while CLDN-4 levels remain unchanged.

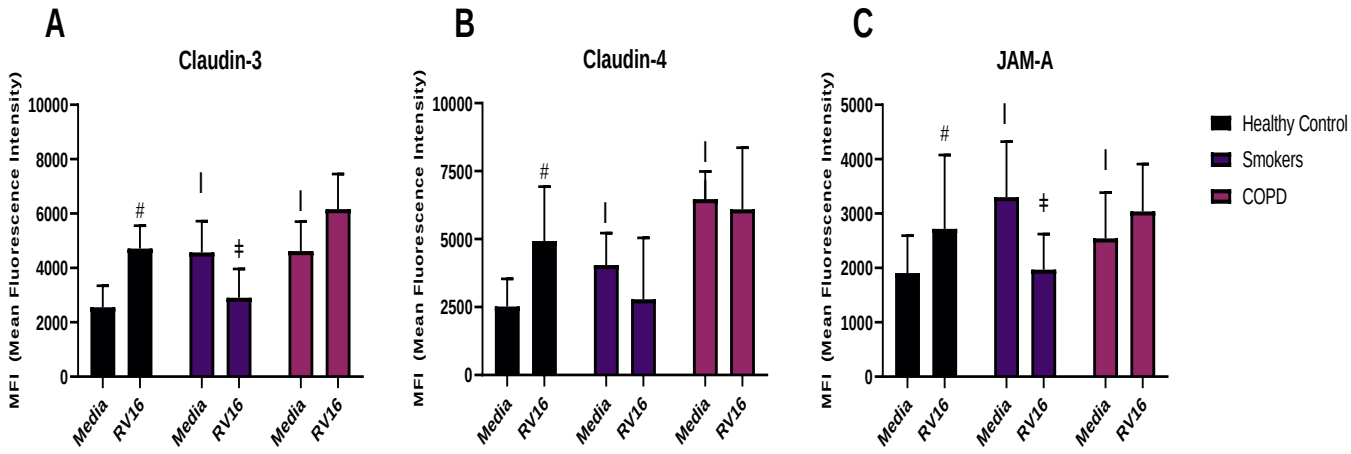


Figure 4.18: CLDN-3, CLDN-4, and JAM-A expression in response to RV16 infection in HBECs. *MFI of the TJ molecules **(A)** CLDN-3, **(B)** CLDN-4, and **(C)** JAM-A in healthy, smoker, and COPD HBECs in response to 24 h of RV16 infection of 0.1 MOI. Error bars are representative of medians with 95% CI. Welch t-tests, and ratio paired t-tests performed. #/I: P<0.05 compared to unstimulated healthy controls. ‡: P<0.05 compared to unstimulated smokers (N: Healthy=3, smokers=3, COPD=6).*

4.1.19 Effect of RV16 infection of HBECs on Colocalization of CLDN-3, -4, and JAM-A

A moderate colocalization of CLDN-3 and CLDN-4 was seen in healthy HBECs after RV16 infection from a strong one at basal conditions (R=0.61) **(Figure 4.19a)**. CLDN-3 and CLDN-4 remained moderately colocalized in smoker(R=0.68) and COPD HBECs (R=0.62) even after RV16 infections **(Figure 4.19a)**. CLDN-3 and JAM-A colocalization changed from a weak to a moderate colocalization after RV16 infection in healthy HBECs (R=0.69) **(Figure 4.19b)**. Both TJ molecules were still moderately colocalized in smoker (R=0.54) and COPD HBECs (R=0.61) after infection **(Figure 4.19c)**.

Finally, CLDN-4 and JAM-A were still weakly colocalized in healthy HBECs after RV16 infection (R=0.44) while smoke (R=0.22) r and COPD HBECs (R=0.28) remained very

weakly colocalized in response to RV16 infection and less so than healthy HBECs **(Figure 4.19c)**.

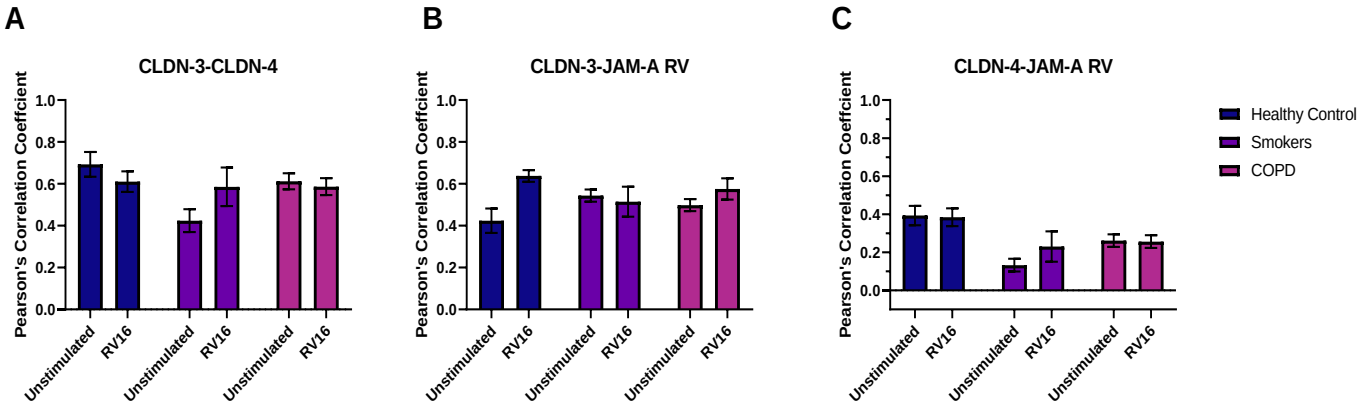


Figure 4.19: Colocalization analysis of TJ molecules after RV16 infection: *Pearson correlation coefficient to assess colocalization between the TJ molecules **(A)** CLDN-3 and CLDN-4, **(B)** CLDN-3 and JAM-A, and **(C)** CLDN-4 and JAM-A in healthy, smoker, and COPD HBECs after 24 h with or without RV16 infection at 0.1 MOI. Error bars are representative of means with SEM.*

4.1.20 Gene expression of CLDN-3, CLDN-4, and JAM-A in HBECs after NTHi and RV16 infections

To assess whether the TJ molecules measured through microscopy are changed after NTHi or RV16 infection through a transcriptional or post-translational level, gene expression measurement of CLDN-3, -4, and JAM-A were performed through RT-qPCR. CLDN-3 gene expression was significantly upregulated in healthy HBECs after RV16 infection with a 1.83-log fold increase after infection (p=0.0022) **(Figure 4.20a)**. There were no significant changes in healthy HBECs however after NTHi infection (p=0.200). No significant differences were found in CLDN-3 gene expression after NTHi infection in smoker HBECs (p=0.6372) but there was a significant downregulation in CLDN-3 compared to healthy controls after RV16 stimulation

(p=0.0436) **(Figure 4.20b)**. In COPD HBECs, expression of CLDN-3 was unchanged after either NTHi or RV16 infections (p=0.5581 and p=0.1939) **(Figure 4.20c)** .

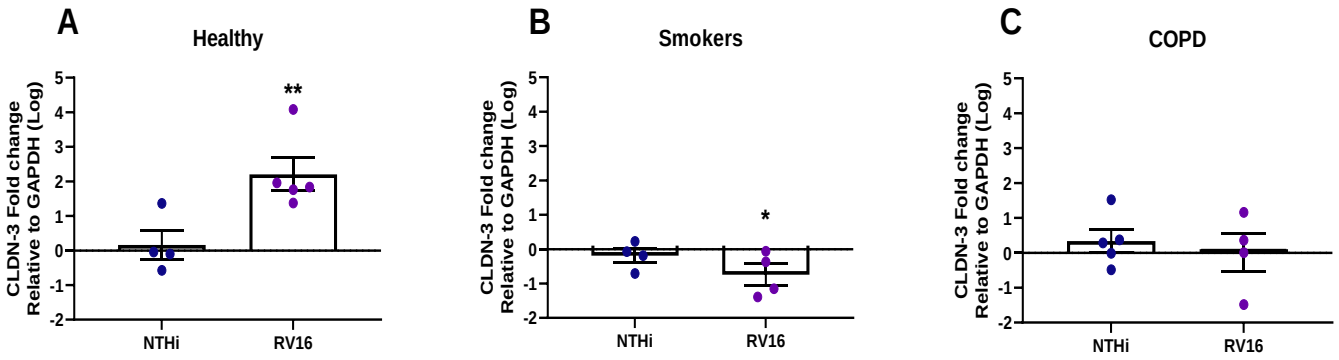


Figure 4.20: Gene expression of CLDN-3 in HBECs after NTHi and RV16 stimulation: Relative gene *expression of CLDN-3 relative to unstimulated HBECs after 24 hours of stimulation of either 10 MOI of NTHi or 0.01 MOI of RV16 in **(A)** Healthy, **(B)** Smokers, **(C)** COPD HBECs. N: Healthy=4-5, Smokers=4, COPD=4-5. Error bars are representative of means with SEM. Ratio paired t-tests and Wilcoxon correction tests performed. *: p<0.05 compared to unstimulated controls. **: p<0.005 compared to unstimulated controls. Each dot represents a biological replicate.*

Unlike CLDN-3 there were no significant differences in CLDN-4 expression after either NTHi or RV16 stimulation in healthy HBECs despite an increase seen after RV16 stimulation (p=0.6250 and p=3125) **(Figure 4.21a)**. Similarly, no fold changes were observed in CLDN-4 expression in smoker HBECs after either NTHi or RV16 stimulation (p=0.9680 and p=0.6446) and no significant differences seen in COPD HBECs either after infection (p=0.3636 and p=3864) **(Figure 4.21b, c)**.

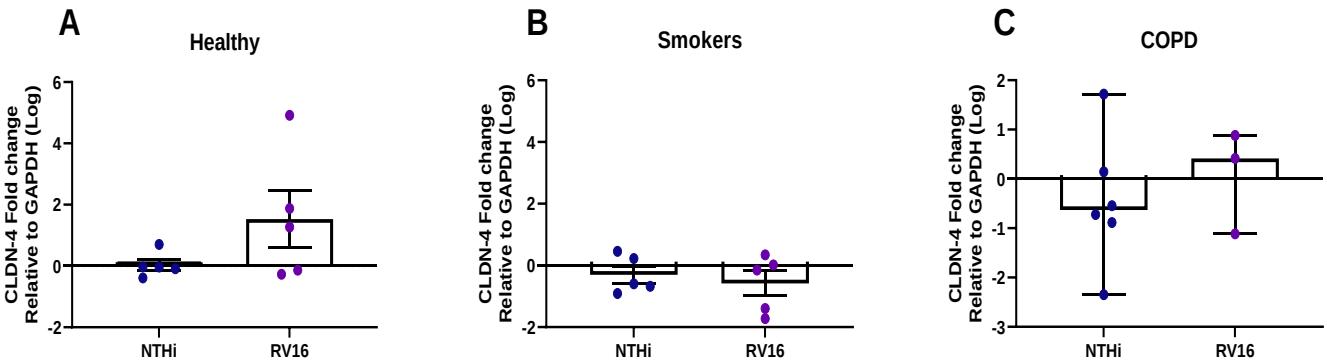


Figure 4.21: Gene expression of CLDN-4 in HBECs after NTHi and RV16 stimulation: Relative gene *expression of CLDN-4 relative to unstimulated HBECs after 24 hours of stimulation of either 10 MOI of NTHi or 0.01 MOI of RV16 in* ***(A)*** *Healthy,* ***(B)*** *Smokers,* ***(C)*** *COPD HBECs. N: Healthy=5-6., Smokers=5, COPD=3-6. Error bars are representative of means with SEM. Ratio paired t-tests and Wilcoxon correction tests performed. Each dot represents a biological replicate.*

Lastly, gene expression of JAM-A was unchanged in healthy HBECs after stimulation with either NTHi or RV16 (p=0.6055 and p=0.5693) as well as infected smoker HBECs (p=0.7933 and p=0.8882) and the HBECs of COPD patients (p=0.4738 and 0.3855) **(Figure 4.22a, b, c)**. Overall, these results indicate that there are no significant transcriptional differences in CLDN-3, CLDN-3, and JAM-A after NTHi or RV16 stimulation in all three groups with the exception of a significant 1.83 log-fold increase in CLDN-3 after RV16 stimulation in healthy HBECs.

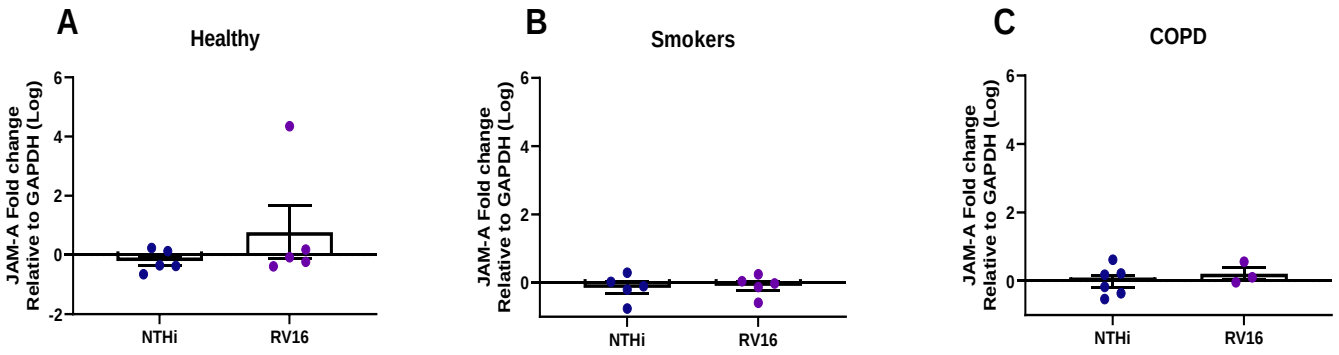


Figure 4.22: Gene expression of JAM-A in HBECs after NTHi and RV16 stimulation: Relative gene *expression of JAM-A compared to unstimulated HBECs after 24 hours of stimulation of either 10 MOI of NTHi or 0.01 MOI of RV16 in* ***(A)*** *Healthy,* ***(B)*** *Smokers,* ***(C)*** *COPD HBECs. Error bars are representative of means with SEM. Ratio paired t-tests performed. N: Healthy=5, Smokers=5, COPD=3-6. Each dot represents a biological replicate.*

4.1.21 Tight Junction Molecules Occludin and ZO-1 gene expression after NTHi and RV16 infection

The TJ molecules ZO-1 and Occludin were subsequently measured as they have been found to be highly expressed in the bronchioles and are physiologically altered in some disease states such as asthma and smoking. Changes in gene expression in both ZO-

1 and Occludin were measured in all three groups after 24 h of either NTHi or RV16 infections

Gene expression of Occludin remained unchanged in healthy HBECs after NTHi or RV16 stimulation (p=0.8125 and p=0.5693) **(Figure 4.23a)**. Neither the HBECs of smokers (p=0.6203 and p=0.4482) or COPD patients (p=0.0781 and p=0.7660) had any significant changes in Occludin after NTHi and RV16 infection as well compared to the unstimulated HBECs **(Figure 4.23b, c)**.

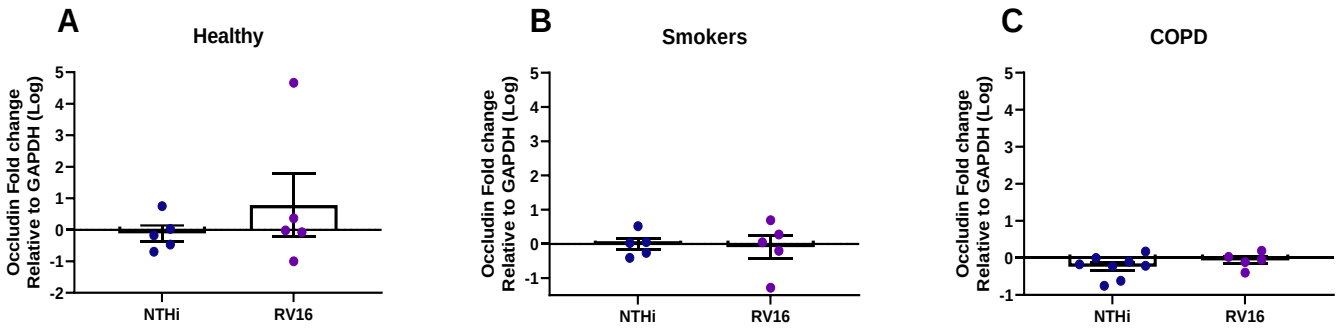


Figure 4.23: Gene expression of Occludin in HBECs after NTHi and RV16 stimulation: Relative gene *expression of Occludin compared to unstimulated HBECs after 24 hours of stimulation of either 10 MOI of NTHi or 0.01 MOI of RV16 in **(A)** Healthy, **(B)** Smokers, **(C)** COPD HBECs. Ratio paired t-tests performed. N: Healthy=5, Smokers=5, COPD=5-8. Error bars are representative of means with SEM. Each dot represents a biological replicate.*

ZO-1 levels were also unchanged after NTHi or RV16 infection in healthy HBECs (p=0.7502 and p=0.5693) **(Figure 4.24a)**. However, ZO-1 levels were significantly downregulated by approximately a 0.5 log-fold after NTHi infection in smoker HBECs (p=0.0228) **(Figure 4.24b)**. No changes were observed however in smoker HBECs after RV16 infection (p=0.3815). In contrast to smoker or healthy HBECs, there was a significant 0.5 log-fold upregulation in ZO-1 in COPD HBECs after NTHi infection (p=0.0285) **(Figure 4.24c)**. No significant changes were observed in ZO-1 after RV16 infection in COPD HBECs (p=0.4950) **(Figure 4.24c)**. The data indicates that Occludin gene expression remained unchanged in all groups after either NTHi or RV16

infection. ZO-1 expression however seemed to have different trends in all groups after NTHi infection with no changes observed in healthy HBECs, a significant decrease in smokers, and a significant upregulation in COPD patients with no changes observed after RV16 infection in all groups.

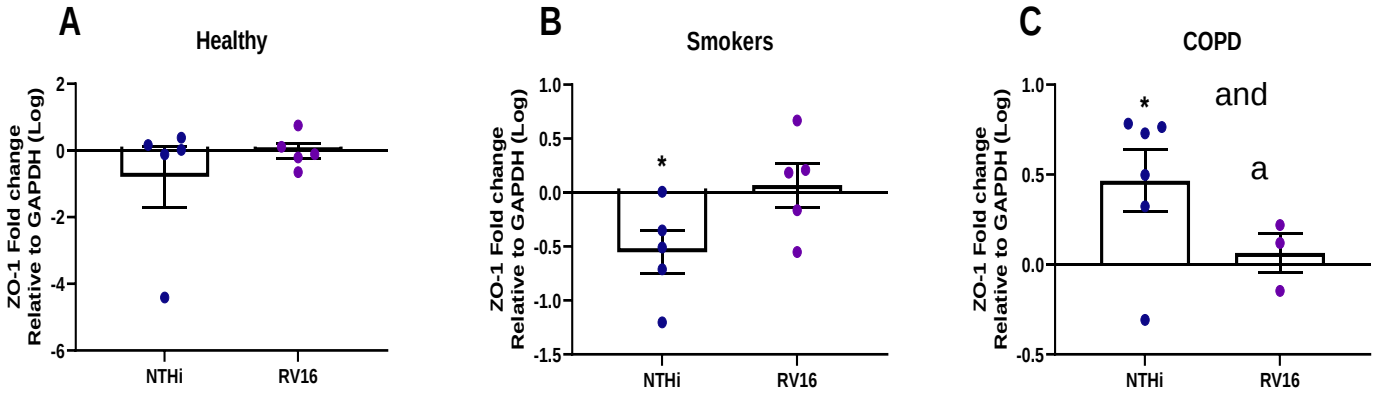


Figure 4.24: Gene expression of ZO-1 in HBECs after NTHi and RV16 stimulation: Relative gene *expression of ZO-1 compared to unstimulated HBECs after 24 hours of stimulation of either 10 MOI of NTHi or 0.01 MOI of RV16 in **(A)** Healthy, **(B)** Smokers, **(C)** COPD HBECs. N: Healthy=5, Smokers=5, COPD=3-6. Error bars are representative of means with SEM. Ratioed paired and Wilcoxon correction t-tests performed. *: p<0.05 compared to unstimulated controls. Each dot represents a biological replicate.*

Discussion

Despite the importance of the epithelial barrier and in particular TJ proteins, there are only a few studies looking at them in COPD. In fact, the majority of studies on the epithelial barrier and TJ proteins have been done either in the intestines, another mucosal barrier, or through the use of established cell lines instead of primary cells. In this study, epithelial primary cells from the lungs of healthy, smokers, and COPD patients were utilized in order to elucidate phenotypes and mechanisms that are more physiologically relevant. In addition, I attempted to establish different facets of expression and behavior of the TJ proteins from spatial behavior to expression of TJ molecules at either a genetic or protein level under different contexts.

4.2.1 TJ molecule expression differences in HBECs

The results show that the behavior and expression of the TJ proteins measured differed between all three groups and in different conditions. Perhaps most interestingly, the data seems to indicate that the expression of CLDN-3, CLDN-4, and JAM-A, at a protein level at least, were significantly higher under basal conditions in smokers and COPD patients than in healthy HBECs. The implications of having significantly greater expression of the aforementioned TJ molecules may be substantial in playing a protective role either structurally through interactions with the ECM or barrier integrity or by aiding host immune responses.

While it has been shown that CSE decreases gene expression of TJ molecules such as CLDN-1, -3, -4, ZO-1, and Occludin, this does not fall in line with the findings here[256]. However, there may be a few reasons why the findings were different. Firstly, while the cells culture here belonged to smokers, they were not exposed to any CSE during culturing. Secondly, while gene expression of TJ molecules was decreased in

response to CSE, protein expression was largely unchanged with the exception of Occludin, which was still decreased. Finally, experiments of epithelial cells exposed to CSE were done in a lung cancer cell line which differs from the primary epithelial cells acquired from smokers during this study. Another comparable lung disease where these results may be compared is asthma. In the plasma of asthma patients, CLDN-4 was found to be significantly greater than healthy controls and even greater in exacerbating asthma patients[257]. CLDN-4 in plasma however indicates that it has been either secreted or shed from the plasma membrane in endothelial or epithelial cells which could either mean it has a higher expression on the cell surface or is not able to properly function.

The significant increase in CLDN-3, -4, and JAM-A under basal condition may be due to the amount of lung injury observed in smokers and COPD patients. A study by Jin et. al on rats that attempted to induce lung injury through bacterial infection in the lungs found that rats expressed higher amounts of CLDN-3, CLDN-4, and CLDN-18 in the lungs and BAL after the induction of a lung injury compared to uninjured rats[258]. The grade of lung injury was also moderately correlated with the amount of CLDN-3, -4, and -18 that was present in the BALF of the rats. The majority of TJ molecules in the lungs are expressed in either epithelial or endothelial cells and thus the source of the TJ proteins in the lungs were likely from those cell types. Kage et. al did a study in mice where they found that water induced lung injury in the mice significantly upregulated the amount of CLDN-4 in the lungs. Furthermore, CLDN-4 deficient mice had more severe lung injury such as increased cells in BAL and water in the lungs and increased IL-1β gene expression[259]. This indicates that CLDN-4 may functions by attempting to protect the lungs and sealing the epithelial barrier during a lung injury and making it less permeable to pathogens or noxious substances which may explain

why healthy HBECs significantly upregulate TJ molecules after infection. In the case of the HBECs of smokers and COPD patients, it may be that the lungs from those respective groups are chronically injured which is why the TJ molecules are programmed to remain significantly higher under basal conditions. In addition, it could also be that the increase of the TJ molecules are attempting to offset or prevent serious lung injury but are unable to fully because of other pathological factors such as apoptosis and chronic inflammation.

For example, it has been shown that increased expression of JAM-A on epithelial cells can increase EMT, a characteristic that is observed to be higher in the epithelium of COPD patients and smokers[255]. EMT was increased through phospho-Akt signaling, a common pathway for the process of EMT. A study on JAM-A expression in nasal epithelial cells showed that JAM-A expression decreased in response to poly I:C stimulation and mediated IL-8 secretion while my experiments demonstrated no changes in JAM-A expression in all three groups but localization changes instead[231]. However, the nasal epithelial cells in the aforementioned study were modified and came from patients with chronic sinusitis which may differentiate it from my results in physiological context.

4.2.2 Role of JAM-A expression in transmigration of leukocytes

Inflammatory environments increase migration of leukocytes into inflamed tissue. However, leukocyte transmigration was blunted in JAM-A deficient mice and was abrogated post lung injury compared to WT mice indicating that JAM-A is necessary in some for leukocyte transmigration in some capacity[260]. More specifically, JAM-A KO mice significantly reduces neutrophil transmigration into the lungs and the alveolar space as well as expression of the chemokine CXCL1[260]. This is of particular relevance to COPD and smokers as infiltration of leukocytes and especially

neutrophils heavily infiltrate the lungs of COPD and smokers in their inflammatory environment and the increased expression of JAM-A may help facilitate an increasing and perpetual influx of leukocytes.

JAM-A expression significantly increased in healthy HBECs after NTHi or RV16 infections. Since JAM-A has been shown to facilitate the transmigration of neutrophils as well as leukocytes in general, this would fall in line with an inflammatory response where recruitment of leukocytes would be necessary to fight off and clear an infection. However, it is not yet clear what causes the upregulation in JAM-A, whether it is directly upregulated from a pro-inflammatory cytokine or from a specific factor secreted by the pathogen, whether it be structural or secreted. The data seem to indicate that it may be dependent on pathogen infection as when healthy HBECs were stimulated with a bacterial or viral analogue, LPS or Poly I:C respectively, a significant increase in JAM- A was not observed unlike what was seen when infected with NTHi or RV16. More studies need to be done and for the specific cause of the upregulated JAM-A to be elucidated.

Unlike with healthy HBECs, JAM-A levels in COPD HBECs were unchanged with whatever stimulus given to them indicating that the HBECs in COPD were unresponsive. This could be for several reasons. One reason may be that levels of JAM-A were already so high that there was a negative feedback loop that was being induced in order to prevent levels of JAM-A from going any higher. Another reason may be that signaling to upregulate JAM-A may be desensitized due to the inflammatory environment as JAM-A is already higher in COPD HBECs.

4.2.3 TER and Spatial effects of TJ molecules in HBECs

The TERs in the HBECs did not significantly differ between the different groups. Nor were there any significant changes post-infection or stimulation in any group from the

media controls indicating that the TER is unaffected. A previous study of kidney or intestinal epithelial cell lines infected with pathogenic *E. coli* significantly decreased TERs post-infection. However, the change in TER was only observed at an early timepoint pf 6 hours post-infection[261]. A study on Caco-2 cells, an intestinal epithelial cell line, demonstrated that when they were stimulated with TNF-α, the TER significantly concentration-dependently decreased after 48 hours[262]. Hardyman et. al showed a similar decrease in TER in differentiated HBECs after TNFα stimulation[263]. Data from **Chapter 3** showed that concentrations of TNF-α increased with NTHi infection in basal cultures however there was still no effect on TERs post-infection with NTHi. This may occur for several reasons. Firstly the aforementioned studies only measured TERs between 48-96 hours after stimulation which is far longer than the 24 hour timepoint utilized in this study. Secondly, the concentrations of TNF-α used in these studies were 100s to 1000s of times greater than the concentrations that were secreted by the HBECs after NTHi infection and thus no effect was observed in the TERs here. Finally, there is a delay between infection and TNF-α synthesis and secretion which may further delay any effects on TER changes.

TER changes may be tissue dependent when exposed to poly I:C. It has been shown that the intestinal tract of rats showed a significant decrease and no change in TERs upon stimulation with poly I:C at an early timepoint of 1 or 3 hours[264]. The significant decrease in the ileum however was only significant at a very high dose of poly I:C (200 μg/ml). Another study on differentiated human keratinocytes showed that TERs actually increased in response to poly I:C stimulation at 24 and 48 hours while no changes were observed in nasal epithelial cells in response to either LPS or poly I:C[265,266]. Bronchial epithelial cell lines however had their TERs significantly decrease in response to either poly I:C or RV stimulation however they were immortalized

bronchial epithelial cells unlike the primary cells used in my study which showed a decreased capacity for growth after passage 6 with fibroblastic morphological changes[267].

Exposure of immortalized lung cells to CSE significantly decreased TERs and also decreased gene expression of CLDN-3, CLDN-4, and JAM-A[256]. The HBECs in this chapter however were not exposed to CSE but came from chronic smokers instead and were also primary cells.

Under basal conditions, the TJ molecules investigated were mostly diffused across the cell surface while TJ molecules were more clustered in smoker and COPD HBECs with JAM-A being localized to the intercellular junction as well. Localization of TJ molecules in lung cell lines are often found to be at the intercellular junctions of the cells which was not found in this study were the TJs were either diffused or cultured. However lung cell lines are cultured on surfaces that are not precoated with ECM proteins such as collagen which was used in this study to aid in HBEC attachment and growth. In addition, primary HBECs were used in this study instead of epithelial cell lines as it is more physiologically relevant. A study by Koval et. al however found that when alveolar cells were cultured on ECM coated surfaces including TJ molecules were found to be away from the intercellular junctions[268]. CLDN-4 for example, was diffused across the cell surface when the alveolar cells were cultured on collagen and some clustering was observed in CLDN-7 however higher magnification images are needed to confirm the findings[268].

There are a few reasons why polarization may be occurring in certain groups or conditions particularly in COPD or smoker HBECs. Firstly, as previously mentioned, the ECM and particularly collagen or other secreted ECMs may play a role in the

localization of TJ molecules in HBECs. Another reason is that in the COPD group for example, TJ proteins are being polarized but are unable to form intercellular tight junctions which may compromise barrier integrity. TJ regulation can be mediated by multiple proteins. The induction of the protein Scribble for example increased the ability for TJ formation through the suppression of ERK and EMT in an epithelial cell line[269]. MMPs, which have been found to be upregulated in COPD patients, can also abrogate tight junction formation in epithelial cells[270]. Interestingly, EMT in COPD HBECs are significantly higher than healthy HBECs and are more prone to inflammation induce EMT and can be induced with CSE exposure as well[271,272]. The lack of TJ distribution or intercellular junction formations may mean that TJ proteins cannot exhibit their protective effect in COPD or smoker HBECs even when upregulated.

When stimulating with LPS or infecting with NTHi the TJ molecules became clustered in healthy HBECs with some JAM-A localization at the intercellular junctions. Smoker and COPD HBECs however remained mostly unchanged with less clustering and more polarization observed under LPS stimulation. Thus, this may indicate that under basal conditions, COPD and smoker HBECs are exhibiting a phenotype where they are programmed to behave like they are being stimulated despite no stimulation given to the cells beforehand. The clustering observed in healthy HBECs may also be directed towards where the pathogen is most concentrated or adhered to in order to prevent transmigration or entry. This is unlikely to be a NTHi specific phenomenon as it is also observed upon stimulation with LPS indicating that localization is perhaps dependent on PRR stimulation such as TLR4.

4.2.4 Transcriptional Regulation of TJ Molecules

Infection can trigger a myriad of changes on a transcriptional and translational level, however they can be controlled individually. Therefore, for a full understanding of the molecular mechanisms, an investigation/measurement of mRNA and protein level is needed. Changes in TJ transcription and gene expression were measured post-infection with either NTHi or RV16. CLDN-3 was significantly upregulated in healthy HBECs and significantly downregulated in smoker HBECs post-infection with RV16. This follows the of the protein levels of CLDN-3 in healthy and smoker HBECs suggesting that the transcriptional changes are subsequently being translated to protein changes. Unlike CLDN-3 however, there were no changes in CLDN-4 or JAM-A in terms of gene expression post-infection with NTHi or RV16. This could mean that the regulation of CLDN-4 and JAM-A may be regulated post-transcriptionally or through post-translational modification as both TJ proteins were significantly upregulated in healthy HBECs post-infection and JAM-A was downregulated in smoker HBECs post-infection with NTHi or RV16.

Protein levels of Occludin and ZO-1 were not measured however relative gene expression was measured post-infection with NTHi or RV16 in healthy, smokers, and COPD HBECs. There were no changes in Occludin expression in all three groups post-infection suggesting that infection does not alter any changes in gene expression. ZO-1 also was unchanged post-infection in healthy HBECs however NTHi infection significantly downregulated or upregulated ZO-1 expression in smoker and COPD HBECs respectively. Previous studies have shown that levels ZO-1 was significantly decreased after CSE exposure or in smoker and COPD HBECs[197,273]. However, no comparisons have been made in HBECs post-infection with NTHi and thus it was yet to be explored. ZO-1 is an important TJ molecule in the lung and thus a decrease in

ZO-1 may impair barrier function or if ZO-1 was functionally dysregulated to perform other functions that would disrupt the epithelium. A study on enteropathogenic *E. coli* (EPEC) demonstrated that EPEC was able to recruits ZO-1 to their actin tails and for pedestal formation which may help in their virulence by facilitating their invasion of cells[274]. It would be interesting to investigate whether NTHi is capable of utilizing similar mechanisms in the lungs as there is evidence that NTHi can reside intracellularly as well[275,276]. If true, this may be one mechanism that NTHi can persist in the lungs of COPD patients since NTHi significantly upregulated ZO-1 post-infection.

While relative gene expression within groups post-infection was possible, comparison of gene expression between groups in different conditions and baseline measurements of TJ proteins were not possible. This was mainly due to different amounts of RNA starting material between donors which can be compared between conditions in the same donor but not between different donors with the same condition.

4.2.5 Limitations and Further Investigations

The current chapter has demonstrated several interesting findings on the role of TJ molecules in epithelial cells and particularly under the context of stimulation or infection. However, this chapter has several limitations. Firstly, all experiments in this chapter have been done on HBECs that were cultured at a monolayer. This is a useful and straightforward method to elucidate the roles that TJ proteins play in the epithelium with or without infection and a plethora of parameters can be measured such as fluorescence, colocalization, and gene expression and spatial changes can be examined. However, monolayer cultures are not the perfect model in terms of establishing something as complex as the lung microenvironment since for example paracellular permeability and gradients, which is regulated by CLDNs, does not apply

as strongly in a monolayer culture. This may influence localization and expression of CLDNs and hinder their ability to form intercellular junctions however it could also be due to reasons previously described here. A physiologically closer model would be to culture and stain differentiated HBECs cultured at ALI as the HBECs can differentiate into different subtypes. A differentiated model may show a different or more complicated picture than what was demonstrated in the current chapter. My previous attempts to stain differentiated HBECs however were unsuccessful and thus it was not possible to do in this study.

Another interesting investigation would have been to look at spatial changes of HBECs and TJ protein expression changes through different timepoints. Currently, the only timepoint that was utilized in this study was at 24 hours but an earlier timepoint between 4-8 hours and a later timepoint at 48 or 72 hours would have also been interesting to examine any changes in TJs through time and to investigate if they can recover to baseline post-infection.

Finally, while TJs in HBECs were investigated across different groups and conditions, any signalling changes that TJ molecules can mediate were unexplored. Whether this was upstream signaling by investigating the effect of inflammation on TJ expression or downstream signaling where TJ protein signalling can affect barrier integrity or processes such as EMT.

Chapter 5: RNA-seq Study of HBECs in COPD During Bacterial or Viral Infection

Introduction

COPD is a complex and multi-factorial disease. As such, elucidating which factors would contribute to COPD pathogenesis and the interplay of different genes and proteins in such a complex system has proven challenging thus far. In particular, there has not been as much focus on the epithelial barrier which contributes to both immune and inflammatory processes as well as lung barrier integrity and repair.

In order to capture gene expression and regulation in a particular disease like COPD, there are several techniques that may be utilized. One of the most useful of these techniques is bulk RNA-seq as it is able to capture all the genes that are expressed in cells under different contexts. Thus, all the RNA in the cells would be sequenced and compared to different disease groups or conditions. Since the role of epithelial cells in COPD are understudied, I sought to explore its genetic profile and compare it to the healthy control group and smokers which may be regarded as an intermediary group between healthy and COPD patients as it is one of the largest risk factors for COPD. Bulk RNA-seq was chosen instead of single cell RNA-seq as monolayer cells are undifferentiated and would be highly unlikely to show distinct genetic profiles from different cell populations.

Not only would it be of importance to compare gene expression between healthy, smokers, and COPD HBECs but it would also be important to compare them under the context of a bacterial or viral infection. Both bacterial and viral infections are strongly associate with exacerbations risks in COPD and in particular NTHi and RV are among the most prominent pathogens linked to exacerbations. Therefore,

comparing differential gene expression (DGE) of healthy, smokers and COPD HBECs post-infection may elucidate some important factors that contribute to the incidence of exacerbation.

There have been a few studies that have investigated the lung epithelium in COPD or healthy HBECs through either microarray or sequencing assays with either different contexts or methods[173,226,277]. For example, Baddal et. al investigated the response of primary differentiated healthy HBECs in response to an NTHi infection but only utilized one donor in triplicate which may make the results in need of more robustness[277]. Veerati et. al infected differentiated HBECs of healthy, asthma, and COPD patients with RV-A1 at a 0.001 MOI and then sequenced the HBECs at 24-96 hours with 5 donors per group and found that viral titers and IFNs peaked at 24-48 hours[226]. There were also no significant differences in viral titers or IFN levels in healthy HBECs when the dose was increased to 0.01, 0.1, or 1 MOI.

Culturing primary epithelial cells in monolayer cultures is valuable as it produces a tissue to study under different contexts directly from patients which can lead to further *in vivo* studies for example. However, differentiating basal epithelial cells into different epithelial subtypes such as goblet cells produces an epithelial layer that is physiologically closer to the lung epithelium despite the difficulties in differentiating basal cultures. Thus in this chapter DGE is assessed in healthy controls, smokers, and COPD HBECs in different contexts in a supervised and unsupervised manner. Firstly, DGE within groups are assessed post-infection with NTHi or RV. Secondly, DGE between groups are elucidated whether it is an unstimulated condition or post-infection with NTHi or RV. Finally, the aforementioned differences are investigated in both HBECs cultured at a monolayer or HBECs cultured at ALI in order to assess whether DGE changes depending on the culturing method. Investigating DGE in those

contexts helps capture a fuller picture of what is happening in the complex COPD epithelium and how that may relate to the pathogenesis of the disease. In particular, during a supervised analysis, DGE of genes of interest such as innate immune genes, PRRs, and TJ molecules are assessed in all three groups of HBECs to pinpoint any target genes of interest.

Results

5.1.1 Dispersion Estimates of sequenced samples

A dispersion plot of the sequenced samples were graphed to determine the variability from the mean counts of the individual genes. The majority of the genes had a low amount of variability and fell within the fitted curved drawn on the dispersion plot **(Figure 5.1)**. This indicates that the majority of the genes had low variability between each other even with increasing mean counts which usually tend to increase in variability.

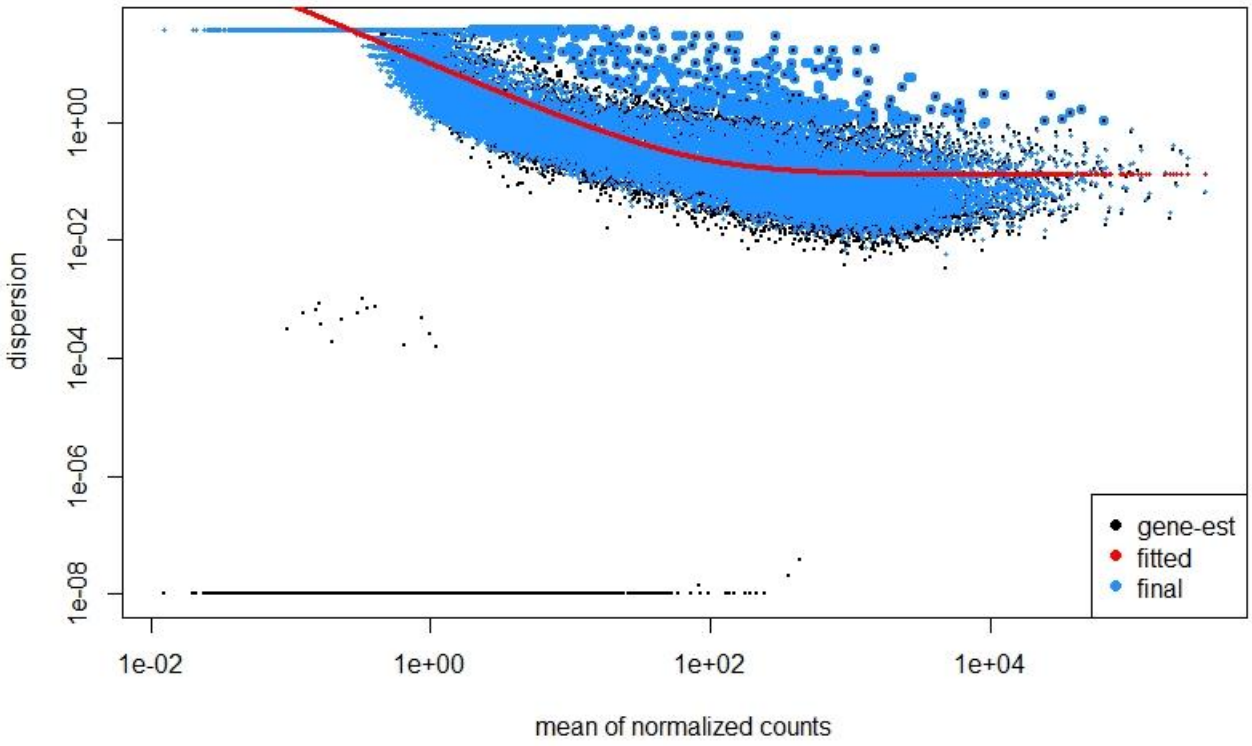


Figure 5.1: Dispersion Plot for the RNA-seq dataset. *A dispersion plot for all the samples was plotted with the x-axis being the mean of normalized counts of a gene and the y-axis is the variation in individual genes. Each dot is representative of a gene count and its respective variation. The red line represents the estimated variance of genes given their expression level.*

5.1.2 Principle Component Analysis of the sequenced samples within different groups and culture conditions

A principle component analysis (PCA) was then done to assess variability between samples and particularly the variability in samples within the same groups or different groups. A PCA plot was first plotted to compare variability between healthy, smoker, and COPD groups. Two clusters were identified on the PCA plot with sample groups having a small amount of variability within the clusters indicating that HBEC groups were not the factor responsible for the over 80% of variation between the two clusters on the PC1 access **(Figure 5.2a)**. In order to assess which factor was responsible for the generation of the two clusters, a PCA plot was graphed whilst stratifying the points by culture method. Indeed, it emerged that one cluster belonged to samples cultured at a monolayer and the other cluster for samples cultured at ALI **(Figure 5.2b)**. Variation within each cluster was much lower considering biological replicates with the ALI clusters having a mean variation of 12.1% on the PC1 access and 3.2% on the PC2 access. In the monolayer cluster, there was a mean variation of 19.7% on the PC1 axis and a 1.4% variation on the PC2 axis. ALI and monolayer subjects were different but the variations between subjects was much lower than the variation between the two culturing methods.

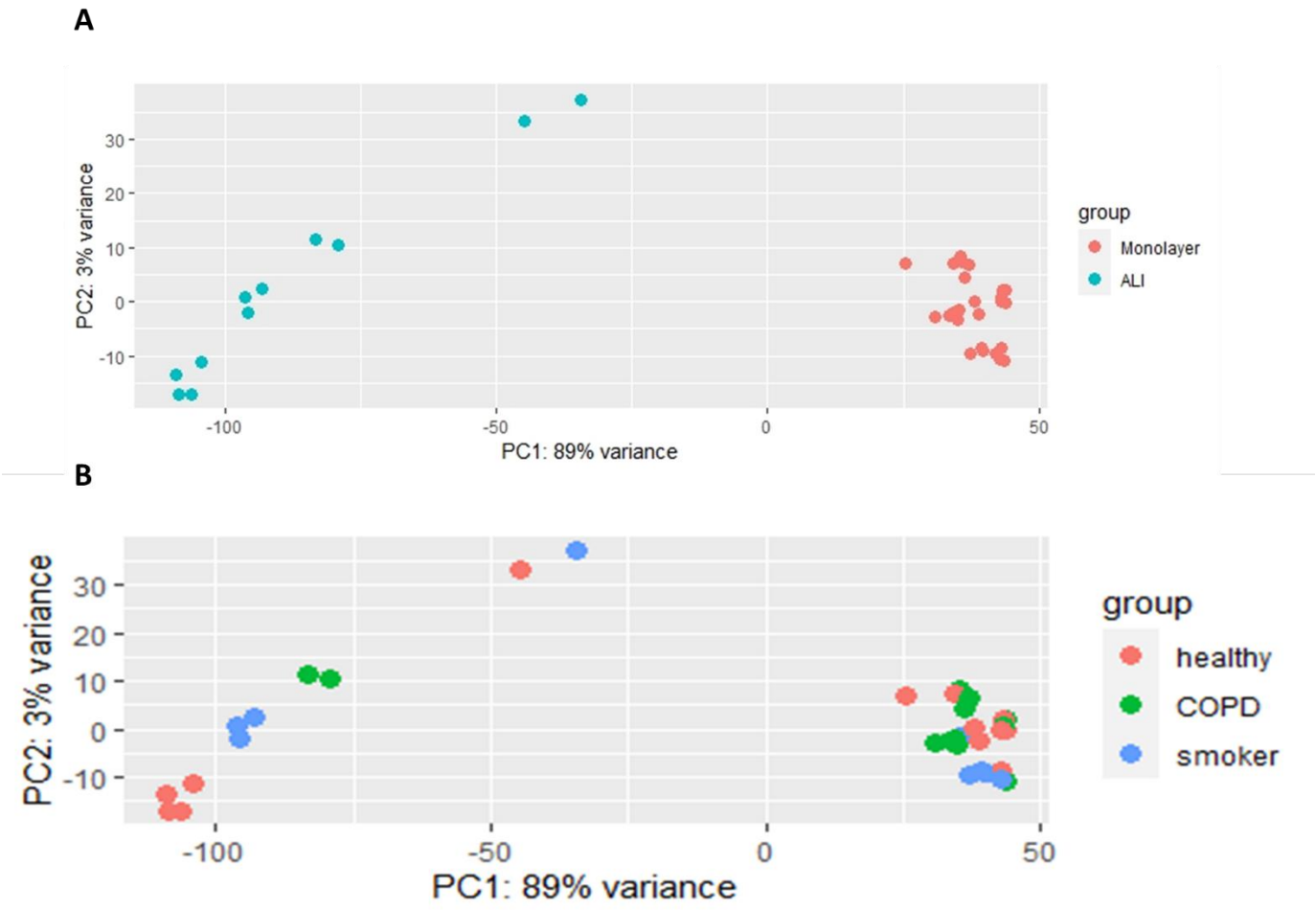


Figure 5.2: Principal Component Analysis for the RNA-seq HBECs samples. *PCA plots for the different samples of HBECs stratified by **(A)** Culture method and subsequently by **(B)** The three diseases groups of healthy, smokers, and COPD HBECs. Total number of samples=36 with each dot representative of a different subject in a certain condition.*

5.1.3 Distance Matrix between samples within different HBEC groups and conditions

In order to assess variations between individual samples, a distance matrix was plotted between the individual samples. Based on the results from the PCA plot a distance matrix was plotted while stratifying HBEC samples that were cultured at ALI and HBEC samples cultured at a monolayer. Similar to what was observed in the PCA plots, there was a great amount of variation between samples that were cultured at

ALI compared to the samples cultured at a monolayer regardless of the group or condition **(Figure 5.3a)**. Thus, in order to look at variations between groups or stimulations and remove the culturing method variable, Monolayer and ALI samples were split up and a distance matrix was plotted for each and the variation between samples were examined.

Differences between samples were less extreme upon culture method segregation with differences observed between biological replicates. On the monolayer distance matrix, the biggest differences were observed between unstimulated HBECs or HBECs stimulated with NTHi as well as differences between healthy and COPD HBECs **(Figure 5.3b)**. ALI samples were fewer in number with variation between biological replicates and between healthy and COPD HBECs **(Figure 5.4c)**.

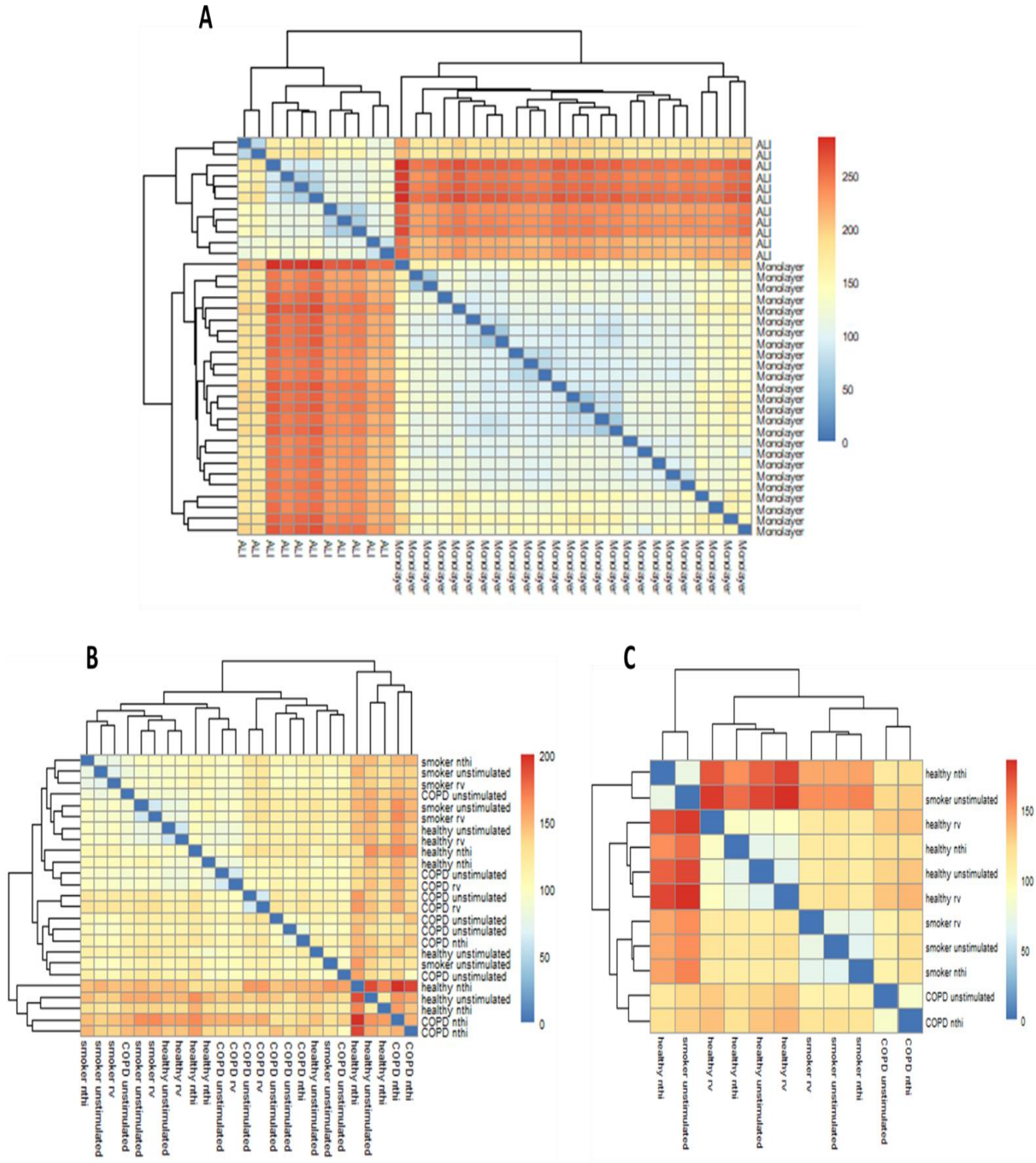


Figure 5.3: Variation for the sequenced HBEC samples in different culture methods and groups. *A distance matrix was plotted to visualized variation between HBEC samples by **(A)** Stratification of samples between basal and differentiated HBEC culture methods. Distance matrices were plotted for **(B)** Basal cultured HBECs and **(C)** ALI cultured HBECs stratified by healthy, smokers, and COPD HBECs and stimulations conditions. N=36.*

5.1.4 log 2-Fold changes and significance comparisons between HBEC groups and stimulations

Comparison between different groups and conditions were then performed to generate DGE through log2fold changes and p-values. MA plots were then generated for each comparison with logfold changes plotted and stringent p-adjusted values highlighted in order to take into account and curtail the False Discovery Rate. The lfcShrink() function was used to shrink the data points during visualization and to take into account outliers. There were significant DGE genes in various comparisons in all three groups, conditions, and both culture methods. MA plots for all comparisons are displayed in the **Appendix**. There were DGEs in COPD HBECs stimulated with NTHi or between healthy and COPD HBECs stimulated with NTHi cultured at a monolayer for example **(Figure 5.4a,b)**. For differentiated HBECs, there were differences found between healthy and smoker HBECs at basal conditions as well as between healthy and smoker HBECs stimulated with NTHi **(Figure 5.4c,d)**.

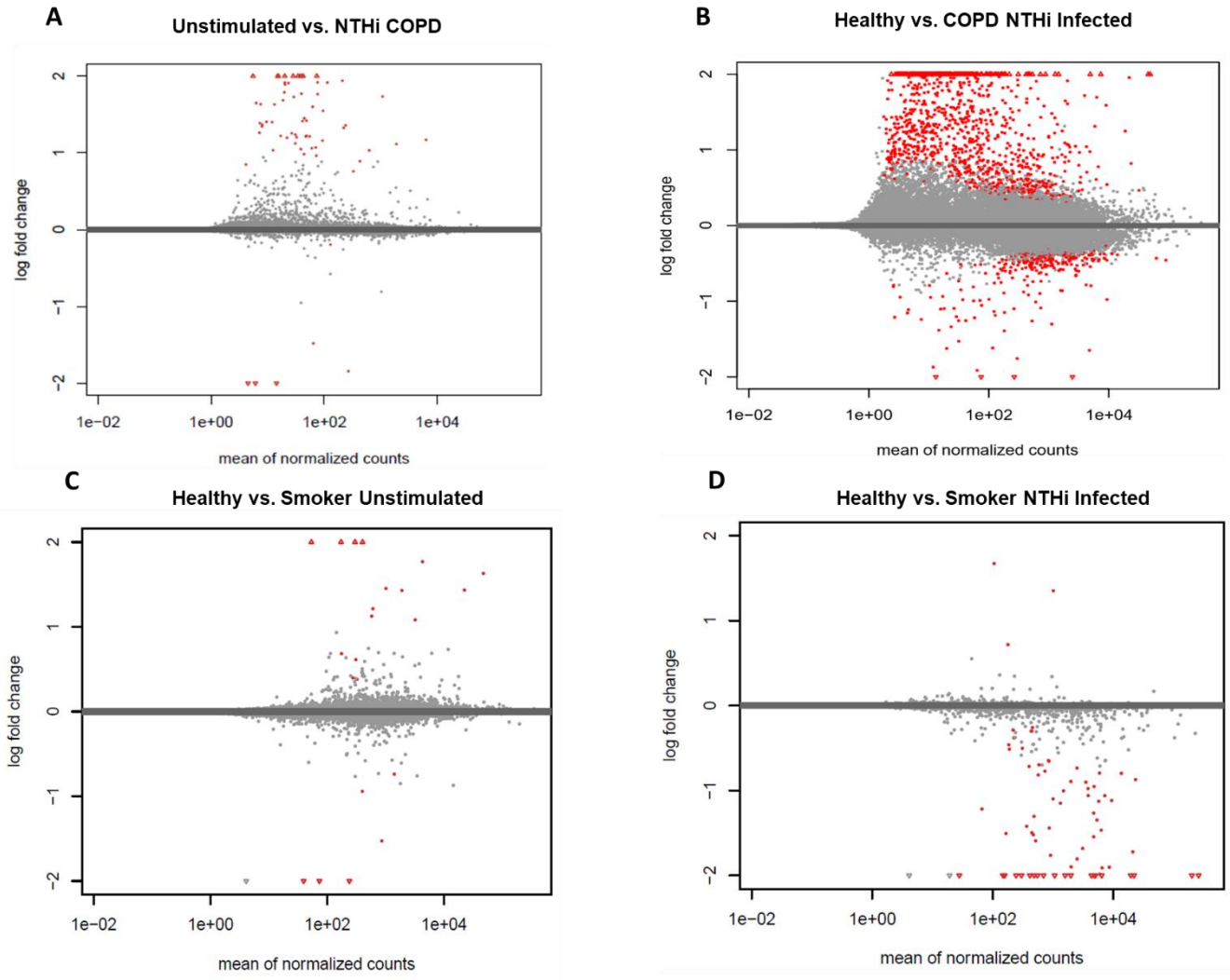


Figure 5.4: MA plots for DEGs in different HBEC groups and conditions. *MA plots were graphed to visualize DGE in HBECs in* ***(A)*** *Unstimulated vs. NTHi infected COPD HBECs and* ***(B)*** *Healthy vs. COPD NTHi infected HBECs at basal cultures. MA plots for differentiated HBECs were also graphed for DGE in* ***(C)*** *Unstimulated healthy vs. unstimulated smokers and* ***(D)*** *Healthy vs Smokers infected with NTHi. Red dots are genes that are found to be significant.*

5.1.5 DGE between unstimulated healthy HBECs and smoker or COPD HBECs in basal cultures

In order to assess gene expression differences between different conditions and groups, DGE was assessed in an unsupervised manner by looking at log2fold changes and p-values for significance. To take into account outliers in log2fold changes and attempt to mitigate the effects of low group sizes, the lfcShrink() function was utilized

to assess DGE. In addition, the cut off for log2fold changes was put at -12 and 12 as it is likely that any greater effect size is due to low gene reads in a group or a low group size. The log2fold change cutoff utilized was -1 and 1 while the p-value used to establish significance was $1x10^{-4}$.

DGE between unstimulated healthy HBECs and unstimulated smoker HBECs were first measured and volcano plots were used to visualize DEGs using the Enhance Volcano package. There were no high log2fold differences found between unstimulated smokers and unstimulated healthy HBECs. The gene *SYT11* however still had a significant decrease in smokers compared to healthy controls despite having a low log2fold decrease of 0.04 **(Figure 5.5a)**.

Unstimulated COPD HBECs were subsequently compared to unstimulated healthy HBECs for differentially expressed genes (DEGs). Similar to smoker HBECs, there were no DEGs that passed the log2fold cutoff however there was significance in the genes of *CLDN11* and *LINC01436* **(Figure 5.5b)**. Overall, the results demonstrate that there are few differences between COPD and smoker HBECs under basal conditions compared to healthy controls in monolayer cultures.

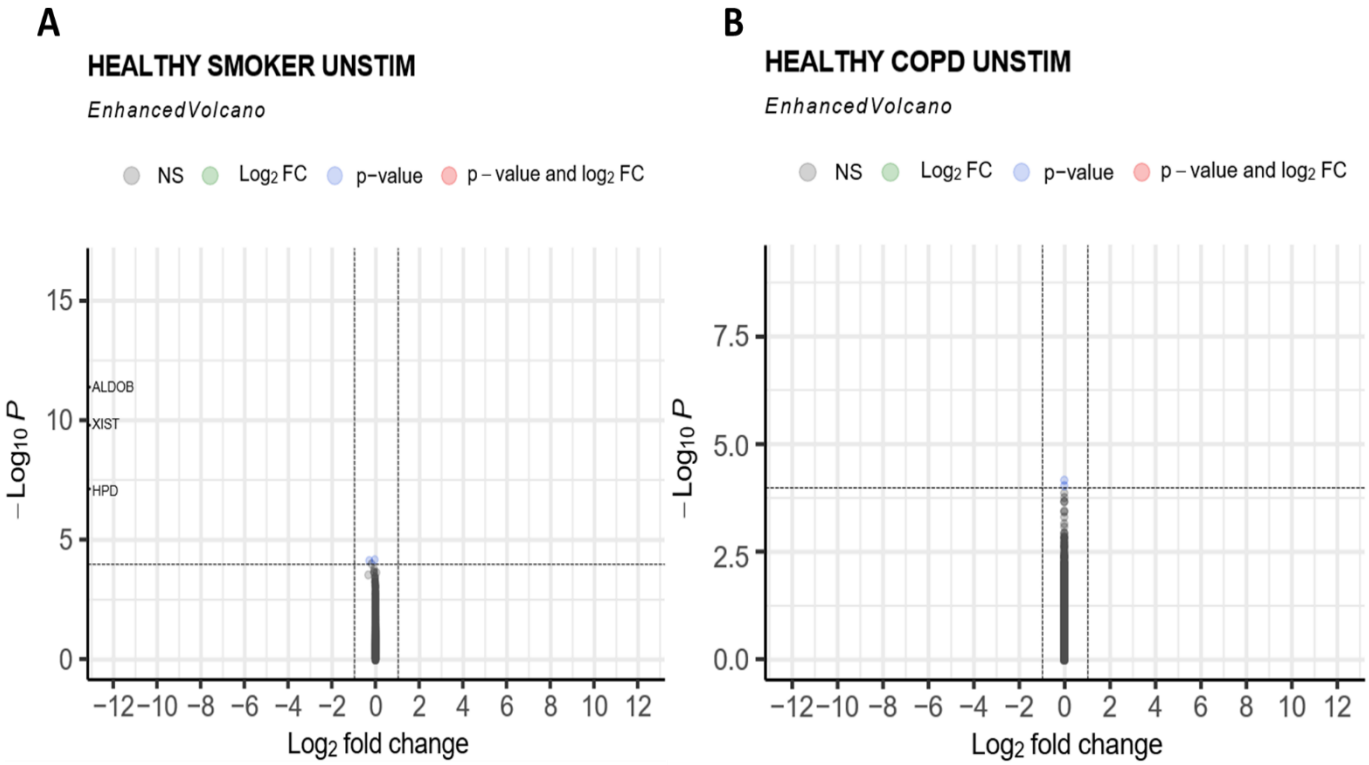


Figure 5.5: DEGs in unstimulated COPD and smokers compared to unstimulated healthy HBECs. *Volcano plots were graphed to visualize DGE of **(A)** Smoker and **(B)** COPD HBECs compared to healthy HBECs when unstimulated in basal cultures with Log2fold change on the x-axis and transformed p-values on the y-axis**.** N: Healthy=3, Smokers=3, COPD=6.*

5.1.6 DEGs in differentiated HBEC cultures under basal conditions in COPD, smokers, and healthy HBECs

Following the examination of unstimulated HBEC DEGs in basal cultures, DGE was looked at in differentiated HBECs at ALI. Unlike what was observed in basal cultures, there were significant DEGs in unstimulated smokers compared to unstimulated healthy HBECs in ALI cultures. The genes *SLC26A2* and *OSBPL6* were significantly decreased in unstimulated smokers compared to unstimulated healthy HBECs by a decrease of 1.5 and 2-log2fold changes respectively. *OSBPL6* is a transporter that is responsible for the efflux of cholesterol in the cells while *SLC26A2* is responsible for the transport of sulfates in cells **(Figure 5.6a)**.

The most upregulated gene in unstimulated smoker is the non-coding RNA gene *XIST* which responsible for X-chromosome inactivation with 6.1 log2fold upregulation. *SLC39A8*, which is responsible for the transport of important ions like Zinc, is also upregulated in smoker HBECs. *DHCR7, DHCR24, and SC5D,* are enzymes that play a role in cholesterol biosynthesis and were also upregulated in unstimulated smokers compared to unstimulated healthy HBECs by approximately 1.8, 1.4, and 1.4 log2folds respectively. *LDOC1* was also upregulated by 1.1 log2fold and is a pro-apoptotic protein and implicated in the suppression of NFκB activation **(Figure 5.6a)**.

Similar to what was seen in basal cultures, there were no DEGs found in unstimulated COPD HBECs compared to unstimulated healthy HBECs that met the criteria. However, the genes *PPP1R14C* and MPC1 were statistically significant despite only have a log2fold change of -0.3 and 0.2 respectively **(Figure 5.6b)**.

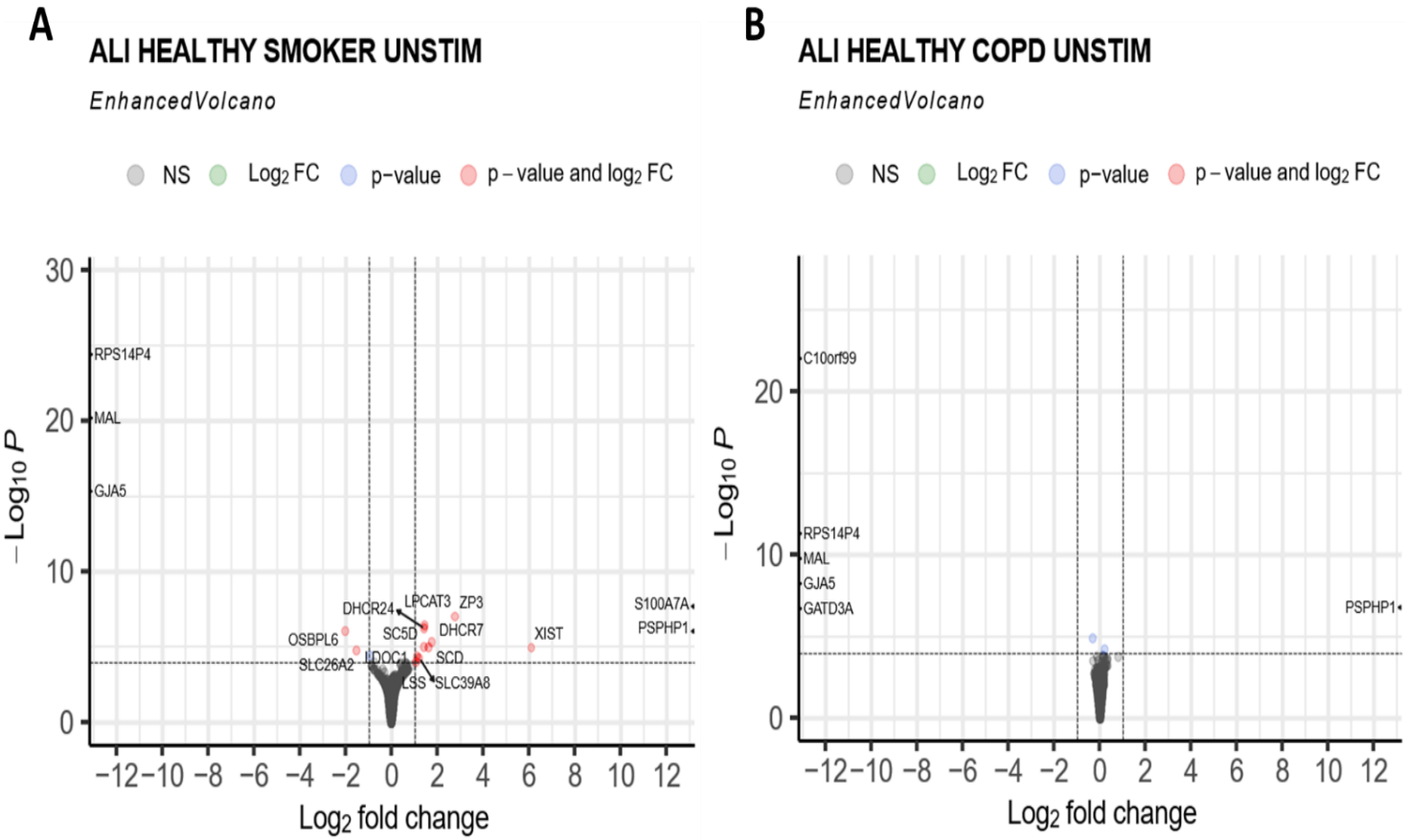


Figure 5.6: Unstimulated HBEC DEGs in differentiated cultures. *Volcano plots showing DEGs in differentiated* ***(A)*** *Unstimulated smokers and* ***(B)*** *Unstimulated COPD HBECs compared to unstimulated healthy HBECs. Log2fold change is on the x-axis and transformed p-values on the y-axis. N: Healthy=1, Smoker=2, COPD=1.*

5.1.7 DEGs of healthy HBECs stimulated with NTHi in basal cultures

DEGs were then examined in healthy HBECs that were stimulated with an MOI of 10 of NTHi for 24 hours in basal cultures. There were very few DEGs found when healthy HBECs were stimulated with NTHi with *CP* and *APOA1-AS* among them which were significantly downregulated by 4 and 2.7 log2folds respectively **(Figure 5.7)**.

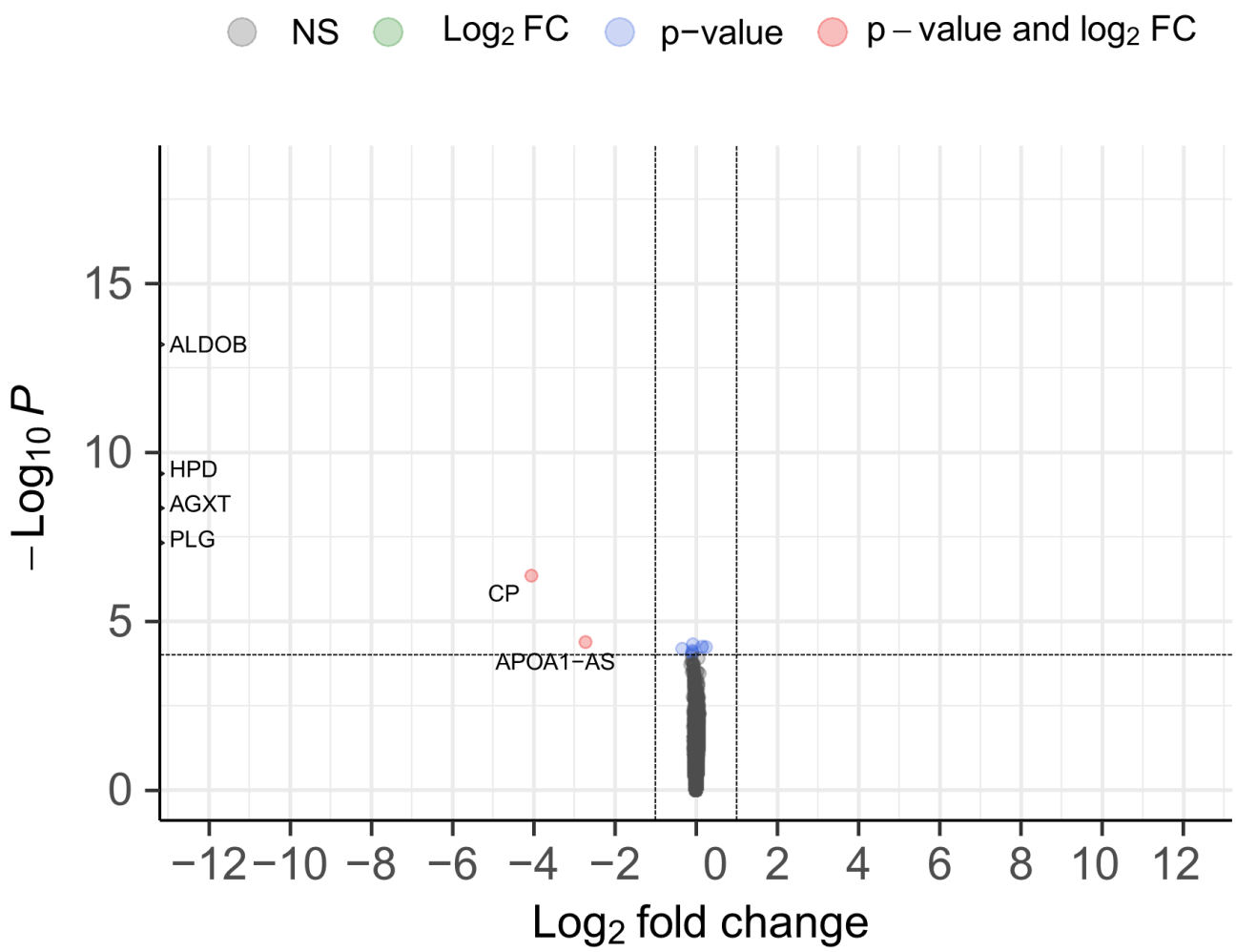


Figure 5.7: DGE in healthy HBECs post-infection with NTHi. *Volcano plot to visualize DEGs in NTHi infected healthy HBECs at 10 MOI for 24 hours compared to uninfected HBECs in basal cultures. Log2fold change on the x-axis and transformed p-values on the y-axis. N: Unstimulated=3, NTHi=4.*

5.1.8 Effect of NTHi infection on smoker HBECs in basal cultures

Smoker HBECs were then assessed for DEGs after NTHi infection first in comparison to unstimulated smokers and then compared to healthy HBECs stimulated with NTHi. There were 53 DEGs in smokers stimulated with NTHi compared to unstimulated smoker HBECs with only 1 downregulated gene.

Among the upregulated genes, there were many DEGs that are involved in the innate immune response and IFN signaling. The RNA sensor *DDX58* for example was

upregulated as well as the genes *STAT1* and *IRF7* that are important for innate IFN signaling. Several ISGs were also upregulated such as *ISG15, ETV7, OAS1, OAS2,* and *OAS3* as well as the chemokines *CXCL10* and *CXCL11*. Several Tripartite Motif (TRIM) genes were significantly upregulated such as *TRIM4, TRIM5, TRIM14, and TRIM69* which are involved in different immune mechanisms such as enhancing Type I IFN responses during infections **(Figure 5.8a)**.

When comparing infected smoker HBECs to infected healthy HBECs, a similar set of genes were significantly upregulated such as the immune genes and ISGs *ISG15* and *OAS3*. There were 5 DEGs that were downregulated in NTHi infected smoker HBECs compared to infected healthy HBECs **(Figure 5.8b)**. *ANXA10* for example, a marker of some carcinomas, was downregulated in NTHi infected smoker HBECs. Other genes that were downregulated include *CERK, MTURN, FAM172A, and TNFRSF10D*.

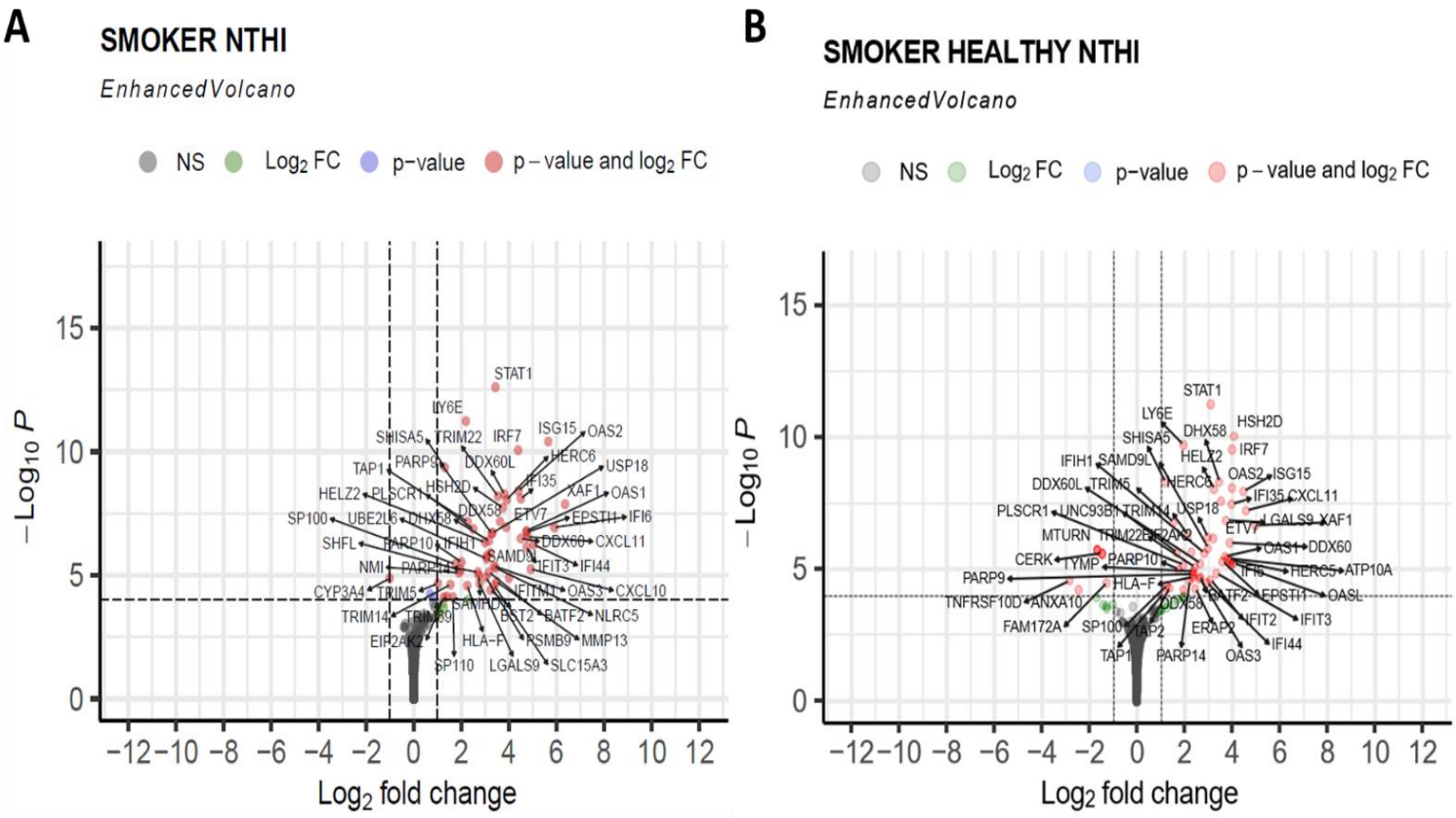


Figure 5.8: DGE in smoker HBECs post-infection with NTHi. *DGE visualized by volcano plots in* ***(A)*** *smoker HBECs post-infection with NTHi compared to unstimulated smoker HBECs and* ***(B)*** *smoker HBECs compared to healthy HBECs post-infection with NTHi at a monolayer. Log2fold change on the x-axis and transformed p-values on the y-axis****.*** *N: NTHi infected Healthy=4, Unstimulated smokers=3, NTHi infection smokers=1.*

5.1.9 NTHi Infected COPD HBECs DEGs in basal culture

DEGs were then compared in NTHi infected HBECs of COPD patients compared to unstimulated COPD HBECs. There were 5 genes that were downregulated and 39 that were upregulated when post-infection with NTHi. *PLG*, the gene that encodes plasminogen, was downregulated by 2.1 log2folds **(Figured 5.9a)**.

PTX3 is involved in innate immune responses, inflammation, and tissue repair and was upregulated by 3.2 log2fold in NTHi infected COPD HBECs. *TNFRSF1B* and *TNFAIP* encode for a TNFα receptor and a TNF-α inducible gene 6 (TSG-6) respectively and they were both significantly upregulated post-infection with NTHi in

COPD HBECs. *MAP3K8* was also upregulated and is responsible for the transduction of inflammatory signaling through the MAPK/ERK pathway **(Figure 5.9a)**.

When compared to NTHi infected healthy HBECs, COPD HBECs had 5 genes that were significantly lower and 212 that were significantly increased post-NTHi infection. Among the downregulated genes *IGFBP6* was significantly decreased in COPD HBECs post-infection by 2.5 log2folds and is responsible for the inhibition of insulin growth factor (IGF) signaling. *DH3,* which mediates the metabolism of retinoic acid, was also decreased in NTHi infected COPD HBECs compared to infected healthy controls **(Figure 5.9b)**.

In terms of increased genes, there are several similarities in DEGs between NTHi infected COPD HBECs and NTHi infected healthy HBECs compared to DEGs in unstimulated COPD HBECs compared to infected COPD HBECs. The genes *TNFAIP, PTX3, TNFRSF1B, IL20, SLC7A7* for example were also significantly higher in COPD infected HBECs compared to infected healthy HBECs. *MMP3* was also significantly higher by 3.5 log2folds as well as *MMP12* by 1.2 log2folds although it wasn't significant (p=0.0036). *ERAP2* mediates the presentation of MHC class I epitopes through its peptidase activity and was also increased in infected COPD HBECs by 3.6 log2fold compared to infected health HBECs **(Figure 5.9b)**.

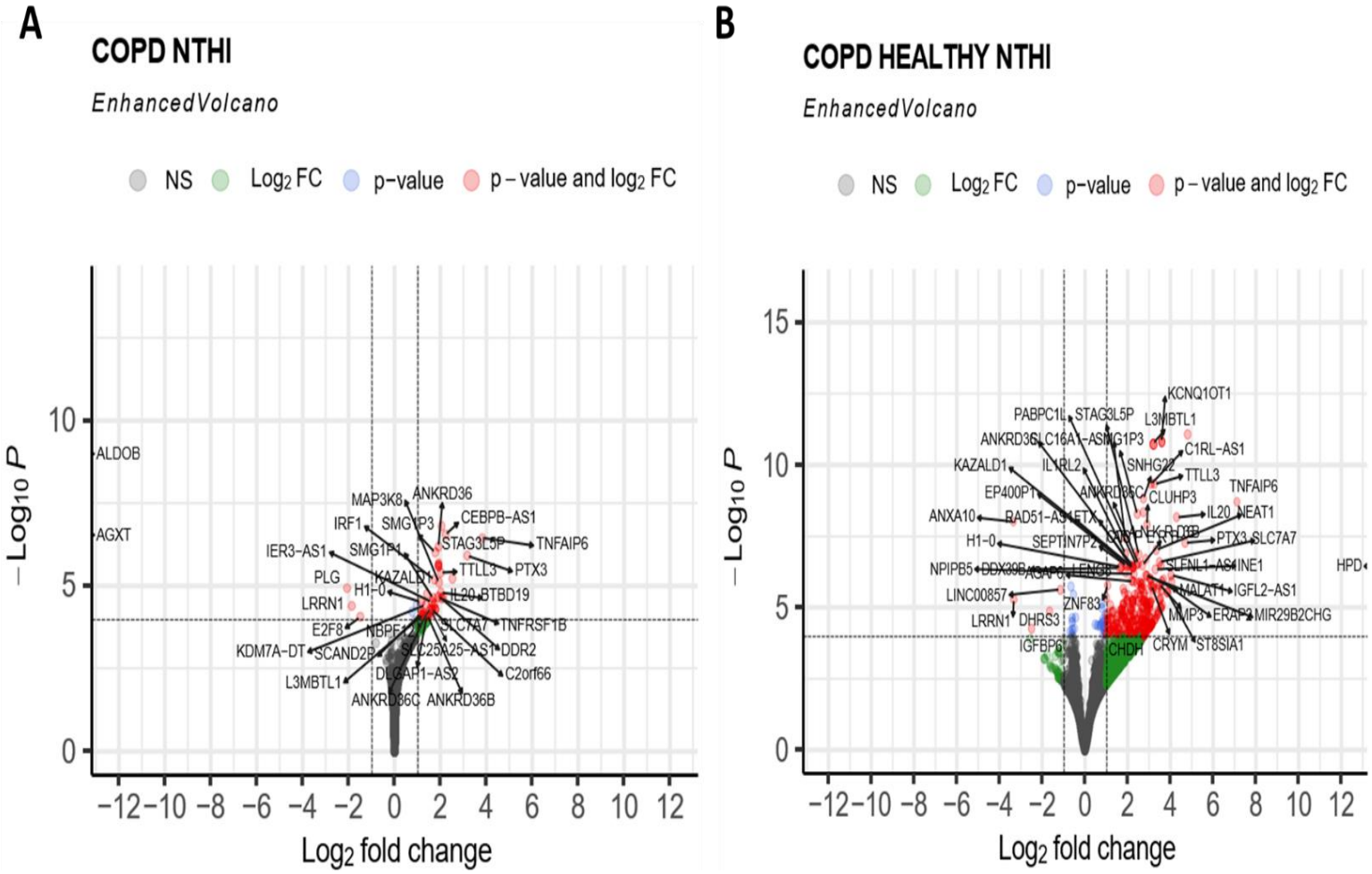


Figure 5.9: DGE in COPD HBECs post-infection with NTHi. *DGE visualized by volcano plots in **(A)** COPD HBECs post-infection with NTHi compared to unstimulated COPD HBECs and **(B)** COPD HBECs compared to healthy HBECs post-infection with NTHi in basal cultures. Log2fold change on the x-axis and transformed p-values on the y-axis**.** N: NTHi infected Healthy=4, Unstimulated COPD=6, NTHi infected COPD=3.*

5.1.10 Differentiated healthy HBECs are unaffected by NTHi infection

Healthy HBECs that were differentiated behaved similarly to undifferentiated HBECs when infected with NTHi. There were no DEGs with the exception of the X-linked RNA coding gene *XIST* which was upregulated by around 10 log2folds **(Figure 5.10)**.

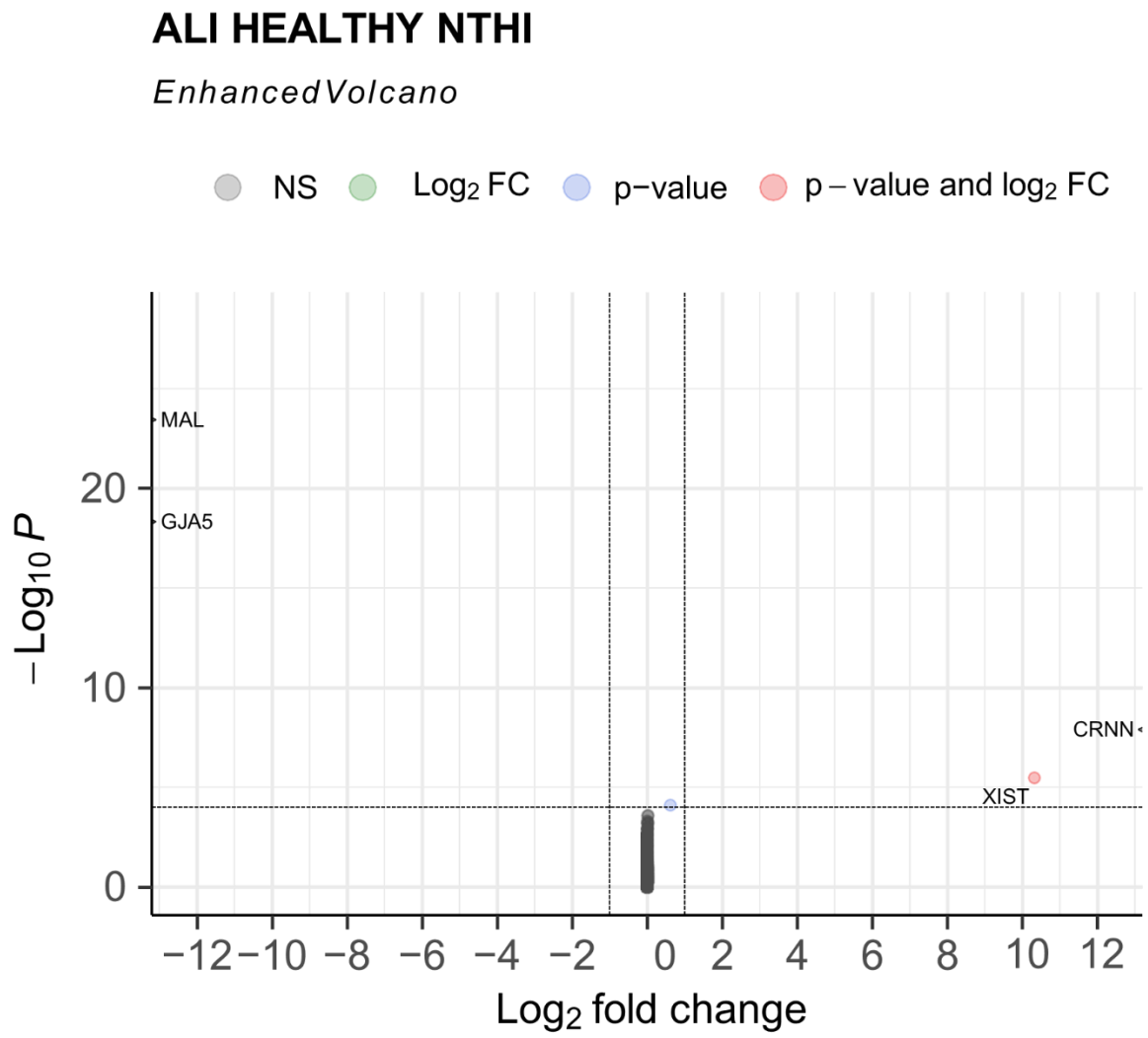


Figure 5.10: DGE in healthy HBECs post-infection with NTHi at ALI. *Volcano plot to visualize DEGs in NTHi infected healthy HBECs compared to uninfected HBECs in differentiated cultures. Log2fold change on the x-axis and transformed p-values on the y-axis. N: Unstimulated=1, NTHi=2.*

5.1.11 DEGs of smoker HBECs infected with NTHi in differentiated cultures

The effect of NTHi on differentiated smoker HBECs was assessed by first comparing NTHi infected smoker HBECs with unstimulated smoker HBECs at ALI. There were few DEGs in infected smoker HBECs compared to uninfected smokers. *NIPAL4,* a Magnesium ion transporter was downregulated by 1.1 log2folds and while the log2fold decrease did not pass the threshold, IL-33 still significantly decreased by 0.16 log2folds **(Figure 5.11`a)**.

When compared to NTHi infected healthy HBECs, there were 41 DEGs that were increased and 2 that were decreased in infected smoker HBECs. The metalloproteinase inhibitor *TIMP1* for example was significantly lower in smokers compared to healthy HBECs post-infection with NTHi as well as the chemokine *CXCL2*. *SERPINB2,* the gene name for the PAI-2 protein, was also lower in smoker HBECs as well as the anti-inflammatory and pro-fibrotic cytokine *TGFβ1* **(Figure 5.11b)**.

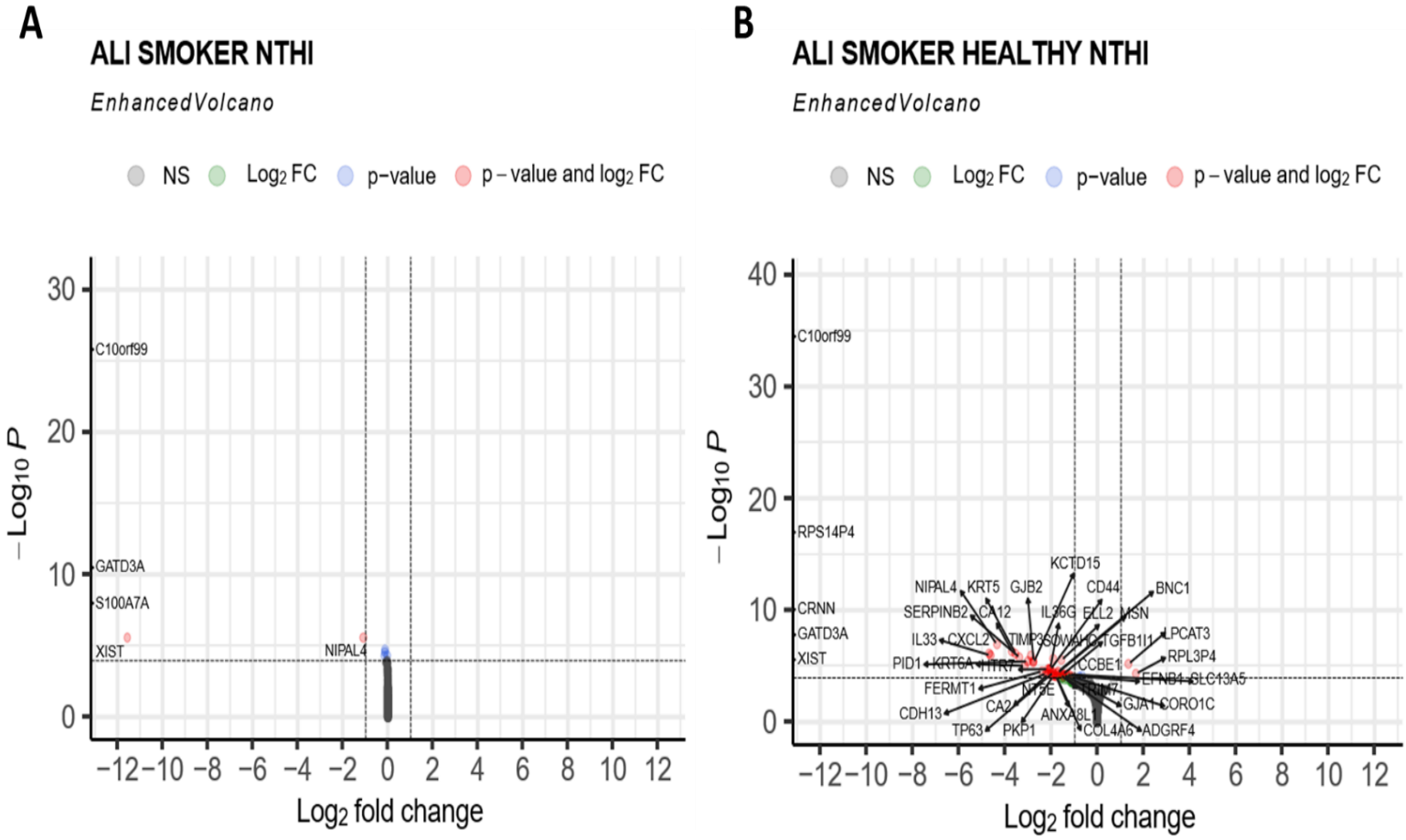


Figure 5.11: DGE in smoker HBECs post-infection with NTHi at ALI. *DGE visualized by volcano plots in* ***(A)*** *smoker HBECs post-infection with NTHi compared to unstimulated smoker HBECs and* ***(B)*** *smoker HBECs compared to healthy HBECs post-infection with NTHiin differentiated cultures. Log2fold change on the x-axis and transformed p-values on the y-axis.* ***N****: NTHi infected Healthy=2, Unstimulated smokers=2, NTHi infected smokers=1.*

5.1.12 DEGs in NTHi infected COPD HBECs in ALI cultures

Next, the effect of NTHi infection on COPD HBECs was examined compared to unstimulated COPD HBECs in differentiated cultures at ALI. Unlike what was observed in basal cultures, there were no significant changes in COPD HBECs pre and post-infection at ALI **(Figure 5.12a)**.

There were also no DEGs that met the criteria in NTHi infected HBECs of COPD patients when compared to NTHi infected health HBECs although there was a statistically significant decrease in *STAT4* and *LDAH* despite only having a slight decrease compared to healthy HBECs post-infection **(Figure 5.12b)**.

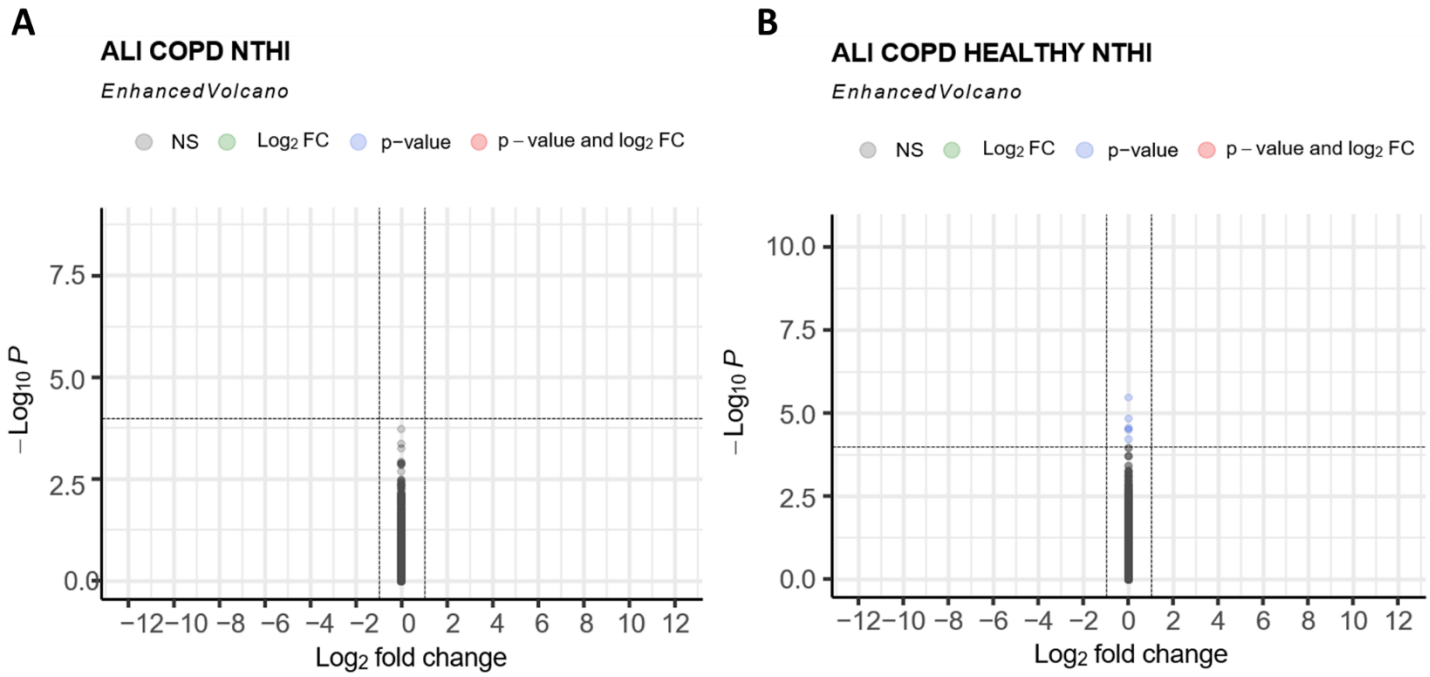


Figure 5.12: DGE in COPD HBECs post-infection with NTHi at ALI. *DGE visualized by volcano plots in **(A)** COPD HBECs post-infection with NTHi compared to unstimulated COPD HBECs and **(B)** COPD HBECs compared to healthy HBECs post-infection with NTHi in differentiated cultures. Log2fold change on the x-axis and transformed p-values on the y-axis**.** N: NTHi infected Healthy=2, Unstimulated COPD=1, NTHi infected COPD=1.*

5.1.13 Response of healthy HBECs when infected with RV in basal cultures

HBECs were infected with RV16 for 24 hours at an MOI of 0.01 and the DEGs assessed. There were not many DEGs that met the criteria and only 5 genes that were significantly downregulated including the demethylase *UTY*, as well as *DDX3Y* which may be implicated with the enhancement of the antiviral response **(Figure 5.13).**

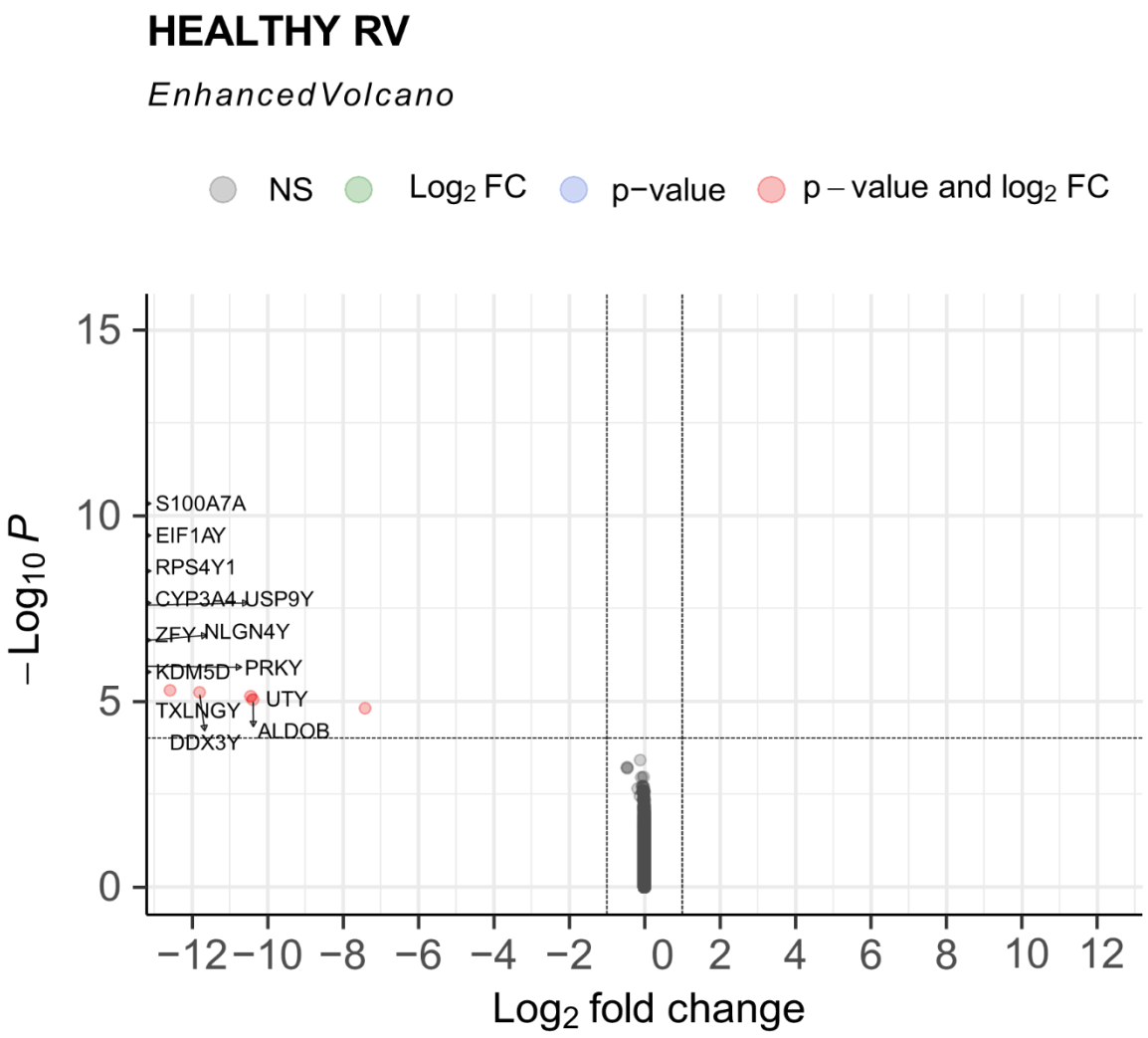


Figure 5.13: Effect of RV16 infection on DEG in healthy HBECs at basal cultures. *DEGs were graphed in a volcano plot for healthy HBECs infected 0.01 MOI of RV16 for 24 hours compared to unstimulated healthy HBECs at basal cultures. Log2fold change on the x-axis and transformed p-values on the y-axis. N: Unstimulated healthy=3, RV16 infected healthy=1.*

5.1.14 No effect of RV infection on DEGs in smoker HBECs at basal cultures

The response of smoker HBECs to RV16 infection was then compared for DEG expression compared to unstimulated smokers. Similar to what was observed in healthy HBECs, there were no DEGs in smoker HBECs infected with RV16 compared to unstimulated smoker HBECs **(Figure 5.14a)**.

There were also no significant differences found between smoker HBECs infected with RV16 and healthy HBECs infected with RV16 with the exception of a much great amount of the pseudogene *TXLNGY* in infected smokers HBECs **(Figure 5.14b)**.

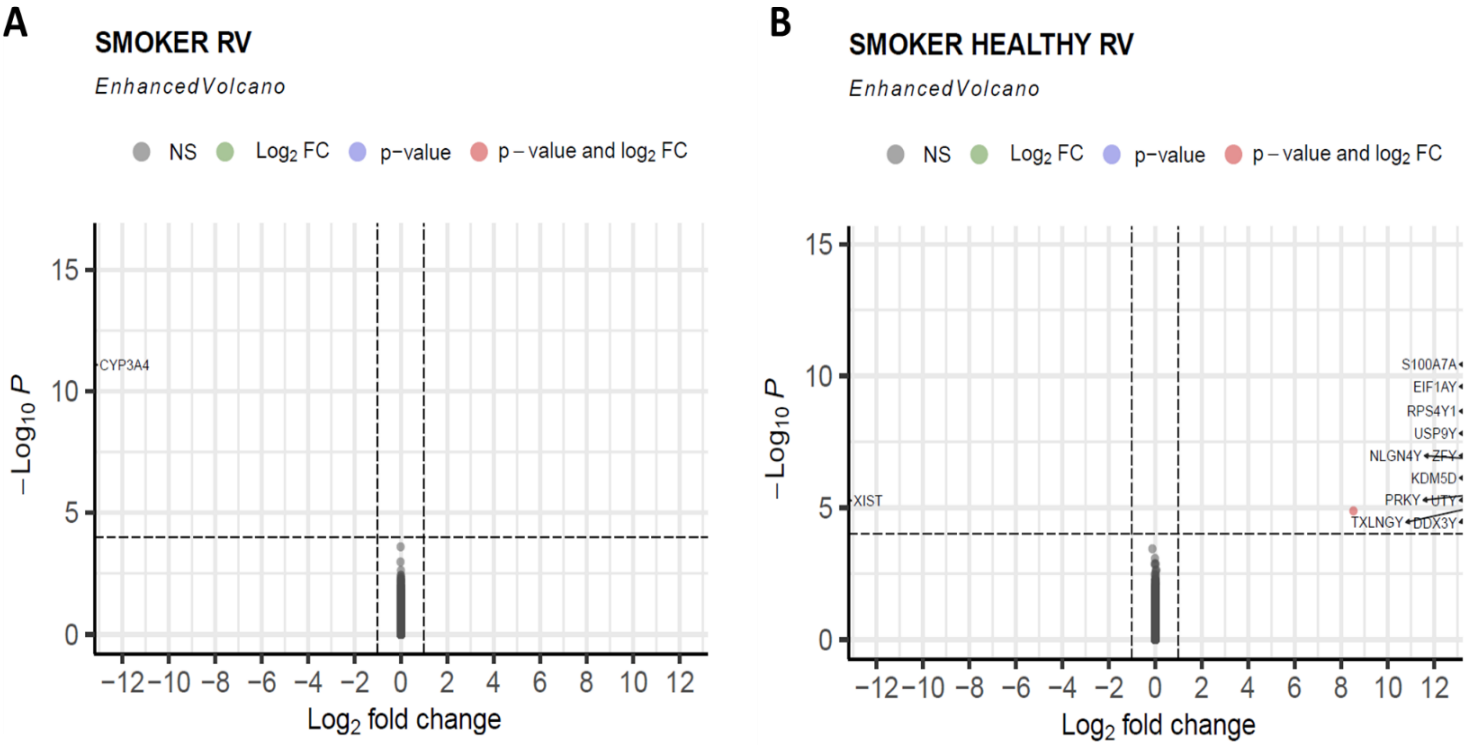


Figure 5.14: RV16 Expression effect on smoker HBEC gene expression. *DGE of smoker HBECs infected with 0.01 RV16 for 24 hours compared to* ***(A)*** *Unstimulated smoker HBECs and* ***(B)*** *RV16 infected healthy HBECs in basal cultures. Log2fold change on the x-axis and transformed p-values on the y-axis. N: RV16 infected Healthy=1, Unstimulated Smoker=3, RV16 infected smoker=2.*

5.1.15 COPD HBECs responses during RV infection in basal cultures

When COPD HBECs were infected with RV16, there were few DEGs which were *AGXT* and *HPD* as well as *DELEC1* only being slightly downregulated by 0.3 log2folds.

PLG was also downregulated by around 1.2 log2folds but was not significant ($p=1.4x10^{-4}$) **(Figure 5.15a)**.

There were also no DEGs in COPD HBECs infected with RV16 when compared to healthy HBECs infected with RV16.*GDF1,* a member of the TGFβ1 superfamily, was significantly higher in infected COPD HBECs compared to healthy infected HBECs despite a relatively small increase of 0.25 log2folds in infected COPD HBECs **(Figure 5.15b)**.

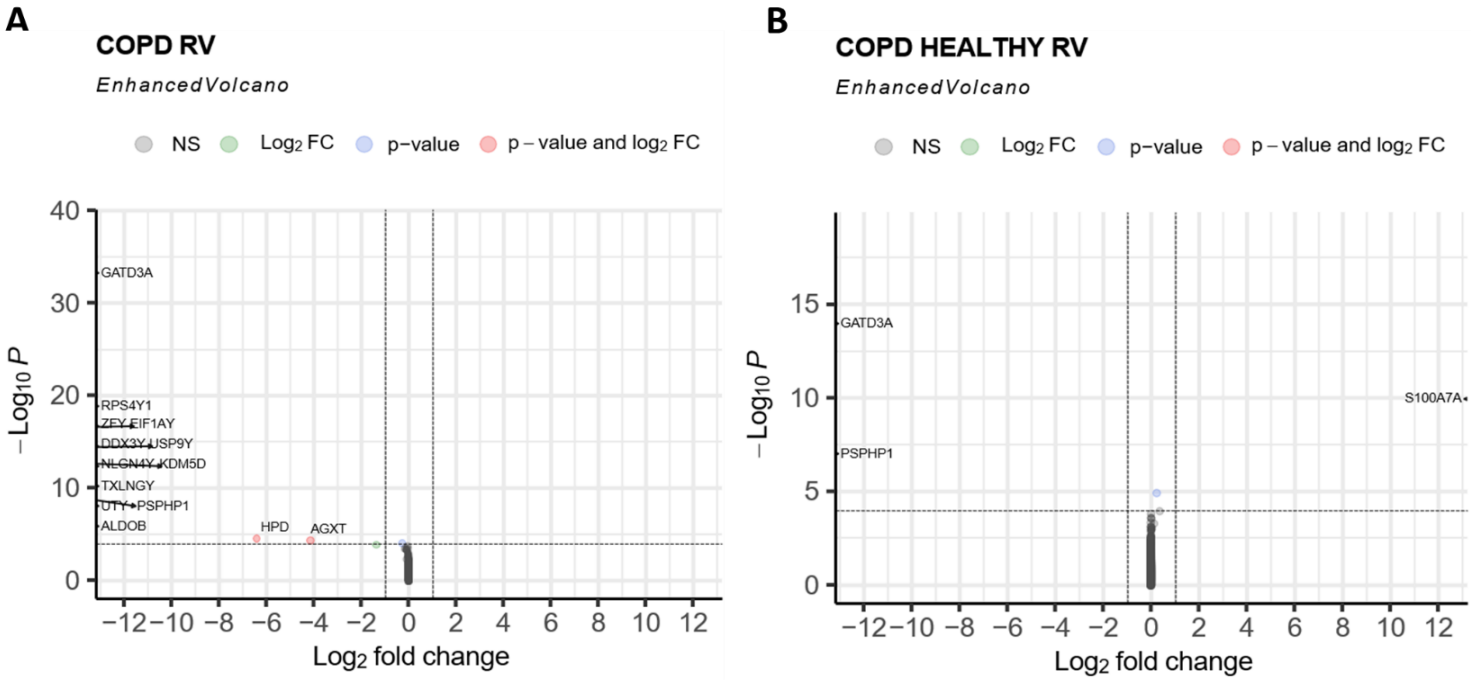


Figure 5.15: RV16 Expression effect on COPD HBEC gene expression. *DGE of COPD HBECs infected with 0.01 RV16 for 24 hours compared to* ***(A)*** *Unstimulated COPD HBECs and* ***(B)*** *RV16 infected healthy HBECs in basal cultures. Log2fold change on the x-axis and transformed p-values on the y-axis. N: RV16 infected Healthy=1, Unstimulated Smoker=6, RV16 infected COPD=2.*

5.1.16 RV infection in differentiated healthy HBECs have no effect

DEGs were then investigated under the context of RV16 infection in differentiated healthy HBECs. There were no significant differences between unstimulated healthy

HBECs and healthy HBECs post-infection in differentiated HBECs which is similar to what was observed under basal culture **(Figure 5.16).**

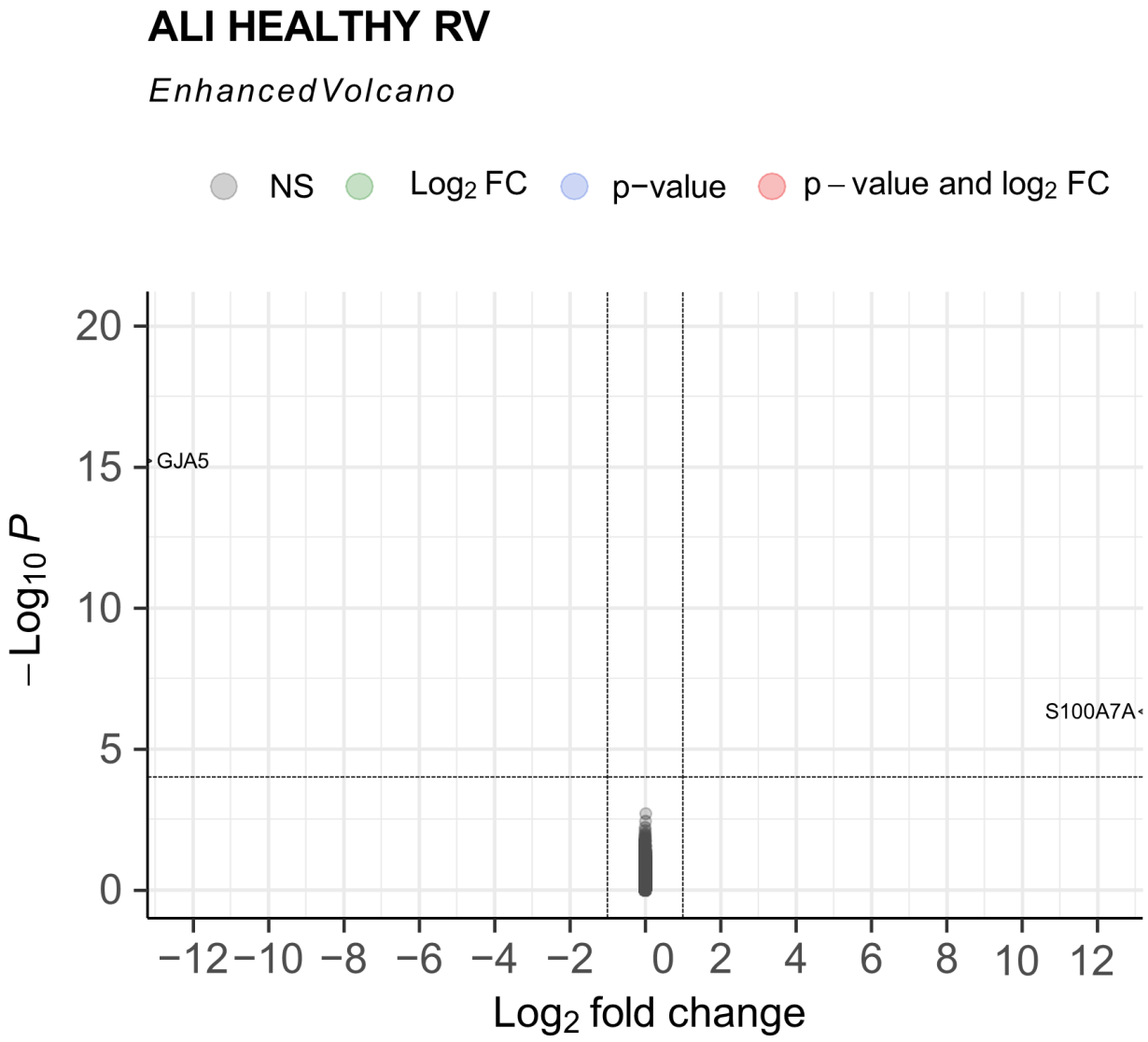


Figure 5.16: DGE in differentiated healthy HBECs post-infection with RV16. *Volcano plot for DEGs of differentiated healthy HBECs post-infection with 0.01 MOI of RV16 for 24 hours. Log2fold change on the x-axis and transformed p-values on the y-axis. N: Unstimulated=1, Infected=2.*

5.1.17 DEGs in differentiated smoker HBECs post-infection with RV

Changes in smoker HBECs were then examined post-infection with RV16 after 24 h. There were few DEGs post-infection with RV16 in smoker HBECs in comparison with unstimulated HBECs in ALI cultures. *XIST* was the only DEG that was downregulated

by approximately 5-log2fold changes and *NIPAL4* was also significant in its decrease but only by 0.06 log2folds with a base mean of 1066.3 read counts **(Figure 5.17a)**.

When compared to RV16 infected healthy HBECs, infected smoker HBECs had 5 DEGs that were significantly higher and 5 DEGs that were significantly lower in differentiated cultures. Genes that encode for proteins that are involved in triglyceride and fat modification and breakdown, *PNPLA3* and *LPCAT3*, were significantly upregulated in infected smoker HBECs by 2.1 and 1.4-log2fold increases respectively. *LARGE1* is a gene that was also significantly increased and is involved in glycosylation of saccharides that can lead to binding to ECM proteins like laminin **(Figure 5.17b)**.

The sulfate transporter *SLC26A2* was significantly lower in RV16 infected smoker HBECs compared to infected healthy HBECs as well as the gene *OSBPL6* which is responsible for the efflux of cholesterol. *SERPINB2,* which inhibits urokinase plasminogen kinase, was also significantly lower as well as *CA12* which is responsible for the hydration of carbon dioxide **(Figure 5.17b)**.

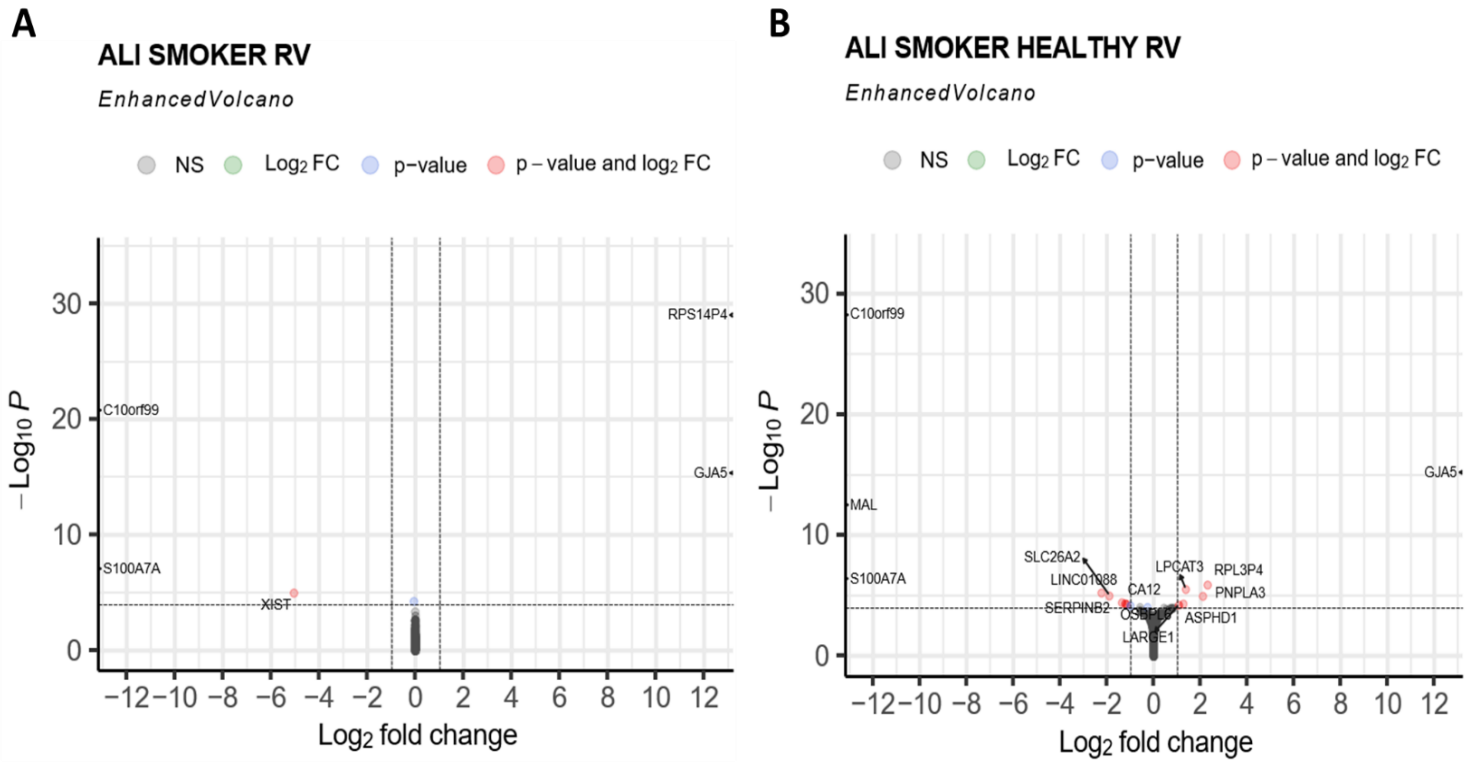


Figure 5.17: RV16 Infection DEGs in differentiated smoker HBECs. *DGE of differentiated smoker HBECs infected with 0.01 RV16 for 24 hours compared to* ***(A)*** *Unstimulated smoker HBECs and* ***(B)*** *RV16 infected healthy HBECs. Log2fold change on the x-axis and transformed p-values on the y-axis. N: RV16 infected Healthy=1, Unstimulated Smoker=2, RV16 infected smoker=1*

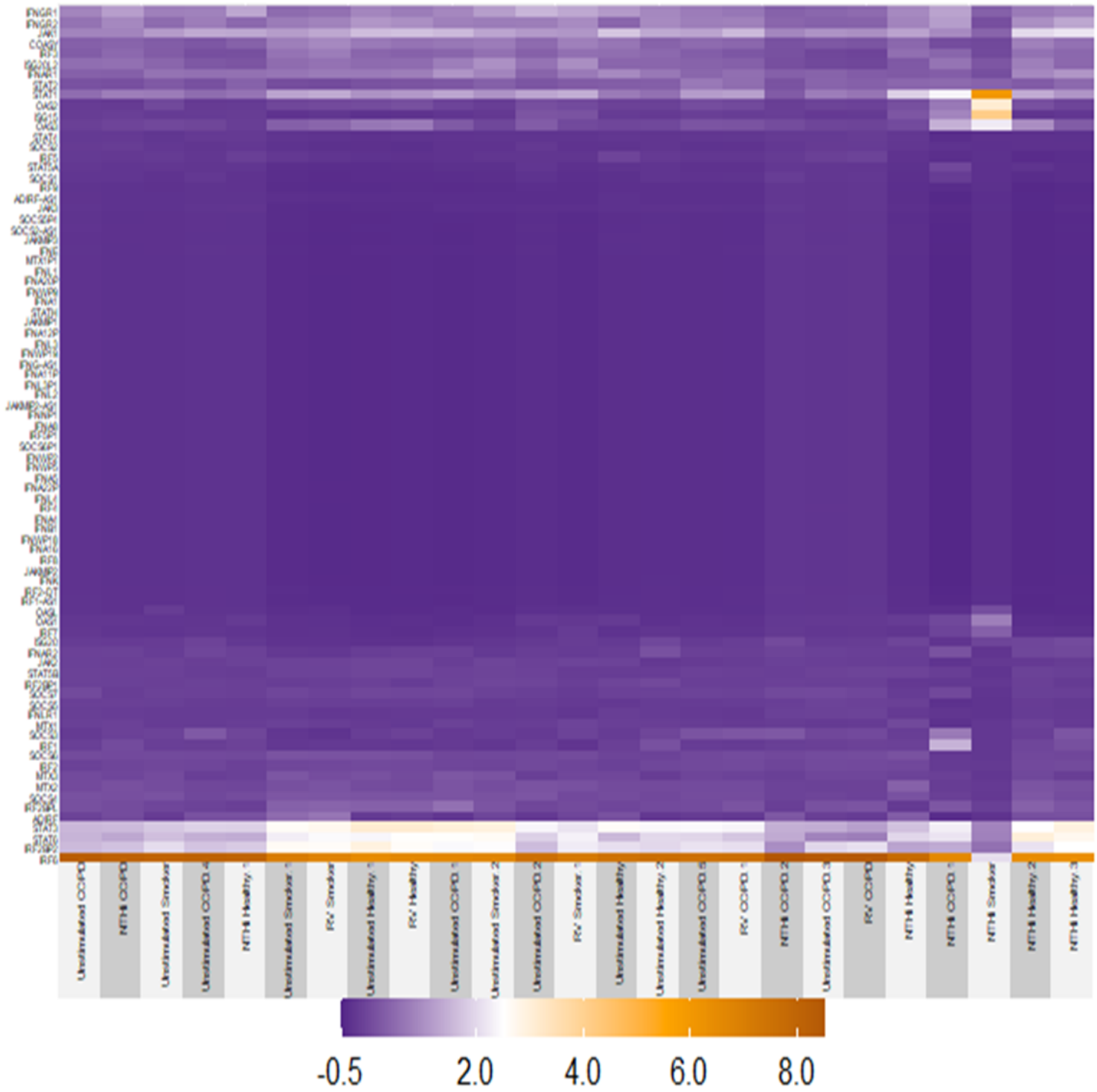
5.1.18 Supervised analysis for DEGs involved in IFN signaling or innate anti-viral immunity

After making all the comparisons between different conditions and groups to identify DEGs, the list of genes was narrowed down to investigate any significant changes in genes of interest. The first set of genes that were investigated were genes involved in IFN signaling or innate anti-viral immunity. Thus, a heatmap was first graphed with the counts of the different genes of interest as well as an adjusted scale. Two heatmaps were graph to segregate samples that were cultured at a monolayer and samples that were cultured at ALI due to the variation between those two groups and in order to be able visualize the gene counts better **(Figure 5.18a,b)**.

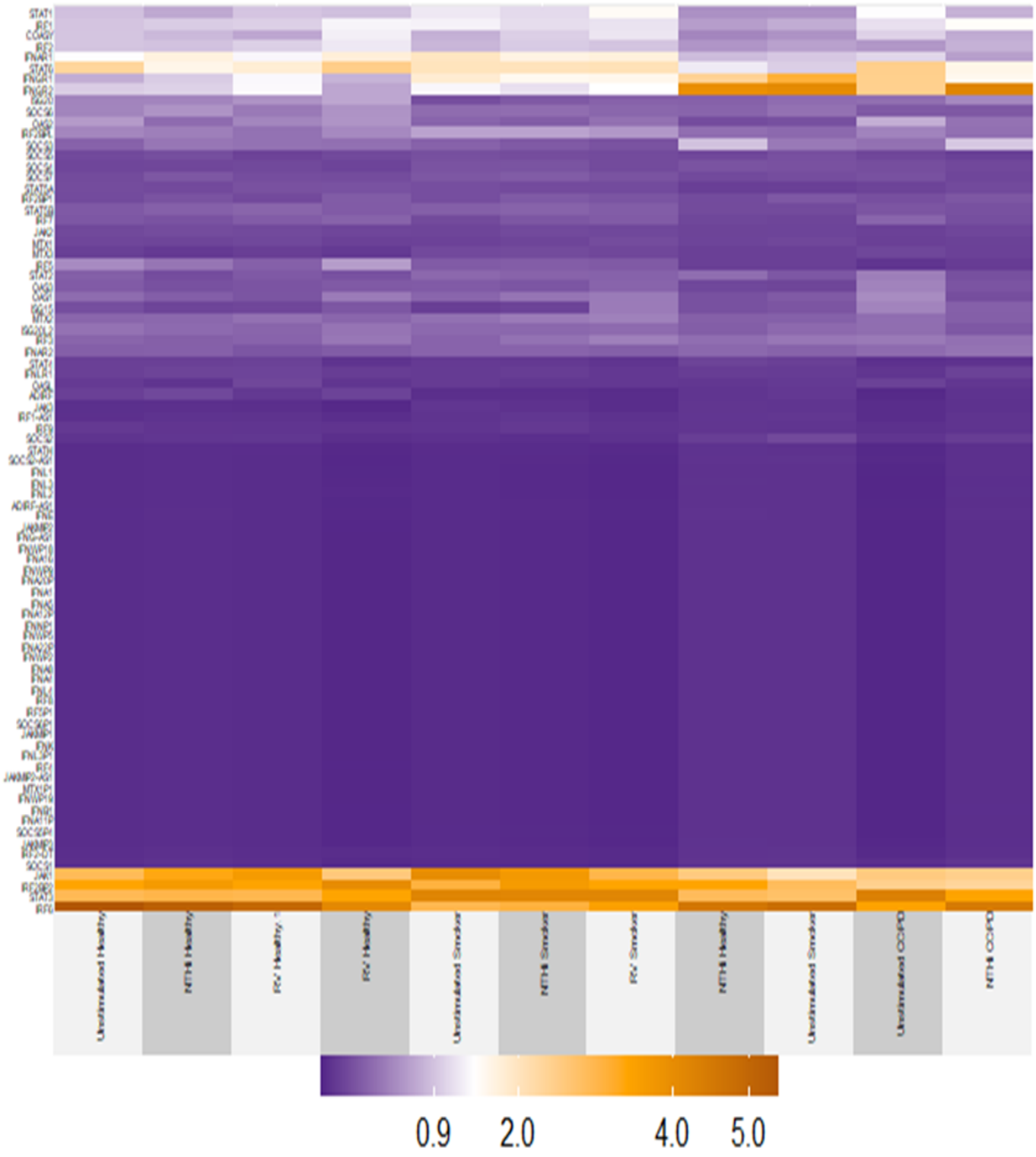
In basal cultures, COPD significantly upregulated the transcription factor *IRF1* by 1.7 log2fold post-infection with NTHi which dimerizes with *IRF7* to express type I and type III IFNs **(Figure 5.18c)**. When compared to healthy HBECs infected with NTHi, COPD HBECs had significantly higher amounts of *IRF9* post-infection which is the transcription factor responsible for mediating the expression of ISGs after STAT1 phosphorylation and dimerization **(Figure 5.18d)**. *SOCS1* however was also significantly higher in NTHi infected COPD HBECs by 2.1 log2folds and negatively regulates Type I and Type III IFN activity through its phosphatase activity **(Figure 5.18e)**.

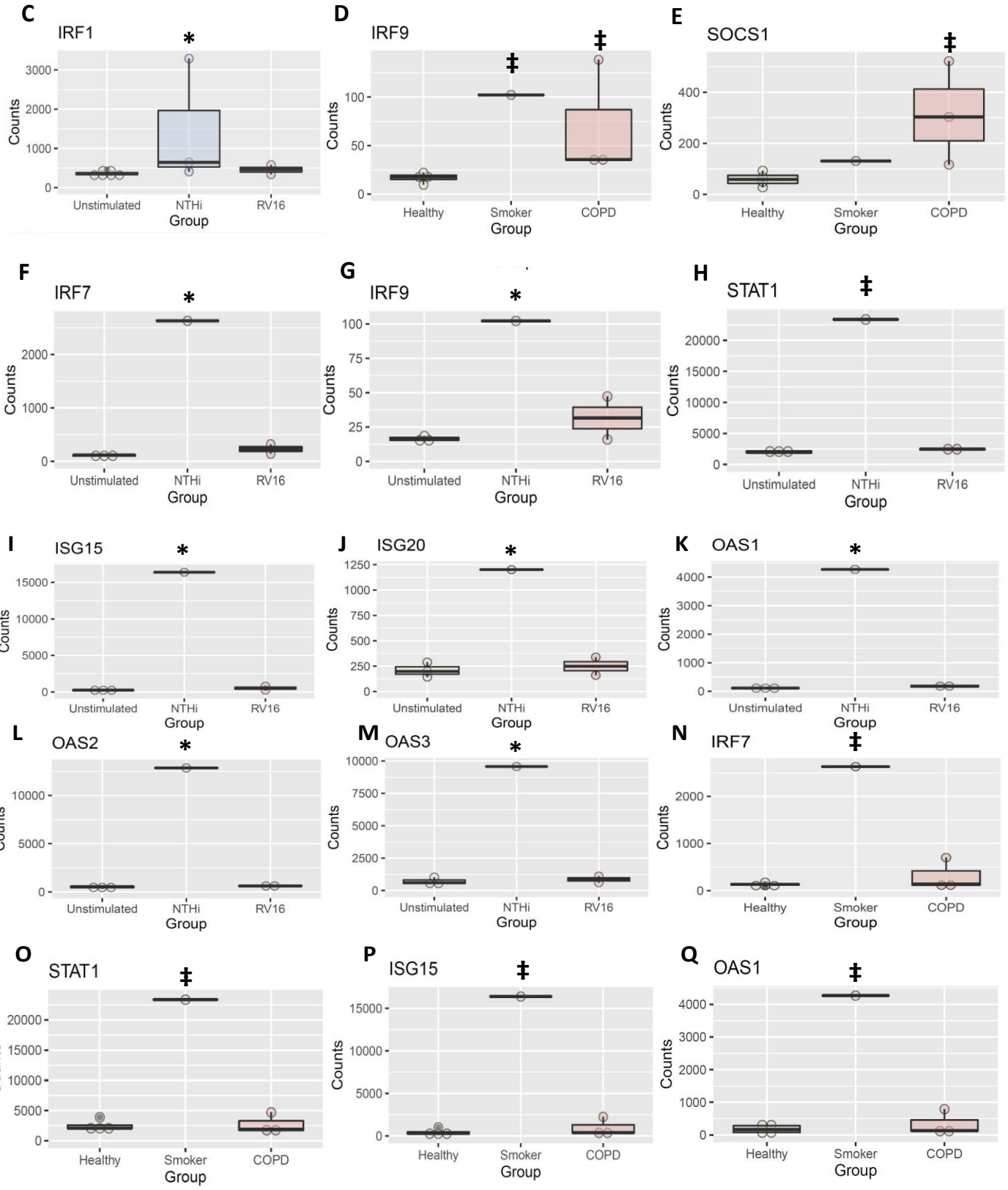
Smoker HBECs had several anti-viral genes that were significantly upregulated post-infection with NTHi. The transcription factors *IRF7* and *IRF9* were significantly higher post-infection in smoker HBECs with NTHi **(Figure 5.18f,g)**. *STAT1* was also higher post-infection with NTHi **(Figure 5.18h)**. The ISGs *ISG15, ISG20, OAS1, OAS2,* and *OAS3* were also significantly upregulated in after infection with NTHi in smoker HBECs **(Figure 5.18i-m)**. Similar genes were significantly higher in NTHi infected smoker HBECs in comparison to healthy HBECs infected with NTHi. *IRF7* and *IRF9* were significantly higher in smoker HBECs post-infection as well as *STAT1* **(Figure 5.18n,o)**. The ISGs *ISG15, OAS1, OAS2, OAS3,* and *OASL* were also significantly higher in smoker HBECs post-infection with NTHi **(Figure 5.18p-t)**.

A



B




C
IRF1
*
Counts
3000
2000
1000
0
Unstimulated
NTHi
RV16
Group
D
IRF9
‡
‡
Counts
100
50
0
Healthy
Smoker
COPD
Group
E
SOCS1
‡
Counts
400
200
0
Healthy
Smoker
COPD
Group
F
IRF7
*
Counts
2000
1000
0
Unstimulated
NTHi
RV16
Group
G
IRF9
*
Counts
100
75
50
25
0
Unstimulated
NTHi
RV16
Group
H
STAT1
‡
Counts
20000
15000
10000
5000
0
Unstimulated
NTHi
RV16
Group
I
ISG15
*
Counts
15000
10000
5000
0
Unstimulated
NTHi
RV16
Group
J
ISG20
*
Counts
1250
1000
750
500
250
0
Unstimulated
NTHi
RV16
Group
K
OAS1
*
Counts
4000
3000
2000
1000
0
Unstimulated
NTHi
RV16
Group
L
OAS2
*
Counts
10000
5000
0
Unstimulated
NTHi
RV16
Group
M
OAS3
*
Counts
10000
7500
5000
2500
0
Unstimulated
NTHi
RV16
Group
N
IRF7
‡
Counts
2000
1000
0
Healthy
Smoker
COPD
Group
O
STAT1
‡
Counts
20000
15000
10000
5000
0
Healthy
Smoker
COPD
Group
P
ISG15
‡
Counts
15000
10000
5000
0
Healthy
Smoker
COPD
Group
Q
OAS1
‡
Counts
4000
3000
2000
1000
0
Healthy
Smoker
COPD
Group

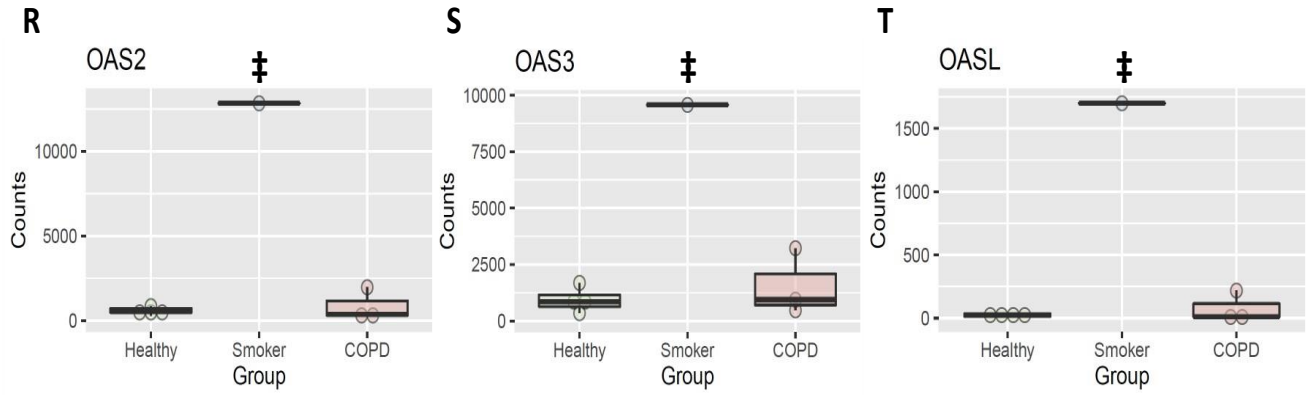


Figure 5.18: Gene expression of genes involved in IFN signaling and anti-viral genes in HBECs. *DEGs of IFN signaling and anti-viral genes in different HBEC groups and conditions visualized by a heatmap when in* ***(A)*** *Basal Cultures and at* ***(B)*** *ALI. The innate anti-viral DEGs that were significant in basal cultures were* ***(C)*** *IRF1 post-infection with 10 MOI of NTHi in COPD infected HBECs and* ***(D)*** *IRF9 in smoker and COPD HBECs post-infection with NTHi and* ***(E)*** *SOCS1 post-infection with NTHi in COPD HBECs compared to healthy HBECs. The genes* ***(F)*** *IRF7,* ***(G)*** *IRF9,* ***(H)*** *STAT1,* ***(I)*** *ISG15,* ***(J)*** *ISG20,* ***(K)*** *OAS1,* ***(L)*** *OAS2,* ***(M)*** *OAS3 were all significant in smoke HBECs post-infection with NTHi compared to unstimulated. Compared to NTHi infected healthy HBECs, infected smoker HBECs had significantly higher* ***(N)*** *IRF7,* ***(O)*** *STAT1,* ***(P)*** *ISG15,* ***(Q)*** *OAS1,* ***(R)*** *OAS2,* ***(S)*** *OAS3 and* ***(T)*** *OASL. *: $p<5x10^{-4}$ compared to unstimulated. ‡: $p<5x10^{-4}$ compared to NTHi infected healthy HBECs.*

5.1.19 Gene counts and changes in PRRs in healthy, smoker, and COPD HBECs

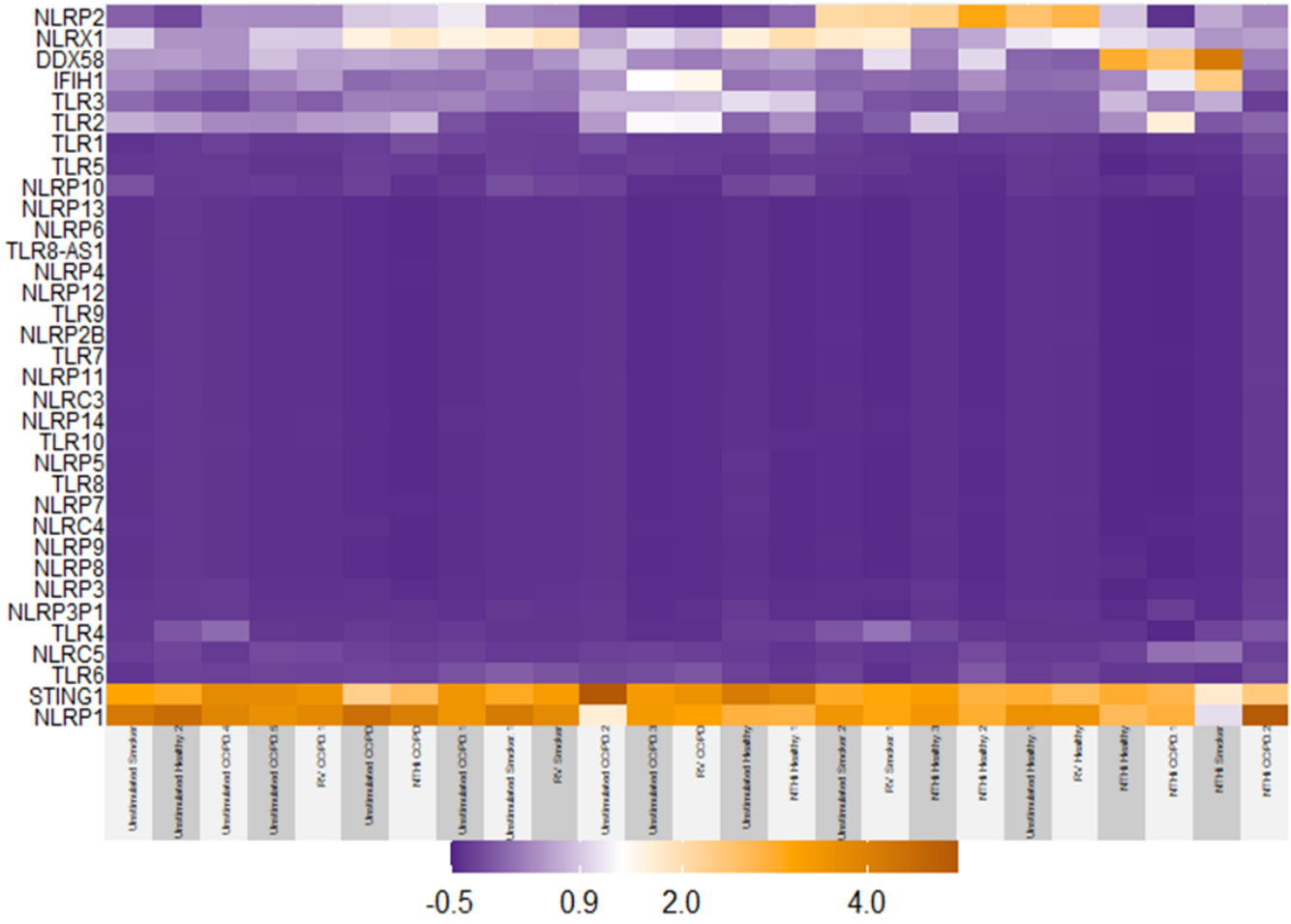
Following investigating genes involved in IFN signaling and innate anti-viral immunity, changes for any PRRs were investigated between groups or conditions. Two heatmaps with the gene counts were graphed for Monolayer or ALI cultured HBECs separately with gene counts for PRRs such as TLRs, NLRs, as well as other PRRs such as *IFIH1* or *STING* which are involved with viral sensing **(Figure 5.19a,b)**.

In terms of significant changes in PRR expression, there were significant changes found only in NTHi infected smokers compared to unstimulated controls or compared to NTHi infected healthy HBECs. *DDX58* and *IFIH1,* which are intracellular RNA sensors, were upregulated in NTHi infected smoker HBECs compared to unstimulated smoker HBECs **(Figure 5.19c,d)**. *NLRC5,* a member of the NLR family of sensors, was also significantly upregulated post-infection with NTHi **(Figure 5.19e)**. Similarly,

compared to healthy HBECs stimulated with NTHi, smoker HBECs had significantly higher levels of *DDX58* and *IFIH1* post-infection with NTHi **(Figure 5.19f,g)**.

There were no significant DEGs for any PRRs in any of the comparisons made for HBECs that were cultured at ALI.

A



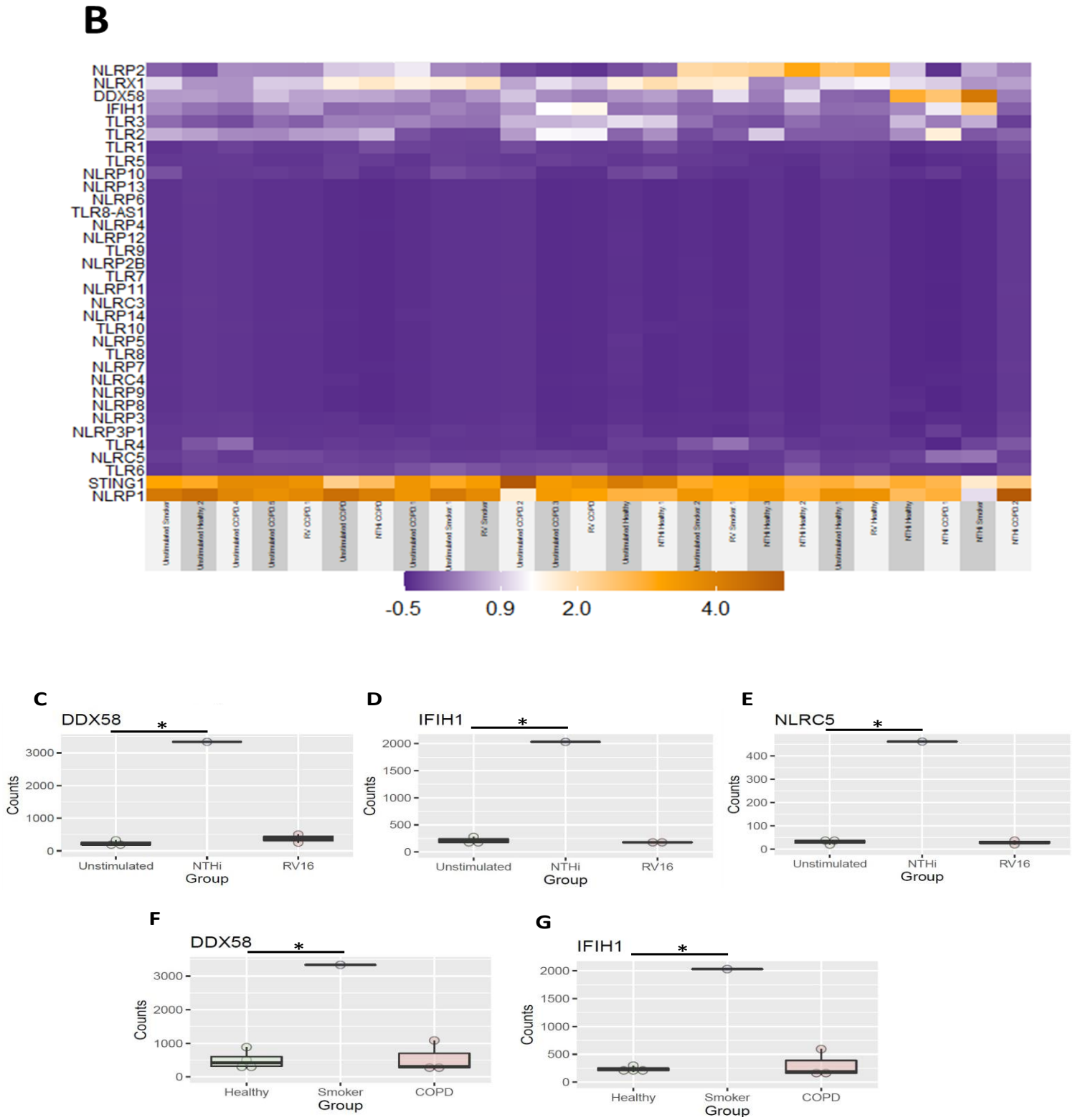


Figure 5.19: PRR gene counts in healthy, smoker, and COPD HBECs. *DEGs of different PRRs in different HBEC groups and conditions visualized by a heatmap when in* ***(A)*** *Basal Cultures and at* ***(B)*** *ALI. Gene counts of the PRRs* ***(C)*** *DDX58,* ***(D)*** *IFIH1, and* ***(E)*** *NLRC5 were plots comparing unstimulated smoker HBECs with HBECs stimulated with 10 MOI of NTHi or 0.01 MOI of RV16. in basal cultures. NTHi infected HBECs in all three groups were plotted for gene counts of* ***(F)*** *DDX58 and* ***(G)*** *IFIH1 *: $p<5x10^{-4}$*

5.1.20 DGE of Interleukins, Interleukin Receptors, and Cytokines in HBECs

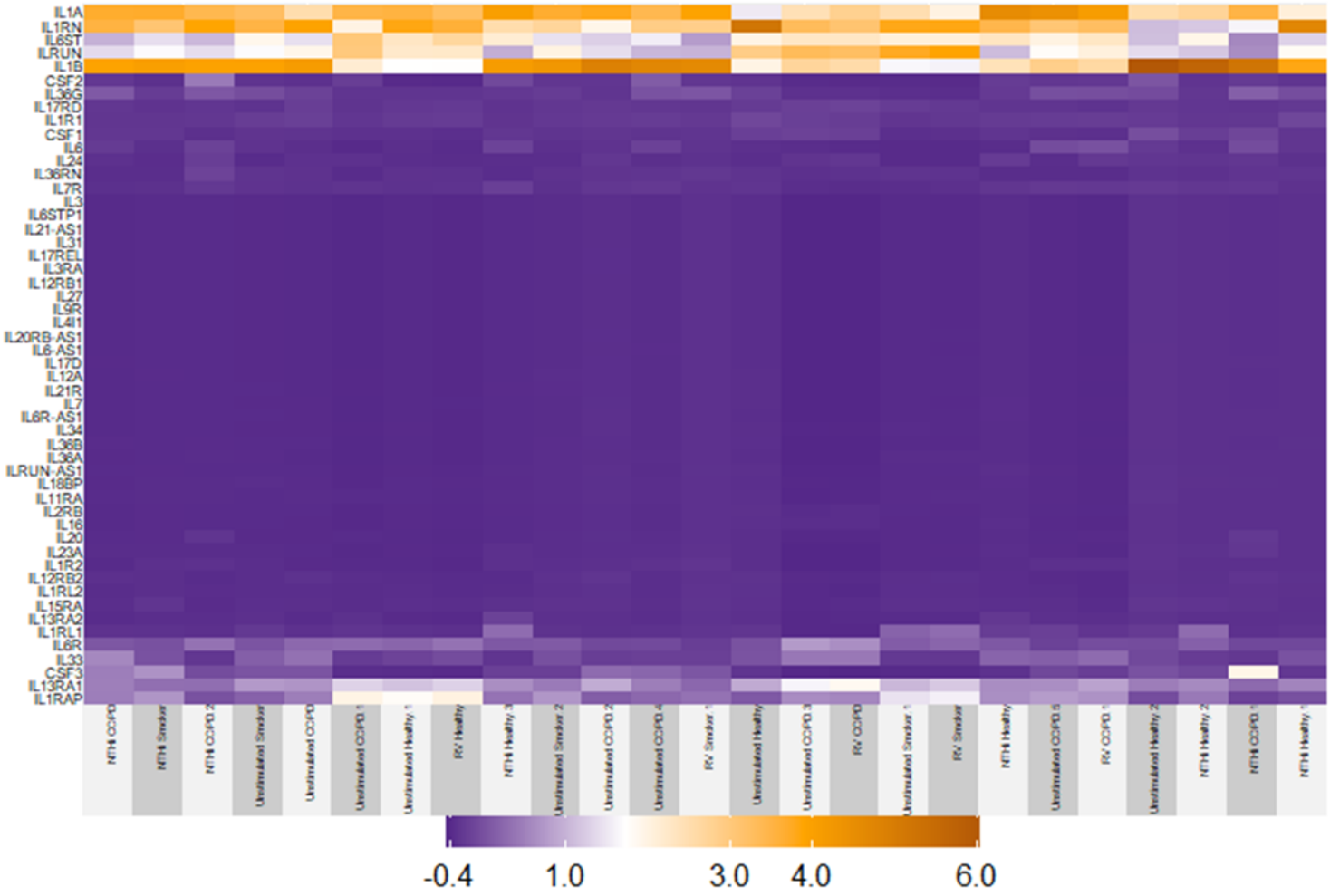
Cytokines and cytokine signaling have a myriad of functions that can be pro-inflammatory or anti-inflammatory depending on the cytokine with several cytokines being produced by HBECs. Thus, different cytokines were investigated between groups and conditions for any significant changes. A heatmap was generated with the gene counts of the different cytokines and cytokine receptors in different HBEC groups and conditions at a basal culture and another for HBECs cultured at ALI **(Figure 5.20a-d)**.

When compared to unstimulated HBECs in COPD at basal cultures, the genes *IL17C* and *IL20* were significantly upregulated by 0.46 and 2.12 log2folds after infection with NTHi **(Figure 5.20e,f)**. *IL17C* and *IL20* were also significantly higher in COPD HBECs post-infection with NTHi by 3.1 and 4.3 log2folds compared to healthy HBECs after NTHi infection **(Figure 5.20g,h)**. *IL34* and the IL18 inhibitor *IL18BP* were also significantly higher in NTHi infected COPD HBECs compared to infected healthy HBECs by 1.75 and 1.33 log2folds respectively **(Figure 5.20i,j)**. In terms of cytokine receptors, the receptors *IL11RA* and *IL1RL2* were significantly higher in NTHi infected COPD HBECs by 1.88, and1.89 log2folds respectively compared to infected healthy HBECs **(Figure 5.20k,l)**. *IL36RN,* an antagonist of the IL-36 receptor, was also significantly higher in NTHi infected COPD HBECs by 2.12 log2folds compared healthy HBECs post-infection with NTHi **(Figure 5.20m)**. The cytokines from the IL36 family were all increased in NTHi infected COPD HBECs compared to unstimulated HBECs or NTHi infected healthy HBECs however the increase was not significant.

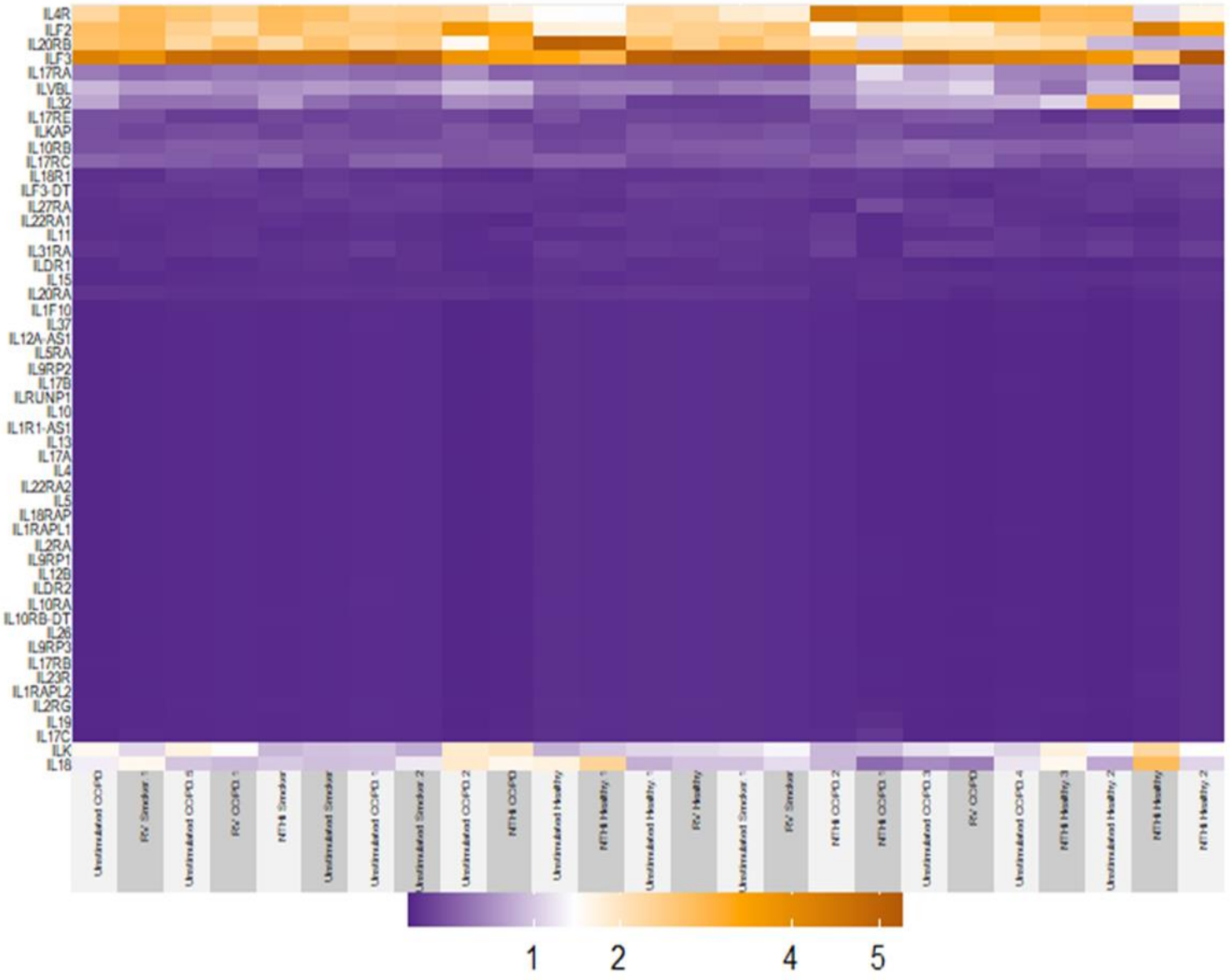
In differentiated unstimulated smoker HBECs, *CSF1* which encodes for M-CSF is significantly higher compared to unstimulated healthy HBECs but by only 0.38 log2folds. In addition, NTHi infected smoker HBECs had significantly lower levels of

IL33 and *IL36G* compared to unstimulated smoker however it was only by 0.16 and 0.07 log2folds respectively **(Figure 5.20n,o)**. When compared to NTHi infected healthy HBECs, smoker HBECs also had significantly lower levels of *IL33* and *IL36G* by 4.63 and 2.04 log2fold respectively post-infection with NTHi **(Figure 5.20p,q)**. *IL1B* as well as *IL1RN*, an inhibitor of IL-1β signaling, were also significantly lower by 0.42and 1.13 log2folds respectively in NTHi infected smoker HBECs compared to infected healthy HBECS **(Figure 5.20r,s)**.

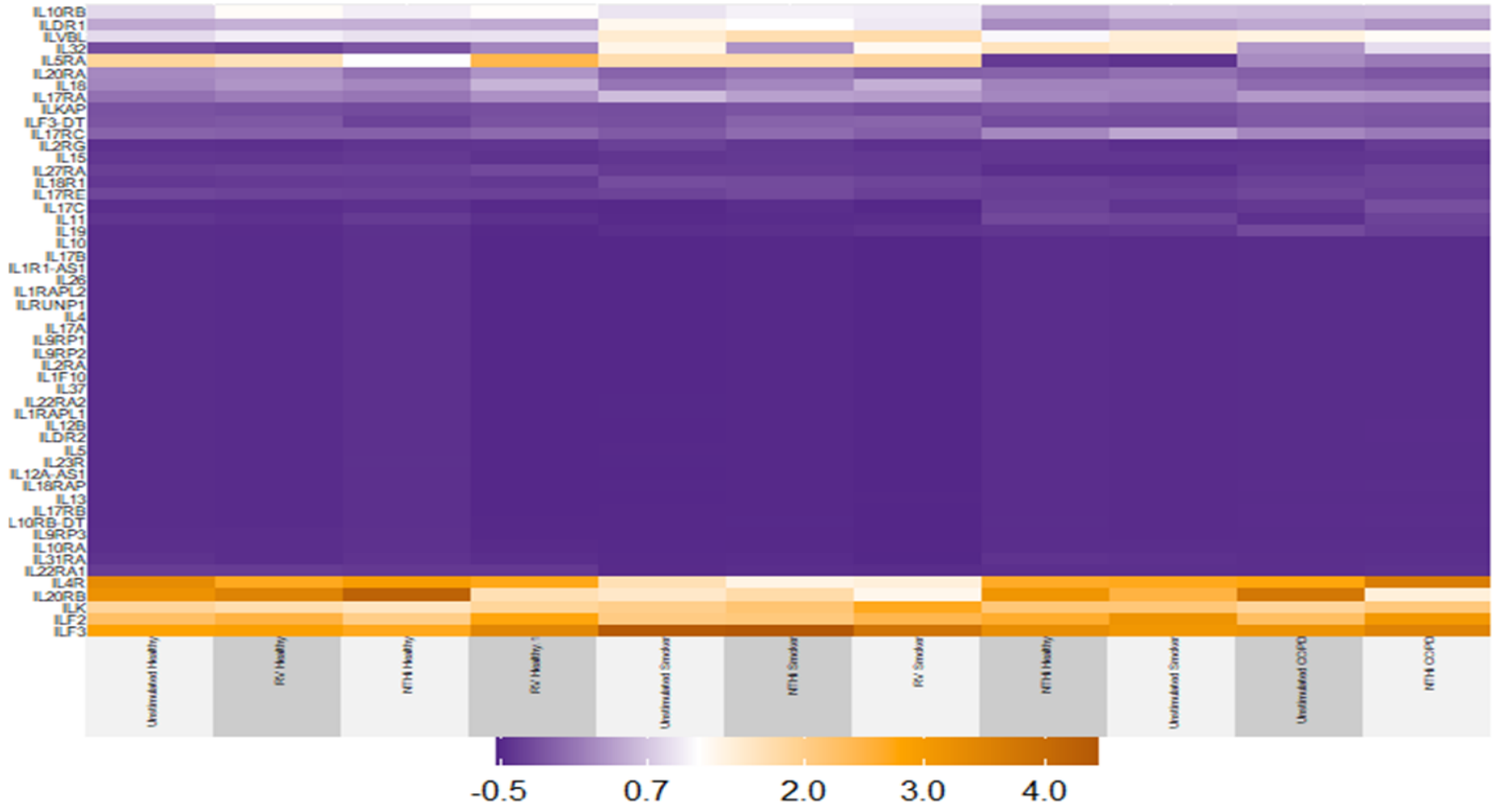
A



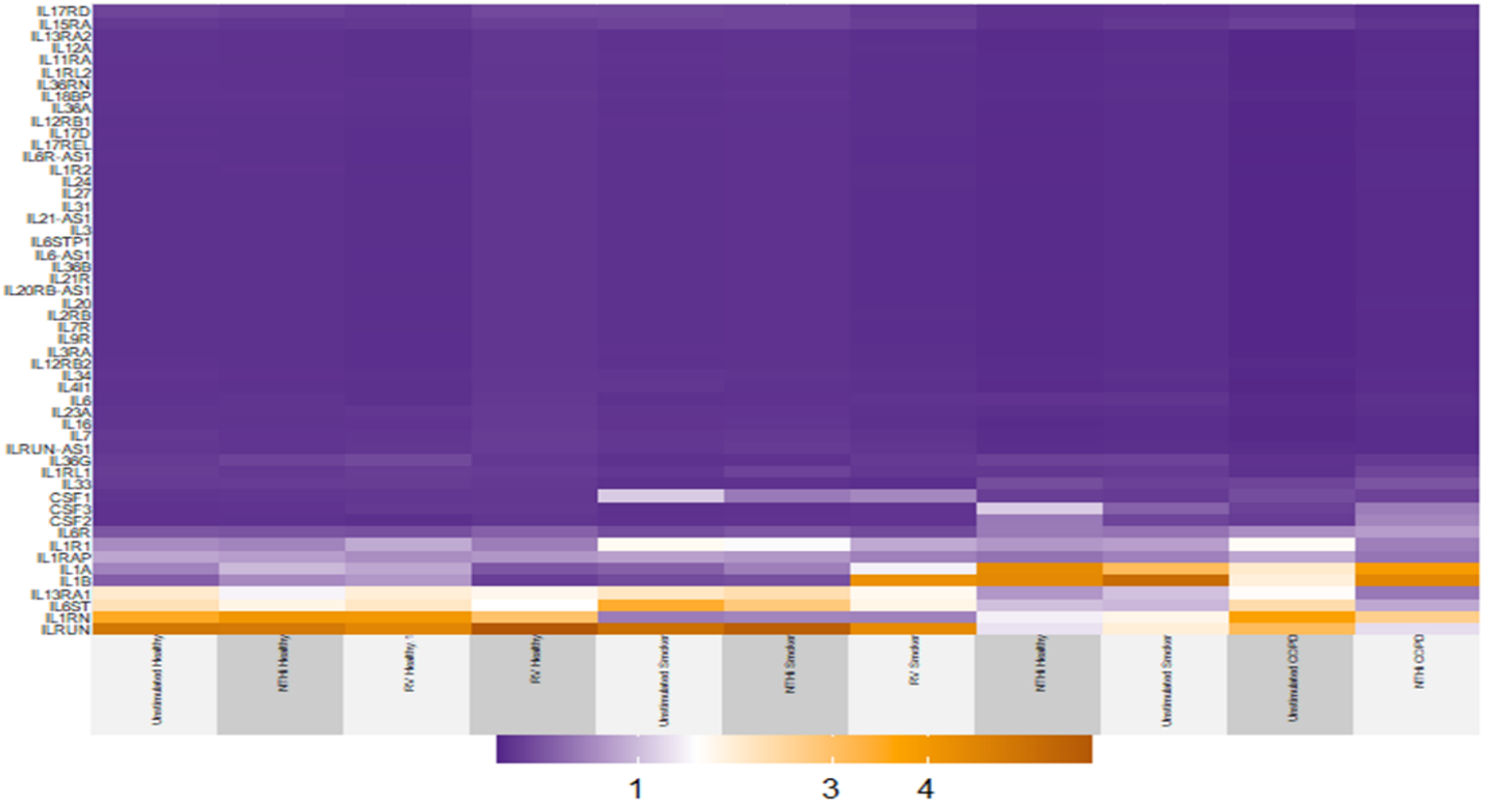
B

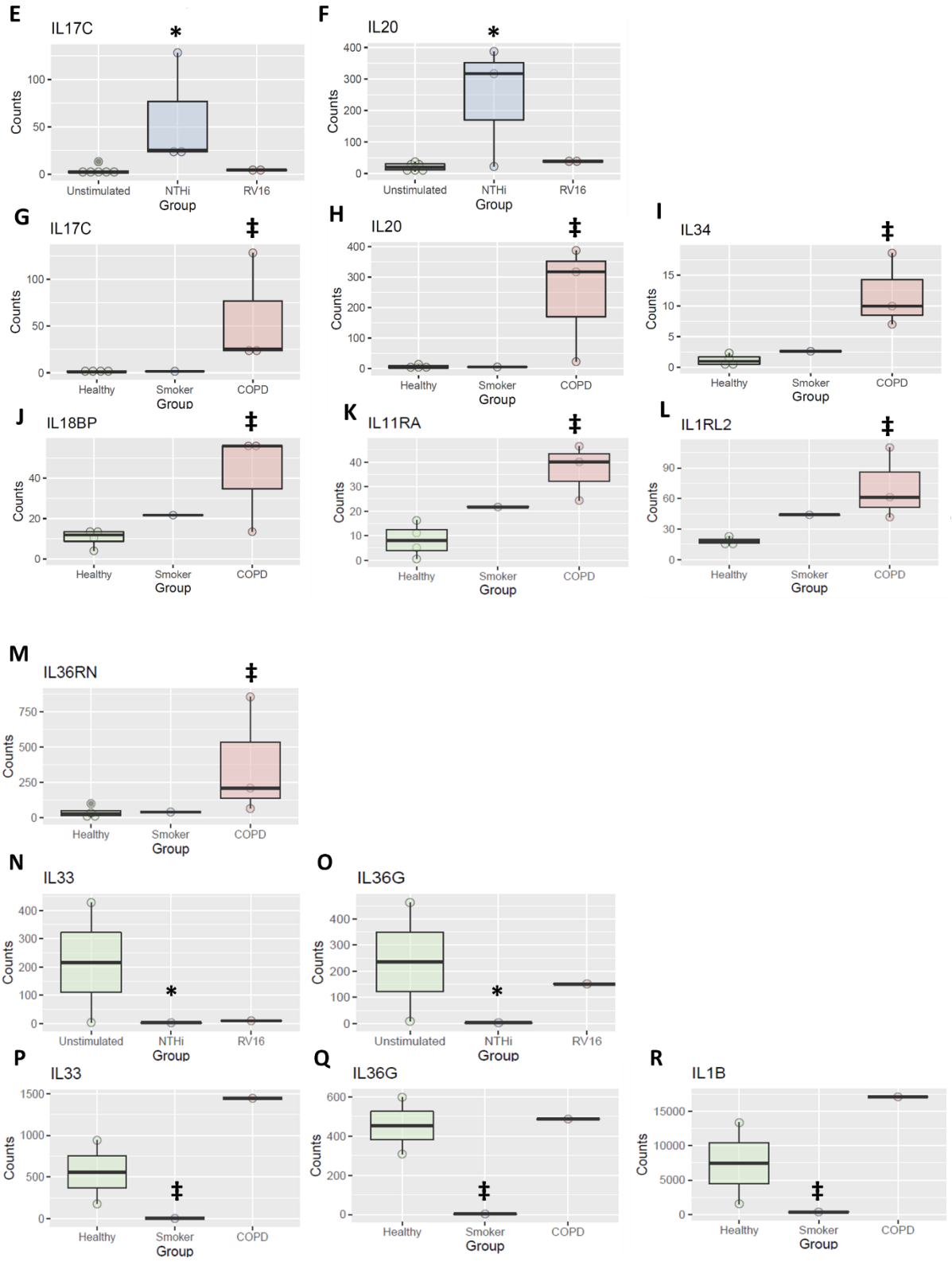

IL4R
ILF2
IL20RB
ILF3
IL17RA
ILVBL
IL32
IL17RE
ILKAP
IL10RB
IL17RC
IL18R1
ILF3-DT
IL27RA
IL22RA1
IL11
IL31RA
ILDR1
IL15
IL20RA
IL1F10
IL37
IL12A-AS1
IL5RA
IL9RP2
IL17B
ILRUNP1
IL10
IL1R1-AS1
IL13
IL17A
IL4
IL22RA2
IL5
IL18RAP
IL1RAPL1
IL2RA
IL9RP1
IL12B
ILDR2
IL10RA
IL10RB-DT
IL26
IL9RP3
IL17RB
IL23R
IL1RAPL2
IL2RG
IL19
IL17C
ILK
IL18
1
2
4
5

C


IL10RB
ILDR1
ILVBL
IL32
IL5RA
IL20RA
IL18
IL17RA
ILKAP
ILF3-DT
IL17RC
IL2RG
IL15
IL27RA
IL18R1
IL17RE
IL17C
IL11
IL19
IL10
IL17B
IL1R1-AS1
IL26
IL1RAPL2
ILRUNP1
IL4
IL17A
IL9RP1
IL9RP2
IL2RA
IL1F10
IL37
IL22RA2
IL1RAPL1
IL12B
ILDR2
IL5
IL23R
IL12A-AS1
IL18RAP
IL13
IL17RB
L10RB-DT
IL9RP3
IL10RA
IL31RA
IL22RA1
IL4R
IL20RB
IL2
ILF2
ILF3
-0.5
0.7
2.0
3.0
4.0

D


IL17RD
IL15RA
IL13RA2
IL12A
IL11RA
IL1RL2
IL36RN
IL18BP
IL36A
IL12RB1
IL17D
IL17REL
IL6R-AS1
IL1R2
IL24
IL27
IL31
IL21-AS1
IL3
IL6STP1
IL6-AS1
IL36B
IL21R
IL20RB-AS1
IL20
IL2RB
IL7R
IL9R
IL3RA
IL12RB2
IL34
IL4I1
IL6
IL23A
IL16
IL7
ILRUN-AS1
IL36G
IL1RL1
IL33
CSF1
CSF3
CSF2
IL6R
IL1R1
IL1RAP
IL1A
IL1B
IL13RA1
IL6ST
IL1RN
ILRUN
1
3
4


E
IL17C
*
Counts
Unstimulated
NTHi
RV16
Group
F
IL20
*
Counts
Unstimulated
NTHi
RV16
Group
G
IL17C
‡
Counts
Healthy
Smoker
COPD
Group
H
IL20
‡
Counts
Healthy
Smoker
COPD
Group
I
IL34
‡
Counts
Healthy
Smoker
COPD
Group
J
IL18BP
‡
Counts
Healthy
Smoker
COPD
Group
K
IL11RA
‡
Counts
Healthy
Smoker
COPD
Group
L
IL1RL2
‡
Counts
Healthy
Smoker
COPD
Group
M
IL36RN
‡
Counts
Healthy
Smoker
COPD
Group
N
IL33
*
Counts
Unstimulated
NTHi
RV16
Group
O
IL36G
*
Counts
Unstimulated
NTHi
RV16
Group
P
IL33
‡
Counts
Healthy
Smoker
COPD
Group
Q
IL36G
‡
Counts
Healthy
Smoker
COPD
Group
R
IL1B
‡
Counts
Healthy
Smoker
COPD
Group

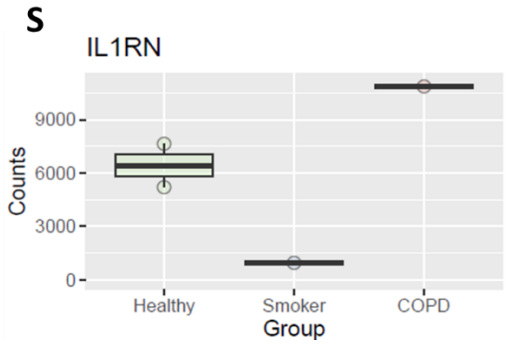


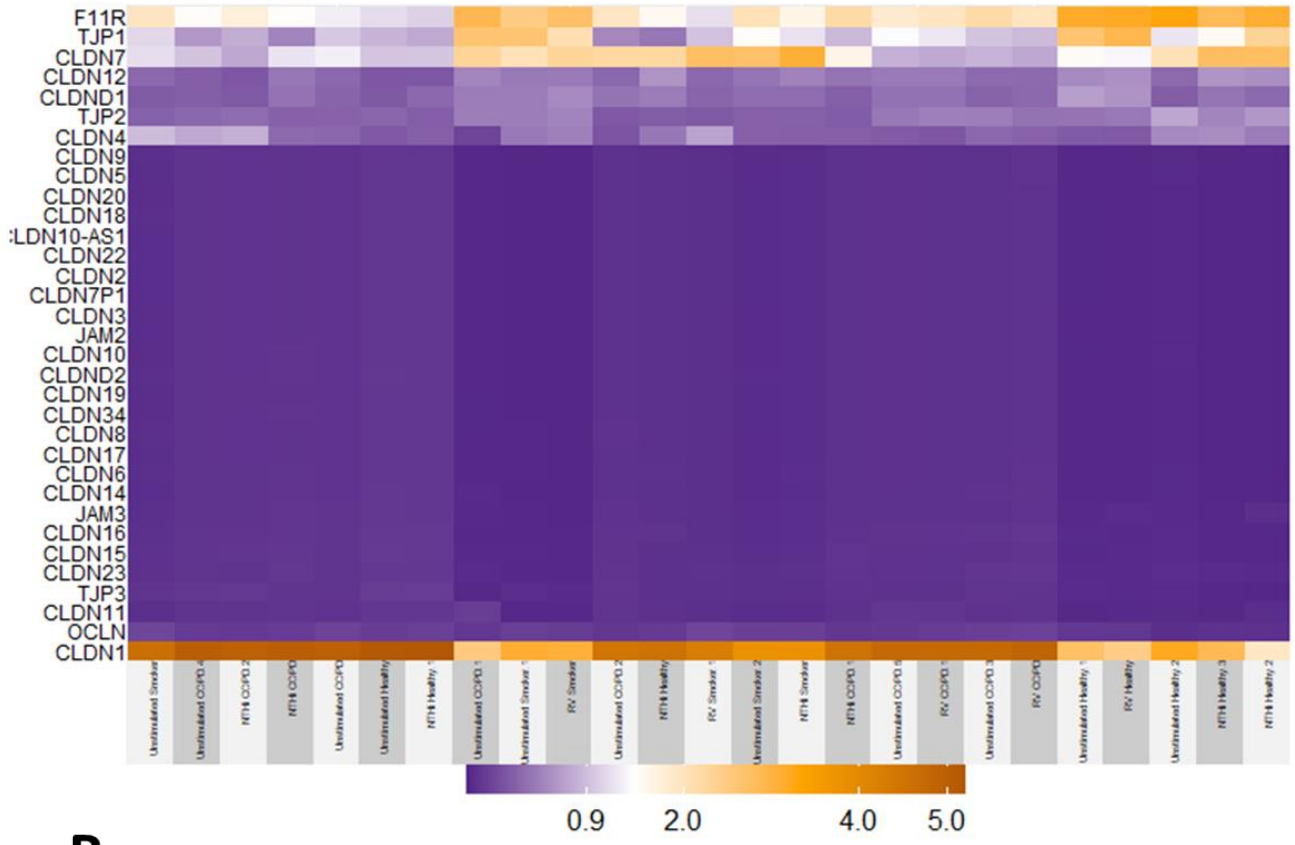
Figure 5.20: DEGs of cytokines and cytokine receptors in HBECs. *DEGs of IFN signaling and anti-viral genes in different HBEC groups and conditions visualized by a heatmap when in **(A,B)** Basal Cultures and at **(C,D)** ALI. Boxplots of significant DEGs of cytokines and cytokine receptors **(E)** IL17C and **(F)** IL20 in COPD HBECs infected with 10 MOI of NTHi and **(G)** IL17C, **(H)** IL20, **(I)** IL34, **(J)** IL18BP, **(K)** IL11RA, **(L)** IL1RL2, and **(M)** IL36N in NTHi infected COPD HBECs compared to infected healthy HBECs. **(N)** IL33 and **(O)** IL36G are significantly downregulated genes in NTHi infected differentiated smoker HBECs compared to unstimulated smokers. **(P)** IL33, **(Q)** IL36G, **(R)** IL1B, and **(S)** IL1RN are significantly lower in smoker HBECs compared to healthy HBECs post-infection with NTHi. *: $p<5x10^{-4}$ compared to unstimulated. ‡: $p<5x10^{-4}$ compared to NTHi infected healthy HBECs.*

5.1.21 DGE of TJ molecules in healthy, smoker, and COPD HBECs

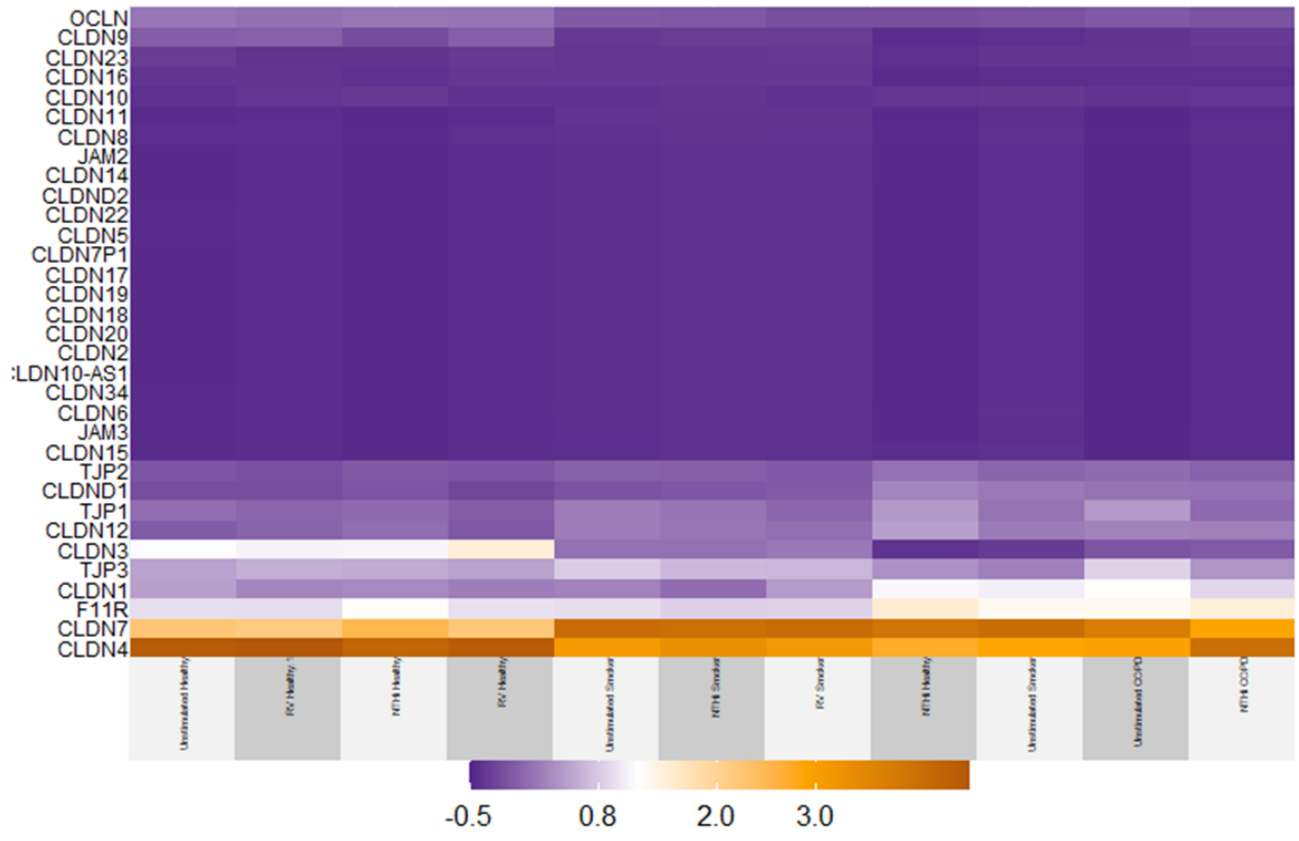
Lastly, DGE of different TJ molecules between different groups and conditions were examined. Two heatmaps for basal and differentiated cultures were graphed separately to visualize DGE of the different TJ molecules in the respective HBEC groups **(Figure 5.21a,b)**.

There were no significant differences between any of the TJ molecules in any group or condition that was investigated with the exception of a significant increase in *CLDN11* in differentiated smoker HBECs infected with RV compared with differentiated RV infected healthy HBECs **(Figure 5.21c)**. However despite the significant increase in RV infected smoker HBECs, it was only an increase of 0.17 log2folds.

A


F11R
TJP1
CLDN7
CLDN12
CLDND1
TJP2
CLDN4
CLDN9
CLDN5
CLDN20
CLDN18
:LDN10-AS1
CLDN22
CLDN2
CLDN7P1
CLDN3
JAM2
CLDN10
CLDND2
CLDN19
CLDN34
CLDN8
CLDN17
CLDN6
CLDN14
JAM3
CLDN16
CLDN15
CLDN23
TJP3
CLDN11
OCLN
CLDN1
0.9
2.0
4.0
5.0

B


OCLN
CLDN9
CLDN23
CLDN16
CLDN10
CLDN11
CLDN8
JAM2
CLDN14
CLDND2
CLDN22
CLDN5
CLDN7P1
CLDN17
CLDN19
CLDN18
CLDN20
CLDN2
:LDN10-AS1
CLDN34
CLDN6
JAM3
CLDN15
TJP2
CLDND1
TJP1
CLDN12
CLDN3
TJP3
CLDN1
F11R
CLDN7
CLDN4
-0.5
0.8
2.0
3.0

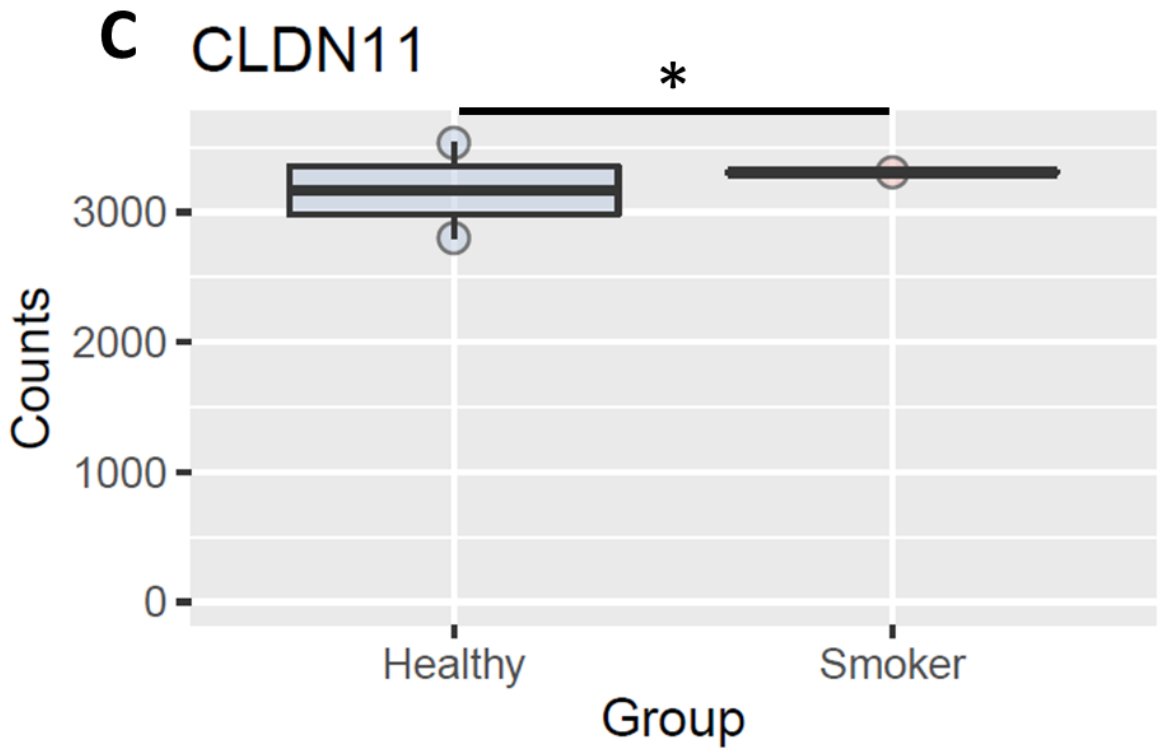


Figure 5.21: Gene expression of TJ Molecules in HBEC groups. *Gene counts of TJ molecules in healthy, smoker, and COPD HBECs visualized as a heatmap in* ***(A)*** *Basal conditions and at* ***(B)*** *ALI.* ***(C)*** *Gene counts of CLDN 11 post-infection with 0.01 MOI of RV16 in differentiated HBECs. *: $p<5x10^{-4}$*

Discussion

5.2.1 Variation between sequenced HBEC samples

There was not a lot of variation in mean gene counts for individual genes however there was variation between different samples depending on the condition or culture method. The biggest amount of variation observed were the differences between samples that were cultured at a monolayer and samples that were cultured at ALI. This was observed both in the PCA plot and the distance matrix for variation in individual plots. The donors that were cultured at a monolayer were different from the donors cultured at ALI and thus one explanation may be that it may be due to donor variation. However, donors within the same culture method were different as well such as between COPD and healthy donors for example and there was far less variation between these different donors than the differences observed between different culture conditions as seen in the PCA plot.

5.2.2 DGE in COPD or smokers compared to healthy HBECs when unstimulated

At basal conditions, there were no DEGs observed in either unstimulated COPD or smoker HBECs when compared to unstimulated healthy HBECs. This could either be because a stimulus such as a bacterial infection is required to assess DEGs between the different groups or any changes are occurring at a post-transcriptional or post-translational level which cannot be captured in an RNA-seq experiment.

In differentiated cultures however, some differences were observed in DGE between unstimulated smokers and unstimulated healthy HBECs. There were changes in different transporters in unstimulated smoker HBECs such as the gene for the cholesterol efflux transporter *OSPBL6* and the sulfate transporter *SLC26*. In addition, genes for cholesterol and fatty acid biosynthesis such as *DHCR7* and *SCD* were also

upregulated. Cholesterol biosynthesis has been shown to be increased in smokers high cholesterol is associated with atherosclerosis and other co-morbidities such as coronary heart disease that are found in COPD patients and smokers[278,279]. The decrease in cholesterol efflux also means that cholesterol may be more concentrated in smoker HBECs than healthy HBECs.

LDOC1 was also upregulated in smokers and a previous study on thyroid cancer cells has shown that it is capable of mediating apoptosis through the inhibition of NFκB[280]. The inhibition of NFκB by *LDOC1* may also contribute to the decreased expression of inflammatory cytokines in the epithelial cells of smokers. The effect on cigarette exposure on HBECs can be sometimes contradictory however and has previously been shown to actually increase inflammation rather than curtail it[281].

Unlike in a context of infection, there were no DEGs in differentiated unstimulated COPD HBECs compared to differentiated unstimulated healthy HBECs.

5.2.3 Effect of NTHi on smoker HBECs in comparison to NTHi infected healthy HBECs

When healthy HBECs were infected with NTHi, there were only 2 DEGs. It is unclear whether 10 MOI was insufficient to elicit a response in healthy HBECs as there were many more DEGs in NTHi infected smokers and COPD HBECs or if a 24 hours timepoint is too late to see any DGE. Only *CP* and *APOA1-AS* were differentially expressed and significantly downregulated post-infection with NTHi in healthy HBECs. CP is a protein that is responsible for the oxidation of iron in the cells while APOA1-AS is an inhibitor of APOA1 which forms a part of high density lipoproteins and their efflux from tissue to live.

In contrast to healthy HBECs, there were many DEGs in smoker HBECs post-infection with NTHi. In particular there were several ISGs and genes involved in IFN signaling were significantly upregulated. ISGs can have a variety of functions and can sometimes be antagonistic in their functions. *XAF1 and IFI27* for example, are ISGs that were significantly upregulated and have been shown to have pro-apoptotic activity in epithelial cells[282]. On the other hand, *IFI6* and *IFIT3* were also upregulated which are ISGs that have been shown to be anti-apoptotic[283]. The resolution of those antagonistic genes is unclear and it may be that what is observed on a transcriptional level may be different at a translational level or a later timepoint may be needed to notice any predominant shifts in their upregulation.

The chemokines CXCL10 and CXCL11 were both also significantly upregulated in smoker HBECs post-infection and both bind to the chemokine receptor CXCR3[284]. CXCR3 is expressed on effector and memory T-cells and monocytes and thus activation of CXCR3 by CXCL10 and CXCL11 would lead to more infiltrating T-cells and monocytes which has been found in the lungs of chronic smokers[285].

Previous studies have shown that IFN responses can combat bacterial infections such as NTHi. However, it is uncertain whether smokers have an upregulated IFN response in order combat the infection or if it is a misfiring of the innate immune response as gene expression of other classical pro-inflammatory cytokines such as CXCL8, IL-1β, TNFα, and IL-6 were not found to be significantly upregulated. Some evidence on the immune response misfiring or not fully functioning comes from evidence that smokers are at an increased risk of infection including bacterial infection[286]. If the epithelial immune response were functional, then perhaps an opportunistic pathogen like NTHi would not be able to infect smokers. Of course, epithelial cells are only one type of innate immune cells and leukocytes may act very differently and produce significantly

higher pro-inflammatory cytokines than epithelial cells with epithelial cells attempting to function as resolving cells by inducing apoptosis of infected cells for example. In fact, leukocytes and the pro-inflammatory cytokines TNFα and IL-6 were significantly higher in the BAL of NTHi infected mice that were expose to CS than mice that were exposed to NTHi on its own[287].

Negative regulators of IFN signaling were also significantly upregulated. *ETV7* and *USP18* are both genes that can suppress IFNAR signaling after IFN desensetization or suppress ISG expression[253,288]. However despite them being significantly upregulated, ISGs and genes involved in IFN signaling such as *IRF7* were still significantly upregulated indicating that either it was too early to detect full suppression, or that smoker HBECs failed to successfully repress IFN signaling post-infection with NTHi. The protein *BATF2* was also upregulated which are involved with the inhibition of the expression of pro-inflammatory cytokines like IL-17 and IL-23[289]. *LGALS9*, which encodes for the galectin-9 protein, was significantly increased and has been shown before in neutrophils to mediate intracellular respiratory bacterial killing and phagocytosis and can induce the production of CXCL8[290]. Interestingly, bacterial killing was only observed on Gram negative bacteria in the study on galectin-9.

Several genes involved in the mediation of MHC class I antigen presentation were also increased post-infection with NTHi. The genes include *TAP1, ERAP2,* and the immunoproteasome *PSMB9.* This may indicate that NTHi that have become intracellular to epithelial cells are having their proteins processed and presented as antigen peptides on MHC class I proteins on the cell surface. The MHC class I protein *HLA-F* was also significantly upregulated although its function is not as well defined as other MHC class I molecules. Interestingly, genes involved in MHC class II peptide processing and presentation such as *CLIP* were unchanged which could mean that

the ability to endocytose and present peptides from extracellular bacteria is blunted. *PLSCR1* was also upregulated and it is involved in the negative regulation of Fc receptor mediated phagocytosis. While epithelial cells are not professional antigen presenting cells they could enact changes in phagocytosis on macrophages for example as another study demonstrated[291].

There were also several poly ADP-ribose polymerases (PARPs) that were upregulated post-infection and in particular *PARP9, 10,* and *14*. PARPs transfer modifies proteins by ribosylating them with an ADP-ribose molecule. PARPs have a variety of functions from mediating DNA repair to mediating inflammatory and anti-viral immune responses. PARP14 has been shown to mediate IL-4 signaling through STAT6 and subsequently mediating type 2 responses by promoting the binding of STAT6 to its promoter[292]. Furthermore, PARP14 has also been shown to promote type 17 responses in mice[293]. PARP9 on the other hand has been shown to have an opposing role to PARP14 and facilitates the phosphorylation of STAT1 by ribosylation and the subsequent enhancement of the anti-viral response in macrophages[294]. Finally, PARP10 has been shown to inhibit NFκB through an E3 ubiquitin ligase and thus inhibits the production of pro-inflammatory cytokines[295]. The upregulation of PARPs with different functions indicates that the innate immune response in epithelial cells against NTHi is either broad or not specific or targeted. NTHi is a Gram negative bacteria however and thus has LPS on its cells surface. LPS activates TLR4 signaling which is a TLR that can undergo signaling through either the MYD88 or TRIF pathways which activates both NFκB and IRF3 respectively[296]. This leads to the production of both pro-inflammatory cytokines and type I and type III IFNs.

Another piece of evidence on the mediation of pro-inflammatory responses in smokers post-infection is the upregulation of the *NMI* gene. NMI has been demonstrated to be

able to act as a DAMP and induce activation of NFκB which upregulates the production of pro-inflammatory cytokines[297]. In addition, NMI has been inhibit the innate anti-viral response by facilitating the degradation of IRF7[298]. However, there were none of the classical pro-inflammatory cytokine upregulated in the dataset indicating that there are factors inhibiting their production that are not able to be overridden by proteins like NMI or that their upregulation would have been captured at a different timepoint.

There were also several genes from the tripartite motif (TRIM) family that were upregulated after NTHi infection in smoker infection. *TRIM5, 14, 22,* and *69* were all significantly increased post-infection. The TRIM family proteins have several function with many having functions that restrict viral replication or enhancing the anti-viral response. TRIM5 for example has been shown to restrict the invasion of retroviruses by binding to their capsid[299]. TRIM14 however regulates the immune response by enhancing or inhibiting type I IFN responses depending on the context. For example, in response to *Mycobacterium tuberculosis* infections, TRIM14 inhibited the production of type I IFNs[300]. In another study however TRIM14 was able to activate type I IFN production in A549 cells after Sendai virus infection[301]. In addition, it is able enhances signaling through the cGAS pathway which detects DNA from different pathogens by inhibiting its degradation[302]. Interestingly, NTHi has been previously shown to upregulate type I IFNs through the STING-cGAS pathway in BEAS2B cells[303].

The Metalloproteinase MMP13 was also significantly upregulated post-infection indicating a higher rate of the breakdown of ECM proteins like collagen.

When comparing NTHi infected smoker HBECs to infected healthy HBECs, the set of DEGs were similar to what was observed in the DEGs between infected and unstimulated smokers. This includes PARPs, TRIMs, and IFI genes as well as genes

mediating MHC class I presenting gene including *TAP2.* The gene *UNC93B1* was also significantly higher in smoker HBECs and is responsible for the transport of TLRs from the endoplasmic reticulum to the endosome to sense any pathogens. This shows that IFN responses and ISGs are more robust in infected smoker HBECs than infected healthy HBECs. As previously discussed, this could indicate smokers have untargeted clearance of NTHi or that NTHi can more easily manipulate host factors which affect the innate immune response. Alternatively, it is also possible that these responses are either repressed when epithelial cells are interacting with other leukocytes in the lung microenvironment. Thus epithelial cells become programmed to compensate for this negative regulation which results in a significantly higher response when stimulated in isolation with no external factors other than the infection.

There were however several genes that were significantly lower in NTHi infected smokers HBECs compared to infected healthy HBECs. *TNFRSF10D* for example was significantly lower and is involved in the inhibition of apoptosis[304]. The gene encoding type VIII collagen *COL8A1* was also lower.

The aforementioned discussed findings were all in basal smoker HBECs however when looking at differentiated smoker HBECs, a different picture emerges. When smoker HBECs were infected with NTHi, only *NIPAL4* emerge as a DEG that was downregulated. *NIPAL4* is a Magnesium transporter but it has not been implicated in lung diseases or defects and thus its relation to infection, if one exists, is yet to be discovered.

In comparison to healthy HBECs however, smoker HBECs had several DEGs that were downregulated post-infection. *IL33, IL36G,* and *CXCL2* were significantly lower in differentiated smokers compared to healthy HBECs post-infection with NTHi. IL-33

has been mainly been shown to be and inducer of type 2 cytokines production. IL-36γ has been increasingly shown to be an important activator of NFκB and mediator of pro-inflammatory cytokine production and neutrophilic inflammation particularly in mucosal tissue like the lungs[305,306]. Its pro-inflammatory role has also been shown in the context of lung injury and infection. CXCL2 has been shown to be a strong granulocyte and monocyte chemoattractant and mediator of proinflammatory cytokine production as well[307]. This may imply that infected smoker HBECs have a reduced capacity to produce type 2 cytokines or proinflammatory cytokines in the context of an infection.

The inhibitor of MMP3, *TIMP3* was also significantly lower in smoker HBECs compared to healthy HBECs indicating a curtailed ability to regulate MMP3 which was not significantly changed post-infection.

Anti-apoptotic genes such as *KCTD15* were also significantly lower in smoker HBECs relatively to healthy HBECs indicating that the smoker HBECs had a higher propensity to undergo apoptosis compared to health HBECs post-infection[308].

Genes involved in junctional formation and adhesion between cells were also lower in smoker HBECs. *CDH13,* which encodes for cadherin-13, and *FERMT1* were significant lower. Cadherin-13 is an adheren molecules that homodimerizes while FERMT1 activates and interacts with the integrin β subunit in epithelial cells and their decrease indicates an impaired ability for barrier and junctional formation in smoker HBECs. CD44 is also an adhesion molecule and helps recruit leukocytes into inflamed tissues however gene expression of *CD44* was found to be lower in smoker HBECs post-infection with NTHi which is evidence for lower inflammation in smokers after infection.

5.2.4 Changes in COPD HBECs post-infection with NTHi

COPD HBECs underwent several changes post-infection with NTHi. One change observed was the upregulation of inflammatory factors. *TNFRSF1B*, which codes for a gene for a TNF receptor, was significantly upregulated post-infection with NTHi which may increase TNF mediated signaling on HBECs. Evidence for TNFα mediated signaling increasing comes from the TNFα inducible protein (TNFAIP) 1,5 (More commonly named PTX3), and 6 were significantly upregulated post-infection with NTHi. TNFAIP6, or TSG6, has been shown to have anti-inflammatory activity . TSG6 prevented LPS induced lung injury and inhibited the association of TLR4 with MyD88 thus preventing TLR4 signaling and expression of pro-inflammatory cytokines[309]. TNFAIP1 has also been shown to inhibit inflammation and have anti-apoptotic activity and can induce the production of MMP2[310]. PTX3 on the other hand, has been shown to mediate inflammation and in some contexts has been shown to be important fight infections. For example, a study on OVA mice which are often an asthmatic model in mice, showed that PTX3 promoted inflammation and airway hyperresponsiveness in the lungs[311]. *MAP3K8*, which mediates LPS induced signaling and pro-inflammatory cytokine production was also upregulated in COPD HBECs after infection with NTHi[312]. The cytokine *IL20* was upregulated in NTHi infected COPD HBECs. Treating cells with IL20 have been demonstrated to significantly increased the production of pro-inflammatory cytokines, MMP1 and 9, and increased MMP activity[313]. These data were also shown again in the context of *S. pneumoniae* infection where neutralizing IL-20 abrogated inflammation[314]. The study also demonstrated that IL-20 limited bacterial clearance and neutralizing IL-20 decreased bacterial load. Another study demonstrated that IL20 significantly increased production of MMP2 and MMP9 and mediate ERK signaling by increasing the phosphorylation of ERK[315].

This shows that there are multiple TNFAIPs induced with various functions induced by NTHi with both inflammatory and anti-inflammatory activity. Whether or not the anti-inflammatory TNFAIPs have their activity blunted due to desensitization or some other signaling defect or that their activity is insufficient to curtail chronic inflammation in COPD is yet to be studied. Interestingly, the gene for the transcription factor *IRF1,* was also upregulated and it functions by transcribing ISGs following type I and type III IFN signaling.

There were also genes other than *IL20* that were involved in ECM regulation and production that were upregulated post-infection with NTHi. *DDR2,* which was also upregulated, has been shown to be activated by ECM proteins like collagen and can upregulate the production of MMP1 and MMP13[316,317]. Interestingly *E2F8*, which has been associated with EMT and cell proliferation, was significantly downregulated post-infection with NTHi[318]. Thus, COPD HBECs seem to upregulated several pro-inflammatory and ECM regulatory factors post-infection with NTHi indicating that there is high inflammation. However, there are also anti-inflammatory factors such as TSG6 but they are also regulated by pro-inflammatory cytokines such as TNFα, and their activity may not be sufficient to regulate excessive inflammation as we will see that NTHi infected COPD HBECs are more inflammatory than infected health HBECs.

Compared to NTHi infected healthy HBECs, infected COPD HBECs had many DEGs that were significantly higher including several uncategorized genes. Inflammatory genes such as *IL20, TNFRS1B,* and *PTX3* were still higher in infected COPD HBECs compared to infect healthy HBECs as well as other genes involved in the inflammatory pathway such as *TNFAIP6. TNFRS25,* named Apo-3 as well, was also higher in COPD HBECs compared to infected healthy HBECs and it has previously been shown to be able to activate NFκB and apoptosis[319]. The type 17 cytokine *IL17C* was significantly

higher in COPD HBECs than infected healthy HBECs. IL17C is an inflammatory cytokine that can induce the production of cytokines such as CXCL8 which induces the recruitment of leukocytes including neutrophils as well as inducing AMP production. A study by Vella et. al demonstrated that NTHi can significantly upregulate the production of IL-17C and other pro-inflammatory cytokines in mice which is abrogated in IL-17C deficient mice. In addition, they showed that severe COPD patients had significantly higher production of IL-17C in their sputum potentially because NTHi colonizes the airways of COPD patients[320]. *C1R* was also higher in COPD HBECs and is a gene that forms a part of the complement system and initiates the complement pathway. Activation of this pathway results in bacterial killing and opsonization by leukocytes such as macrophages.

In terms of cytokine receptors, *IL1RL2* and *IL11RA* were significantly higher in COPD HBECs post-infection than healthy HBECs. The increase in receptors may indicate that there is a higher amount of signaling of the their respective cytokine through the receptors. IL-11 is part of the IL-6 family of cytokines and can also induce the phosphorylation of STAT3 but can also mediate ERK signaling as well[321]. IL-11 is also significantly higher in the epithelium of severe asthmatic patients and can induce fibrosis in the lungs[322,323]. IL-1RL2 forms parts of the receptor complex for IL-36 which is an inflammatory cytokine and IL-1RL2 can also be a receptor for IL-1 cytokines. IL-36 has also been shown to be able to induce innate anti-viral immunity pathways through IRF1 which was also upregulated post-infection in COPD HBECs[324]. However in a chronic inflammatory environment such as what is found in COPD the ability to mediate innate anti-viral immunity may be blunted due to chronic desensitization. This in turn may hinder the ability for COPD patients to fight viral infections such as RVs as

they would be colonized by NTHi which has induced a blunted response due to a chronic infection.

There were also genes involved in the innate anti-viral pathway that were significantly higher in NTHi infected COPD HBECs than infected healthy HBECs. *IRF9* was significantly higher for example and it functions as a co-factor of phosphorylated STAT1 and STAT2 in order to mediate the transcription of ISGs. However, *SOCS1* was also significantly higher in infected COPD HBECs. SOCS1 is a phosphatase that is capable of dephosphorylating STAT1 and STAT2 and thus inhibits their activation and production of ISGs[325]. Inhibition of ISG production can facilitate viral infection and increase viral load which what was found in fibroblasts that constitutively express SOCS1[326]. In COPD, this may have implications on the susceptibility of COPD patients to be infected with viruses such as RV and induce exacerbations due to their inability to mount a proper anti-viral immune response.

The anti-microbial protein *BPFIA1* was also higher in COPD HBECs and has been found to be able to decrease bacterial load during infection in bronchial epithelial cells and decrease lung inflammation in mice[327]. *PTGS2,* which can mediate the production of pro-inflammatory prostaglandins, was also significantly higher in infected COPD HBECs compared to infected healthy HBECs[328]. *ZBTB20* was also higher and has been shown to facilitate pro-inflammatory cytokine production by repressing the transcription of the NFκB repressor, IκBα[329].

The MMP regulating factor *DDR2* was also significantly higher in infected COPD HBECs as well as the metalloproteinase MMP3 indicating that significantly higher ECM degradation is occurring in COPD HBECs post-infection with NTHi . Several Zinc finger proteins (ZNFs) were also higher in COPD HBECs and they have each have a

myriad of functions from transcriptional regulation to modification and degradation of different proteins.

5.2.5 RV16 Infection did not induce any DEGs in HBECs

Upon infection with RV16, there were no significant changes of HBECs in healthy, smokers, or COPD patients at monolayer cultures. This is also true when RV16 infected smoker and COPD HBECs were compared to infected healthy HBECs. This can be due to two factors. Firstly, the samples were sequenced at 24 hours and the biggest changes may occur at later timepoints such as 48 or 72 hours post-infections. Some studies have shown that IFN responses for example continue to grow up to 72 or 96 hours post-infection. In addition, this may be true in particular for RV16 as it has been shown that RV16 out of several RV strains tested elicited the weakest immune and IFN responses in HBECs upon infection and thus this may also be why no DEGs or immune responses were found[250]. Another study showed that different low doses of RV16 had similar copy number of RV16 24 hours post-infection[330]. Finally, the dose utilized in this study was 0.01 MOI which has been found to elicit a robust immune response in another study on RV infection of HBECs and has been shown to induce significant changes in previous a chapter. However, for the purposes of an RNA-seq experiment and with the number of samples sequenced it may have been too low of a MOI to capture any changes.

In differentiated HBECs, there were some changes that were induced in smoker HBECs upon infection with RV16 compared to infected healthy HBECs which include genes involved in fatty acid biosynthesis and regulation like *PNPLA3* and post-translational modifications such as *LARGE1*.

5.2.6 Limitations and further investigations

This chapter mainly focused on DEGs in HBECs of different groups and conditions and has produced a wealth of interesting and novel data to be looked at in COPD. However there are a few limitations to be pointed out. Firstly, the sample sizes in some conditions were low particularly in the differentiated samples mainly due to several samples not undergoing successful library preparation and differentiated COPD HBECs infected with RV16 did not make it through library prep either. While I attempted to mitigate that by having a large number of reads of 30M reads/sample which increases read depth and performing the analysis to take into account low sample sizes and outliers, the problem can still persist despite that and decrease data reliability and makes it difficult to identify outliers when group sizes are two or less.

Secondly, RV16 infection experiments did not detect meaningful changes in infected HBECs. There were no DEGs found in any condition with infected RV16 and thus it may be that either it was too early to detect any changes or that the dose was too low. As previously mentioned, RV16 in particular does not elicit as strong immune responses as other strains of RV despite a study by Mallia finding that it was possible to induce exacerbations after subjecting COPD patients with RV16[95].

Finally, while RNA-seq experiments are useful to assess DEGs between different conditions or groups and is able to give a wealth of data, it cannot fully assess or capture the changes and complexity of a biological system. Changes, or lack thereof, in a transcriptional context of RNA-seq does not necessarily translate well to changes in protein expression. In fact, the correlation between transcriptional changes and protein quantities are relatively weak to moderate. Another factor is that proteins can undergo a multitude of modifications that can change their structure and function from glycosylations to phosphorylations that are not necessarily reliant on changes in gene

expression. For example, while IRF3 was significantly upregulated in NTHi infected smoker HBECs, this does not necessarily mean that there were any functional changes as phosphorylation of IRF3 is required in order for it to exert its transcriptional function. Further investigations would be required to assess whether the gene expression changes are impacting functional changes within the cell by protein measurements and functional studies such as by measuring protein levels of different ISGs and TNFα inducible proteins in HBECs. Staining for the phosphorylation for STAT1 or IRF3 in HBECs on a Western blot can also be done to assess whether the changes from our RNA-seq experiments can be translated to their functional role as well.

Chapter 6: Concluding Discussion

6.1 Summary

The current body of work attempted to elucidate several different aspects on epithelial cell function in COPD. Comparisons were made to healthy HBECs as well as to smoker HBECs as it is the biggest risk factor in causing COPD and it can potentially inform us of a transition from a healthy epithelium to the epithelium of COPD patients. Firstly, the innate immune and anti-viral response were investigated in the three groups of HBECs in response to infection. It should be noted that no significant changes on a protein level were induced at an early four hour timepoint. NTHi induced a concentration-dependent increase of TNFα secretion particularly in COPD and healthy HBECs in basal cultures at 24 hours with TNFα having the highest concentration in COPD HBECs despite not being significantly higher than the healthy or smoker epithelial cells. GM-CSF however remained unchanged with all stimulations with the exception of poly I:C were GM-CSF was upregulated in all three groups but was only significant in smokers. Concentrations in COPD HBECs also appeared to have the highest concentrations after poly I:C stimulation. In terms of alarmins, smokers and COPD HBECs had significantly higher levels of IL-25 post-infection with NTHi in basal cultures depending on the dose utilized. Under RV16 infection however, healthy HBECs seemed to have the higher IL-25 concentrations although it should be noted that IL-25 levels were generally low. There was a concentration-dependent increase in TSLP concentrations post-infection in HBECs particularly in smokers and it was also regulated after poly I:C stimulation of healthy and COPD HBECs though not significantly. IL-33 was generally undetectable in all groups and conditions however it was still detectable in cell lysates indicating it is present but hasn't been

secreted. Finally type I and type III IFNs were measured in HBECs. No response was observed to LPS stimulation however COPD HBECs secreted significantly higher IFNλ1 than healthy HBECs post-infection with NTHi. Interestingly, while NTHi infection decreased IFNβ1 production in healthy HBECs, the trend was broken in COPD and healthy HBECs with IFNβ1 levels starting to increase from a MOI of 10 onwards. This may indicate that a negative feedback mechanism is dysfunctional in COPD and smoker HBECs at higher doses of NTHi. In response to poly I:C, type I and type III IFNs were significantly upregulated in healthy and COPD HBECs but not in smokers where there was no upregulation, and they were significantly lower than healthy and COPD HBECs. RV16 did not elicit IFNβ1 production in all three groups however while healthy HBECs maintain similar levels of IFNβ1, smoker and COPD HBECs had decreased levels of IFNβ1 indicating that RV16 is able to more efficiently inhibit or evade immunity in those two groups. IFNλ1 secretion was less affected however with secretion increasing concentration-dependently in healthy HBECs but not in smokers which had significantly lower levels. In terms of IFNRs, there were no changes found in any of the three groups post-infection with NTHi or RV16 with the exception of healthy HBECs where the higher affinity IFNAR2 was upregulated post-infection with RV16 as well as the ISG OAS1. This may indicate that health HBECs have a more robust IFN signalling pathway than smoker or COPD HBECs even at low doses of RV16.

In **Chapter 4**, the tight junctions in COPD HBECs were investigated to assess barrier changes in COPD compared to healthy and smoker HBECs. Interestingly, no changes were found in TER in any of the three groups under any stimulation indicating that changes may be functional or that TJ molecules are not playing a role in barrier integrity. CLDN-3, CLDN-4, and JAM-A in particular were studied as they are TJs that

have relatively higher expression in the lungs. Smoker and COPD HBECs had significantly higher levels of the TJ proteins under basal levels than healthy controls and all three groups did not response to either LPS or poly I:C stimulation. Post-infection with either NTHi or RV16 significantly upregulated CLDN-3, CLDN-4, and JAM-A in healthy HBECs indicating that TJ molecules are responsive during an infection in healthy HBECs. COPD HBECs however were unresponsive post-infection and in fact smoker HBECs downregulated CLDN-3 and JAM-A in particular post-infection indicating defective signalling or an increase in cell death in smoker HBECs compared to the healthy or COPD groups. Spatially, COPD and smoker HBECs had a phenotype under unstimulated conditions that resembled healthy HBECs post-infections indicating that COPD and smoker HBECs are behaving like they are infected in basal conditions. Some of those spatial characteristics are in fact mitigated during poly I:C stimulation or RV16 infection indicating that a negative feedback loop may be triggered due to excessive stimulation compared to when they are unstimulated. The spatial characteristics of the TJ proteins are listed in **Table 6.1** Protein expression however with gene expression with only CLDN-3 being upregulated post-infection with RV16 in healthy HBECs indicating that TJ regulation may be primarily translational or post-translational. ZO-1 however seemed to be downregulated in smoker HBECs and upregulated in COPD HBECs post-infection with NTHi but it is unclear if gene expression would translate well to protein expression.

Tight Junction Protein		Claudin-3			Claudin-4			JAM-A		
		H	S	C	H	S	C	H	S	C
Unstimulated	Diffused	++	-	-	++	-	-	++	-	-
	Polarized	-	++	+	-	++	++	-	++	++
	Clustered	-	++	+	-	+	+	-	++	++
LPS	Diffused	-	++	-	-	-	-	-*	-*	-*
	Polarized	++	+	++	++	+	+	++	-	+
	Clustered	++	-	+	+	-	-	++	-	+
NTHi	Diffused	-	-	-	-	-	+	-	-*	-*
	Polarized	++	++	++	++	++	-	++	++	++
	Clustered	++	++	++	+	+	-	++	++	++
Poly I:C	Diffused	-	++	++	-	+	+	-	+*	-*
	Polarized	++	-	+	+	-	-	++	+	-
	Clustered	++	-	-	+	-	-	++	-	-
RV16	Diffused	-	++	++	-	++	-	-	-	-
	Polarized	++	-	+	++	-	+	++	-	+
	Clustered	++	-	-	-	-	-	++	-	-

Table 6.1: Summary of spatial changes of TJ proteins CLDN-3, CLDN-4, and JAM-A in HBECs under different conditions. ++: Strong/Very strong, +: Moderate, - : Little/none. H; Healthy, S: Smokers, C: COPD. *: Localization at intercellular junctions observed for JAM-A.

In **Chapter 5**, an RNA-seq experiment was performed and analyzed on all three HBEC groups post-infection with NTHi or RV16 in basal or differentiated cultures. It was observed that monolayer and ALI cultures were drastically different from each other indicating that careful interpretation of the results need to be taken from experiments with each culturing model.

Infection with NTHi induced the greatest change in HBECs particularly in monolayer cultures and in smoker and COPD HBECs. Smoker HBECs upregulated several ISGs and anti-viral genes upon NTHi infection but few pro-inflammatory genes compared to healthy HBECs. This may indicate that smoker HBECs form an untargeted response against NTHi and potentially other bacterial infections because while the anti-viral response may be important in a bacterial infection, the induction of pro-inflammatory cytokines are also important for leukocyte recruitment. In addition, in differentiated cultures smoker HBECs had significantly lower inflammatory genes post-infection with NTHi such as *IL-33* and *IL-36G*. In COPD HBECs, NTHi induced a significantly greater inflammatory response than NTHi infected healthy HBECs with several TNFAIPs upregulated in COPD HBECs. This indicates that COPD HBECs are more susceptible to an exaggerated inflammatory response upon bacterial infection. RV16 did not induce many significant changes in all three groups indicating that RV16 can efficiently evade any immune responses or that the dose was too low or the timepoint too early to capture any changes. Of course all the data for **Chapter 5** can only be discussed in the context of gene expression. The picture that may emerge in terms of functional protein expression may potentially be different and the current data shown in this thesis are summarized in **Figure 6.1**.

6.2 Future Investigations

The current thesis has demonstrated several insights into the epithelium and differences in epithelial cells from COPD patients compared to healthy controls and smoker epithelial cells as well as they are the largest risk factor for causing COPD. While I believe that the insights uncovered were valuable, in several instances it opened up more questions than answers that can be pursued for a more granular picture of what is occurring in COPD.

The innate anti-viral immune response is a complex regulatory network with many proteins playing a role in media or negatively regulating IFN responses. Post-translational modifications such as phosphorylation and ubiquitination are important to regulate anti-viral responses. For example, IRF3 needs to be phosphorylated in order to translocate to the nucleus and induce IFN production and STAT1 needs to be phosphorylated in order to induce ISG production. Alarmins such as IL-33 also signal through ERK and phosphorylation of ERK and indeed IFNλ has been shown to mediate TSLP production and thus alarmins may be able to regulate anti-viral responses as well[331]. Studying anti-viral and host response regulation in HBECs may uncover more specific therapeutic targets that can be developed to mitigate any dysregulated responses.

Tight junction proteins can have several relevant functions such as mediating neutrophil recruitment through JAM-A. The regulation of TJs has not been extensively studied and it is thought that there are several pathways to regulating them including through pro-inflammatory cytokines. The data in **Chapter 4** showed that TJ molecules were spatially similar in smoker and COPD HBECs when unstimulated to when healthy HBECs were infected. Experiments exploring why TJ proteins in unstimulated COPD and smoker HBECs have this ‘infected’ phenotype would be an interesting path to

explore and whether their phenotype can be reverted to how TJ localize in healthy HBECs.

In **Chapter 5,** it was shown that the ALI model of epithelial cell culture varied greatly to the model of monolayer cell culture. This could mean that going forward ALI cultures should be more of the norm as they are differentiated epithelial cells despite more difficulty with differentiating HBECs than culturing them basally. Differentiated cultures can then undergo single cell RNA-seq to assess gene expression for different epithelial subtypes such as goblet cells and examine the immune response between groups and conditions.

The current thesis demonstrates that epithelial cells are functioning differently in COPD HBECs than healthy HBECs. In addition, smoker HBECs exhibit similarities and differences between COPD HBECs depending on what is being measured or investigated leading me to believe that COPD HBECs are phenotypically distinct to smokers. Differences were observed between healthy, smoker, and COPD HBECs in immune and anti-viral responses as well as in TJ protein localization and expression. Interactions between epithelial cells and other cell types that have prominent roles in COPD such as neutrophils need to also be examined through co-culture models and whether neutrophils can prime COPD epithelial cells for inflammation more than healthy epithelial cells for example. In addition, a co-infection models where HBECs are infected with RV and then NTHi can also be investigated for any host response differences as previous studies on epithelial cells have shown that co-infection can significantly change immune responses[176,332]. Further investigations need to be undertaken to elucidate mechanistic differences between the three groups in order to develop targets that more holistically target a complex disease like COPD. The hypothesis outlined at the beginning of the thesis was that HBECs were dysregulated

in terms of their barrier function and immune responses in the context of an infection. Indeed, as I have demonstrated, COPD HBECs were dysregulated in both aspects and thus the hypothesis can be accepted.

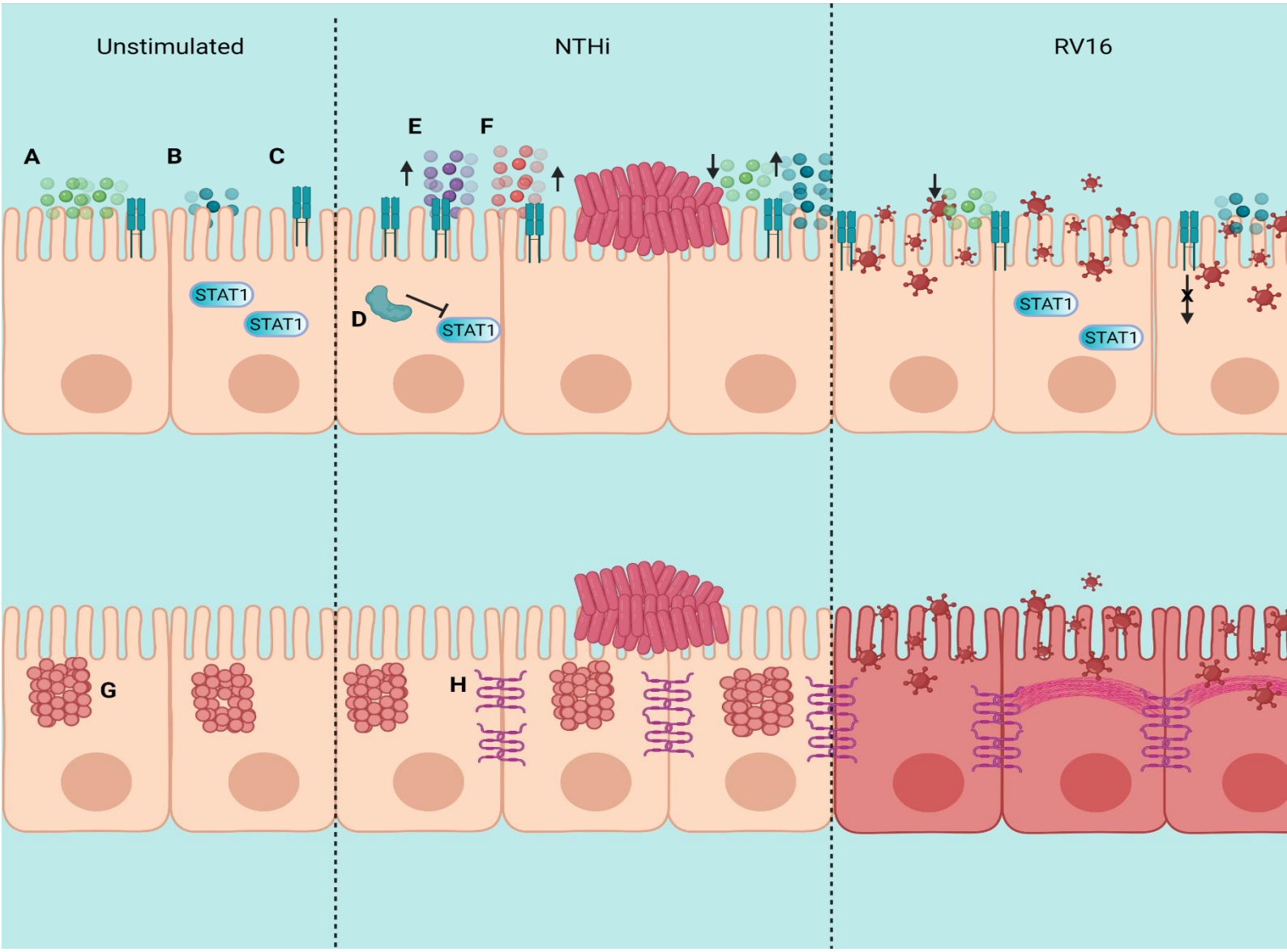


Figure 6.1: Changes observed in the HBECs of COPD patients. *Top Panel: Innate immune responses in COPD HBECs.* ***(A)*** *IFNβ1 decreased post-infection to either NTHi or RV16 indicating a dysfunction anti-viral response however* ***(B)*** *IFNλ1 was upregulated post-infection with NTHi but not with RV16.* ***(C)*** *IFNAR2 was upregulated post-infection with RV16 in healthy but not COPD HBECs indicating decrease IFN signalling and* ***(D)*** *SOCS1 expression was also higher than healthy HBECs which inhibits IFN signalling through dephosphorylation of STATs such as STAT1.* ***(E)*** *The alarmins TSLP and IL-25 but not IL-33 were upregulated after infection with NTHi but not with RV16 and* ***(F)*** *Pro-inflammatory mediators such as TNFα and TNFα inducible proteins were also upregulated post-infection with NTHi but not with RV16 demonstrating higher inflammation in COPD. Bottom Panel: Tight Junction Proteins in COPD HBECs.* ***(G)*** *TJ proteins CLDN-3, CLDN-4, and JAM-A were polarized and clustered on the surface of the epithelial cells of smoker and COPD HBECs at basal conditions and with NTHi infection but TJ proteins were unchanged showing a lack of responsiveness in COPD. However, TJ proteins then diffused across the cell surface with a little polarization in COPD HBECs when infected with RV16.* ***(H)*** *JAM-A was able to localized at the intercellular junctions as well upon infection with either NTHi or RV16 and may be able to assist with neutrophil transmigration into the lungs. Transepithelial resistances however were unchanged in HBECs upon infection.*

Chapter 7: The Covid-19 Pandemic Effect On the Thesis and Research

The Covid-19 virus spread throughout the globe from January 2020 and caused the UK government to call for a complete lockdown from March 2020 to mitigate the amount of deaths and sustained pressure on the health service. The lockdown included the closing down of university facilities and research labs. Thus, I was unable to do any lab research for my thesis from March 2020 until August 2020 when the labs reopened. Despite reopening however labs remained at a third capacity which further restricted access to spend time in the lab to do research for my DPhil. In addition, recruitment for patient samples has completely halted since March 2020 and therefore I could not receive any more bronchoscopy samples to do research on and had to utilize the epithelial cells I have acquired beforehand. This unfortunately meant that I was unable to do all the experiments that I had planned and had to make the best of the time remaining for my three year DPhil project.

I would have generally liked to do more experiments to test and optimize different timepoints for my stimulations such as later timepoints at 48 or 72 hours as well as different doses during those timepoints. HBECs would have potentially responded differently over time or at different doses in terms of immune and anti-viral responses. TJ proteins may have also acted differently over time and changed their behavior and localization. The availability of cells was also a limiting factor on the expansion of different conditions.

For **Chapter 3**, more mechanistic studies investigating IFN signalling would have added a layer of complexity to the function of HBECs. Flow cytometry experiments to examine IFNRs on HBECs in healthy, smokers, and COPD patients in response to

infection were started but were not optimized in time for the end of the project. In addition, plans to do western blots on phosphorylated STAT1 and phosphorylated IRF3 were planned in order to look at IFN signaling activation in response to infection and stimulation.

For **Chapter 4**, I would have spent more time trying to grow and stain differentiated HBECs to see if there were any changes in TJ expression or investigated spatial changes. In addition, investigating the migration of neutrophils through a transwell with or without JAM-A neutralizing antibodies in HBECs would also be pursued to examine if JAM-A blocking can inhibit neutrophil migration in COPD during an infection.

For **Chapter 5**, I would have attempted to increase the samples sizes for my RNA-seq experiment to give it more robustness and reliability. However this was difficult due to the halted recruitment of patients due to Covid-19 as well as the difficulty in growing up differentiated cultures. Polysomal fractionations on mRNA for sequencing were also attempted through myself doing work in collaboration with Rocio Martine Nunez at King's College London but the work was unable to continue after the beginning of lockdown on March 2020.

Appendix

Analyte	***LLOD (pg/ml)***	***ULOD (pg/ml)***
IFNλ1	1.2	18750
IFNβ1	3.1	48437.5
TSLP	0.2	3125
IL-33	0.59	9218.75
IL-25	0.58	9062.5
TNF-α	0.51	7968.75
GM-CSF	0.12	1875
IFN-α2a	4	62500

Table S1 : Lower and upper limits of detection for the analytes measured using the multiplex MSD platform.

Polysomal Fractionation

From 4 degrees, the 45% and 15% sucrose solutions were warmed to room temperature. The 15% sucrose solution was then pipette carefully into an ultracentrifuge tube until the halfway mark. The 45% sucrose solution was then injected slowly in the bottom of the ultracentrifuge tube going up slowly with the meniscus that separates both sucrose solutions until the tube is full. The ultracentrifuge tube is then carefully capped. The tube is then put on a rack and taken to the polysomal fractionation machine that is levelled and then tilts and spins the rack for 2 min until a 15%-45% sucrose density gradient is formed. Sucrose gradient is carefully put at 4 degrees until required.

Gradient tube is carefully put into an ultracentrifuge bucket on ice. 250ul of the lysed samples are inserted into the tube slowly by pipetting into the tube sideways. Ultracentrifuge buckets are weighed to ensure balance and slowly hooked onto the rotor. Samples are then ultracentrifuged at 40,000g for 1:25 h at 4 degrees.

Following ultracentrifugation, the buckets are carefully removed and put on ice. The tube is then put under the polysomal fractionation machine to allow the reading of different polysomal fractions into different tubes.

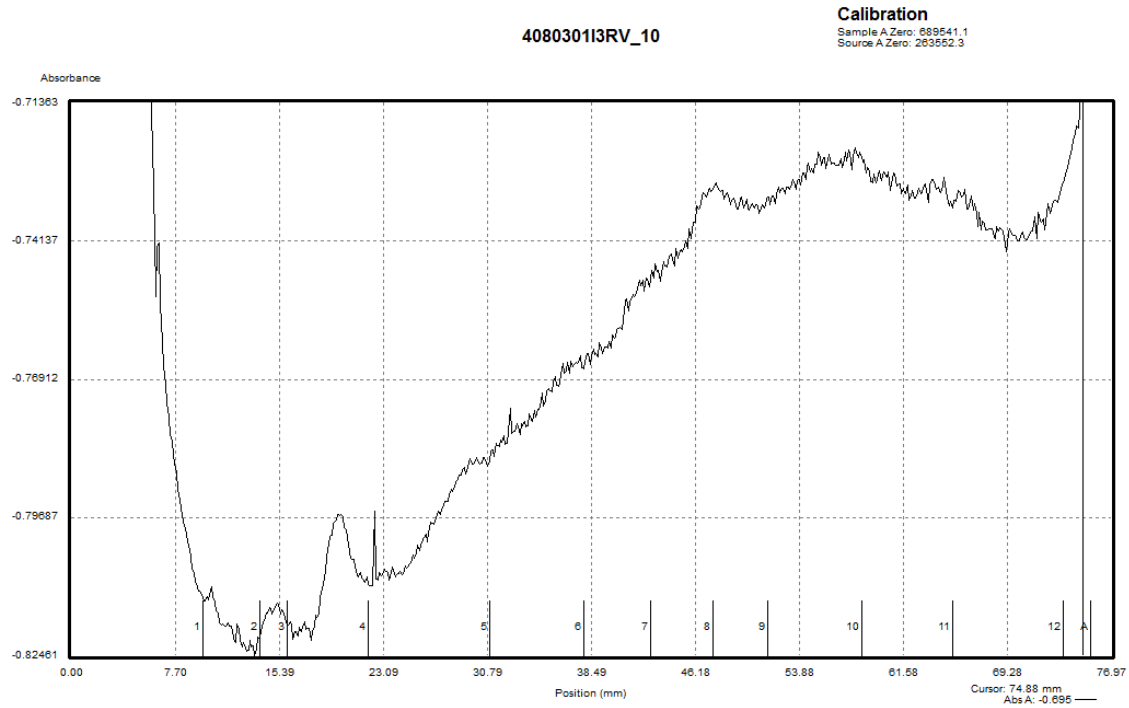


Figure S1: Graph of a polysomal fractionation from a gradient with each number showing a fraction.

HGNC_symbol	log2FoldChange	pvalue
XAF1	6.358619	1.34E-08
IFI6	5.901783	1.17E-07
ISG15	5.654756	3.91E-11
IFI44	5.036859	5.78E-07
CXCL10	4.915933	5.66E-06
CXCL11	4.782156	2.82E-07
OAS1	4.739722	1.61E-07
IFIT3	4.73961	7.19E-07
EPSTI1	4.737432	1.85E-07
IFI35	4.501078	8.02E-09
DDX60	4.496758	3.28E-07
OAS2	4.398773	3.87E-09
IRF7	4.382843	8.73E-11
IFITM1	4.002182	1.30E-05
HERC6	3.908812	8.76E-09
ETV7	3.880447	1.15E-07
DDX60L	3.808552	5.33E-09
HSH2D	3.74083	1.86E-08
DDX58	3.622924	6.73E-08
TRIM22	3.54103	6.42E-09
MMP13	3.483006	1.87E-05
NLRC5	3.449628	5.10E-06
STAT1	3.43206	2.47E-13
SLC15A3	3.374453	2.60E-05
OAS3	3.368703	4.27E-06
USP18	3.312652	1.94E-07
PARP9	3.269134	2.04E-07
BST2	3.225401	4.03E-05
SAMD9L	3.220642	1.25E-06
BATF2	3.166028	7.51E-06
DHX58	3.161842	4.07E-07
IFIH1	3.064	1.72E-06
UBE2L6	3.061985	2.18E-06
PSMB9	3.033051	1.22E-05
HELZ2	2.997139	4.69E-07
LGALS9	2.761304	2.17E-05
SAMHD1	2.732016	1.02E-05
PARP14	2.693799	7.58E-06

PLSCR1	2.507221	1.37E-07
BISPR	2.280613	0.0001
TAP1	2.266426	6.89E-08
HLA-F	2.249727	2.66E-05
LY6E	2.189839	5.85E-12
PARP10	2.005912	2.96E-06
SHFL	1.96888	6.19E-06
NMI	1.901884	7.95E-06
SP100	1.745846	3.58E-06
SP110	1.645532	7.68E-05
TRIM14	1.539091	2.42E-05
TRIM69	1.38792	7.21E-05
SHISA5	1.306336	4.32E-10
GMPR	1.276095	0.000225
EIF2AK2	1.253256	7.97E-05
TYMP	1.229522	0.000131
RTP4	1.081418	0.000335
IFI27	1.068002	0.000374
CMPK2	1.021903	0.000229
TRIM5	1.015323	2.15E-05
DTX3L	0.865377	0.0002
UNC93B1	0.825881	8.13E-05
PSMB10	0.817349	0.000138
CMTR1	0.682565	5.80E-05
SAMD9	0.575989	0.00048
TRIM21	0.430698	0.000369
CYP3A4	-1.01391	1.34E-05

Table S2: DEGs for NTHi infected smokers vs. unstimulated smokers

hgnc_symbol	log2FoldChange	pvalue
XAF1	4.996664	2.22E-07
CXCL11	4.598639	6.08E-08
ISG15	4.48676	1.13E-08
HSH2D	4.076801	9.12E-11
OASL	4.058161	6.05E-06
OAS2	4.00541	8.38E-09
IFI35	3.987187	3.43E-08
IRF7	3.986419	2.99E-10
HERC5	3.956211	4.74E-06
IFI6	3.95099	6.91E-06
DDX60	3.911195	1.01E-06
ATP10A	3.837354	4.00E-06
LGALS9	3.753268	1.43E-07
OAS1	3.714295	3.35E-06
EPSTI1	3.598747	5.16E-06
HERC6	3.54317	2.63E-08
DHX58	3.463334	4.88E-09
IFIT3	3.345215	1.46E-05
HELZ2	3.245061	9.30E-09
ETV7	3.216859	6.76E-07
IFIT2	3.097003	2.57E-05
STAT1	3.080943	5.57E-12
SAMD9L	2.99019	1.62E-06
USP18	2.974489	6.10E-07
IFI44	2.943187	3.33E-05
IFIH1	2.834225	2.52E-06
BATF2	2.674908	1.96E-05
DDX60L	2.668657	6.17E-06
OAS3	2.646353	2.32E-05
ERAP2	2.461338	5.50E-05
TRIM22	2.438407	8.63E-06
TYMP	2.374465	1.24E-05
PARP9	2.362336	1.57E-05
HLA-F	2.350705	2.02E-05
EIF2AK2	2.298251	2.26E-06
PARP14	2.21379	2.82E-05
TRIM14	2.139351	5.25E-07
DDX58	1.969285	5.99E-05

TNFSF13B	1.962425	0.000108
PLSCR1	1.960757	6.99E-06
LY6E	1.946321	1.97E-10
IFITM1	1.941488	0.000126
PARP10	1.7562	1.06E-05
NLRC5	1.732006	0.000135
UNC93B1	1.68033	2.39E-06
TRIM5	1.531765	1.70E-07
LAMP3	1.504684	0.000221
TAP2	1.374575	5.15E-05
GMPR	1.261238	0.00029
SP100	1.255735	4.15E-05
SAMD9	1.217643	0.000209
SHISA5	1.180896	5.01E-09
TAP1	1.09585	8.86E-05
IRF9	1.019522	0.000362
ZNF385C	1.008366	0.000373
SP110	0.935218	0.000356
UBE2L6	0.780341	0.000498
TRIM69	0.752303	0.000378
NMI	0.718508	0.000285
PNPT1	0.677661	0.000454
SHFL	0.638866	0.000355
XIST	-0.15462	4.32E-06
CYP3A4	-0.15826	0.000262
HAS2	-0.67799	0.000449
H2BC5	-0.85288	0.000411
REPS2	-1.00028	0.000219
ROR1	-1.25688	0.000319
FAM172A	-1.26911	3.31E-05
COL8A1	-1.27091	0.00025
ERO1B	-1.40635	0.000224
CERK	-1.48132	2.52E-06
H2AC6	-1.68127	0.000118
MTURN	-1.68777	1.83E-06
ANXA10	-2.45065	6.12E-05
TNFRSF10D	-2.84019	2.82E-05

Table S3: DEGs between NTHi infected smokers vs NTHi infected healthy HBECs

HGNC Symbol	log2FoldChange	pvalue
RPL3P4	1.672144	4.78E-05
LPCAT3	1.351563	6.44E-06
MORN4	0.717605	0.000186
FOLR3	-0.25981	0.000434
SLAMF9	-0.30175	0.000265
H19	-0.37995	0.000166
EIF4A1	-0.45722	0.000454
KRTAP2-3	-0.46195	0.00048
GJC1	-0.50417	0.000377
LY6D	-0.51235	0.000491
NEK6	-0.6475	0.000204
CSF3	-0.65537	7.15E-05
	-0.69782	0.00019
UBA6	-0.73569	0.000247
RIC1	-0.77336	8.91E-05
FSTL3	-0.79508	0.000498
FSCN1	-0.79776	0.000377
MN1	-0.81743	0.000443
ITGA6	-0.8722	0.00039
VCAN	-0.89404	0.000415
SPHK1	-0.90286	0.000427
CLCA2	-0.95359	0.000345
FRMD6	-0.9775	0.000217
ZBED2	-1.00439	0.000344
MCAM	-1.06026	0.000313
CORO1C	-1.06132	9.19E-05
CLMP	-1.0988	0.000214
TNC	-1.11776	0.000281
IL1RN	-1.12794	0.00027
MXD1	-1.15017	0.000114
SLC13A5	-1.21868	5.42E-05
ANXA8	-1.26697	0.000168
CCBE1	-1.30541	5.54E-05
EFNB1	-1.34844	6.37E-05
MYOSLID	-1.42185	0.000162
ADGRF4	-1.44256	9.04E-05

GJA1	-1.46807	5.69E-05
TGFB1I1	-1.49795	5.58E-05
INKA1	-1.50675	0.000113
GJB6	-1.52215	0.00012
ELL2	-1.54622	2.88E-06
TRIM7	-1.59354	6.08E-05
BNC1	-1.68303	2.98E-05
MSN	-1.72293	4.20E-05
COL4A6	-1.76431	8.78E-05
ANXA8L1	-1.80705	7.08E-05
SOWAHC	-1.90026	2.23E-06
PKP1	-1.90427	7.56E-05
TP63	-1.91184	3.74E-05
NT5E	-1.98595	5.76E-05
CD44	-2.02773	1.94E-05
IL36G	-2.04161	1.70E-05
HTR7	-2.12432	1.90E-05
CA2	-2.13438	5.13E-05
CDH13	-2.20833	4.49E-05
FERMT1	-2.37768	2.87E-05
KCTD15	-2.7568	4.82E-06
GJB2	-2.75874	3.59E-06
TIMP3	-2.86265	1.16E-06
PID1	-2.99754	3.74E-06
KRT6A	-3.13057	9.39E-06
SERPINB2	-3.36385	1.71E-06
KRT5	-3.53725	7.85E-07
CA12	-3.68642	5.07E-07
NIPAL4	-4.35446	1.14E-07
IL33	-4.63211	1.10E-06
CXCL2	-4.69764	7.42E-07
XIST	-21.4737	7.86E-07
CRNN	-25.2502	1.10E-09
RPS14P4	-32.6473	1.06E-17
GATD3A	-33.0269	1.46E-09
C10orf99	-41.0401	3.14E-35

Table S4: DEGs in differentiated NTHi infected smokers vs. differentiated NTHi infected healthy HBECs.

HGNC Symbol	Log2FoldChange	pvalue
TNFAIP6	3.840531	3.57E-07
PTX3	3.167985	1.22E-06
CEBPB-AS1	2.226045	2.87E-07
IL20	2.115617	2.20E-05
DDR2	2.055703	2.41E-05
BTBD19	2.013981	1.59E-05
TTLL3	2.012053	3.99E-06
MAP3K8	1.940394	7.93E-06
ANKRD36	1.920314	6.51E-07
ZNF83	1.915909	2.61E-06
STAG3L5P	1.911062	2.41E-06
TNFRSF1B	1.891491	2.18E-05
SMG1P3	1.772393	9.80E-07
SLC7A7	1.766394	5.18E-05
IRF1	1.734972	6.41E-06
SMG1P1	1.686627	2.36E-05
C2orf66	1.635019	5.16E-05
IER3-AS1	1.631901	3.07E-05
SLC25A25-AS1	1.60171	5.97E-05
ANKRD36B	1.45145	7.84E-05
DLGAP1-AS2	1.420285	8.01E-05
KAZALD1	1.414425	1.74E-05
LINC01465	1.405167	0.000119
KDM7A-DT	1.358388	3.78E-05
ANKRD36C	1.326961	9.13E-05
PCNPP3	1.26342	0.000161
L3MBTL1	1.255797	7.45E-05
NPIPP1	1.222489	0.000136
RASD1	1.221798	0.000173
NPIPB4	1.214849	0.00016
RNF207	1.214387	0.000186
C15orf62	1.204531	0.000202
H1-0	1.170171	3.06E-05
SCAND2P	1.160533	6.95E-05
NMRAL2P	1.1241	0.000195
TNFAIP2	1.115672	0.000247

SDHAP1	1.070626	0.000118
CLUHP3	1.060867	0.000228
NPIPB5	1.049313	0.000193
CCT6P3	1.034311	0.000174
LENG8	1.033223	0.000123
MPP3	0.98433	0.000142
NBPF12	0.962714	3.70E-05
CROCCP3	0.895687	0.000426
DDX39B	0.891577	0.000115
NFKBIZ	0.886937	0.000434
STX11	0.884121	0.000379
C1RL-AS1	0.881569	0.000337
MIR29B2CHG	0.838933	0.000486
TNFSF15	0.828469	0.000499
LIF	0.817525	0.000423
FTX	0.785841	0.000337
AGAP6	0.767653	0.000459
MUC20-OT1	0.748334	0.000406
CHKB	0.640928	0.000387
RERG	0.467182	0.000415
ZNF814	0.444822	0.000381
ESRRA	0.14459	0.000309
APOA1-AS	-0.12263	0.000482
GSTM1	-0.19471	0.000266
E2F8	-1.48281	8.78E-05
LRRN1	-1.84468	3.99E-05
PLG	-2.05992	1.19E-05
ALDOB	-17.788	1.02E-09
AGXT	-18.2476	2.96E-07

Table S5: DEGs of COPD HBECs infected with NTHi vs unstimulated COPD HBECs

HGNC symbol	log2FoldChange	pvalue
HPD	18.93746	3.63E-07
TNFAIP6	7.12525	1.98E-09
PTX3	4.685111	5.52E-08
IL20	4.289368	6.99E-09
IGFL2-AS1	4.02772	7.49E-07
ST8SIA1	3.839705	2.91E-06
TNFRSF1B	3.616959	8.33E-06
ERAP2	3.598798	1.24E-06
KCNQ1OT1	3.585082	1.51E-11
PAIP1P1	3.575074	1.05E-05
SLFNL1-AS1	3.562611	3.59E-07
PRECSIT	3.539362	1.03E-05
MMP3	3.49149	1.63E-06
SLC7A7	3.484236	2.61E-07
N4BP2L1	3.398952	2.29E-06
RN7SL600P	3.390054	1.87E-05
NEAT1	3.33124	9.79E-08
SPOCK2	3.301361	2.45E-05
INE1	3.289387	4.71E-07
TMEM225B	3.252876	2.82E-05
TTLL3	3.249122	4.72E-10
L3MBTL1	3.183774	1.77E-11
PSMD6-AS2	3.164031	4.73E-06
ZNF385C	3.149546	3.55E-05
HSPE1P5	3.13729	3.90E-05
BPIFA1	3.137063	3.85E-05
CRYM	3.121603	1.80E-06
PHF24	3.104246	2.49E-05
IL17C	3.090992	4.07E-05
C1RL-AS1	3.090368	4.70E-10
ATP2A1	3.087482	4.48E-05
TRIM17	3.083249	6.66E-06
KIF17	3.069931	1.27E-05
LINC00342	3.062819	1.03E-06
ARHGAP27P1-BPTFP1-KPNA2P3	3.046549	1.00E-06
C1R	3.028454	9.74E-06
COLQ	3.016878	4.92E-05
LINC00685	2.929013	9.57E-06

SCIN	2.905027	3.74E-05
CLUHP3	2.903523	1.26E-08
FAM227A	2.900407	2.18E-05
MIR29B2CHG	2.898841	7.98E-07
PDXDC2P	2.875208	6.72E-06
TMPRSS11A	2.872897	6.81E-05
EGR3	2.870777	2.76E-05
SPRY4IT1	2.867032	7.79E-05
MALAT1	2.846266	7.38E-07
CATSPERB	2.845305	2.03E-07
C15orf62	2.819722	3.08E-05
CHDH	2.807038	8.38E-05
ST7-AS1	2.804609	6.41E-05
HERC2P9	2.790749	4.35E-06
PDE4DIPP2	2.770068	6.09E-06
C2orf66	2.761628	3.29E-06
STAC3	2.756136	2.86E-05
SNHG22	2.733307	1.54E-09
NBPF19	2.724339	5.72E-06
SLCO4A1	2.721985	1.72E-05
RASGEF1B	2.701176	1.07E-05
SMG1P5	2.698625	1.50E-06
ANKRD36B	2.689647	3.39E-07
SLC25A25-AS1	2.663997	2.05E-06
BTN2A3P	2.633039	1.51E-06
NPIPB3	2.614039	7.99E-06
STAG3L5P-PVRIG2P-PILRB	2.594117	8.24E-05
TNFRSF25	2.592764	4.19E-06
LENG8-AS1	2.578787	1.31E-06
STAG3L5P	2.525414	1.41E-07
ADAMTSL4-AS1	2.522831	9.33E-05
EBLN2	2.511881	4.30E-05
PTGS2	2.504573	6.20E-06
ANKRD36C	2.491181	2.94E-07
NPIPA1	2.479655	3.17E-06
SMG1P3	2.450184	5.35E-09
CEBPB-AS1	2.448269	1.41E-06
DDR2	2.42612	9.50E-05
GHRLOS	2.42582	7.20E-05

MIR23AHG	2.413953	2.58E-05
PABPC1L	2.40378	3.20E-07
CROCCP3	2.40268	5.08E-05
LIME1	2.361845	8.98E-05
DICER1-AS1	2.356449	2.82E-05
NPIPP1	2.339501	3.59E-06
CRYGS	2.339469	6.78E-05
NPIPB5	2.29686	6.89E-07
AGAP4	2.287127	1.75E-05
SMG1P1	2.264151	5.62E-06
AGAP6	2.262207	1.26E-06
KAZALD1	2.258063	4.16E-07
RSKR	2.252847	6.37E-06
PILRB	2.246076	7.82E-06
ANKRD36	2.230212	3.56E-07
CCT6P1	2.224943	2.96E-05
ZBTB20	2.220751	5.76E-06
NPIPB4	2.219393	1.27E-05
RAD51-AS1	2.197697	4.02E-07
BTBD19	2.159818	7.64E-05
SEPTIN7P13	2.146488	3.58E-05
GABRE	2.145426	1.26E-05
PPFIA4	2.13003	8.07E-05
SOCS1	2.128745	1.18E-05
NBPF12	2.114881	1.81E-05
FTX	2.109767	3.22E-07
SH3BP5-AS1	2.097212	5.58E-05
MIR222HG	2.090425	5.95E-05
ADAMTS13	2.088075	6.06E-05
EREG	2.061192	4.42E-05
NOTCH2NLA	2.027348	3.75E-06
GIPR	2.016462	7.67E-05
CLEC2D	1.951216	3.58E-05
SEPTIN7P2	1.947051	3.53E-07
LENG8	1.908613	6.00E-07
EP400P1	1.902428	2.90E-07
IL1RL2	1.892575	1.31E-07
CTC338M12	1.885575	1.36E-05
IL11RA	1.884945	4.84E-05

SLC16A1-AS1	1.882475	3.61E-08
CENATAC	1.854501	2.44E-05
SNHG12	1.848064	3.13E-06
MAP3K8	1.83166	9.46E-05
PKD1P6	1.82411	2.03E-05
MUC20-OT1	1.82186	7.55E-06
SCAND2P	1.793208	2.26E-06
DNHD1	1.787568	1.43E-05
KDM7A-DT	1.779935	7.71E-06
IRF9	1.753638	6.90E-05
LINC-PINT	1.74718	2.41E-05
GTF2IP20	1.732288	1.16E-05
CATSPER2	1.726088	2.97E-05
AFG3L1P	1.717104	1.28E-05
H1-0	1.696549	3.92E-07
CBX7	1.657743	8.97E-05
MMP25-AS1	1.644261	1.31E-05
DDX39B	1.62576	4.23E-07
MRPL45P2	1.600963	6.00E-05
WASH7P	1.547267	9.12E-05
SNHG17	1.547071	8.85E-05
CROCCP2	1.531389	2.01E-05
MPP3	1.481134	2.83E-05
C6orf141	1.447314	3.97E-05
AHSA2P	1.39882	6.63E-05
ZNF354B	1.378755	4.49E-05
CCNL1	1.328584	1.40E-05
GADD45A	1.313384	4.97E-05
SEPTIN7P14	1.3066	9.32E-05
RP9P	1.264261	1.46E-05
HDAC10	1.228813	6.34E-05
RDH13	1.227206	2.47E-05
PLA2R1	1.205822	6.03E-05
PVT1	1.193949	8.38E-06
GARS1-DT	1.189582	2.60E-05
ZNF692	1.126167	7.20E-05
ZNF276	1.089423	4.89E-05
BTN2A1	1.075417	2.61E-05
ZNF502	1.072993	3.42E-05

ZNF83	1.067485	1.69E-06
ANKRD13D	1.002166	4.49E-06
SNHG3	1.001486	8.28E-05
NUP50-DT	0.963813	1.81E-05
ZNF26	0.930696	3.08E-05
FNBP4	0.930135	8.28E-05
PNISR	0.924464	4.40E-05
USP36	0.916579	6.44E-05
CCNL2	0.897276	4.97E-05
ZNF44	0.846989	8.47E-05
KCTD13	0.843237	2.58E-05
ZBTB48	0.809183	3.42E-05
N4BP2L2	0.792246	1.05E-05
DDX55	0.788737	7.33E-06
ZNF839	0.758673	4.05E-05
TRIM39	0.709963	4.51E-05
ZNF274	0.595612	4.33E-05
MAPKAPK5	0.486438	4.00E-05
PSMF1	-0.43207	2.29E-05
CUL3	-0.48421	5.61E-05
CUL2	-0.52821	3.61E-06
DOCK7	-0.58077	6.00E-05
MTMR14	-0.59403	2.37E-05
HDAC1	-0.59488	3.24E-05
WARS1	-0.60336	9.09E-05
CHTF8	-0.65348	1.85E-06
TTI2	-0.69123	6.96E-05
LINC00857	-1.14938	2.43E-06
DH3	-1.64907	1.39E-05
IGFBP6	-2.48952	5.58E-05
LRRN1	-3.31756	5.39E-06
ANXA10	-3.34288	9.91E-09

Table S6: DEGs between NTHi infected COPD HBECs and healthy HBECs infected with NTHi.

References

1. Lozano, R. *et al.* Global and regional mortality from 235 causes of death for 20 age groups in 1990 and 2010: a systematic analysis for the Global Burden of Disease Study 2010. *Lancet (London, England)* **380**, 2095–2128 (2012).

2. Marcoa, R. *et al.* Classification of Chronic Obstructive Pulmonary Disease (COPD) according to the new Global Initiative for Chronic Obstructive Lung Disease (GOLD) 2017: Comparison with GOLD 2011. *COPD* **15**, 21–26 (2018).

3. Pallasaho, P., Kainu, A., Sovijärvi, A., Lindqvist, A. & Piirilä, P. L. Combined effect of smoking and occupational exposure to dusts, gases or fumes on the incidence of COPD. *COPD J. Chronic Obstr. Pulm. Dis.* **11**, 88–95 (2014).

4. Paulin, L. M. *et al.* Occupational exposures are associated with worse morbidity in patients with chronic obstructive pulmonary disease. *Am. J. Respir. Crit. Care Med.* **191**, 557–565 (2015).

5. *Global Strategy for the Diagnosis, Management, and Prevention of Chronic Obstructive Pulmonary Disease*. www.goldcopd.org (2020).

6. Schneider, D. *et al.* Increased cytokine response of rhinovirus-infected airway epithelial cells in chronic obstructive pulmonary disease. *Am. J. Respir. Crit. Care Med.* **182**, 332–340 (2010).

7. Bafadhel, M. *et al.* Airway bacteria measured by quantitative polymerase chain reaction and culture in patients with stable COPD: relationship with neutrophilic airway inflammation, exacerbation frequency, and lung function. *Int. J. Chron. Obstruct. Pulmon. Dis.* **10**, 1075–1083 (2015).

8. Bafadhel, M. *et al.* Acute exacerbations of chronic obstructive pulmonary disease: identification of biologic clusters and their biomarkers. *Am. J. Respir. Crit. Care Med.* **184**, 662–671 (2011).

9. Saha, S. & Brightling, C. E. Eosinophilic airway inflammation in COPD. *Int. J. Chron. Obstruct. Pulmon. Dis.* **1**, 39–47 (2006).

10. Green, R. H. *et al.* Asthma exacerbations and sputum eosinophil counts: a randomised controlled trial. *Lancet (London, England)* **360**, 1715–1721 (2002).

11. Bafadhel, M. *et al.* Blood eosinophils to direct corticosteroid treatment of exacerbations of chronic obstructive pulmonary disease: a randomized placebo-controlled trial. *Am. J. Respir. Crit. Care Med.* **186**, 48–55 (2012).

12. Pavord, I. D. *et al.* Mepolizumab for Eosinophilic Chronic Obstructive Pulmonary Disease. *N. Engl. J. Med.* **377**, 1613–1629 (2017).

13. Albert, R. K. *et al.* Azithromycin for prevention of exacerbations of COPD. *N. Engl. J. Med.* **365**, 689–698 (2011).

14. Parnham, M. J. *et al.* Azithromycin: mechanisms of action and their relevance for clinical applications. *Pharmacol. Ther.* **143**, 225–245 (2014).

15. Snell, N. *et al.* S32 Epidemiology of chronic obstructive pulmonary disease

(COPD) in the uk: findings from the british lung foundation's 'respiratory health of the nation' project. *Thorax* **71**, A20.1-A20 (2016).

16. Ciapponi, A. *et al.* The epidemiology and burden of COPD in latin America and the caribbean: Systematic review and meta-analysis. *COPD J. Chronic Obstr. Pulm. Dis.* **11**, 339–350 (2014).

17. Blanco, I. *et al.* Geographical Distribution of COPD Prevalence in the Americas. *COPD J. Chronic Obstr. Pulm. Dis.* **15**, 317–325 (2018).

18. Blanco, I. *et al.* Geographical distribution of COPD prevalence in Europe, estimated by an inverse distance weighting interpolation technique. *Int. J. COPD* **13**, 57–67 (2018).

19. Aaron, S. D., Gershon, A. S., Gao, Y., Yang, J. & Whitmore, G. A. Influence of country-level differences on COPD prevalence. *Int. J. COPD* **11**, 2305–2313 (2016).

20. Lõpez-Campos, J. L., Tan, W. & Soriano, J. B. Global burden of COPD. *Respirology* vol. 21 14–23 (2016).

21. Zhu, B., Wang, Y., Ming, J., Chen, W. & Zhang, L. Disease burden of COPD in china: A systematic review. *International Journal of COPD* vol. 13 1353–1364 (2018).

22. *Stemming the Rising Tide of Non-Communicable Diseases*.

23. Xu, G. *et al.* NSFC Health Research Funding and Burden of Disease in China. *PLoS One* **9**, e111458 (2014).

24. Wang, C. *et al.* Prevalence and risk factors of chronic obstructive pulmonary disease in China (the China Pulmonary Health [CPH] study): a national cross-sectional study. *Lancet* **391**, 1706–1717 (2018).

25. Ntritsos, G. *et al.* Gender-specific estimates of COPD prevalence: a systematic review and meta-analysis. *Int. J. Chron. Obstruct. Pulmon. Dis.* **13**, 1507–1514 (2018).

26. Zysman, M. *et al.* Relationship between gender and survival in a real-life cohort of patients with COPD. *Respir. Res.* **20**, (2019).

27. DeMeo, D. L. *et al.* Women manifest more severe COPD symptoms across the life course. *Int. J. COPD* **13**, 3021–3029 (2018).

28. Golpe, R. *et al.* Mortality in COPD patients according to clinical phenotypes. *Int. J. COPD* **13**, 1433–1439 (2018).

29. Asthma, COPD, and Asthma-COPD Overlap Syndrome - Global Initiative for Chronic Obstructive Lung Disease - GOLD. https://goldcopd.org/asthma-copd-asthma-copd-overlap-syndrome/.

30. Kerkhof, M. *et al.* Blood eosinophil count and exacerbation risk in patients with COPD. *European Respiratory Journal* vol. 50 (2017).

31. Bafadhel, M. *et al.* Blood Eosinophils and Outcomes in Severe Hospitalized Exacerbations of COPD. in *Chest* vol. 150 320–328 (Elsevier B.V., 2016).

32. Vedel-Krogh, S., Nielsen, S. F., Lange, P., Vestbo, J. & Nordestgaard, B. G. Blood eosinophils and exacerbations in chronic obstructive pulmonary disease: The copenhagen general population study. *Am. J. Respir. Crit. Care Med.* **193**, 965–974 (2016).

33. Couillard, S., Larivée, P., Courteau, J. & Vanasse, A. Eosinophils in COPD Exacerbations Are Associated With Increased Readmissions. *Chest* **151**, 366–373 (2017).

34. Yun, J. H. *et al.* Blood eosinophil count thresholds and exacerbations in patients with chronic obstructive pulmonary disease. *J. Allergy Clin. Immunol.* **141**, 2037-2047.e10 (2018).

35. Shin, S. H. *et al.* Serial blood eosinophils and clinical outcome in patients with chronic obstructive pulmonary disease. *Respir. Res.* **19**, (2018).

36. Xu, W., Li, R. & Sun, Y. Increased IFN-γ-producing Th17/Th1 cells and their association with lung function and current smoking status in patients with chronic obstructive pulmonary disease. *BMC Pulm. Med.* **19**, (2019).

37. Kunisaki, K. M. *et al.* Exacerbations of chronic obstructive pulmonary disease and cardiac events a post hoc cohort analysis from the SUMMIT randomized clinical trial. *Am. J. Respir. Crit. Care Med.* **198**, 51–57 (2018).

38. Butler, S. J., Ellerton, L., Goldstein, R. S. & Brooks, D. Prevalence of lung cancer in chronic obstructive pulmonary disease: A systematic review. *Respiratory Medicine: X* vol. 1 100003 (2019).

39. Yamada, K. *et al.* Impaired nuclear factor erythroid 2-related factor 2 expression increases apoptosis of airway epithelial cells in patients with chronic obstructive pulmonary disease due to cigarette smoking. *BMC Pulm. Med.* **16**, 27 (2016).

40. Snider, G., Kleinerman, J., Thurlbeck, W. & Bengali, Z. The Definition of Emphysema. *Am. Rev. Repiratory Dis.* **132**, 182–185 (1985).

41. Hochhegger, B. *et al.* Pulmonary Acinus: Understanding the Computed Tomography Findings from an Acinar Perspective. *Lung* vol. 197 259–265 (2019).

42. Barker, A. F. Alpha 1-antitrypsin-deficiency-related emphysema. *J. Am. Board Fam. Pract.* **5**, 489–93 (1992).

43. Guyot, N. *et al.* Unopposed cathepsin G, neutrophil elastase, and proteinase 3 cause severe lung damage and emphysema. *Am. J. Pathol.* **184**, 2197–2210 (2014).

44. Duan, M. C. *et al.* Infiltration of IL-17-Producing T Cells and Treg Cells in a Mouse Model of Smoke-Induced Emphysema. *Inflammation* **39**, 1334–1344 (2016).

45. Meng, X. M., Nikolic-Paterson, D. J. & Lan, H. Y. TGF-β: The master regulator of fibrosis. *Nature Reviews Nephrology* vol. 12 325–338 (2016).

46. Kim, V. & Criner, G. J. Chronic bronchitis and chronic obstructive pulmonary disease. *American Journal of Respiratory and Critical Care Medicine* vol. 187

228–237 (2013).

47. Georas, S. N. & Rezaee, F. Epithelial barrier function: at the front line of asthma immunology and allergic airway inflammation. *The Journal of allergy and clinical immunology* vol. 134 509–520 (2014).

48. Baraniuk, J. N. *et al.* Protein networks in induced sputum from smokers and COPD patients. *Int. J. Chron. Obstruct. Pulmon. Dis.* **10**, 1957–1975 (2015).

49. Chen, L. *et al.* Imbalance between subsets of CD8+ peripheral blood T cells in patients with chronic obstructive pulmonary disease. *PeerJ* **2016**, (2016).

50. Rogers, D. F. Mucus hypersecretion in chronic obstructive pulmonary disease. *Novartis Found. Symp.* **234**, 65–83 (2001).

51. Chen, G. *et al.* Foxa3 induces goblet cell metaplasia and inhibits innate antiviral immunity. *Am. J. Respir. Crit. Care Med.* **189**, 301–313 (2014).

52. Yaghi, A. & Dolovich, M. Airway Epithelial Cell Cilia and Obstructive Lung Disease. *Cells* **5**, 40 (2016).

53. Yonker, L. M. *et al.* Development of a Primary Human Co-Culture Model of Inflamed Airway Mucosa. *Sci. Rep.* **7**, 8182 (2017).

54. Kim, V. *et al.* The chronic bronchitic phenotype of COPD: An analysis of the COPDGene study. *Chest* **140**, 626–633 (2011).

55. Andersen, K. H. *et al.* Prevalence, predictors, and survival in pulmonary hypertension related to end-stage chronic obstructive pulmonary disease. *J. Hear. Lung Transplant.* **31**, 373–380 (2012).

56. Santos, S. *et al.* Enhanced expression of vascular endothelial growth factor in pulmonary arteries of smokers and patients with moderate chronic obstructive pulmonary disease. *Am. J. Respir. Crit. Care Med.* **167**, 1250–1256 (2003).

57. Wagner, P. D. The critical role of VEGF in skeletal muscle angiogenesis and blood flow. in *Biochemical Society Transactions* vol. 39 1556–1559 (Biochem Soc Trans, 2011).

58. Barberà, J. A. *et al.* Pulmonary vascular abnormalities and ventilation-perfusion relationships in mild chronic obstructive pulmonary disease. *Am. J. Respir. Crit. Care Med.* **149**, 423–429 (1994).

59. Aleva, F. E. *et al.* Prevalence and Localization of Pulmonary Embolism in Unexplained Acute Exacerbations of COPD: A Systematic Review and Meta-analysis. *Chest* **151**, 544–554 (2017).

60. BD, K., PD, M. & WT, M. Hypoxemia in patients with COPD: cause, effects, and disease progression. *Int. J. Chron. Obstruct. Pulmon. Dis.* **6**, 199–208 (2011).

61. Hoenderdos, K. *et al.* Hypoxia upregulates neutrophil degranulation and potential for tissue injury. *Thorax* **71**, 1030 LP – 1038 (2016).

62. Nishimura, M. Lessons for COPD from the GOLD 2017 report. *Respirology (Carlton, Vic.)* vol. 22 621 (2017).

63. Gorre, F. & Vandekerckhove, H. Beta-blockers: focus on mechanism of action. Which beta-blocker, when and why? *Acta Cardiol.* **65**, 565–570 (2010).

64. Trevethick, M., Clarke, N., Strawbridge, M. & Yeadon, M. Inhaled muscarinic antagonists for COPD--does an anti-inflammatory mechanism really play a role? *Curr. Opin. Pharmacol.* **9**, 250–255 (2009).

65. Ferguson, G. T. *et al.* Triple therapy with budesonide/glycopyrrolate/formoterol fumarate with co-suspension delivery technology versus dual therapies in chronic obstructive pulmonary disease (KRONOS): a double-blind, parallel-group, multicentre, phase 3 randomised controlled tr. *Lancet Respir. Med.* **6**, 747–758 (2018).

66. Yang, I. A., Shaw, J. G., Goddard, J. R., Clarke, M. S. & Reid, D. W. Use of inhaled corticosteroids in COPD: improving efficacy. *Expert Rev. Respir. Med.* **10**, 339–350 (2016).

67. Finney, L. *et al.* Inhaled corticosteroids and pneumonia in chronic obstructive pulmonary disease. *Lancet. Respir. Med.* **2**, 919–932 (2014).

68. Lipson, D. A. *et al.* Once-Daily Single-Inhaler Triple versus Dual Therapy in Patients with COPD. *N. Engl. J. Med.* **378**, 1671–1680 (2018).

69. Papi, A. *et al.* Extrafine inhaled triple therapy versus dual bronchodilator therapy in chronic obstructive pulmonary disease (TRIBUTE): a double-blind, parallel group, randomised controlled trial. *Lancet* **391**, 1076–1084 (2018).

70. Yang, I. A., Clarke, M. S., Sim, E. H. A. & Fong, K. M. Inhaled corticosteroids for stable chronic obstructive pulmonary disease. *Cochrane database Syst. Rev.* CD002991 (2012) doi:10.1002/14651858.CD002991.pub3.

71. Agusti, A. *et al.* Inhaled corticosteroids in COPD: friend or foe? *Res. Cent. Asthma COPD* doi:10.1183/13993003.01219-2018.

72. Siva, R. *et al.* Eosinophilic airway inflammation and exacerbations of COPD: a randomised controlled trial. *Eur. Respir. J.* **29**, 906–913 (2007).

73. Bafadhel, M. *et al.* Predictors of exacerbation risk and response to budesonide in patients with chronic obstructive pulmonary disease: a post-hoc analysis of three randomised trials. *Lancet. Respir. Med.* **6**, 117–126 (2018).

74. Brightling, C. E. *et al.* Benralizumab for chronic obstructive pulmonary disease and sputum eosinophilia: a randomised, double-blind, placebo-controlled, phase 2a study. *Lancet Respir. Med.* **2**, 891–901 (2014).

75. Criner, G. J. *et al.* Benralizumab for the Prevention of COPD Exacerbations. *N. Engl. J. Med.* NEJMoa1905248 (2019) doi:10.1056/NEJMoa1905248.

76. Ying, S. *et al.* Expression and Cellular Provenance of Thymic Stromal Lymphopoietin and Chemokines in Patients with Severe Asthma and Chronic Obstructive Pulmonary Disease. *J. Immunol.* **181**, 2790–2798 (2008).

77. Calvén, J. *et al.* Viral Stimuli Trigger Exaggerated Thymic Stromal Lymphopoietin Expression by Chronic Obstructive Pulmonary Disease Epithelium: Role of Endosomal TLR3 and Cytosolic RIG-I-Like Helicases. *J. Innate Immun.* **4**, 86–99 (2012).

78. Corren, J. *et al.* Tezepelumab in Adults with Uncontrolled Asthma. *N. Engl. J. Med.* **377**, 936–946 (2017).

79. Rennard, S. I. *et al.* The safety and efficacy of infliximab in moderate to severe chronic obstructive pulmonary disease. *Am. J. Respir. Crit. Care Med.* **175**, 926–934 (2007).

80. O'Dwyer, D. N., Dickson, R. P. & Moore, B. B. The Lung Microbiome, Immunity and the Pathogenesis of Chronic Lung Disease. *J. Immunol.* **196**, 4839 (2016).

81. Monsó, E. *et al.* Bacterial infection in chronic obstructive pulmonary disease. A study of stable and exacerbated outpatients using the protected specimen brush. *Am. J. Respir. Crit. Care Med.* **152**, 1316–20 (1995).

82. Sethi, S., Evans, N., Grant, B. J. B. & Murphy, T. F. New strains of bacteria and exacerbations of chronic obstructive pulmonary disease. *N. Engl. J. Med.* **347**, 465–471 (2002).

83. Patel, I. S. *et al.* Relationship between bacterial colonisation and the frequency, character, and severity of COPD exacerbations. *Thorax* **57**, 759–764 (2002).

84. Miravitlles, M. *et al.* Relationship between bacterial flora in sputum and functional impairment in patients with acute exacerbations of COPD. *Chest* **116**, 40–46 (1999).

85. Marin, A. *et al.* Effect of bronchial colonisation on airway and systemic inflammation in stable COPD. *COPD J. Chronic Obstr. Pulm. Dis.* **9**, 121–130 (2012).

86. Wang, Z. *et al.* Lung microbiome dynamics in COPD exacerbations. *Eur. Respir. J.* **47**, 1082–1092 (2016).

87. Kolsum, U. *et al.* Blood and sputum eosinophils in COPD; Relationship with bacterial load. *Respir. Res.* **18**, (2017).

88. Mayhew, D. *et al.* Longitudinal profiling of the lung microbiome in the AERIS study demonstrates repeatability of bacterial and eosinophilic COPD exacerbations. *Thorax* **73**, 422–430 (2018).

89. Rodrigo-Troyano, A. *et al.* Pseudomonas aeruginosa resistance patterns and clinical outcomes in hospitalized exacerbations of COPD. *Respirology* **21**, 1235–1242 (2016).

90. Rodrigo-Troyano, A. *et al.* Pseudomonas aeruginosa in chronic obstructive pulmonary disease patients with frequent hospitalized exacerbations: A prospective multicentre study. *Respiration* **96**, 417–424 (2018).

91. Kherad, O. *et al.* Upper-respiratory viral infection, biomarkers, and COPD exacerbations. *Chest* **138**, 896–904 (2010).

92. Seemungal, T. *et al.* Respiratory viruses, symptoms, and inflammatory markers in acute exacerbations and stable chronic obstructive pulmonary disease. *Am. J. Respir. Crit. Care Med.* **164**, 1618–1623 (2001).

93. Dimopoulos, G. *et al.* Viral epidemiology of acute exacerbations of chronic

obstructive pulmonary disease. *Pulm. Pharmacol. Ther.* **25**, 12–18 (2012).

94. George, Ŝ. N. *et al.* Human rhinovirus infection during naturally occurring COPD exacerbations. *Eur. Respir. J.* **44**, 87–96 (2014).

95. Mallia, P. *et al.* An experimental model of rhinovirus induced chronic obstructive pulmonary disease exacerbations: A pilot study. *Respir. Res.* **7**, (2006).

96. Mallia, P. *et al.* Experimental rhinovirus infection as a human model of chronic obstructive pulmonary disease exacerbation. *Am. J. Respir. Crit. Care Med.* **183**, 734–742 (2011).

97. Singanayagam, A. *et al.* Corticosteroid suppression of antiviral immunity increases bacterial loads and mucus production in COPD exacerbations. *Nat. Commun.* **9**, (2018).

98. Pettigrew, M. M. *et al.* Dynamic changes in the Streptococcus pneumoniae transcriptome during transition from biofilm formation to invasive disease upon influenza A virus infection. *Infect. Immun.* **82**, 4607–4619 (2014).

99. Karppinen, S. *et al.* Acquisition and transmission of streptococcus pneumoniae are facilitated during rhinovirus infection in families with children. *Am. J. Respir. Crit. Care Med.* **196**, 1172–1180 (2017).

100. Wark, P. A. B., Tooze, M., Powell, H. & Parsons, K. Viral and bacterial infection in acute asthma and chronic obstructive pulmonary disease increases the risk of readmission. *Respirology* **18**, 996–1002 (2013).

101. Wilkinson, T. M. A. *et al.* Effect of interactions between lower airway bacterial and rhinoviral infection in exacerbations of COPD. *Chest* **129**, 317–324 (2006).

102. Mallia, P. *et al.* Rhinovirus infection induces degradation of antimicrobial peptides and secondary bacterial infection in chronic obstructive pulmonary disease. *Am. J. Respir. Crit. Care Med.* **186**, 1117–1124 (2012).

103. Molyneaux, P. L. *et al.* Outgrowth of the bacterial airway microbiome after rhinovirus exacerbation of chronic obstructive pulmonary disease. *Am. J. Respir. Crit. Care Med.* **188**, 1224–1231 (2013).

104. Metcalfe, H. J. *et al.* Effects of cigarette smoke on Toll-like receptor (TLR) activation of chronic obstructive pulmonary disease (COPD) macrophages. *Clin. Exp. Immunol.* **176**, 461–472 (2014).

105. Chen, H., Cowan, M. J., Hasday, J. D., Vogel, S. N. & Medvedev, A. E. Tobacco Smoking Inhibits Expression of Proinflammatory Cytokines and Activation of IL-1R-Associated Kinase, p38, and NF-κB in Alveolar Macrophages Stimulated with TLR2 and TLR4 Agonists. *J. Immunol.* **179**, 6097–6106 (2007).

106. Sethi, S., Maloney, J., Grove, L., Wrona, C. & Berenson, C. S. Airway inflammation and bronchial bacterial colonization in chronic obstructive pulmonary disease. *Am. J. Respir. Crit. Care Med.* **173**, 991–998 (2006).

107. Berenson, C. S., Garlipp, M. A., Grove, L. J., Maloney, J. & Sethi, S. Impaired Phagocytosis of Nontypeable Haemophilus influenzae by Human Alveolar

Macrophages in Chronic Obstructive Pulmonary Disease . *J. Infect. Dis.* **194**, 1375–1384 (2006).

108. Hodge, S., Hodge, G., Scicchitano, R., Reynolds, P. N. & Holmes, M. Alveolar macrophages from subjects with chronic obstructive pulmonary disease are deficient in their ability to phagocytose apoptotic airway epithelial cells. *Immunol. Cell Biol.* **81**, 289–296 (2003).

109. Sapey, E. *et al.* Behavioral and structural differences in migrating peripheral neutrophils from patients with chronic obstructive pulmonary disease. *Am. J. Respir. Crit. Care Med.* **183**, 1176–1186 (2011).

110. Qiu, Y. *et al.* Biopsy Neutrophilia, Neutrophil Chemokine and Receptor Gene Expression in Severe Exacerbations of Chronic Obstructive Pulmonary Disease. *Am. J. Respir. Crit. Care Med.* **168**, 968–975 (2003).

111. Hoenderdos, K. & Condliffe, A. The neutrophil in chronic obstructive pulmonary disease: Too little, too late or too much, too soon? *American Journal of Respiratory Cell and Molecular Biology* vol. 48 531–539 (2013).

112. W, H., M, L., Y, Z., C, Z. & Y, X. Expressions of MMP-12, TIMP-4, and Neutrophil Elastase in PBMCs and Exhaled Breath Condensate in Patients With COPD and Their Relationships With Disease Severity and Acute Exacerbations. *J. Immunol. Res.* **2019**, (2019).

113. Genschmer, K. R. *et al.* Activated PMN Exosomes: Pathogenic Entities Causing Matrix Destruction and Disease in the Lung. *Cell* **176**, 113-126.e15 (2019).

114. Grabcanovic-Musija, F. *et al.* Neutrophil extracellular trap (NET) formation characterises stable and exacerbated COPD and correlates with airflow limitation. *Respir. Res.* **16**, (2015).

115. Dicker, A. J. *et al.* Neutrophil extracellular traps are associated with disease severity and microbiota diversity in patients with chronic obstructive pulmonary disease. *J. Allergy Clin. Immunol.* **141**, 117–127 (2018).

116. Eriksson Ström, J. *et al.* Cytotoxic lymphocytes in COPD airways: Increased NK cells associated with disease, iNKT and NKT-like cells with current smoking. *Respir. Res.* **19**, (2018).

117. HODGE, G., MUKARO, V., HOLMES, M., REYNOLDS, P. N. & HODGE, S. Enhanced cytotoxic function of natural killer and natural killer T-like cells associated with decreased CD94 (Kp43) in the chronic obstructive pulmonary disease airway. *Respirology* **18**, 369–376 (2013).

118. Galgani, M. *et al.* Imbalance of circulating dendritic cell subsets in chronic obstructive pulmonary disease. *Clin. Immunol.* **137**, 102–110 (2010).

119. Qiu, S. lin *et al.* Enhanced activation of circulating plasmacytoid dendritic cells in patients with Chronic Obstructive Pulmonary Disease and experimental smoking-induced emphysema. *Clin. Immunol.* **195**, 107–118 (2018).

120. Stoll, P. *et al.* Imbalance of dendritic cell co-stimulation in COPD. *Respir. Res.* **16**, (2015).

121. Demedts, I. K. *et al.* Accumulation of dendritic cells and increased CCL20 levels in the airways of patients with chronic obstructive pulmonary disease. *Am. J. Respir. Crit. Care Med.* **175**, 998–1005 (2007).

122. Freeman, C. M. *et al.* Lung CD8+ T cells in COPD have increased expression of bacterial TLRs. *Respir. Res.* **14**, (2013).

123. Eustace, A. *et al.* Identification of cells expressing IL-17A and IL-17F in the lungs of patients with COPD. *Chest* **139**, 1089–1100 (2011).

124. Sileikiene, V. *et al.* Levels of CD4+ CD25+ T regulatory cells in bronchial mucosa and peripheral blood of chronic obstructive pulmonary disease indicate involvement of autoimmunity mechanisms. *Adv. Respir. Med.* **87**, 159–166 (2019).

125. Eriksson Ström, J. *et al.* Cytotoxic lymphocytes in COPD airways: Increased NK cells associated with disease, iNKT and NKT-like cells with current smoking. *Respir. Res.* **19**, (2018).

126. Gosman, M. M. E. *et al.* Increased number of B-cells in bronchial biopsies in COPD. *Eur. Respir. J.* **27**, 60–64 (2006).

127. Bracke, K. R. *et al.* Role of CXCL13 in cigarette smoke-induced lymphoid follicle formation and chronic obstructive pulmonary disease. *Am. J. Respir. Crit. Care Med.* **188**, 343–355 (2013).

128. Ladjemi, M. Z. *et al.* Increased IgA production by B-cells in COPD via lung epithelial interleukin-6 and TACI pathways. *Eur. Respir. J.* **45**, 980–993 (2015).

129. Gohy, S. T. *et al.* Polymeric immunoglobulin receptor down-regulation in chronic obstructive pulmonary disease: Persistence in the cultured epithelium and role of transforming growth factor-β. *Am. J. Respir. Crit. Care Med.* **190**, 509–521 (2014).

130. Byrne, R., Todd, I., Tighe, P. J. & Fairclough, L. C. Autoantibodies in chronic obstructive pulmonary disease: A systematic review. *Immunology Letters* vol. 214 8–15 (2019).

131. Weitnauer, M., Mijošek, V. & Dalpke, A. H. Control of local immunity by airway epithelial cells. *Mucosal Immunol.* **9**, 287 (2015).

132. Gon, Y. & Hashimoto, S. Role of airway epithelial barrier dysfunction in pathogenesis of asthma. *Allergol. Int.* **67**, 12–17 (2018).

133. Schlingmann, B., Molina, S. A. & Koval, M. Claudins: Gatekeepers of lung epithelial function. *Semin. Cell Dev. Biol.* **42**, 47–57 (2015).

134. Ridley, C. & Thornton, D. J. Mucins: the frontline defence of the lung. *Biochem. Soc. Trans.* **46**, 1099–1106 (2018).

135. Linden, S. K., Sutton, P., Karlsson, N. G., Korolik, V. & McGuckin, M. A. Mucins in the mucosal barrier to infection. *Mucosal Immunol.* **1**, 183 (2008).

136. Roy, M. G. *et al.* Muc5b is required for airway defence. *Nature* **505**, 412–416 (2014).

137. Zuo, W.-L. *et al.* Ontogeny and Biology of Human Small Airway Epithelial Club

Cells. *Am. J. Respir. Crit. Care Med.* **198**, 1375–1388 (2018).

138. Wang, Y. *et al.* Pulmonary alveolar type I cell population consists of two distinct subtypes that differ in cell fate. *Proc. Natl. Acad. Sci.* **115**, 2407 LP – 2412 (2018).

139. Guillott, L. *et al.* Response of human pulmonary epithelial cells to lipopolysaccharide involves toll-like receptor 4 (TLR4)-dependent signaling pathways: Evidence for an intracellular compartmentalization of TLR4. *J. Biol. Chem.* **279**, 2712–2718 (2004).

140. Otvos, L. J. Immunomodulatory effects of anti-microbial peptides. *Acta Microbiol. Immunol. Hung.* **63**, 257–277 (2016).

141. Funderburg, N. *et al.* Human -defensin-3 activates professional antigen-presenting cells via Toll-like receptors 1 and 2. *Proc. Natl. Acad. Sci.* **104**, 18631–18635 (2007).

142. Boniotto, M. *et al.* Human beta-defensin 2 induces a vigorous cytokine response in peripheral blood mononuclear cells. *Antimicrob. Agents Chemother.* **50**, 1433–41 (2006).

143. Wan, M. *et al.* Antimicrobial peptide LL-37 promotes bacterial phagocytosis by human macrophages. *J. Leukoc. Biol.* **95**, 971–981 (2014).

144. Lishko, V. K., Moreno, B., Podolnikova, N. P. & Ugarova, T. P. Identification of Human Cathelicidin Peptide LL-37 as a Ligand for Macrophage Integrin α(M)β(2) (Mac-1, CD11b/CD18) that Promotes Phagocytosis by Opsonizing Bacteria. *Res. reports Biochem.* **2016**, 39–55 (2016).

145. Levanen, B. *et al.* Impact of tobacco smoking on cytokine signaling via interleukin-17A in the peripheral airways. *Int. J. Chron. Obstruct. Pulmon. Dis.* **11**, 2109–2116 (2016).

146. Gabryelska, A., Kuna, P., Antczak, A., Białasiewicz, P. & Panek, M. IL-33 Mediated Inflammation in Chronic Respiratory Diseases—Understanding the Role of the Member of IL-1 Superfamily. *Front. Immunol.* **10**, (2019).

147. Honda, K. *et al.* IL-17A synergistically stimulates TNF-alpha-induced IL-8 production in human airway epithelial cells: A potential role in amplifying airway inflammation. *Exp. Lung Res.* **42**, 205–216 (2016).

148. Schoenbeck, S., McKenzie, D. T. & Kagnoff, M. F. Interleukin 5 is a differentiation factor for IgA B cells. *Eur. J. Immunol.* **19**, 965–969 (1989).

149. Seibold, M. A. Interleukin-13 Stimulation Reveals the Cellular and Functional Plasticity of the Airway Epithelium. *Ann. Am. Thorac. Soc.* **15**, S98–S102 (2018).

150. Fukaya, T. *et al.* Pivotal Role of IL-22 Binding Protein in the Epithelial Autoregulation of Interleukin-22 Signaling in the Control of Skin Inflammation . *Frontiers in Immunology* vol. 9 1418 (2018).

151. Totemeyer, S. *et al.* IFN-gamma enhances production of nitric oxide from macrophages via a mechanism that depends on nucleotide oligomerization domain-2. *J. Immunol.* **176**, 4804–4810 (2006).

152. Lee, H. C., Chathuranga, K. & Lee, J. S. Intracellular sensing of viral genomes and viral evasion. *Experimental and Molecular Medicine* vol. 51 1–13 (2019).

153. Triantafilou, K. *et al.* Human rhinovirus recognition in non-immune cells is mediated by Toll-like receptors and MDA-5, which trigger a synergetic pro-inflammatory immune response. *Virulence* **2**, 22 (2011).

154. Sanders, S. P. *et al.* Nitric Oxide Inhibits Rhinovirus-Induced Granulocyte Macrophage Colony-Stimulating Factor Production in Bronchial Epithelial Cells. *https://doi.org/10.1165/ajrcmb.24.3.4131* **24**, 317–325 (2012).

155. Jarjour, N. N. *et al.* The effect of an experimental rhinovirus 16 infection on bronchial lavage neutrophils. *J. Allergy Clin. Immunol.* **105**, 1169–1177 (2000).

156. Liu, C. *et al.* Role of epithelial chemokines in the pathogenesis of airway inflammation in asthma (Review). *Mol. Med. Rep.* **17**, 6935–6941 (2018).

157. McGuinness, A. J. A. & Sapey, E. Oxidative Stress in COPD: Sources, Markers, and Potential Mechanisms. *J. Clin. Med.* **6**, (2017).

158. Saetta, M. *et al.* Goblet cell hyperplasia and epithelial inflammation in peripheral airways of smokers with both symptoms of chronic bronchitis and chronic airflow limitation. *Am. J. Respir. Crit. Care Med.* **161**, 1016–1021 (2000).

159. Song, J. *et al.* Aberrant DNA methylation and expression of SPDEF and FOXA2 in airway epithelium of patients with COPD. *Clin. Epigenetics* **9**, 42 (2017).

160. Ghosh, M. *et al.* Exhaustion of airway basal progenitor cells in early and established chronic obstructive pulmonary disease. *Am. J. Respir. Crit. Care Med.* **197**, 885–896 (2018).

161. Yang, J. *et al.* Smoking-Dependent Distal-to-Proximal Repatterning of the Adult Human Small Airway Epithelium. *Am. J. Respir. Crit. Care Med.* **196**, 340–352 (2017).

162. Rostami, M. R. *et al.* Smoking shifts human small airway epithelium club cells toward a lesser differentiated population. *npj Genomic Med.* **6**, (2021).

163. de Boer, W. I. *et al.* Monocyte chemoattractant protein 1, interleukin 8, and chronic airways inflammation in COPD. *J. Pathol.* **190**, 619–626 (2000).

164. Di Stefano, A. *et al.* Bronchial inflammation and bacterial load in stable COPD is associated with TLR4 overexpression. *Eur. Respir. J.* **49**, (2017).

165. Macredmond, R. E., Greene, C. M., Dorscheid, D. R., Mcelvaney, N. G. & O'Neill, S. J. Epithelial expression of TLR4 is modulated in COPD and by steroids, salmeterol and cigarette smoke. *Respir. Res.* **8**, 84 (2007).

166. Xia, J. *et al.* Increased IL-33 expression in chronic obstructive pulmonary disease. *Am. J. Physiol. Lung Cell. Mol. Physiol.* **308**, L619-27 (2015).

167. Byers, D. E. *et al.* Long-term IL-33-producing epithelial progenitor cells in chronic obstructive lung disease. *J. Clin. Invest.* **123**, 3967–3982 (2013).

168. Kearley, J. *et al.* Cigarette smoke silences innate lymphoid cell function and

facilitates an exacerbated type I interleukin-33-dependent response to infection. *Immunity* **42**, 566–579 (2015).

169. Brandelius, A. *et al.* Selective inhibition by simvastatin of IRF3 phosphorylation and TSLP production in dsRNAchallenged bronchial epithelial cells from COPD donors. *Br. J. Pharmacol.* **168**, 363–374 (2013).

170. Anzalone, G. *et al.* IL-17A-associated IKK-α signaling induced TSLP production in epithelial cells of COPD patients. *Exp. Mol. Med.* **50**, (2018).

171. Yao, Y., Zhou, J., Diao, X. & Wang, S. Association between tumor necrosis factor-α and chronic obstructivepulmonary disease: a systematic review and meta-analysis. *Ther. Adv. Respir. Dis.* **13**, (2019).

172. Day, A., Barnes, P. & Donnelly, L. Elevated GM-CSF in COPD may drive defective macrophage phenotype. *Eur. Respir. J.* **44**, P1482 (2014).

173. Baines, K. J. *et al.* Novel immune genes associated with excessive inflammatory and antiviral responses to rhinovirus in COPD. *Respir. Res.* **14**, (2013).

174. Singanayagam, A. *et al.* Antiviral immunity is impaired in COPD patients with frequent exacerbations. *Am. J. Physiol. Cell. Mol. Physiol.* **317**, L893–L903 (2019).

175. Andresen, E., Gunther, G., Bullwinkel, J., Lange, C. & Heine, H. Increased expression of beta-defensin 1 (DEFB1) in chronic obstructive pulmonary disease. *PLoS One* **6**, e21898 (2011).

176. Arnason, J. W. *et al.* Human beta-defensin-2 production upon viral and bacterial co-infection is attenuated in COPD. *PLoS One* **12**, e0175963 (2017).

177. Baines, K. J. *et al.* Airway beta-Defensin-1 Protein Is Elevated in COPD and Severe Asthma. *Mediators Inflamm.* **2015**, 407271 (2015).

178. Guillon, A. *et al.* Neutrophil proteases alter the interleukin-22-receptor-dependent lung antimicrobial defence. *Eur. Respir. J.* **46**, 771–782 (2015).

179. Wittekindt, O. H. Tight junctions in pulmonary epithelia during lung inflammation. *Pflugers Archiv European Journal of Physiology* vol. 469 135–147 (2017).

180. Bhat, A. A. *et al.* Tight junction proteins and signaling pathways in cancer and inflammation: A functional crosstalk. *Frontiers in Physiology* vol. 10 (2019).

181. Aghapour, M., Raee, P., Moghaddam, S. J., Hiemstra, P. S. & Heijink, I. H. Airway Epithelial Barrier Dysfunction in Chronic Obstructive Pulmonary Disease: Role of Cigarette Smoke Exposure. *Am. J. Respir. Cell Mol. Biol.* **58**, 157–169 (2018).

182. Koval, M. Claudin Heterogeneity and Control of Lung Tight Junctions. *Annu. Rev. Physiol.* **75**, 551–567 (2013).

183. Itoh, M. *et al.* Direct binding of three tight junction-associated MAGUKs, ZO-1, ZO-2, and ZO-3, with the COOH termini of claudins. *J. Cell Biol.* **147**, 1351–1363 (1999).

184. Furuse, M., Sasaki, H. & Tsukita, S. Manner of interaction of heterogeneous claudin species within and between tight junction strands. *J. Cell Biol.* **147**, 891–903 (1999).

185. Van Itallie, C. M. & Anderson, J. M. Phosphorylation of tight junction transmembrane proteins: Many sites, much to do. *Tissue Barriers* vol. 6 (2018).

186. D'Souza, T., Agarwal, R. & Morin, P. J. Phosphorylation of Claudin-3 at threonine 192 by cAMP-dependent protein kinase regulates tight junction barrier function in ovarian cancer cells. *J. Biol. Chem.* **280**, 26233–26240 (2005).

187. Mitchell, L. A., Overgaard, C. E., Ward, C., Margulies, S. S. & Koval, M. Differential effects of claudin-3 and claudin-4 on alveolar epithelial barrier function. *Am. J. Physiol. - Lung Cell. Mol. Physiol.* **301**, 40–49 (2011).

188. Van Itallie, C., Rahner, C. & Anderson, J. M. Regulated expression of claudin-4 decreases paracellular conductance through a selective decrease in sodium permeability. *J. Clin. Invest.* **107**, 1319–1327 (2001).

189. LaFemina, M. J. *et al.* Claudin-18 deficiency results in alveolar barrier dysfunction and impaired alveologenesis in mice. *Am. J. Respir. Cell Mol. Biol.* **51**, 550–558 (2014).

190. Kotton, D. N. Claudin-18: Unexpected regulator of lung alveolar epithelial cell proliferation. *Journal of Clinical Investigation* vol. 128 903–905 (2018).

191. Looi, K. *et al.* Effects of human rhinovirus on epithelial barrier integrity and function in children with asthma. *Clin. Exp. Allergy* **48**, 513–524 (2018).

192. Sweerus, K. *et al.* Claudin-18 deficiency is associated with airway epithelial barrier dysfunction and asthma. *J. Allergy Clin. Immunol.* **139**, 72-81.e1 (2017).

193. De Boer, W. I. *et al.* Altered expression of epithelial junctional proteins in atopic asthma: Possible role in inflammation. *Can. J. Physiol. Pharmacol.* **86**, 105–112 (2008).

194. Hamilton, L. M. *et al.* Altered protein tyrosine phosphorylation in asthmatic bronchial epithelium. *Eur. Respir. J.* **25**, 978–985 (2005).

195. Kim, B. G. *et al.* Impact of the endothelial tight junction protein claudin-5 on clinical profiles of patients with COPD. *Allergy, Asthma Immunol. Res.* **10**, 533–542 (2018).

196. Milara, J., Peiró, T., Serrano, A. & Cortijo, J. Epithelial to mesenchymal transition is increased in patients with COPD and induced by cigarette smoke. *Thorax* **68**, 410–420 (2013).

197. Schamberger, A. C. *et al.* Cigarette smoke-induced disruption of bronchial epithelial tight junctions is prevented by transforming growth factor-β. *Am. J. Respir. Cell Mol. Biol.* **50**, 1040–1052 (2014).

198. Bouvry, D., Planès, C., Malbert-Colas, L., Escabasse, V. & Clerici, C. Hypoxia-induced cytoskeleton disruption in alveolar epithelial cells. *Am. J. Respir. Cell*

Mol. Biol. **35**, 519–527 (2006).

199. Greve, J. M. *et al.* The major human rhinovirus receptor is ICAM-1. *Cell* **56**, 839–847 (1989).

200. Avadhanula, V., Rodriguez, C. A., Ulett, G. C., Bakaletz, L. O. & Adderson, E. E. Nontypeable Haemophilus influenzae adheres to intercellular adhesion molecule 1 (ICAM-1) on respiratory epithelial cells and upregulates ICAM-1 expression. *Infect. Immun.* **74**, 830–838 (2006).

201. Shukla, S. D. *et al.* The main rhinovirus respiratory tract adhesion site (ICAM-1) is upregulated in smokers and patients with chronic airflow limitation (CAL). *Respir. Res.* **18**, (2017).

202. Thews, O. *et al.* Impact of reactive oxygen species on the expression of adhesion molecules in vivo. in *Advances in Experimental Medicine and Biology* vol. 645 95–100 (Adv Exp Med Biol, 2009).

203. Inumaru, J. *et al.* Molecular mechanisms regulating dissociation of cell-cell junction of epithelial cells by oxidative stress. *Genes to Cells* **14**, 703–716 (2009).

204. Dongre, A. & Weinberg, R. A. New insights into the mechanisms of epithelial–mesenchymal transition and implications for cancer. *Nature Reviews Molecular Cell Biology* vol. 20 69–84 (2019).

205. Wang, Q., Wang, Y., Zhang, Y., Zhang, Y. & Xiao, W. The role of uPAR in epithelial-mesenchymal transition in small airway epithelium of patients with chronic obstructive pulmonary disease. *Respir. Res.* **14**, (2013).

206. Boxio, R. *et al.* Neutrophil elastase cleaves epithelial cadherin in acutely injured lung epithelium. *Respir. Res.* **17**, (2016).

207. Mi, S. *et al.* Blocking IL-17A Promotes the Resolution of Pulmonary Inflammation and Fibrosis Via TGF-β1–Dependent and –Independent Mechanisms. *J. Immunol.* **187**, 3003–3014 (2011).

208. Bruewer, M. *et al.* Interferon-γ induces internalization of epithelial tight junction proteins via a macropinocytosis-like process. *FASEB J.* **19**, 923–933 (2005).

209. Mazzon, E. & Cuzzocrea, S. Role of TNF-α in lung tight junction alteration in mouse model of acute lung inflammation. *Respir. Res.* **8**, 75 (2007).

210. Chen, H., Lu, R., Zhang, Y. guo & Sun, J. Vitamin D Receptor Deletion Leads to the Destruction of Tight and Adherens Junctions in Lungs. *Tissue Barriers* **6**, 1–13 (2018).

211. Sundar, I. K., Hwang, J. W., Wu, S., Sun, J. & Rahman, I. Deletion of vitamin D receptor leads to premature emphysema/COPD by increased matrix metalloproteinases and lymphoid aggregates formation. *Biochem. Biophys. Res. Commun.* **406**, 127–133 (2011).

212. Short, K. R. *et al.* Influenza virus damages the alveolar barrier by disrupting epithelial cell tight junctions. *Eur. Respir. J.* **47**, 954–966 (2016).

213. Yeo, N. K. & Jang, Y. J. Rhinovirus infection-induced alteration of tight junction

and adherens junction components in human nasal epithelial cells. *Laryngoscope* **120**, 346–352 (2010).

214. Kast, J. I. *et al.* Respiratory syncytial virus infection influences tight junction integrity. *Clin. Exp. Immunol.* **190**, 351–359 (2017).

215. Clarke, T. B., Francella, N., Huegel, A. & Weiser, J. N. Invasive bacterial pathogens exploit TLR-mediated downregulation of tight junction components to facilitate translocation across the epithelium. *Cell Host Microbe* **9**, 404–414 (2011).

216. Hua, K. *et al.* Haemophilus parasuis Infection Disrupts Adherens Junctions and Initializes EMT Dependent on Canonical Wnt/β-Catenin Signaling Pathway. *Front. Cell. Infect. Microbiol.* **8**, (2018).

217. Guo, S., Al-Sadi, R., Said, H. M. & Ma, T. Y. Lipopolysaccharide Causes an Increase in Intestinal Tight Junction Permeability in Vitro and in Vivo by Inducing Enterocyte Membrane Expression and Localization of TLR-4 and CD14. *Am. J. Pathol.* **182**, 375–387 (2013).

218. Lee, C. S. *et al.* Simvastatin suppresses RANTES-mediated neutrophilia in polyinosinic–polycytidylic acid-induced pneumonia. *Eur. Respir. J.* **41**, 1147–1156 (2013).

219. Wira, C. R., Schaefer, T. M., Fahey, J. V & Wright, J. A. Poly(I:C) Uterine Epithelial Cells to the TLR3 Agonist Reproductive Tract: Antiviral Response of Innate Immunity in the Human Female. (2021) doi:10.4049/jimmunol.174.2.992.

220. Takizawa, Y., Kishimoto, H., Tomita, M. & Hayashi, M. Changes in the expression levels of tight junction components during reconstruction of tight junction from mucosal lesion by intestinal ischemia/reperfusion. *Eur. J. Drug Metab. Pharmacokinet.* **39**, 211–220 (2014).

221. Monnappa, A. K., Bari, W., Choi, S. Y. & Mitchell, R. J. Investigating the Responses of Human Epithelial Cells to Predatory Bacteria. *Sci. Reports 2016 61* **6**, 1–14 (2016).

222. Stephens, M. False discovery rates: a new deal. *Biostatistics* **18**, 275–294 (2017).

223. Yang, D., Han, Z. & Oppenheim, J. J. Alarmins and immunity. *Immunol. Rev.* **280**, 41–56 (2017).

224. HM Lazear, T. N. M. D. Interferon-λ: immune functions at barrier surfaces and beyond. *Immunity* **43**, 15–28 (2015).

225. García-Valero, J. *et al.* Deficient pulmonary IFN-β expression in COPD patients. *PLoS One* **14**, (2019).

226. Veerati, P. C. *et al.* Airway Epithelial Cell Immunity Is Delayed During Rhinovirus Infection in Asthma and COPD. *Front. Immunol.* **11**, (2020).

227. Kotenko, S. V., Rivera, A., Parker, D. & Durbin, J. E. Type III IFNs: Beyond antiviral protection. *Seminars in Immunology* vol. 43 (2019).

228. Cohen, T. S. & Prince, A. S. Bacterial Pathogens Activate a Common Inflammatory Pathway through IFNλ Regulation of PDCD4. *PLoS Pathog.* **9**, (2013).

229. Mubarak, R. Al, Roberts, N., Mason, R. J., Alper, S. & Chu, H. W. Comparison of pro- and anti-inflammatory responses in paired human primary airway epithelial cells and alveolar macrophages. *Respir. Res. 2018 191* **19**, 1–14 (2018).

230. Unger, B. L. *et al.* Rhinovirus Attenuates Non-typeable Hemophilus influenzae-stimulated IL-8 Responses via TLR2-dependent Degradation of IRAK-1. *PLOS Pathog.* **8**, e1002969 (2012).

231. Ohkuni, T. *et al.* Poly(I:C) reduces expression of JAM-A and induces secretion of IL-8 and TNF-α via distinct NF-κB pathways in human nasal epithelial cells. *Toxicol. Appl. Pharmacol.* **250**, 29–38 (2011).

232. Lee, J. E., Kim, Y. H., Rhee, C. S. & Kim, D. Y. AntibiSynergistic effect of Dermatophagoides farinae and lipopolysaccharides in human middle ear epithelial cells. *Allergy, Asthma Immunol. Res.* **8**, 445–456 (2016).

233. Cakarova, L. *et al.* Macrophage Tumor Necrosis Factor-α Induces Epithelial Expression of Granulocyte–Macrophage Colony-stimulating Factor. *https://doi.org/10.1164/rccm.200812-1837OC* **180**, 521–532 (2012).

234. Tengroth, L. *et al.* Functional Effects of Toll-Like Receptor (TLR)3, 7, 9, RIG-I and MDA-5 Stimulation in Nasal Epithelial Cells. *PLoS One* **9**, e98239 (2014).

235. J, K., SP, S., ES, S., V, C. & D, P. Role of NF-kappa B in cytokine production induced from human airway epithelial cells by rhinovirus infection. *J. Immunol.* **165**, 3384–3392 (2000).

236. Caruso, R. *et al.* Interleukin-25 Inhibits Interleukin-12 Production and Th1 Cell-Driven Inflammation in the Gut. *Gastroenterology* **136**, 2270–2279 (2009).

237. J, S. *et al.* IL-25 downregulates Th1/Th17 immune response in an IL-10-dependent manner in inflammatory bowel disease. *Inflamm. Bowel Dis.* **19**, 720–728 (2013).

238. Cheng, D. *et al.* Epithelial Interleukin-25 Is a Key Mediator in Th2-High, Corticosteroid-Responsive Asthma. *https://doi.org/10.1164/rccm.201403-0505OC* **190**, 639–648 (2014).

239. Paplińska-Goryca, M. *et al.* Sputum interleukin-25 correlates with asthma severity: a preliminary study. *Adv. Dermatology Allergol. Dermatologii i Alergol.* **35**, 462 (2018).

240. J, B. *et al.* Rhinovirus-induced IL-25 in asthma exacerbation drives type 2 immunity and allergic pulmonary inflammation. *Sci. Transl. Med.* **6**, (2014).

241. Ponce-Gallegos, M. A., Ramirez-Venegas, A. & Falfan-Valencia, R. Th17 profile in COPD exacerbations. *Int. J. Chron. Obstruct. Pulmon. Dis.* **12**, 1857–1865 (2017).

242. Shimura, E. *et al.* Potential role of myeloid cell/eosinophil-derived IL-17 in LPS-induced endotoxin shock. *Biochem. Biophys. Res. Commun.* **453**, 1–6 (2014).

243. Hui, C. C. K. *et al.* Thymic stromal lymphopoietin (TSLP) secretion from human nasal epithelium is a function of TSLP genotype. *Mucosal Immunol. 2015 85* **8**, 993–999 (2014).

244. Sommereyns, C., Paul, S., Staeheli, P. & Michiels, T. IFN-Lambda (IFN-λ) Is Expressed in a Tissue-Dependent Fashion and Primarily Acts on Epithelial Cells In Vivo. *PLOS Pathog.* **4**, e1000017 (2008).

245. Cohen, T. S. & Prince, A. S. Bacterial Pathogens Activate a Common Inflammatory Pathway through IFNλ Regulation of PDCD4. *PLoS Pathog.* **9**, (2013).

246. MR, H. *et al.* Respiratory syncytial virus infection enhances Pseudomonas aeruginosa biofilm growth through dysregulation of nutritional immunity. *Proc. Natl. Acad. Sci. U. S. A.* **113**, 1642–1647 (2016).

247. Kawashima, T. *et al.* Double-Stranded RNA of Intestinal Commensal but Not Pathogenic Bacteria Triggers Production of Protective Interferon-β. *Immunity* **38**, 1187–1197 (2013).

248. McNab, F., Mayer-Barber, K., Sher, A., Wack, A. & O'Garra, A. Type I interferons in infectious disease. *Nat. Rev. Immunol. 2015 152* **15**, 87–103 (2015).

249. Duffney, P. F. *et al.* Cigarette smoke dampens antiviral signaling in small airway epithelial cells by disrupting TLR3 cleavage. *Am. J. Physiol. - Lung Cell. Mol. Physiol.* **314**, L505 (2018).

250. Wark, P. A. B., Grissell, T., Davies, B., See, H. & Gibson, P. G. Diversity in the bronchial epithelial cell response to infection with different rhinovirus strains. *Respirology* **14**, 180–186 (2009).

251. Schneider, D. *et al.* Increased cytokine response of rhinovirus-infected airway epithelial cells in chronic obstructive pulmonary disease. *Am. J. Respir. Crit. Care Med.* **182**, 332–340 (2010).

252. Niwa, M. *et al.* IL-17A Attenuates IFN-λ Expression by Inducing Suppressor of Cytokine Signaling Expression in Airway Epithelium. *J. Immunol.* **201**, 2392–2402 (2018).

253. François-Newton, V. *et al.* USP18-based negative feedback control is induced by type I and type III interferons and specifically inactivates interferon α response. *PLoS One* **6**, (2011).

254. Cera, M. R. *et al.* JAM-A promotes neutrophil chemotaxis by controlling integrin internalization and recycling. *J. Cell Sci.* **122**, 268–277 (2009).

255. Y, T. *et al.* Junctional adhesion molecule-A, an epithelial-mesenchymal transition inducer, correlates with metastasis and poor prognosis in human nasopharyngeal cancer. *Carcinogenesis* **36**, 41–48 (2015).

256. Tatsuta, M. *et al.* Effects of cigarette smoke on barrier function and tight junction proteins in the bronchial epithelium: protective role of cathelicidin LL-37. *Respir. Res.* **20**, 251 (2019).

257. Lee, P.-H. *et al.* Alteration in Claudin-4 Contributes to Airway Inflammation and

Responsiveness in Asthma. *Allergy. Asthma Immunol. Res.* **10**, 25 (2018).

258. Jin, W. *et al.* Increased claudin-3, -4 and -18 levels in bronchoalveolar lavage fluid reflect severity of acute lung injury. *Respirology* **18**, 643–651 (2013).

259. Kage, H. *et al.* Claudin 4 knockout mice: normal physiological phenotype with increased susceptibility to lung injury. *Am. J. Physiol. - Lung Cell. Mol. Physiol.* **307**, L524 (2014).

260. Woodfin, A. *et al.* JAM-A mediates neutrophil transmigration in a stimulus-specific manner in vivo: evidence for sequential roles for JAM-A and PECAM-1 in neutrophil transmigration. *Blood* **110**, 1848–1856 (2007).

261. Canil, C. *et al.* Enteropathogenic Escherichia coli decreases the transepithelial electrical resistance of polarized epithelial monolayers. *Infect. Immun.* **61**, 2755–2762 (1993).

262. Ma, T. Y. *et al.* TNF-α-induced increase in intestinal epithelial tight junction permeability requires NF-κB activation. *https://doi.org/10.1152/ajpgi.00173.2003* **286**, (2004).

263. Hardyman, M. A. *et al.* TNF-α–mediated bronchial barrier disruption and regulation by src-family kinase activation. *J. Allergy Clin. Immunol.* **132**, 665-675.e8 (2013).

264. Moyano-Porcile, V., Olavarría-Ramírez, L., González-Arancibia, C., Bravo, J. A. & Julio-Pieper, M. Short-term effects of Poly(I:C) on gut permeability. *Pharmacol. Res.* **101**, 130–136 (2015).

265. Borkowski, A. W. *et al.* Toll-Like Receptor 3 Activation Is Required for Normal Skin Barrier Repair Following UV Damage. *J. Invest. Dermatol.* **135**, 569–578 (2015).

266. Ramezanpour, M., Bolt, H., Psaltis, A. J., Wormald, P.-J. & Vreugde, S. Primary human nasal epithelial cells: a source of poly (I:C) LMW-induced IL-6 production. *Sci. Rep.* **8**, 11325 (2018).

267. Comstock, A. T. *et al.* Rhinovirus-induced barrier dysfunction in polarized airway epithelial cells is mediated by NADPH oxidase 1. *J. Virol.* **85**, 6795–6808 (2011).

268. M, K. *et al.* Extracellular matrix influences alveolar epithelial claudin expression and barrier function. *Am. J. Respir. Cell Mol. Biol.* **42**, 172–180 (2010).

269. IA, E., C, M. & PO, H. Scribble regulates an EMT polarity pathway through modulation of MAPK-ERK signaling to mediate junction formation. *J. Cell Sci.* **126**, 3990–3999 (2013).

270. PD, V. *et al.* MMP9 modulates tight junction integrity and cell viability in human airway epithelia. *Am. J. Physiol. Lung Cell. Mol. Physiol.* **296**, (2009).

271. Carlier, F., Detry, B., Sibille, Y. & Pilette, C. COPD-related epithelial inflammation drives EMT in primary epithelial ALI-cultures. *Eur. Respir. J.* **52**, PA4239 (2018).

272. J, M., T, P., A, S. & J, C. Epithelial to mesenchymal transition is increased in

patients with COPD and induced by cigarette smoke. *Thorax* **68**, 410–420 (2013).

273. Heijink, I. H., Noordhoek, J. A., Timens, W., Oosterhout, A. J. M. van & Postma, D. S. Abnormalities in Airway Epithelial Junction Formation in Chronic Obstructive Pulmonary Disease. *https://doi.org/10.1164/rccm.201311-1982LE* **189**, 1439–1442 (2014).

274. EPEC recruits ZO-1 to site of the bacterial attachment and to the... | Download Scientific Diagram. https://www.researchgate.net/figure/EPEC-recruits-ZO-1-to-site-of-the-bacterial-attachment-and-to-the-distal-part-of-the_fig1_6679010.

275. Hanajima-Ozawa, M. *et al.* Enteropathogenic Escherichia coli, Shigella flexneri, and Listeria monocytogenes Recruit a Junctional Protein, Zonula Occludens-1, to Actin Tails and Pedestals. *Infect. Immun.* **75**, 565–573 (2007).

276. Ikeda, M. *et al.* Nontypeable Haemophilus influenzae exploits the interaction between protein-E and vitronectin for the adherence and invasion to bronchial epithelial cells. *BMC Microbiol. 2015 151* **15**, 1–11 (2015).

277. B, B. *et al.* Dual RNA-seq of Nontypeable Haemophilus influenzae and Host Cell Transcriptomes Reveals Novel Insights into Host-Pathogen Cross Talk. *MBio* **6**, (2015).

278. Goldfarbmuren, K. C. *et al.* Dissecting the cellular specificity of smoking effects and reconstructing lineages in the human airway epithelium. *Nat. Commun. 2020 111* **11**, 1–21 (2020).

279. Attard, R. *et al.* The impact of passive and active smoking on inflammation, lipid profile and the risk of myocardial infarction. *Open Hear.* **4**, e000620 (2017).

280. Zhao, S. *et al.* LDOC1 inhibits proliferation and promotes apoptosis by repressing NF-κB activation in papillary thyroid carcinoma. *J. Exp. Clin. Cancer Res. 2015 341* **34**, 1–12 (2015).

281. GR, H., SB, N., X, K., RF, L. & SS, M. Mechanism of cigarette smoke condensate-induced acute inflammatory response in human bronchial epithelial cells. *Respir. Res.* **3**, (2002).

282. Lee, M.-G. *et al.* XAF1 directs apoptotic switch of p53 signaling through activation of HIPK2 and ZNF313. *Proc. Natl. Acad. Sci.* **111**, 15532–15537 (2014).

283. Liu, Z. *et al.* IFI6 depletion inhibits esophageal squamous cell carcinoma progression through reactive oxygen species accumulation via mitochondrial dysfunction and endoplasmic reticulum stress. *J. Exp. Clin. Cancer Res. 2020 391* **39**, 1–28 (2020).

284. Metzemaekers, M., Vanheule, V., Janssens, R., Struyf, S. & Proost, P. Overview of the Mechanisms that May Contribute to the Non-Redundant Activities of Interferon-Inducible CXC Chemokine Receptor 3 Ligands. *Front. Immunol.* **0**, 1970 (2018).

285. Strzelak, A., Ratajczak, A., Adamiec, A. & Feleszko, W. Tobacco Smoke Induces and Alters Immune Responses in the Lung Triggering Inflammation,

Allergy, Asthma and Other Lung Diseases: A Mechanistic Review. *Int. J. Environ. Res. Public Health* **15**, (2018).

286. Bagaitkar, J., Demuth, D. R. & Scott, D. A. Tobacco use increases susceptibility to bacterial infection. *Tob. Induc. Dis.* **4**, 12 (2008).

287. Lugade, A. A. *et al.* Cigarette Smoke Exposure Exacerbates Lung Inflammation and Compromises Immunity to Bacterial Infection. *J. Immunol.* **192**, 5226–5235 (2014).

288. Froggatt, H. M., Harding, A. T., Chaparian, R. R. & Heaton, N. S. ETV7 limits antiviral gene expression and control of influenza viruses. *Sci. Signal.* **14**, eabe1194 (2021).

289. Kayama, H. *et al.* BATF2 prevents T-cell-mediated intestinal inflammation through regulation of the IL-23/IL-17 pathway. *Int. Immunol.* **31**, 371–383 (2019).

290. Vega-Carrascal, I. *et al.* Galectin-9 Signaling through TIM-3 Is Involved in Neutrophil-Mediated Gram-Negative Bacterial Killing: An Effect Abrogated within the Cystic Fibrosis Lung. *J. Immunol.* **192**, 2418–2431 (2014).

291. C, H. *et al.* Phospholipid Scramblase 1 Modulates FcR-Mediated Phagocytosis in Differentiated Macrophages. *PLoS One* **11**, (2016).

292. Mehrotra, P. *et al.* PARP-14 Functions as a Transcriptional Switch for Stat6-dependent Gene Activation *. *J. Biol. Chem.* **286**, 1767–1776 (2011).

293. Mehrotra, P., Krishnamurthy, P., Sun, J., Goenka, S. & Kaplan, M. H. Poly-ADP-ribosyl polymerase-14 promotes T helper 17 and follicular T helper development. *Immunology* **146**, 537–546 (2015).

294. Iwata, H. *et al.* PARP9 and PARP14 cross-regulate macrophage activation via STAT1 ADP-ribosylation. *Nat. Commun. 2016 71* **7**, 1–19 (2016).

295. Verheugd, P. *et al.* Regulation of NF-κB signalling by the mono-ADP-ribosyltransferase ARTD10. *Nat. Commun.* **4**, (2013).

296. Lu, Y. C., Yeh, W. C. & Ohashi, P. S. LPS/TLR4 signal transduction pathway. *Cytokine* **42**, 145–151 (2008).

297. Z, X. *et al.* NMI and IFP35 serve as proinflammatory DAMPs during cellular infection and injury. *Nat. Commun.* **8**, (2017).

298. Wang, J. *et al.* Negative Regulation of Nmi on Virus-Triggered Type I IFN Production by Targeting IRF7. *J. Immunol.* **191**, 3393–3399 (2013).

299. Ganser-Pornillos, B. K. & Pornillos, O. Restriction of HIV-1 and other retroviruses by TRIM5. *Nat. Rev. Microbiol. 2019 179* **17**, 546–556 (2019).

300. Hoffpauir, C. T. *et al.* TRIM14 Is a Key Regulator of the Type I IFN Response during Mycobacterium tuberculosis Infection. *J. Immunol.* **205**, 153–167 (2020).

301. Zhou, Z. *et al.* TRIM14 is a mitochondrial adaptor that facilitates retinoic acid-inducible gene-I–like receptor-mediated innate immune response. *Proc. Natl. Acad. Sci.* **111**, E245–E254 (2014).

302. Chen, M. *et al.* TRIM14 Inhibits cGAS Degradation Mediated by Selective Autophagy Receptor p62 to Promote Innate Immune Responses. *Mol. Cell* **64**, 105–119 (2016).

303. Lu, C. *et al.* Nontypeable Haemophilus influenzae DNA stimulates type I interferon expression via STING signaling pathway. *Biochim. Biophys. Acta - Mol. Cell Res.* **1865**, 665–673 (2018).

304. Marsters, S. A. *et al.* A novel receptor for Apo2L/TRAIL contains a truncated death domain. *Curr. Biol.* **7**, 1003–1006 (1997).

305. Koss, C. K. *et al.* IL36 is a critical upstream amplifier of neutrophilic lung inflammation in mice. *Commun. Biol. 2021 41* **4**, 1–15 (2021).

306. Foster, A. M. *et al.* IL-36 Promotes Myeloid Cell Infiltration, Activation, and Inflammatory Activity in Skin. *J. Immunol.* **192**, 6053–6061 (2014).

307. Boro, M. & Balaji, K. N. CXCL1 and CXCL2 Regulate NLRP3 Inflammasome Activation via G-Protein–Coupled Receptor CXCR2. *J. Immunol.* **199**, 1660–1671 (2017).

308. Smaldone, G. *et al.* KCTD15 is overexpressed in human childhood B-cell acute lymphoid leukemia. *Sci. Reports 2019 91* **9**, 1–13 (2019).

309. Mittal, M. *et al.* TNFα-stimulated gene-6 (TSG6) activates macrophage phenotype transition to prevent inflammatory lung injury. *Proc. Natl. Acad. Sci.* **113**, E8151–E8158 (2016).

310. Zhang, C. L. *et al.* Knockdown of TNFAIP1 inhibits growth and induces apoptosis in osteosarcoma cells through inhibition of the nuclear factor-κB pathway. *Oncol. Rep.* **32**, 1149–1155 (2014).

311. Gao, P. *et al.* Pentraxin 3 promotes airway inflammation in experimental asthma. *Respir. Res. 2020 211* **21**, 1–10 (2020).

312. Rodríguez, C., Pozo, M., Nieto, E., Fernández, M. & Alemany, S. TRAF6 and Src kinase activity regulates Cot activation by IL-1. *Cell. Signal.* **18**, 1376–1385 (2006).

313. Hsu, Y. H. *et al.* Anti-IL-20 monoclonal antibody inhibited inflammation and protected against cartilage destruction in murine models of osteoarthritis. *PLoS One* **12**, (2017).

314. F, M. *et al.* Production of Interleukin-20 cytokines limits bacterial clearance and lung inflammation during infection by Streptococcus pneumoniae. *EBioMedicine* **37**, 417–427 (2018).

315. Hsieh, M.-Y. *et al.* Interleukin-20 promotes angiogenesis in a direct and indirect manner. *Genes Immun. 2006 73* **7**, 234–242 (2006).

316. Vogel, W., Gish, G. D., Alves, F. & Pawson, T. The Discoidin Domain Receptor Tyrosine Kinases Are Activated by Collagen. *Mol. Cell* **1**, 13–23 (1997).

317. Xu, L. *et al.* Increased expression of the collagen receptor discoidin domain receptor 2 in articular cartilage as a key event in the pathogenesis of osteoarthritis. *Arthritis Rheum.* **56**, 2663–2673 (2007).

318. Kim, L. K. *et al.* E2F8 regulates the proliferation and invasion through epithelial-mesenchymal transition in cervical cancer. *Int. J. Biol. Sci.* **16**, 320–329 (2019).

319. Marsters, S. A. *et al.* Apo-3, a new member of the tumor necrosis factor receptor family, contains a death domain and activates apoptosis and NF-κB. *Curr. Biol.* **6**, 1669–1676 (1996).

320. Vella, G. *et al.* IL-17C contributes to NTHi-induced inflammation and lung damage in experimental COPD and is present in sputum during acute exacerbations. *PLoS One* **16**, e0243484 (2021).

321. Lamertz, L. *et al.* Soluble gp130 prevents interleukin-6 and interleukin-11 cluster signaling but not intracellular autocrine responses. *Sci. Signal.* **11**, 7388 (2018).

322. Minshall, E. *et al.* IL-11 expression is increased in severe asthma: Association with epithelial cells and eosinophils. *J. Allergy Clin. Immunol.* **105**, 232–238 (2000).

323. Ng, B. *et al.* Fibroblast-specific IL11 signaling is required for lung fibrosis and inflammation. *bioRxiv* 801852 (2019) doi:10.1101/801852.

324. Wang, P., Gamero, A. M. & Jensen, L. E. IL-36 promotes anti-viral immunity by boosting sensitivity to IFN-α/β in IRF1 dependent and independent manners. *Nat. Commun.* **10**, (2019).

325. X, X. *et al.* Respiratory syncytial virus NS1 protein degrades STAT2 by inducing SOCS1 expression. *Intervirology* **57**, 65–73 (2014).

326. Giotis, E. S. *et al.* Constitutively elevated levels of SOCS1 suppress innate responses in DF-1 immortalised chicken fibroblast cells. *Sci. Reports 2017 71* **7**, 1–15 (2017).

327. Liu, Y. *et al.* SPLUNC1/BPIFA1 Contributes to Pulmonary Host Defense against Klebsiella pneumoniae Respiratory Infection. *Am. J. Pathol.* **182**, 1519–1531 (2013).

328. J, H. *et al.* Atf3 negatively regulates Ptgs2/Cox2 expression during acute inflammation. *Prostaglandins Other Lipid Mediat.* **116**–**117**, 49–56 (2015).

329. Liu, X. *et al.* Zinc finger protein ZBTB20 promotes toll-like receptor-triggered innate immune responses by repressing IκBα gene transcription. *Proc. Natl. Acad. Sci.* **110**, 11097–11102 (2013).

330. Warner, S. M., Wiehler, S., Michi, A. N. & Proud, D. Rhinovirus replication and innate immunity in highly differentiated human airway epithelial cells. *Respir. Res.* **20**, (2019).

331. Ye, L. *et al.* Interferon-λ enhances adaptive mucosal immunity by boosting release of thymic stromal lymphopoietin. *Nat. Immunol.* **20**, 593–601 (2019).

332. Unger, B. L. *et al.* Rhinovirus Attenuates Non-typeable Hemophilus influenzae-stimulated IL-8 Responses via TLR2-dependent Degradation of IRAK-1. *PLoS Pathog.* **8**, e1002969 (2012).